Migration of cosmetic components into plastic packaging material

Dissertation

der Mathematisch-Naturwissenschaftlichen Fakultät

der Eberhard Karls Universität Tübingen

zur Erlangung des Grades eines

Doktors der Naturwissenschaften

(Dr. rer. nat.)

vorgelegt von

Laetitia Bolte

aus Leipzig

Tübingen

2024

Gedruckt mit Genehmigung der Mathematisch-Naturwissenschaftlichen Fakultät der Eberhard Karls Universität Tübingen.

Tag der mündlichen Qualifikation:	17.03.2025
Dekan:	Prof. Dr. Thilo Stehle
1. Berichterstatter:	Prof. Dr. Rolf Daniels
2. Berichterstatterin:	Prof. Dr. Dominique Jasmin Lunter

Acknowledgements

I would like to express my profound gratitude to all the individuals and groups that have either directly or indirectly contributed to the completion of this PhD.

First and foremost, I am deeply grateful to Prof. Dr. Rolf Daniels, my first supervisor, for his unwavering support and guidance throughout my entire research journey. His dedication of time and energy to assist me in writing this thesis and in the development of my publication has been invaluable. His insightful discussions and advice were critical to advancing this research. I am particularly thankful for his role in facilitating communication between the university and the company, as well as for his efforts to meet with me regularly in Hamburg and Tübingen.

I would also like to express my gratitude to Prof. Dr. Dominique Lunter, my second supervisor, for her support and the productive discussions during PhD seminars, which provided me with additional insights and direction.

A special thanks goes to Dr. Heiner Gers-Barlag, who enabled this work at Beiersdorf and supported me through regular meetings, offering valuable suggestions and advice. His guidance was instrumental during the writing process and in broadening the scope of my research through opportunities for publications, conferences, and presentations.

My sincere thanks also go to my direct supervisor, Guido Heinsohn, for welcoming me into his laboratory group and generously sharing his expertise. His willingness to support me with both minor and significant inquiries, as well as his constructive input on research directions, were immensely beneficial.

I am also grateful to my colleagues, Antje, Imke, Nils, and Marcel, who provided a warm introduction and support within the team, helping me become familiar with laboratory instruments, conducting measurements, and engaging in insightful scientific and personal discussions. My gratitude extends to Sabrina for her expertise and assistance with DSC measurements, as well as her openness to explore new approaches. Further Dr. Peter Philips's team for the use of their balances, and the GC-MS team, including Melanie, Marcel, Sebastian and Karo for their support and capacities for my measurements.

A big thank you goes out to the entire analytical department and the other PhD students for fostering a welcoming and supportive environment, which allowed me to freely explore and experiment with my ideas. I really enjoy our lunches to share scientific ideas, as well to get our minds of.

I am also thankful for the Packaging team, especially Orkun Kaymakci, for generously sharing his expertise and inviting me to workshops and visits, which provided valuable insights and significantly enhanced my knowledge and understanding.

Special thanks to the Body development team, and particularly Alina Brinkmann, for facilitating the production of the emulsions and offering technical guidance. I am equally grateful to the Packaging & Formula Science team for supplying materials for migration measurements and for sharing their expertise.

Further I would like to thank Melanie, Max and Carl for their support in writing the thesis and proofreading it.

On a personal note, I would like to express my gratitude to my parents and my sister, Aurelia, whose encouragement, support, and occasional distractions provided me with the balance needed to see this work through.

I am also deeply grateful to my friends Lukas, Jannik, Max, Markus, Sarah, who have been there with me since we started our studies in chemistry, supporting me along the way, that lead up to this thesis. Further a big thank you to Doro, Jana, Joni, Basti, Nati, and Lina for their continuous encouragement and companionship throughout.

Finally, my deepest appreciation goes to my husband, Juliy, who has been by my side from the beginning, supporting my decisions and providing every bit of motivation and help I needed along the way. I am grateful to you for everything.

This work is dedicated to my parents, my sister, and my husband, in appreciation of their constant presence and support. Thank you, for being there for me.

Publication and presentation

Parts of this dissertation were published in a publication and presented at a conference.

Presentation
Laetitia Bolte
Migration of cosmetic components into packaging material
Conference: POLY-CHAR 2024 – Polymers for our future
27th-31st May 2024

Publication
Laetitia Bolte, Heiner Gers-Barlag, Guido Heinsohn, Rolf Daniels
Migration of cosmetic components into polyolefins, Advances in Polymer Technology. 2024, 2024 (1): 2680899, 13 pages. https://doi.org/10.1155/adv/2680899

Special notes

Legally protected trademarks are used without special identification.

Unless otherwise stated, error bars and values following the designation "±" represent the standard deviation in both positive and negative directions from the mean (n = 3).

In this work, all lipids not miscible with water and liquid at room temperature are referred to as oils.

Unless otherwise noted, percentage values in formulations and mixtures refer to the mass fraction (m/m).

Table of contents

1 Abbreviations

%	Percent
$\Delta H_{x/R}$	Change in enthalpy of sample x/reference
ρ	Density
χ	Crystallinity
$A_{x/R}$	Surface area of sample x/reference
a, b, c, Y	Parameters of the asymptotic function
CIS	Charpy notched impact strength
D	Diffusion coefficient
DSC	Differential scanning calorimetry
E	Extrusion cycles
et al.	And others
F	Ratio of surface-to-volume of the polymer relative to the reference
FT	Fourier transformation
G	Factor considering the geometry of the polymer
g	Gram
GC-MS	Gas chromatography-mass spectrometry
GmbH	Gesellschaft mit beschränkter Haftung
h	Hour
HDPE	High-density polyethylene
IM	Injection molding plate
IR	Infrared
J	Joule
K	Kelvin
k	Slope of the linearized graph
kg	Kilogram
L	Polymer thickness

LC-MS	Liquid chromatography-mass spectrometry
LDPE	Low-density polyethylene
LLDPE	Linear low-density polyethylene
MFR	Melt flow rate
μ	Viscosity
mg	Milligram
min	Minute
mm	Millimeter
MS	Maximum saturation
MW	Molecular weight
MWD	Molecular weight distribution
N	Newton
n	Number of repeated measurements
NMR	Nuclear magnetic resonance
PCR	Post-consumer recyclates
PE	Polyethylene
PET	Polyethylene terephthalate
PO	Polyolefin
PP	Polypropylene
R	Reference
r	Recycled
RI	Retention index
ρ	Density
XRF	X-ray fluorescence spectroscopy
SCB	Short chain branching per 1000 C atoms
TGA	Thermogravimetric analysis
T	Temperature
t	Time

T_c	Crystallizing temperature
T_g	Glass transition temperature
T_m	Melting temperature
TM	Tension modulus
TS	Tension strength
µL	Microliter
µm	Micrometer
v	Virgin
Vm	Molar volume
$V_{x/R}$	Volume of sample x/reference
VOC	Volatile organic compound

2 Introduction

2.1 Plastic

2.1.1 Plastic definition

Plastic materials are categorized under the chemical class of polymers, which are large molecules composed of repeating units of monomers and can be natural or synthetic. Due to their broad abundance and variety of properties, they have a wide range of applications. Polymers are classified into elastomers, thermoplastics, fibers, duroplasts and biopolymers based on their physical and chemical properties. Plastics are materials that exhibit a combination of properties of elastomers and fibers [1-3].

Fibers have a high degree of symmetry, resulting in strong intermolecular interactions within the polymer chains. This configuration exhibits high crystallinity, tensile strength, and tensile modulus. The structure is mainly linear with low amounts of branching and cross-linking and provides great mechanical properties along the direction of the polymer chains. In contrast, elastomers have a high molecular weight with a significant amount of cross-linking, making them predominantly amorphous. Industrial processing requires temperatures above their glass transition temperature (T_g) to gain full chain mobility [1].

Plastic materials typically consist of linear polymer chains with varying degrees of branching and minimal cross-linking, resulting in different levels of crystallinity and the presence of amorphous regions [1-3]. Specific properties are described in more detail in the following sections.

Plastic packaging plays a central role in modern industry, especially in the cosmetics sector. The most common materials for plastic packaging are high-density polyethylene (HDPE), followed by polypropylene (PP), low-density polyethylene (LDPE), linear low-density polyethylene (LLDPE), and polyethylene terephthalate (PET) [2]. All of them are semicrystalline thermoplastics. PP, HDPE, LDPE, and LLDPE are derived from aliphatic hydrocarbons, such as ethylene, propylene, butene, and pentene, and belong to the class of polyolefins (POs). PET, on the other hand, is a polyester made from ethylene glycol and terephthalic acid (Figure 1). Polyethylene (PE) is a type of PO consisting of repeating ethylene monomers, and variations in its chain arrangement and structure result in different properties and applications.

Consequently, PE is classified into HDPE, LDPE, and LLDPE, each with distinct characteristics suitable for various uses, as outlined in the following section [1].

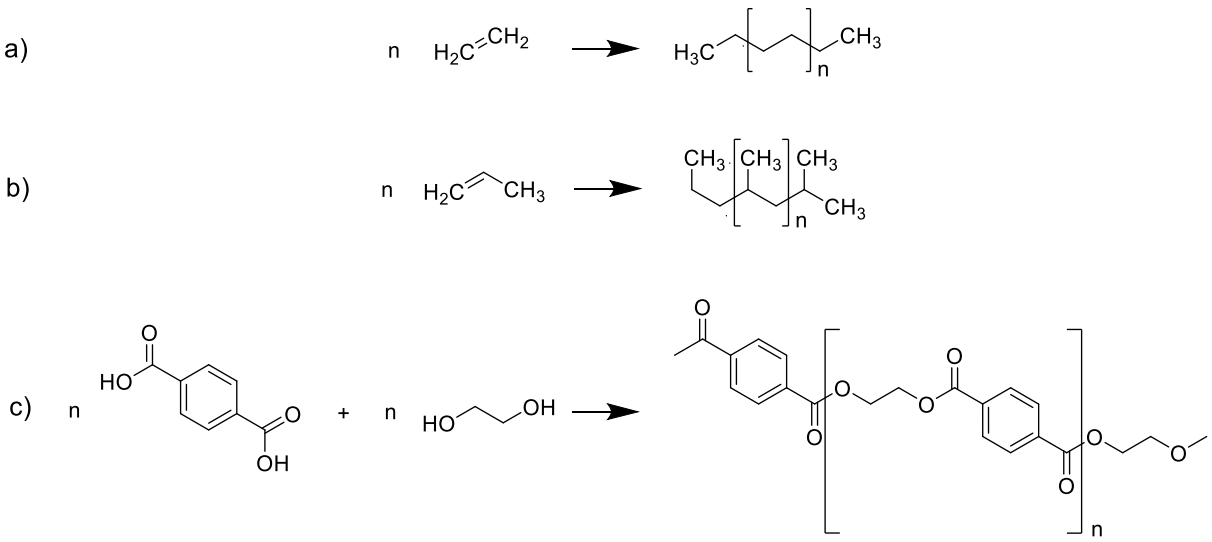

Figure 1 Chemical structure of a) PE, b) PP, and c) PET.

POs are predominantly used for packaging purposes in the cosmetics industry due to their cost-effectiveness and high processability. Their properties, such as molecular weight and molecular weight distribution, significantly influence their mechanical and rheological properties, while branching characteristics, including the degree and distribution frequency of branching, impact the polymer structure and its subsequent use [3-6]. Different POs fulfill different functions based on their properties. While HDPE is commonly used for cosmetic bottles containing lotion, shower gel, shampoo, and soap, LDPE is used for films, labels, squeeze bottles, and as a barrier layer in cosmetic packaging, PP for lids and jars containing cosmetic products, and PET is used for beverage bottles beyond the cosmetic industry [7-9].

2.1.2 Molecular structure

Each polymer exhibits a different polymer structure based on the monomer units, the type and amount of branching, and the presence of heteroatoms, influencing the arrangement of the polymer chains to one another. Chains with dense packaging and high symmetry engage in hydrogen bonding in the presence of heteroatoms. The packaging of the polymer chains depends on the structure of the polymer chain and the attached amount, length, and position of branches. Branched chains occupy more volume than linear ones, affecting properties like crystallinity, density, mechanical, and thermal characteristics. Branching can occur during polymer production with Ziegler-Natta catalysis, but mainly due to free radical polymerization or the intentional introduction of alkene comonomers and intermolecular chain transfer. The formation of *n*-hexyl, *n*-amyl, and *n*-butyl branches from the hydrogen atom of the fifth, sixth, and seventh methylene groups during radical formation is shown in Figure 2. Meanwhile, metallocene and Phillips catalysts would barely provoke any branching because they are single-site catalysts compared to Ziegler-Natta, which has several active sites, leading to more control over polymer tacticity, molecular weight, and its distribution [1, 10].

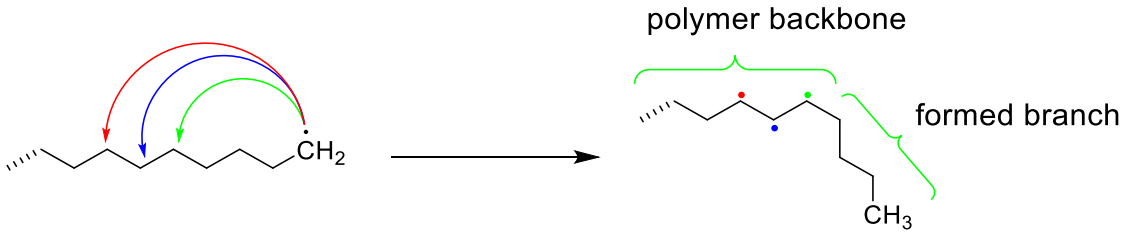

Figure 2 Branch formation after intermolecular chain transfer.

Branching can be distinguished into long and short chain branches. Short chain branches are mainly n-butyl, n-amyl, and n-hexyl branches. At the same time, long chain branches reach chain lengths longer than n-hexyl. The main distinction between polymers is observed in their different short chain branches and their resulting properties and applications. The difference in the chain length of octene and longer comonomers would not show significant variations [1, 10]. The analyzed polymers in this thesis are POs and polyesters, containing long and linear aliphatic chains with varying amounts of branching (Figure 3).

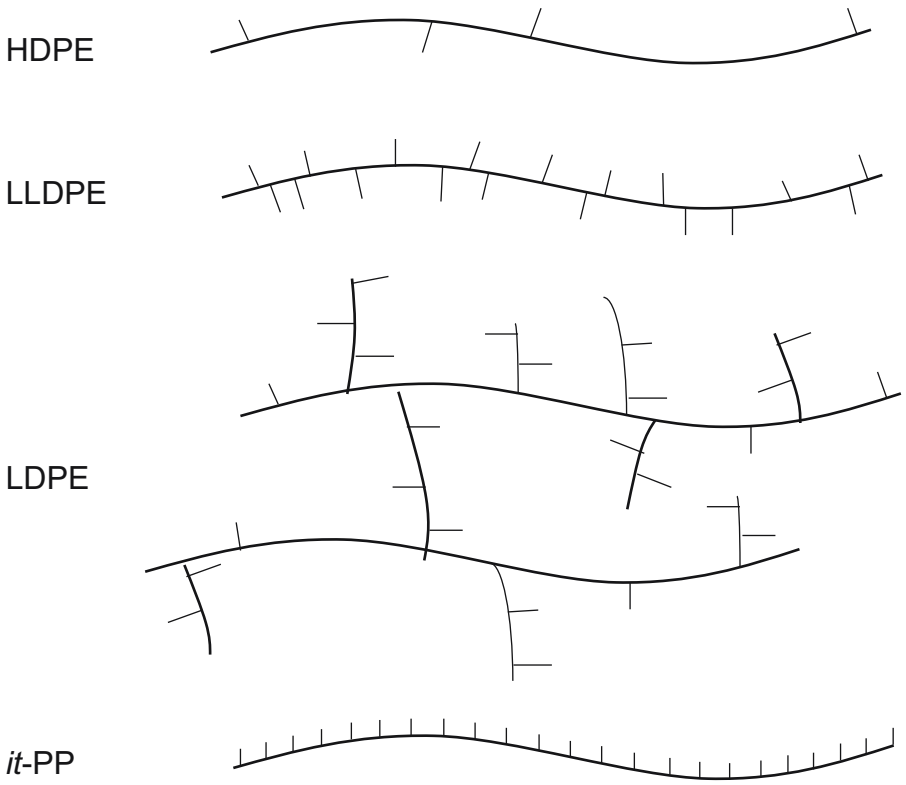

Figure 3 Polymer chains and their structure of different POs.

Apart from branching, the molecular structure is defined by the crystallinity of the polymer in its solid state. The formation of crystalline structures is based on symmetrical chain arrangements, high molecular weight, and minimal irregular branching. These factors allow for close packing and higher density of polymer chains. As a result, density is positively correlated with crystallinity. For instance, as shown in Table 1, HDPE exhibits higher crystallinity compared to LDPE.

Therefore, density shows a positive correlation with crystallinity, as shown in, HDPE provides higher crystallinity than LDPE. Most polymers are a mixture of crystalline and amorphous phases. Even high crystalline structures possess amorphous domains within the intersection of chain folds and end groups. However, the crystalline structure can alter under stress. For example, HDPE has an orthorhombic crystalline structure that forms a monoclinic crystal structure under compressive forces [1].

As depicted in Figure 3, the molecular structure varies significantly between different POs and other polymers, influencing the properties of the material. Table 1 highlights the distinct molecular features within POs and PET, showcasing the diversity and complexity of polymer science.

Table 1 Molecular properties of HDPE, LDPE, LLDPE, PP and PET [1, 6, 10-17].

Property	HDPE	LDPE	LLDPE	PP	PET
Density at 20 °C [g/cm^3]	0.94-0.97	0.91-0.93	0.91-0.94	0.84-0.91	1.30-1.40
Crystallinity [%]	60-90	29-60	30-53	3-67	20-50
MW mass average [g/mol]	1000-1500000	69000-411000	94000-208000	1000-5400000	19000-66000
SCB CH_3/1000C	0-7	8-33	7-26	-	-

HDPE materials have a high structural regularity, consisting mainly of linear polymer chains and fewer than seven ethyl groups per 1000 carbon atoms and, therefore, neglectable amounts of short and long chain branching. Those structure properties facilitate a high order of polymer chain arrangement leading to a large crystalline phase and, as the name implies, a relatively high density of 0.95-0.97 g/cm^3. Therefore, HDPE has the highest crystallinity, up to 90%, within plastic packaging materials. The close arrangement of the polymer chains leads to intermolecular forces as induced dipole-dipole interactions, giving the material good thermal and mechanical properties but also making it more rigid and brittle compared to other PE materials, like LDPE [1]. LDPE is a highly irregular branched polymer with more than 60 SCB of ethyl and butyl groups per 1000 carbon atoms and long chain branches at irregular intervals along the polymer chains. The branching increases the molecular weight (MW) but decreases crystallinity, density, and intermolecular force within the chains, leading to lower mechanical properties and, on the other hand, allowing the material to be more flexible, ductile, and transparent while enhancing entanglement. For example, LDPE has a density of around 0.91 g/cm^3 with a crystallinity of 60%. In comparison, HDPE with no branching has a higher density of 0.95 g/cm^3 due to closer arrangements of the chains, resulting in a crystallinity of up to 90% [1, 18]. A further PE structure is given with LLDPE, which is a copolymer of ethylene and higher-molecular-weight alpha alkenes like 1- butene, 1-hexene, or 1-octene. It has more short chain branching than HDPE along the polymer chain in more regular intervals and lengths. This allows the material to retain good mechanical properties and high flexibility compared to HDPE and LDPE, making it widely used for flexible films and tubing in packaging applications. On the

other hand, LLDPE has a lower crystallinity and density, therefore decreasing viscosity and processability compared to HDPE [1, 18, 19].

Along PE materials, PP is another important PO. It is composed of regularly spaced repeating units of propylene. In industry, mainly isotactic PP is used in which the methyl groups are arranged on the same side of the polymer, compared to atactic PP, in which methyl groups are randomly spread on both sides of the polymer chain. Further, the methyl group attached to every other carbon atom gives the polymer a head-to-tail configuration, as shown before in Figure 3. Isotactic PP has a higher structural arrangement with higher crystallinity than the amorphous atactic-PP. However, due to the methyl groups on the polymer chains, the density is lower than that of HDPE [1]. A study found PP, with lowest density, generates nearly 50% less CO_2-equivalent during transportation than other polymers [20, 21].

Copolymers of HDPE and isotactic-PP can occur due to contamination or intentional production. The copolymer is amorphous and has low crystallizing tendencies due to the randomly arranged length of ethylene and propylene units, which leads to varying properties for each copolymer [1].

Besides the POs, polyester PET is a commonly used packaging material. PET is a crystalline, linear polyester made of carbon, oxygen, and heteroatoms, formed during esterification and polycondensation processes [8]. PET is very stiff due to a lack of methylene groups on the main polymer chain, the presence of aromatic groups, and the strong hydrogen bonding between heteroatoms, which form a zigzag chain structure [1]. Compared to other polymers, PET has the highest density of approximately 1.3 g/cm^3 and is, thereby, almost 40% heavier than POs, leading to a greater environmental impact during transportation [20].

2.1.3 Thermal properties

The molecular structure of polymers directly influences their thermal behavior. The higher the symmetry of the polymer chains and the more intermolecular forces are present, the higher the melting (T_m), crystallization (T_c) and glass transition temperature (T_g). While T_m is a specific and short temperature area from a solid to a liquid state, T_g is the transition of a glassy solid to a leathery and further to a rubbery state within a broad temperature range. T_m is always significantly higher than T_g. Temperature changes below T_g where materials are glass-like solids, would not introduce a great change within the structure until the range of T_g is reached. Most linear polymers are hard and brittle below T_g. Along with the rise in temperature above T_g, the material's stiffness decreases. In the rubbery state, the polymer chains gain mobility, and many different conformations of the polymer chains. Due to long chain branching and low cross-linking, the material shows a high elasticity in the rubber state below T_m. Polymer chains with functional groups in their backbone influence T_g and T_m. While aliphatic and ether groups increase the flexibility and decrease T_g and T_m, other functional groups like aromatic, carbonyl, and amide groups lead to more stiffness and higher T_m and T_g [1].

Table 2 Thermal properties of POs and PET [1, 6, 8, 11-17, 22-24].

Property	HDPE	LDPE	LLDPE	PP	PET
T_m [°C]	125 - 135	105 - 115	120 - 130	147 - 176	245 - 265
T_c [°C]	114 - 120	96 - 100	107 - 123	116 - 140	164
T_g [°C]	(-118) - (-133)	(-103) - (-133)	(-110)	(-8)	60 - 76

Within the used packaging materials, PET has the highest temperatures for melting, glass transition, and crystallization due to its present structure of aromatic moieties and strong intermolecular forces like hydrogen bonding. For the PE materials, T_m, T_g, and T_c increase with higher molecular structure and, therefore, higher intermolecular forces like dispersion forces. HDPE with high crystallinity has the highest temperatures for melting, glass transition, and crystallinity, followed by LLDPE and then LDPE. PP, on the other hand, has lower crystallinity and density than HDPE, but the additional methyl groups allow additional interaction of the chains and, therefore, require more energy to melt, crystallize, or reach the glass transition point of the material [1].

2.1.4 Mechanical properties, chemical and thermal resistance

These unique thermal and molecular properties result in distinct mechanical characteristics for the polymers, as detailed in Table 3. POs, with their exceptional combination of strength and flexibility, are ideal for a wide range of applications [1].

Table 3 Mechanical properties of POs and PET [1, 6, 8, 12-17, 22, 24, 25].

Property	HDPE	LDPE	LLDPE	PP	PET
Tensile strength[1] [MPa]	13-51	10-20	25-45	26-32	24-41
Tensile modulus[2] [MPa]	500-1100	130-300	260-520	825-1700	~2300
Elongation at break[3] [%]	250-1200	130-270	300-830	10-140	100-250
Melt Flow Rate[4] [g/10min]	190 °C/2.2 kg 0.6	230 °C/3.8 kg 0.3-55	190 °C/2.2 kg 0.2-160	230 °C/2.2 kg 4-26	230 °C/3.8 kg 7
Melt Viscosity at 150 °C [kPa*s]	133 °C 0.003-1.6	54.5	25.5	0.1	270 °C 0.2-0.35
Charpy notched impact strength[5] at 23 °C [J/m]	20-220	420	54	18-69	640

While PE has high tensile strength, tensile modulus, and elongation at break to withstand deformation without fracturing, PP exhibits a high stiffness and impact resistance, with a tensile modulus between 825-1700 MPa. Particularly, the close arrangement of the polymer chains in HDPE leads induced dipole-dipole interactions, giving the material a high tensile strength and melting point but also making it more rigid and brittle compared to other PE materials. The branching in LDPE decreases the intermolecular forces within the chains, leading to a high elongation, lower tensile

[1] Tensile strength describes the maximum stress a material can withstand when being stretched [1, 10].
[2] Tensile modulus describes the stiffness and how much a material resists deformation under stress [1].
[3] Elongation at break reflects ductility and describes how much strain a material can withstand before breaking [1].
[4] The MFR indicates the mass of a polymer flowing through a standardized capillary under a certain temperature and load within ten minutes and is a measure of viscosity [26].
[5] Charpy notched impact strength measures the material's toughness and it's ability to absorb energy during impact [1].

strength, and less stiffness. LLDPE only has short chain branches in regular intervals, giving the material high flexibility, elongation and tensile strength. Further MFR is high for highly branched LDPE and LLDPE compared to the high crystalline HDPE. PET is compared to PE materials less brittle and can absorb a high amount of energy, resulting in a high charpy notched impact strength value (640 J/m) [1].

The molecular structure influences thermal and mechanical properties but would also play an important role in its resistance towards external factors. Polymers and mainly POs are non-polar aliphatic hydrocarbons resistant to ionic and most polar chemicals. They exhibit solubility in aliphatic hydrocarbon solvents with similar solubility parameters and react in chemical oxidation, free-radical reactions, chlorination, and nitration. Further, they can absorb non-polar gases and liquids but show no diffusion of water and ethanol [1]. Degradation and aging effects, like discoloration and a decrease in mechanical properties in polymers caused by exposure to light, heat, and oxygen lead to the use of additives. Thereby, slip-agents to reduce film to film friction, as well as anti-static agents, inorganic pigments, plasticizers, stabilizers, antioxidants, and UV-absorber are added to improve the materials properties [27, 28].

The presence of branching decreases the polymer chain's intermolecular forces and its heat resistance. However, the gained flexibility allows more resistance to environmental stress cracking. LLDPE and HDPE have high tensile strength and, therefore, higher impact resistance [1].

2.1.5 Processability

One fundamental property influenced by molecular structure is the melt flow rate (MFR), which reflects the average dimension and entanglement of the molecules. Depending on these properties, certain manufacturing processes are more suitable for specific product types. For plastic materials, injection molding (IM), and extrusion blow molding are the main processes used in packaging production. Injection molding is the most commonly used process for the production of three-dimensional products, like buckets, toys, or jars. In this method, the material is melted and homogenized in an extruder and transported through a nozzle connected to the mold cavity. In the mold, the material is solidified. The mold cavity is opened through the gate, and the specimen can be removed (Figure 4) [7-10, 29-31]. This technique represents a good performance method for PP and HDPE materials, is cost effective, and provides easy and fast responses to changes in consumer needs [10, 31, 32].

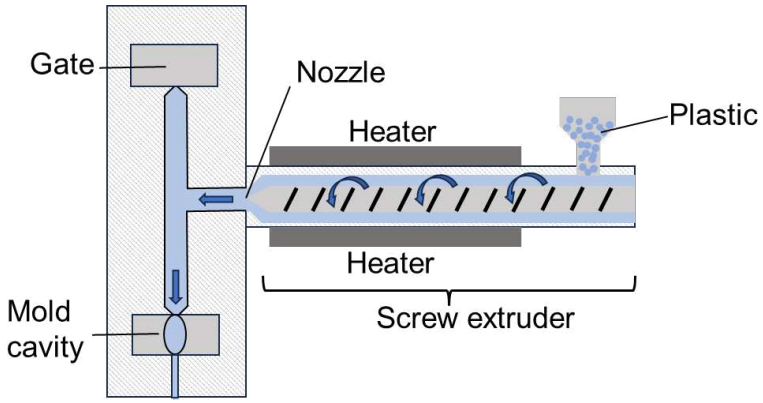

Figure 4 Setup for the injection molding process [10, 31, 32].

Another technique is blow molding, used for hollowing products, for example, bottles in the cosmetic industry. Two methods can be differentiated: extrusion blow molding and injection blow molding. For POs, extrusion blow molding is the main method of choice. The material from the extruder, called a parison, is positioned into the open mold. Once the mold is closed, air pressure is applied to the parison. Thereby, the parison inflates and presses against the mold wall (Figure 5). After cooling down, the specimen can be trimmed and removed. Further, layered products can be produced by coextruding multiple resins [10, 31, 32].

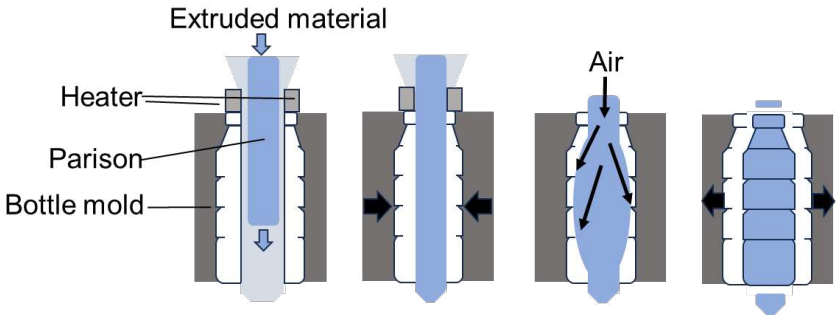

Figure 5 Process of extrusion blow molding [10, 31-33].

Depending on the MFR certain processes are more suitable, as illustrated in Figure 6. MFR values ranging from 0 to 1 g/10 min are ideal for extrusion to produce plastic bags and films, mainly of LDPE and LLDPE. A higher MFR of 0.3 to 5 g/10 min is suitable for blow molding, such as cosmetic HDPE bottles. MFR values above 5 g/10 min are processed by injection molding for products such as jars and lids made from PP, typically for thinner-walled items [7-10, 29, 30].

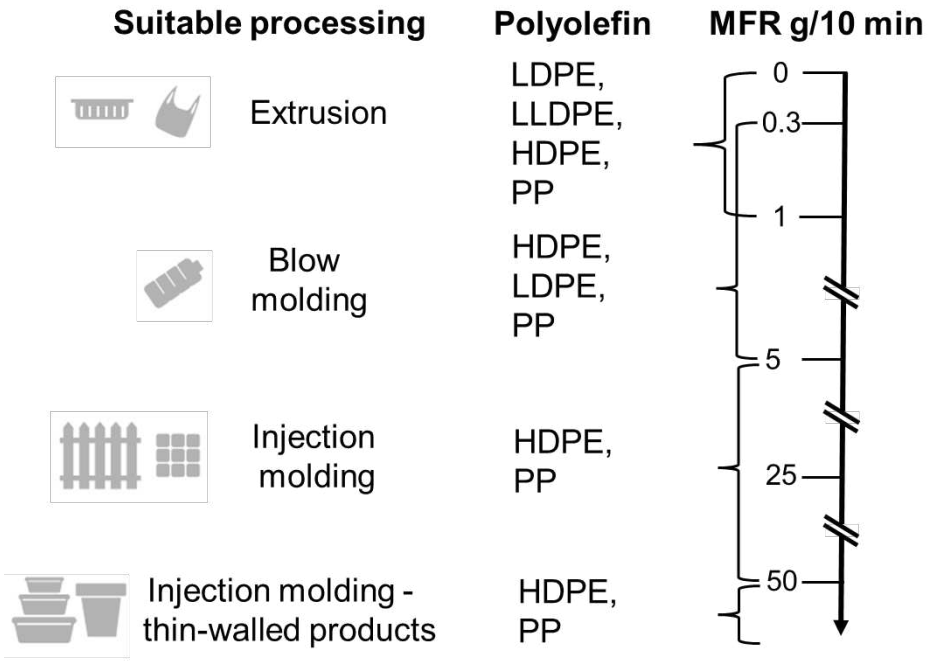

Figure 6 Processing types of POs according to their MFR [3].

2.2 Plastic consumption

Plastic is one of the most widely used packaging materials in the world. In 2009, almost 13 million tonnes of plastic were produced for packaging purposes, increasing to more than 21 million tonnes in 2020 in the EU. That accounts for up to 40% of the total plastic produced [34-37]. By 2030, the global demand is estimated to increase to 417 million tonnes from 236 million tonnes in 2016 [38]. The market for plastic packaging in the cosmetics industry is estimated to be worth around USD 27 billion in 2023 and is expected to be worth around USD 35 billion in 2028 [39, 40]. The demand for POs in the packaging sector continues to grow, leading to a high interest in post-consumer recyclates (PCR) to provide a sustainable solution for the consumers within the packaging industry. Furthermore, EU legislation requires that all plastic packaging materials must be recyclable or reusable by 2030 and that all plastic packaging materials must contain a minimum share of 30% PCR content [34, 41]. Therefore, packaging materials must meet the needs and requirements without compromising functionality and properties [41].

PO plastics are widely used due to their versatility, processability, and low production and processing costs. An analysis conducted in Copenhagen in 2017 examined the source and composition of separated plastic waste, revealing that over 90% of the collected plastic waste comprised equal amounts of PET, PE, and PP. Of this amount, 86% were used for packaging. Within the packaging sector, 19% of the separated plastic was used for bottles containing hygiene and cleaning products, with 86% being PE, 10% PP, and 4% PET. These findings highlight the importance of high-quality recycling for these types of plastic [2].

Currently, the number of plastics in circulation is limited. In 2006, 24.5 million tonnes and in 2020, 29.5 million tonnes of PCR waste were collected, with 19% recycled in 2006 and 35% in 2020. Globally, only 16% of PCR waste was collected for recycling, with the remainder sent to landfill or used for energy recovery. Figure 7 illustrates the development of waste treatment in the EU from 2006 until 2020 [8, 35, 42]. A study by Craft showed that recycling 100% of the POs used for cosmetic packaging compared to 100% landfilling reduces global warming potential by up to 38%.

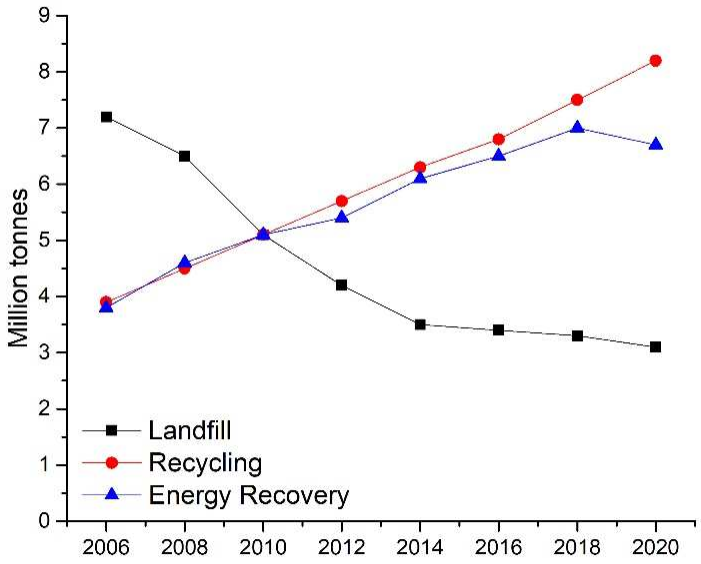

Figure 7 Plastic Post-Consumer Waste Management in the EU from 2006 to 2020 [2, 17, 19].

Fossil-fuel-based feedstock continues to be the primary source for plastic packaging materials, as shown in Figure 8. Approximately 4% of the global oil production was used to produce plastic material in 2009, with another 4% required for the energy consumption plastic production [35, 43]. Besides the fossil-based feedstock, mechanically recycled material and other methods like chemical, bio-based, and carbon-captured feedstocks, are sources for plastic production. These methods are still in development and only comprise less than 1% of plastic sources (Figure 8).

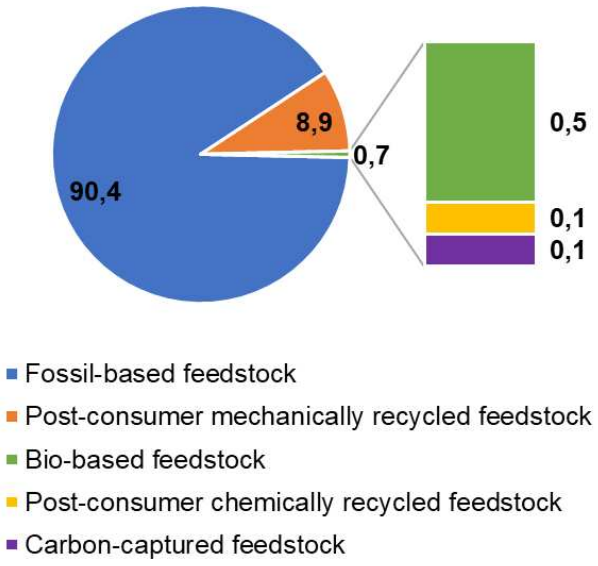

Figure 8 PO sources for polymerization in 2020 in % [2, 17, 19].

Studies have shown that waste separation leads to a 13-times higher recycling rate. In 2021, 5.5 million tonnes of PCR material were integrated into products in Europe,

making up 9.9% of recycling content. That is an increase of 20% compared to 2020. Of these 5.5 million tonnes, 8.5% was used for packaging purposes, compared to 4.6% in 2018 and 6.6% in 2020 [42].

In the following chapter, the entire plastic cycle is represented in Figure 9, showing the sources of the processed plastic and the waste treatment. Thereby, mechanically recycled feedstock makes up the greatest and most important part of the cycle. The mechanical recycling process contains two main steps: first, the sorting and separation, and second, washing, extrusion and degassing, to obtain plastic granules and continue the cycle of plastic production. The goal until 2030 is to increase the amount of post-consumer recycled plastic as a source and waste treatment to over 50% and minimize landfill waste treatment and virgin feedstock.

When comparing POs to other packing materials, like aluminum and bio-based polymers, they have shown the lowest values in environmental impact categories, such as water footprint per gram, except for fossil depletion. However, the environmental footprint will improve due to the possibility of recycling and recycled content. Furthermore, using PCR material for a cosmetic tubes showed a 29% reduction in the impact factor compared to a tube made from virgin material [44].

2.3 Mechanical recycling process

The importance of implementing recycled materials to fulfill sustainability goals and reduce environmental impact has been explained in previous chapters. To gain a deeper insight into the recycled materials and the recycling process, the different steps are highlighted in the following. Recycled materials, such as bottles and jars, are of high interest and are used in the cosmetic industry for packaging purposes [45]. The mechanical recycling process has been well-established and is mainly used to recycle POs. Compared to chemical recycling, in which the material is depolymerized to monomers or degraded, the mechanical recycling process is based on waste separation, decontamination, and reprocessing through extrusion [30]. Post-consumer products are often mixed in the waste, resulting in polymers as a blend of different POs, which requires a high quality separation and recycling process to obtain high quality PCR material suitable for reuse as packaging material [2].

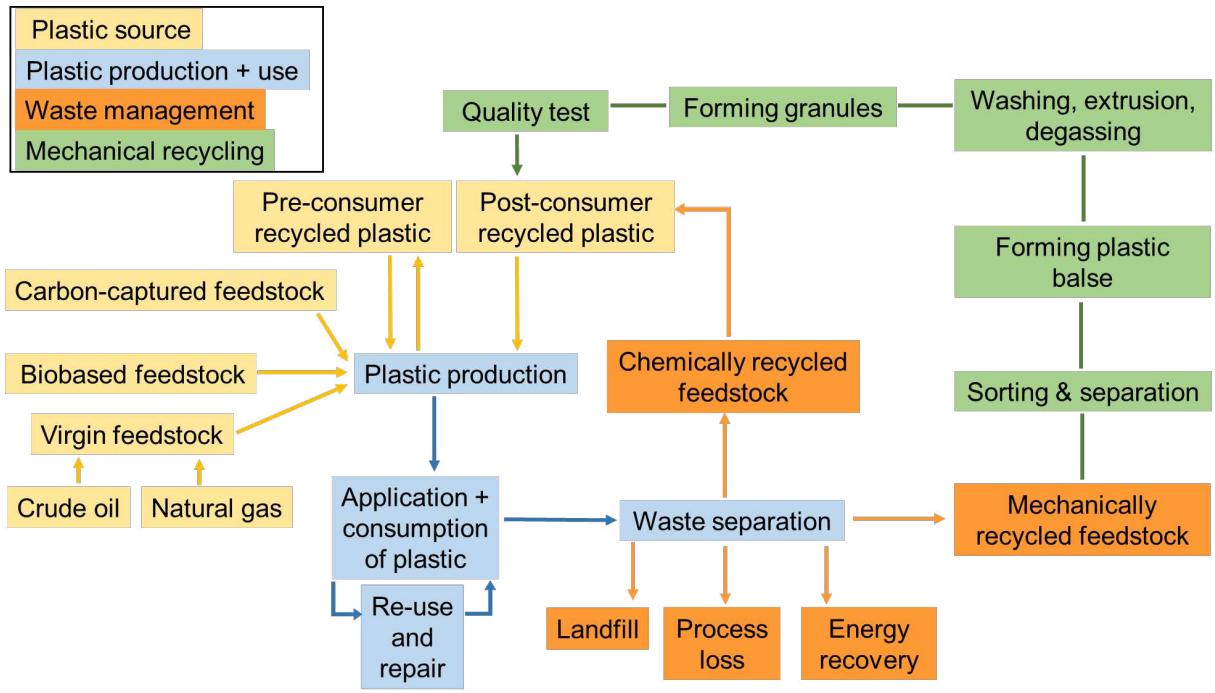

Figure 9 Plastic cycle for plastic production and plastic waste treatment [46].

The mechanical recycling process is divided into different steps of sorting and separation, followed by washing, extrusion, and degassing, as presented in Figure 9. These steps can vary between different recycling plants, leading to a wide variation of PCR materials. Factors such as temperature, equipment, solvents, and feedstock influence the properties of the PCR material. The collected plastic is first processed in a sorting and separation step. The material is sorted by size to eliminate small items and separated by density to isolate lightweight materials like film fractions, followed by

a separation of ferrous metal. With a near-infrared separator, different types of plastic will be sorted, like PP, PE, PET, polystyrene, polyamides, and black items, due to total absorption. Afterward, Eddy current separation is used to differentiate conductive from non-conductive items. After further separation by form, a manual separation and the formation of plastic bales complete the recycling process. These plastic bales are transported to different recycling plants for washing, extrusion, and degassing. The material is again scanned with a near-infrared separator to distinguish plastic types and black plastic, followed by a grinding step into even pieces. Different materials such as metals, minerals, polyvinyl chloride, and polystyrene residues are eliminated based on different densities using the sink-float separation method. The POs are intensively cold-washed by mechanical agitation and then hot-washed at 80 °C to remove solvent residues. In the subsequent extrusion cycle, the material is melted and homogenized under intensive compression at 230-275 °C. The extrusion process is a well-established, cost-effective, and important method in the mechanical recycling industry [8, 10, 46].

The extruder consists of a heated barrel with a rotating single or double screw. It can be divided into three different sections. The first section, the feed zone, introduces and preheats the plastic material, followed by the transition zone, where the material is melted, mixed, compressed, and pumped forward into the third section, known as the metering zone. The last zone applies maximum pressure to pump the material forward while mixing it and eliminating impurities like metal particles and dirt (Figure 10). The melting process is based on heat generated by friction from viscous flow and the mechanical interaction between the screw and the barrel walls [10, 31, 46, 47].

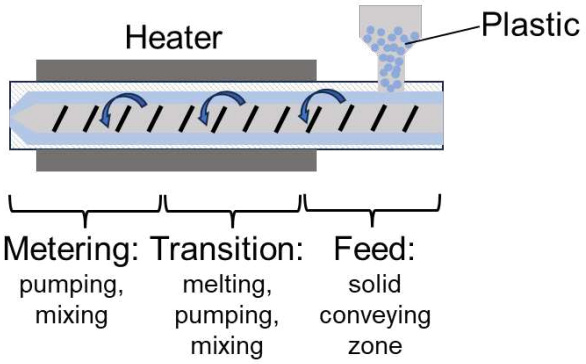

Figure 10 Set up of a single screw extruder.

With the heat and rotating screws, thermal softening or plasticization is induced, producing a homogeneous granulated material. During the extrusion, polymers undergo photo- or thermo-oxidative degradation, and shear-induced stress is applied, which leads to chain scission, chain branching, and crosslinking within the material as shown in Figure 11 [8, 46].

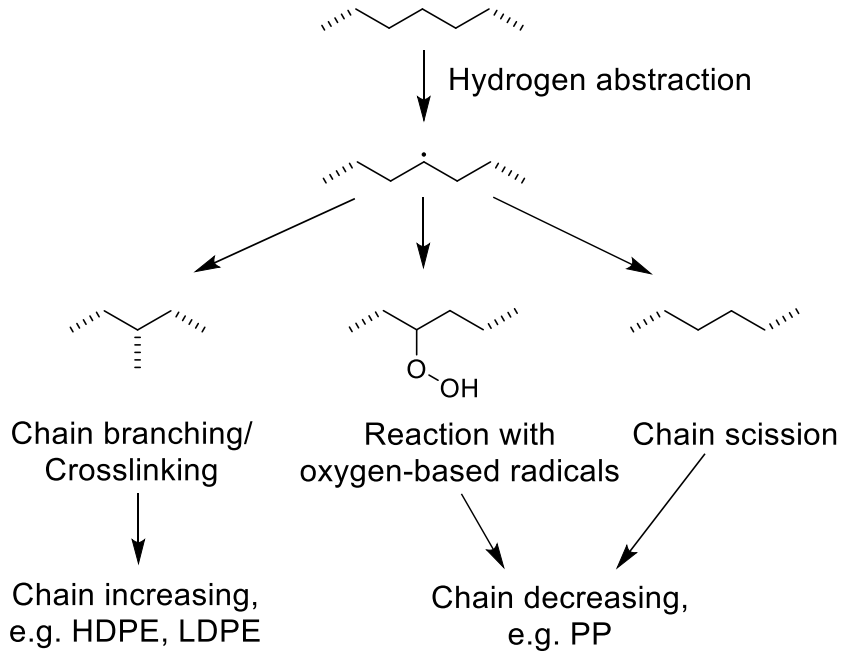

Figure 11 Radical reactions during the extrusion process [8].

During the degradation process, oxygen-induced peroxy radicals and thermally-induced hydrogen atom abstraction leads to the formation of radicals, causing chain-branching or β-scission and decrease the chain length. Chain degradation reduces the polymer length and decreases the mechanical properties while increasing the plasticity. In recycled PP materials, both tensile strength and elongation at break are reduced, while recycled HDPE exhibits decreased tensile strength. For recycled LLDPE, a reduction in elongation at break is observed [8, 48, 49].

At high temperatures during extrusion, volatiles such as solvents and monomers are further removed. In the next steps, the flakes are being analyzed for undesired polymers, colors, and opaque metals. With a zigzag classifier, the materials are separated by size. Under centrifugal forces, the material is dried and further degassed at 110 °C for 48 hours. Before the material is sold, some quality tests are conducted, such as density, color, mechanical properties, crystallinity, and processability.

Cross-contamination among different plastic types is common since almost half of the post-consumer products are made of multiple polymers. Due to the different steps in the mechanical recycling process, most of the different plastic types can be separated from one another, but complete separation is not always achieved [2]. Contamination of different POs, such as LDPE and PP in HDPE, is approximately 6% of the HDPE mass, often resulting from previous labels and caps or intentionally manufactured blends of HDPE with other POs. The presence of PP in HDPE could lead to a decrease in MFR due to reticulation because of MW increase or chain branching during extrusion [22].

However, compared to virgin plastic, recycling often have deteriorated properties due to contamination and degradation. This often leads to different processing methods and, consequently, different application for the material than its original use [3].

2.4 Cosmetic components and emulsions

Emulsions are mixtures of two immiscible liquids stabilized using surfactants or solid particles, known as emulsifiers. One of the liquids is hydrophobic, typically oil components, while the other exhibits hydrophilic behavior, generally water. The surfactants are amphiphilic, reducing the surface tension of the two liquids and preventing the droplets from coalescing. Emulsions can be classified into two types based on the continuous (outer) and dispersed (inner) phases. The oil-in-water (O/W) emulsion has oil droplets dispersed in the water phase, whereas the water-in-oil (W/O) emulsion has oil as an outer phase in which water droplets are dispersed. Furthermore, an appropriate emulsifier system can create complex emulsions such as oil-in-water-in-oil and water-in-oil-in-water [50]. Emulsions are generally thermodynamically unstable systems due to the high interfacial tension of the two immiscible phases, resulting in a high level of free energy in the system that has to be minimized by surfactants. Therefore, the emulsifier's concentration and choice, as well as emulsification conditions like mixing time, speed, and pressure, are critical. The process determines the emulsion's droplet size, which influences rheological properties, texture, appearance, and stability. Thereby, different categories are defined based on the droplet size [51]. Emulsions with droplet sizes from 0.1-5 µm are called macroemulsions. Smaller in size are nanoemulsions, which are kinetically stable and range from 20-100 nm, and thermodynamically stable microemulsions - also termed micellar emulsions - ranging from 5-50 nm. Smaller droplets generate a greater surface area, which allows better stabilization by the surfactant. Larger droplets tend to coalesce, leading to phase separation [51, 52].

In addition to water, oil phases and surfactants, other components are added to the emulsion to improve its properties. Moisturizing substances like butylene glycol, thickeners like cetyl alcohol, preservatives such as ethanol or parabens, and physiologically active ingredients like vitamins are incorporated to achieve the desired effects [53]. In W/O emulsions, salts such as $NaSO_4$ are added alongside thickening agents to enhance stability [54]. Ingredients in the oil phase are referred to as emollients, that act as moisturizing agents to maintain skin softness [55].

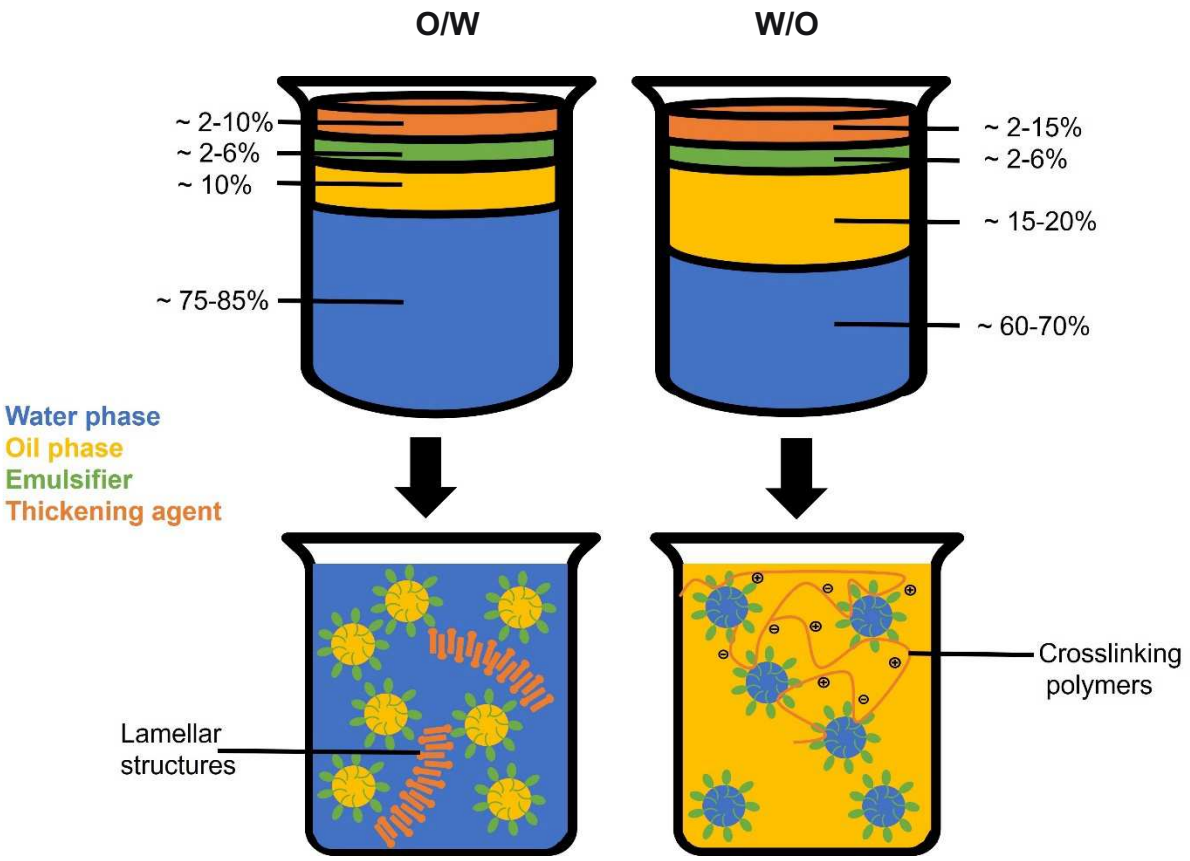

Figure 12 Composition of O/W and W/O.

As mentioned, emulsifiers are the most crucial ingredient for maintaining a stable emulsion. Nonionic surfactants, also known as polymeric surfactants, are particularly effective in preventing coalescence and flocculation. A combination of ionic and nonionic surfactants can further improve the emulsification process, producing smaller droplets. The Hydrophilic-Lipophilic Balance concept by Griffin is a useful tool for selecting the appropriate emulsifier. The concept describes the amount and ratio of hydrophilic and lipophilic groups in the emulsifier, which determines its suitability for certain emulsions such as W/O, O/W, detergents, or solubilizers [52].

A wide variety of lipds are utilized in the cosmetic industry as oil bases, ranging from triglycerides and fatty esters to ethers and compounds with short or low molecular weight chains, as well as long alkyl chains. These lipids vary from 100% natural sources to predominantly mineral-based oils. Often, mixtures of lipids are used to improve the properties of the final product, and the choice would depend on the desired features of the lipid, such as stability, texture, and moisturizing effects. Further, there is a high interest in implementing natural and biodegradable components to replace mineral oil-based substances, aligning with sustainability values. Mineral cosmetic oils like C12-C15 alkyl benzoate or paraffinum liquidum are replaced by natural lipids like

dicaprylyl ether, caprylic/capric triglyceride or sunflower oil, or hybrid lipids from natural and mineral sources like isopropyl palmitate, exemplary shown in Figure 13.

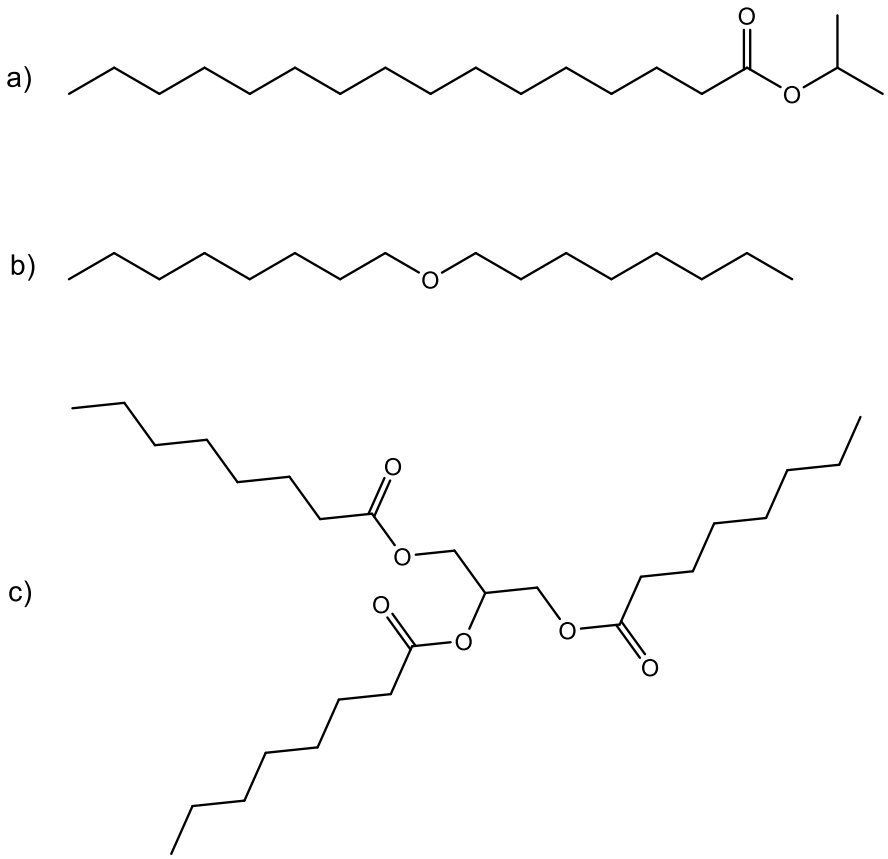

Figure 13 Molecular structure of cosmetic oils a) isopropyl palmitate, b) dicaprylyl ether, c) caprylic acid triglyceride.

Beyond the source of a lipid, the emulsion properties depend on its molecular weight. Heavier oils tend to exhibit lower viscosity and reduced spreadability but higher melting points, as shown in Figure 14. Depending on the type of emulsion and the desired properties, a specific oil mixture is chosen.

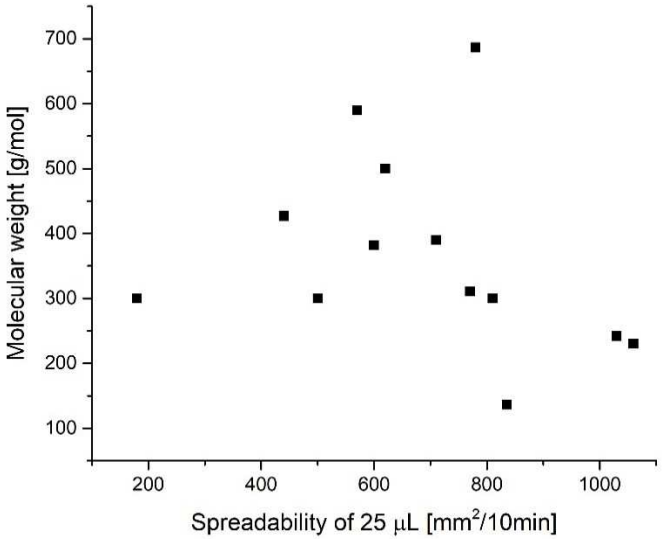

Figure 14 Correlation of molecular weight and spreadability of cosmetic oils.

Thickening agents derived from various chemical classes influence the rheological properties, appearance, and texture of emulsions differently. The thickening effect of these agents depends on the class type, including polysaccharides, fatty alcohols, fatty acid esters, synthetic polymers, proteins, glycerides, and clay minerals, as shown in Figure 15. Substances with hydrophilic groups interact through hydrogen bonds, while hydrophobic polymers interact along their long alkyl chains. Synthetic polymers with crosslinks form interlinks among polymer chains, resulting in steric interaction, while ionic polymers achieve thickening effects by electrostatic interaction forces. All those effects decrease the mobility of molecules, thereby, increasing viscosity. For example, cetyl alcohol is a fatty alcohol with polar and non-polar groups, accumulating at the interface of the two phases. The long alkyl chains form lamellar structures, and the crosslinking of these structured layers restrict movement [56, 57].

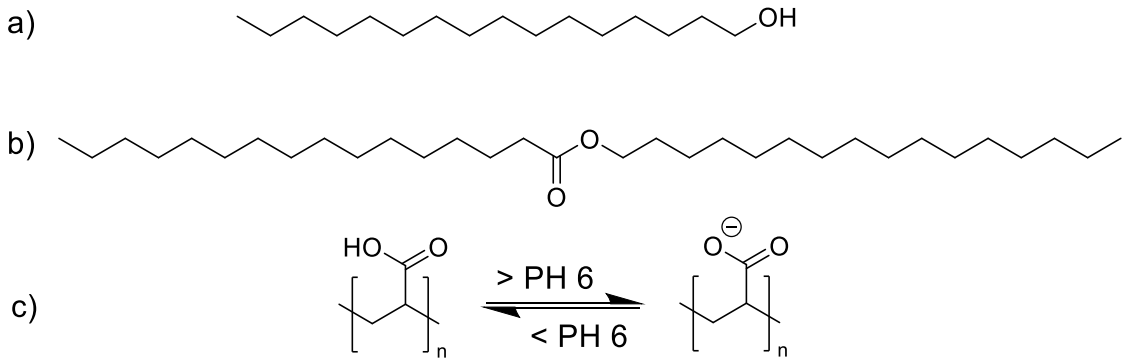

Figure 15 Thickening agents a) fatty alcohol: cetyl alcohol, b) fatty ester: cetyl palmitate, c) synthetic polymer: polyacrylic acid.

2.5 Migration process

Since the products are in direct contact with the packaging material, it is crucial to ensure that no undesired interaction occurs between the product and the packaging material. To date, several studies have shown how components of the PCR material can leach into the product, resulting in contamination that may affect the product's properties and pose a health risk. Plastic packaging materials contain various additives, such as plasticizers, flame retardants, and UV-absorbers, to improve material properties like flexibility, durability, and plasticity while maintaining the color and scent of the cosmetic products. However, some plasticizers, like phthalates and other contaminants like heavy metals and bisphenol A, are often present in plastic packaging and have been associated with a health risk [29, 43, 58-64]. In addition to the leaching from the packaging material into the product, various product components can migrate into the packaging material. In this process, different components from the product are adsorbed by the packaging wall and subsequently diffuse into the polymer chains of the POs, as shown in Figure 16 [23, 65].

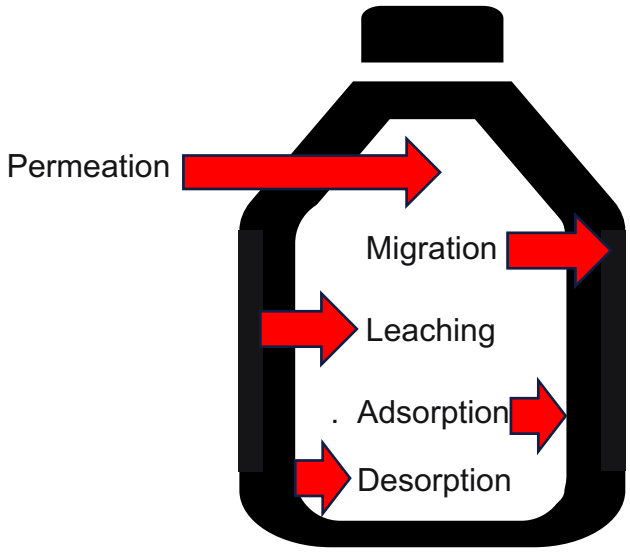

Figure 16 Various interactions of environment, packaging, and product.

Both processes, migration and leaching are based on the adsorption and desorption of a component, which is followed by a diffusion process in which the components are distributed within the material due to concentration differences. Permeation is based on sorption and diffusion processes [66].

The migration is governed by diffusion mechanisms and involves the transfer of substances from the product into the packaging material. The sorption velocity is described by Fick's law of diffusion, which characterizes the molecule movement based on concentration gradients. The diffusion rate R can be described with the diffusion coefficient D as a function of the local diffusion concentration C and L, describing the thickness [67]:

$$R = -D\,(C)\frac{\partial C}{\partial L}$$ **Equation 1** Fick's first law.

Since the diffusion of a substance into the polymer is a non-steady-state process where the concentration of the substance varies with time and position, the Fick's second law is applied.

$$\frac{\partial C}{\partial t} = D\frac{\partial^2 C}{\partial x^2}$$ **Equation 2** Fick's second law.

In this equation, $\frac{\partial C}{\partial t}$ describes the rate of change of concentration over time, while $\frac{\partial^2 C}{\partial x^2}$ is the second spatial derivation of concentration, representing the change in the concentration gradient.

This migration process can lead to deformation of the packaging material, with the outer surface being covered by an oil film and label detachment (Figure 17).

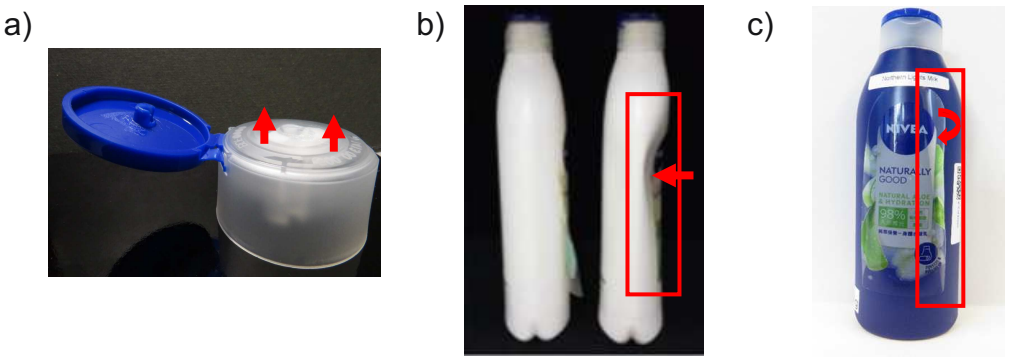

Figure 17 Deformation of a) a lid and b) a bottle and c) label detachment after the migration of oils in the product into the packaging material.

The migration process has been observed in virgin and recycled materials across various cosmetic products. The ongoing investigation of PCRs for their mechanical and chemical properties is significant. Given the diverse feedstock of the PCR materials

and the unique purification processes of each supplier, it is important to evaluate the PCR materials using various quality measurements. For example, GC-MS can be used to identify a wide range of volatile and semi-volatile contaminants. In addition to contamination from the feedstock and the cleaning process, the mixing of different plastic materials, for example, PP and HDPE, and the recycling process, alter the chemical and mechanical properties of the material. This could lead to a greater interaction of the product with the packaging material [68-70]. Studies indicate that the ability to absorb hydrocarbons correlates with the amorphous phase content, which is influenced by the degree of crystallinity and the extent of branching [23].

2.6 Aim

Plastic is one of the most used materials in the packaging industry, with the cosmetic sector relying on different kinds of plastic like HDPE, LDPE, LLDPE, and PP to produce jars, tubes, bottles, caps, and labels to package cosmetic products like emulsions. In this context, it is crucial to ensure that the plastic material does not interact with the product, regardless of storage conditions such as temperature and duration. Previous products containing emulsions exhibited packaging deformations and oily residues on the outer surface over time. Experiments indicate that these oils originate from the contained formulation, migrating into the plastic material and furthermore, the quantitative composition of the product, and thus its stability can be impaired. In addition to that the use of plastic packaging material continues to rise, underscoring the importance of investigating the migration from the product into the material, especially for currently used virgin POs and PCR materials.

Additionally, recycled material is a priority to fulfill sustainability goals. However, recycled materials present many challenges due to a diverse feedstock and the unique purification process of each supplier. That can lead to a broad range of contamination and structural alteration, increasing the risk of interaction between packaging and product. Based on those aspects, this thesis aims to understand the migration process of different cosmetic components into various packaging materials.

The first part of the research aims to analyze migration processes by testing different cosmetic components for their migration into plastic packaging. Oils from different sources and diverse structures will be chosen for comparative analysis. In addition, those oils will be tested as mixtures and incorporated into various oil- and water-based emulsions to understand migration in a realistic system. In the process, the composition of the emulsion will be systematically modified to analyze the influence of specific components on the migration process.

Further, the migration conditions will vary in their temperature, emulsion droplet size, and plastic type. Given that different plastic materials are utilized in the cosmetic industry, the migration will be tested on LDPE, HDPE, LLDPE, PP, and PET, with PET serving as a negative control and migration measurements focusing on the POs. Measurements will be performed on plastic pellets from the suppliers; however, assuming that processing conditions might alter material properties, migration will further be tested on bottles and injection moldings of the same material.

The second part of the thesis aims to examine variations in migration across different plastic materials, specifically focusing on the migration of isopropyl palmitate in virgin and recycled HDPE compared to LDPE, LLDPE and PP. Differences in maximum oil saturation and migration speed are going to be analyzed, and structural properties that influence the process will be defined.

The findings shall provide insights into the migration processes across various components and plastic materials. Based on the conditions, properties of the components and the plastic materials, predictions about the migration process under specific conditions will be made.

3 Materials and methods

3.1 Materials

3.1.1 Polymers

The plastic materials listed in Table 4 were used for the migration measurements. These materials were provided as pellets by various suppliers. The pellets from all suppliers underwent an extrusion and pelletization process, which varied along suppliers, leading to a broad range of pellet shapes and sizes as shown in Table 4. Some pellets were further processed into uniformly shaped injection molding (IM) pellets or extrusion blow molding bottles, facilitated by the company RPC Bramlage. Further, Leibniz Universität Hannover IKK - Institute of Plastics and Circular Economy produced mixtures of HDPE and PP, HDPE with LDPE, and LDPE with LLDPE, along with samples of different numbers of extrusion cycles.

Table 4 Polymers used for migration measurements.

Polymer	Material	Name*	Dimensions [mm]
HDPE	Virgin	vHDPE 1	2.64 x 4.06
		vHDPE 1_IM	0.88 x 4.70
		vHDPE 2	2.16 x 4.38
		vHDPE 4	2.28 x 3.84
		vHDPE 5	0.92 x 4.70
		vHDPE 3	3.35 x 3.98
		vHDPE 3_IM	0.91 x 4.70
		vHDPE 3_ bottle natural	1.04 x 5.10
		vHDPE 3_ bottle white	0.68 x 5.10
		vHDPE 3_ bottle blue	0.99 x 5.10
	Virgin + Recycled	vHDPE 3 + 50% rHDPE 22	9.35 x 5.10
		vHDPE 3 + 70% rHDPE 22	1.04 x 5.10
		vHDPE 3 + 50% rHDPE 23	1.27 x 5.10
		vHDPE 3 + 70% rHDPE 23	1.91 x 5.10
	Recycled	rHDPE 1	2.35 x 4.26

		rHDPE 2	2.19 x 4.56
		rHDPE 2_IM	0.91 x 4.70
		rHDPE 3	1.47 x 4.42
		rHDPE 4	3.24 x 3.23
		rHDPE 5	3.46 x 3.68
		rHDPE 6	2.51 x 4.24
		rHDPE 7	0.90 x 4.70
		rHDPE 8	2.73 x 3.39
		rHDPE 9	2.58 x 2.48
		rHDPE 10	3.93 x 2.40
		rHDPE 11	0.92 x 4.70
		rHDPE 12	0.89 x 4.70
		rHDPE 13	1.90 x 3.96
		rHDPE 14	2.45 x 4.28
		rHDPE 15	1.74 x 4.56
		rHDPE 16	2.36 x 4.30
		rHDPE 17	0.90 x 4.70
		rHDPE 18_a	2.62 x 3.98
		rHDPE 18_b	2.25 x 4.08
		rHDPE 18_c	1.88 x 4.31
		rHDPE 18_d	2.35 x 4.13
		rHDPE 18_e	1.74 x 4.31
		rHDPE 18_f	1.87 x 4.32
		rHDPE 18_g	3.56 x 8.99
		rHDPE 18_h	2.09 x 4.08
		rHDPE 19	2.14 x 4.14
		rHDPE 20_0h	2.87 x 4.08
		rHDPE 20_12h	2.14 x 4.48
		rHDPE 20_24h	2.69 x 3.92
		rHDPE_21	3.52 x 4.43
LDPE	Virgin	vLDPE 1	2.64 x 3.79
		vLDPE 2	0.84 x 4.70
		vLDPE 3	0.88 x 4.70
		vLDPE 4	0.84 x 4.70

	Recycled	rLDPE 1	1.68 x 2.86
		rLDPE 2	2.99 x 2.58
		rLDPE 3	1.60 x 2.86
		rLDPE 4	1.66 x 5.95
		rLDPE 5	1.68 x 6.08
		rLDPE 6	1.99 x 5.20
LLDPE	Virgin	vLLDPE 1	2.44 x 2.26
		vLLDPE 2	0.86 x 4.70
		vLLDPE 3	2.57 x 3.14
PET	Recycled	rPET 1	1.89 x 2.60
HDPE + PP	Virgin	vHDPE_1% vPP	1.43 x 5.10
		vHDPE_3% vPP	1.43 x 5.10
		vHDPE_5% vPP	1.43 x 5.10
PP	Virgin	vPP1	2.68 x 3.30
		vPP 2	2.76 x 3.70
		vPP 3	0.83 x 4.70
		vPP 4	3.33 x 4.35
		vPP 5	0.94 x 4.70
	Recycled	rPP 1	2.28 x 3.46
		rPP 2	2.75 x 4.26
		rPP 3	2.69 x 3.34
		rPP 4	0.93 x 4.70
		rPP 5	3.92 x 4.64
		rPP 6	2.80 x 2.80
HDPE extruded	Virgin	vHDPE_1xE	1.38 x 2.52
		vHDPE_2xE	1.38 x 2.52
		vHDPE_3xE	1.56 x 2.52
		vHDPE_4xE	1.52 x 2.52
		vHDPE 1_5xE	1.43 x 2.52
		vHDPE 1_6xE	1.51 x 2.52
		vHDPE 1_7xE	1.50 x 2.52
		vHDPE 1_8xE	1.46 x 2.52
	Recycled	rHDPE 19_1xE	1.35 x 2.52
		rHDPE 19_ 2xE	1.70 x 2.52

		rHDPE 19_ 3xE	1.65 x 2.52
		rHDPE 19_ 4xE	1.65 x 2.52
		rHDPE 19_ 5xE	1.63 x 2.52
		rHDPE 19_ 6xE	1.61 x 2.52
		rHDPE 19_ 7xE	1.64 x 2.52
		rHDPE 19_ 8xE	1.64 x 2.52
HDPE + LDPE	Virgin	vHDPE + 1% vLDPE	1.46 x 2.52
		vHDPE + 3% vLDPE	1.31 x 2.52
		vHDPE + 5% vLDPE	1.35 x 2.52
		vHDPE + 10% vLDPE	1.25 x 2.52
		vHDPE + 30% vLDPE	1.25 x 2.52
LDPE + LLDPE	Virgin	vLDPE + 1% vLLDPE	1.33 x 2.52
		vLDPE + 3% vLLDPE	1.38 x 2.52
		vLDPE + 5% vLLDPE	1.34 x 2.52
		vLDPE + 10% vLLDPE	1.39 x 2.52
		vLDPE + 30% vLLDPE	1.36 x 2.52

* Symbols indicating injection molding (IM), Extrusion cycle (E), recycled (r), virgin (v).

3.1.2 Components for migration measurements

Fragrance: (R)-(+)-Limonene from Alfa Aesar (Haverhill, MA, USA);

Cosmetic oils: Isopropyl palmitate, Dicaprylyl ether, Caprylic/capric triglyceride from BASF (Ludwigshafen am Rhein, Germany); C12-C15 alkyl benzoate from Evonik (Essen, Germany); Butylene glycol dicaprylate/dicaprate from IOI Oleo (Hamburg, Germany); Castor oil from OPW Ingredients (Niederkrüchten-Dam, Germany); Sunflower oil from Gustav Heess (Leonberg, Germany); Paraffinum liquid from Hansen & Rosenthal (Hamburg, Germany);

Surfactants: Sodium cetearyl sulfate, Diisostearoyl polyglyceryl-3 dimer dilinoleate; Glyceryl stearate SE from BASF (Ludwigshafen am Rhein, Germany); Polyglyceryl-4 diisostearate/polyhydroxystearate/sebacate from Evonik (Essen, Germany);

Thickening additives: Cetyl palmitate, Cetyl alcohol, Tetradecyl tetradecanoate from BASF (Ludwigshafen am Rhein, Germany);

Water solubles: Citric acid from Brenntag GmbH (Hamburg, Germany); Sodium citrate from Merck Chemicals GmbH (Darmstadt, Germany); Potassium sorbate from Newport Industries Ltd. (London, UK); Magnesium sulfate from Reher & Ramsden (Hamburg, Germany)

3.2 Methods

3.2.1 Sample preparation

Migration kinetics were measured at 23 °C, 40 °C, 66 °C, and 105 °C. To this end, glass bottles were filled with an excess amount of the migrating component, and 1 g of weighed plastic pellets was added. The mixture was stored until saturation was reached. For the migration measurement, the pellets were withdrawn, cleaned with wipes, weighed, measured by Infrared (IR) spectroscopy, and then returned to resume the migration process. Measurements were performed in triplicate.

3.2.2 Migration

To describe the migration process, D was calculated. Therefore, the change in weight over time was plotted in the software Origin Pro, as shown in Figure 18. An asymptotic function was fitted in the form of

$$y = a - b \cdot c^t$$ **Equation 3** Asymptotic function.

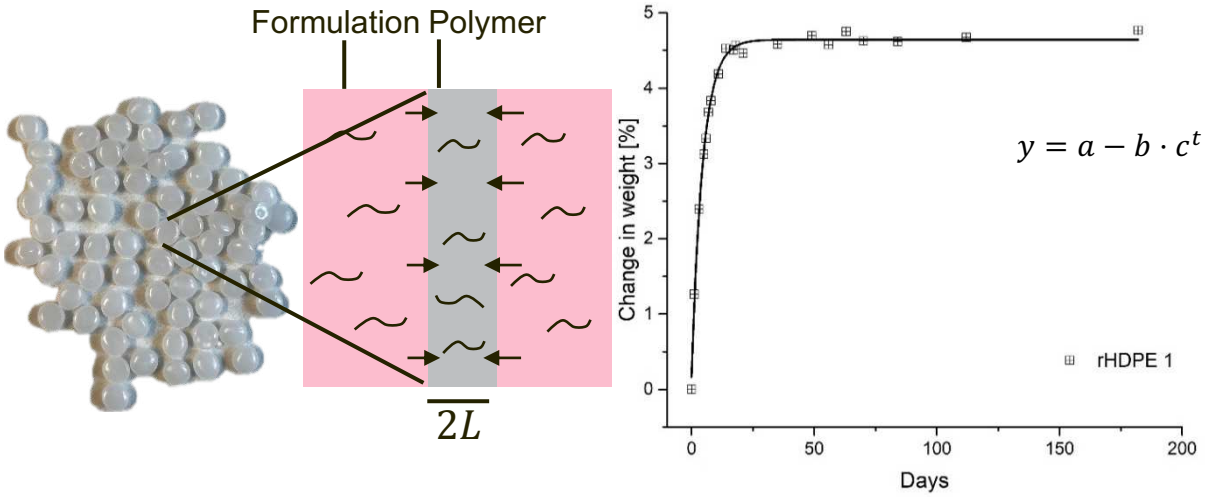

Figure 18 Graphical representation of migration from the product into the packaging material with the corresponding graph of the change in weight over time.

The migration process can be described by Fick's second law as previous shown in Equation 2. The equation can be solved to describe the migration of a substance into a polymer plate, as shown in Equation 4.

$$\frac{Y_t}{Y_\infty} = 1 - \sum_{n=0}^{\infty} \frac{G}{(2n+1)^2\pi^2} e^{\left(\frac{-(2n+1)^2\pi^2 Dt}{L^2}\right)}$$

Equation 4 Solution of the Fick's second law.

Here, Y_t describes the change in weight at a certain time point, Y_∞ represents the maximum change in weight, and G is a factor to consider the geometry of the polymer. For spherical polymers with three-dimensional radial diffusion, G is defined as 6, whereas, for a plate with the diffusion occurs primarily in one direction, G is defined as 8. L describes half the thickness of the polymer because diffusion occurs from both sides. As time increases, the summation term becomes negligibly small, leading to a simplified version Equation 5 of Equation 4, with n=1. The natural logarithm is applied to linearize the values, as shown for Equation 5:

$$\frac{Y_t}{Y_\infty} \approx 1 - \frac{A}{\pi^2} e^{\left(\frac{-\pi^2 Dt}{L^2}\right)}$$

$$\ln\left(1 - \frac{Y_t}{Y_\infty}\right) = \ln\left(\frac{A}{\pi^2}\right) - \frac{\pi^2 Dt}{L^2}$$

Equation 5 Simplification of the Fick's second law.

The values for $\ln\left(1 - \frac{Y_t}{Y_\infty}\right)$ were calculated, using parameter *a* from the asymptotic function for Y_∞. The values for Y_t are calculated with the parameters of the asymptotic function. $\ln\left(1 - \frac{Y_t}{Y_\infty}\right)$ was then plotted against t, resulting in a linear graph (Figure 19). The slope of the graph, k, represents the term $-\frac{\pi^2 D}{L^2}$.

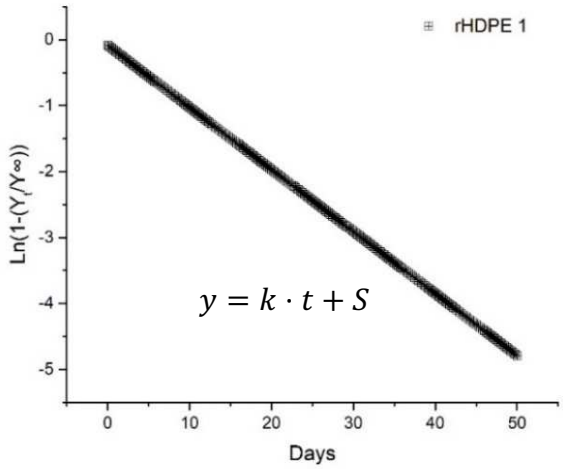

Figure 19 Linearization of the asymptotic function.

Due to variations in geometry and the surface-to-volume-ratio across all pellets, bottles, and injection moldings, a factor F was included to compare the diffusion of various shapes. Leading to the equation for D in a specific polymer x:

$$D_x = -\frac{k\, L_x{}^2 F}{\pi^2} \qquad \textbf{Equation 6} \text{ Calculation of D.}$$

with F as the ratio of surface-to-volume of the calculated polymer relative to the reference:

$$F = \frac{\frac{A_x}{V_x}}{\frac{A_R}{V_R}} \qquad \textbf{Equation 7} \text{ Calculation of F.}$$

The injection molding plate of vHDPE 1 was used as the reference. The surface-to-volume ratio was calculated and set as $\frac{A_R}{V_R} = 3.128$. For all tested materials the $\frac{A_x}{V_x}$ was calculated, and D was determined accordingly. An example of the measurement of different materials compared to the reference is shown in Figure 20.

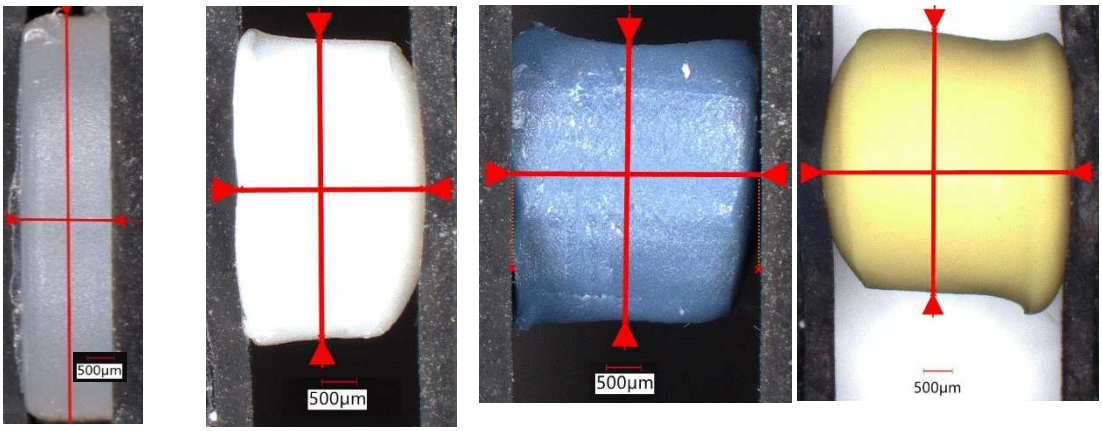

4,75 mm x 1,00 mm 4,36 mm x 2,6 mm 3,91 mm x 3,51 mm 4,23 mm x 4,49 mm

Figure 20 Dimensions of a) IM of vHDPE 1, and pellet of b) rHDPE 19, c) rHDPE 5, and d) rHDPE 13.

The influence of various properties of polymers and cosmetic components and their correlation with the migration process will be described by the Pearson correlation coefficient, Pearson's r. Pearson's r measures the direction and strength of a linear relationship between two continuous variables, with values ranging from -1 to +1. A value of -1 indicates a perfect negative linear relationship, +1 indicates a perfect positive linear relationship, and 0 signifies no correlation between the variables [71].

To analyze the impact of all properties on D, a multiple regression analysis was conducted. The resulting equation quantifies how various parameters (x) influence D, with the coefficients indicating the strength and direction (positive or negative) of the relationship between each parameter and D in one system.

$$D = \text{intercept} + \text{coefficient } 1 * x_1 + \text{coefficent } 2 * x_2 + \cdots + \text{coeffizient n} * x_n$$

Equation 8 General equation of multiple regression analysis.

3.2.3 IR spectroscopy

To identify the migrated components, Fourier Transform (FT) IR spectroscopy was performed using a Vektor 22 spectrometer (Bruker Optics GmbH & Co. KG, Ettlingen, Germany) in transmittance mode with a resolution of 2 cm^{-1}, 20 scans, and a wavenumber range of 4000 – 470 cm^{-1}. Specimens were prepared by pressing pellets in a hydraulic press mold. For visualization of the migration process, pellets were cut into 20 µm thick slices with a Cryotome CM3050 S (Leica, Wetzlar, Germany). Subsequently, they were measured with an IR microscope, Hyperion 3000 (Bruker Optics GmbH & Co. KG, Ettlingen, Germany) in transmittance mode, with a resolution of 4 cm^{-1}, an average of 20 scans and a wavenumber range of 4000-800 cm^{-1}. The microscope was equipped with a 15 X .4NA 160 mm BF objective. Absorbance units in the spectrum were mathematically normalized. Both spectrometers used the signal band of the carbonyl group of the oils in the range of 1800-1700 cm^{-1} to measure the migration into the pellets [17].

3.2.4 Differential scanning calorimetry (DSC)

For thermal analysis of the pellets, 7-20 mg was weighed and encapsulated in aluminum crucibles. An empty crucible was used as a reference. Measurements were performed on a DSC1 Stare System (Mettler Toledo, Columbus, Ohio, USA). Samples were heated from -50 °C to 250 °C at a rate of 10 K/min, then cooled back to -50 °C and reheated under the same conditions. The first heating removed thermal history from the samples, and the second heating was used to determine crystallization. Evaluations were conducted using STARe software. Therefore, enthalpy during the melting process of the second heating curve was defined and used to calculate crystallinity. According to literature, 100% crystalline PE materials have an enthalpy of

ΔH_l = 293 J/g, while PP exhibit an enthalpy of ΔH_l = 170 J/g. The degree of crystallinity χ of a sample was calculated by using Equation 9, with measured enthalpy ΔH_m and enthalpy of 100% crystalline material.

$$x = \frac{\Delta H_m}{\Delta H_l} \cdot 100$$

Equation 9 Calculation of crystallinity.

In addition, the enthalpy of the PO peaks allows the quantification of PP in HDPE. Therefore, a calibration of HDPE with 1%, 3%, 5% PP content was performed, and the enthalpy of PP determined.
Furthermore, the peak of the heating curve indicates the melting point, and the peak of the cooling curve represents the crystallization temperature. Steps within the baseline would represent the glass transition area.

3.2.5 Short chain branching (SCB) and molecular weight (MW)

To determine the MW of the POs and the amount of SCB per 1000 C atoms, samples were measured at the Fraunhofer Institute for Structural Durability and System Reliability LBF using high-temperature gel permeation chromatography with an IR detector, HT-GPC-IR5 (PolymerChar, Valencia, Spain) at 160 °C. The mobile phase was 1,2,4-trichlorobenzene (Thermo Fisher Scientific, Dreieich, Germany) with 0,5 g/L butylhydroxytoluene (Merck, Darmstadt, Germany), and a flow rate of 1 mL/min. For the stationary phase three PSS (Polymer Standards Service GmbH, Mainz, Deutschland) POLEFIN analytical linear XL columns (300 x 8.0 mm) were used. Evaluation of the results was performed with a polystyrene calibration (EasiCal PS-1, Agilent, Waldbronn, Germany) using the Software WinGPC (PSS) as well as Origin Pro. 12 mg of the samples were dissolved in 6 mL of the mobile phase and were shaken at 160 °C for one hour before injection. The sample vials were purged with nitrogen. Measurements were made in duplicate.

3.2.6 X-ray fluorescence spectroscopy (XRF)

The elemental analysis was performed with energy dispersive XRF on a SPECTRO HE (SPECTRO Analytical Instruments GmbH, Kleve, Germany). The XRF has 50W/60kV X-ray tube with four different excitation energies of <3 keV; 3 keV–6 keV; 6keV–19keV and >19 keV. A helium flush was used for lighter elements. 5 g of the samples were weighed in a 24 mm cuvette and then placed in the device for analysis. The sample cuvette rotates during the measurements to analyze different pellets and get an average result. The evaluation was performed with a SPECTRO method, "Powder (organic matrix)". Measurements were performed in duplicate.

3.2.7 Gas chromatography-mass spectrometry (GC-MS)

Beiersdorf AG analyzed volatile and semi-volatile non-intentionally added substances in POs. Volatile components were determined using DHS GC-MS, with Agilent GC 8890 with Mass Selective Detector Agilent 5977B inert plus (Agilent Technologies, Santa Clara, California, USA) and Gerstel KAS4 (Gerstel KG, Mülheim an der Ruhr, Germany). 1 g of the samples was weighed into a screw cap headspace vial, and 10 µL of a 1:10 solution of toluene-D8 (VWR Prolabo, Radnor, Pennsylvania, USA) in methanol (Merck, Darmstadt, Germany) was added as an internal standard. A 1:5 certified alkane multistandard (Sigma-Aldrich, Darmstadt, Germany) in tetrahydrofuran (Merck, Darmstadt, Germany) was used to determine retention indices. 1 µL was added to a separate headspace screw cap vial. The column with the stationary phase Restek "Rxi-624 Sil MS" and Helium gas (Air Liquid, Paris, France) for the mobile phase was used for separation. Semi-volatile components were analyzed by GC-MS, Agilent 7890 GC with 5977 MSD (Agilent Technologies, Santa Clara, California, USA), and Gerstel KAS4 (Gerstel KG, Mülheim an der Ruhr, Germany). 3 g of the sample were weighed into a screw cap glass tube, and 3 mL extraction solvent containing 95% (vol.%) ethanol and 12,85 mg/L 4,4'-difluoro biphenyl as an internal standard were added. The sample is extracted for seven days at 60 °C. A 1:5 certified alkane multistandard (Sigma-Aldrich, Darmstadt, Germany) in tetrahydrofuran (Merck, Darmstadt, Germany) was used to determine retention indices. The column Restek "Rxi-5Sil MS" as a stationary phase and Helium gas (Air Liquid, Paris, France) for the mobile phase was used for separation. The parameters used are shown in Table 5. The identification of the compounds was carried out by mass spectra and the retention indices using an internal library. Measurements were performed in triplicate.

Table 5 GC-MS parameter for the measurements of volatile and semi-volatile components.

Parameter	Volatiles	Semi-volatiles
	Agilent GC 8890	**Agilent 7890 GC**
Injector	Mode: PTV Solvent Vent, Switched Purge Flow to Split Vent: 10 mL/min at 0.02 min Vent 80 mL/min 19.654 psi until 0.01 min	Injection volume 1 µL 40 °C, hold for 0.1 min 12 °C/s - 280 °C 280 °C, hold for 5 min Split: 10:1, Flow 10 mL/min
Carrier gas	He, 1.2 mL/min	Helium, Fluss: 1.0 mL/min
Column	Restek “Rxi-624 Sil MS”, 60 m x 0.25 mm id, 1.4 µm df	Restek Rxi-5Sil MS, 30 m x 0.25 mm id, 0.5 µm df
Oven	40 °C, hold for 2 min 10 °C/min – 280 °C 280 °C hold for 30 min	40 °C for 2 min 5 °C/min till 100 °C 7 °C/min till 150 °C 10 °C/min till 280 °C 280 °C for 12 min 80 °C/min till 320 °C 320 °C for 15 min
Transferline	280 °C	270 °C
	Agilent 5977B	**Agilent MS 5977B**
MS source	230 °C	230 °C
MS Quad	150 °C	150 °C
Scan area	Scan 35 – 300 amu	35-550 amu
	Dynamic Headspace	
Incubation T	110 °C	
Incubation Time	2 min, Agitation 10 s On, 1 s Off, 500 rpm	
Trapping	2 L at 100 mL/min, Trap 40 °C	
Drying	0.2 L at 100 mL/min, Trap 60 °C	
	Thermodesorption	
Initial T Delay Time Initial Time Ramp 1 Rate 1 End Temp 1 Ramp 2 Rate 2 End Temp 2	50 °C 0.5 min 1 min 80.0 °C/min 200 °C 100.0 °C/min 280 °C for 3 min	
Transfer T Desorption Mode	280 °C Splitless	

3.2.8 Thermogravimetric analysis (TGA)

TGA was performed to determine the thermal stability using a DSC1 STARe System (Mettler Toledo, Columbus, Ohio, USA). 12-15 mg of the samples were weighed. Measurements were performed under a constant heating rate of 10 K/min from 25 °C to 850 °C in air. The remaining residue was determined in the minimum weight.

3.2.9 Microscope

Images of the pellets were made with a VHX Digital Microscope (Keyence Deutschland GmbH, Hannover, Germany). To capture the microscopic images of the pellets a magnification of 50-fold was used.

3.2.10 Nuclear magnetic resonance (NMR) measurements

To analyze the migrated components, the pellets were extracted with chloroform for 24 hours. The extract was measured on a NMR spectrometer, Spinsolve 80 Carbon ULTRA (Magritek GmbH, Aachen, Germany). ^{1}H decoupling measurements were performed in chloroform with a 5 mm probe at 24 °C. Tetramethylsilane was used as a reference with a signal at 0 ppm, and the solvent signal was noticed at 7.25 ppm.

3.2.11 Contact angle

Contact angle measurements were performed on a DSA30S Drop Shape Analyzer (Krüss GmbH, Hamburg, Germany). A 2 µL droplet of was applied on the PO surface, and the angle was measured over 20 seconds. Evaluation was performed with Krüss Advance software. Measurements were performed five times, and results were averaged.

3.2.12 Emulsion preparation

Emulsions were produced at a 500 g scale. The composition of the different emulsions is provided in Table 6. The oil-soluble emulsifier was mixed in the oil phase, and the water-soluble emulsifier was dissolved in water at 80 °C. The water phase was added to the oil phase while stirring at 100 rpm for 2 minutes at 80 °C on an RZR 2102 control (Heidolph Instruments GmbH &Co, Schwabach, Germany). The emulsion was homogenized in a Homozenta (Zehnder AG, Gränichen, Switzerland) and stirred for

another 10 minutes at 70 rpm. After a further homogenization step, the emulsion was stored at room temperature. To further reduce the droplet size, some emulsions were processed with a high-pressure homogenizer, PandaPLUS 2000 (GEA, Duesseldorf, Germany), at 900 bar. The composition of the different emulsions is shown in Table 6. Thereby, Lipid 1 indicates isopropyl palmitate, Lipid 2 indicates C12-C15 alkyl benzoate, and Lipid 3 butylene glycol dicaprylate/dicaprate. Sodium cetearyl sulfate was used as an emulsifier in a), diisostearoyl polyglyceryl-3 dimer dilinoleate as an emulsifier in b), glyceryl stearate SE for c), and polyglyceryl-4 diisostearate/polyhydroxystearate/sebacate for d). Thickening emollients were cetyl alcohol in e), tetradecyl tetradecanoate for f), and cetyl palmitate for g). A mixture of citric acid, sodium citrate, potassium sorbate, and magnesium sulphate were used for pH adjustment and as a preservative.

Table 6 Composition of the lipid mixtures, W/O and O/W emulsions.

Mixture/ Emulsion	Water	Lipid 1	Lipid 2	Lipid 3	Emulsifier 1	Emulsifier 2	Thickening Emollient	Salt
M1	-	50%	50%	-	-	-	-	-
M2	-	50%	-	50%	-	-	-	-
E1	88%	10%	-	-	0.36% a	1.64% c	-	-
E2	86%	10%	-	-	0.71% a	3.29% c	-	-
E3	84%	10%	-	-	1.06% a	4.94% c	-	-
E4	86%	10%	-	-	0.40% a	1.60% c	2% e	-
E5	84%	10%	-	-	0.79% a	3.21% c	2% e	-
M3	-	96%	-	-	-	-	4% e	-
E6	86%	10%	-	-	0.40% a	1.60% c	2% f	-
E7	84%	10%	-	-	0.79% a	3.21% c	2% f	-
M4	-	96%	-	-	-	-	4% f	-
E8	76%	18%	-	-	1.00% b	1.00% d	2% g	2%
E9	88%	-	10%	-	0.36% a	1.64% c	-	-
E10	86%	-	10%	-	0.71% a	3.29% c	-	-
E11	84%	-	10%	-	1.06% a	4.94% c	-	-
E12	86%	-	10%	-	0.40% a	1.60% c	2% e	-
E13	84%	-	10%	-	0.79% a	3.21% c	2% e	-
M5	-	-	96%	-	-	-	4% e	-
E14	86%	-	10%	-	0.40% a	1.60% c	2% f	-
E15	84%	-	10%	-	0.79% a	3.21% c	2% f	-
M6	-	-	96%	-	-	-	4% f	-
E16	76%	-	18%	-	1.00% b	1.00% d	2% g	2%

3.2.13 Droplet size

The average droplet size was determined by laser diffraction using a Mastersizer 3000 (Malvern Panalytical, Malvern, UK). Measurements were performed in triplicate, and an average droplet size was calculated.

3.2.14 Surface tension

Tension measurements were performed on K100 tensiometer (Krüss GmbH, Hamburg, Germany) using the Wilhelmy plate method, set at an immersion depth of 3.0 mm at temperatures of 25 °C, 40 °C, and 66 °C with an average of 20 values. The tensiometer range is 1−1000 $mN \cdot m^{-1}$ with 0.01 resolution. Calibration was performed with distilled water.

3.2.15 Density

Measurements were performed with a DMA 4500 (Anton Paar AG, Graz, Austria) using the flexural resonator system. Samples were measured in quintuplicate at 25 °C, 40 °C, and 66 °C with a deviation of less than 0.2%. Calibration was performed at atmospheric pressure using dry air and pure water.

3.2.16 Viscosity

Viscosity measurements were performed on the rheometer ARES 6 (TA Instruments, New Castle, Delaware, USA) with shear rates from log 10 to 1000 s^{-1} with five points per decade, at 25 °C, 40 °C, and 66 °.

4 Results and discussion

4.1 Migration influenced by cosmetic components

4.1.1 Identification of migrating components

For migration analysis, IR spectroscopy was performed to differentiate and identify various polymers and cosmetic components. Thereby, packaging materials before migration was used as a reference to verify the migration of cosmetic components into PO materials by IR spectroscopy. Figure 21 illustrates the IR spectrum of vHDPE 1 in black, which does not show an IR absorption band between 1800-1700 cm^{-1}. The red graph represents the vHDPE 1 after 14 days incubation in isopropyl palmitate. After the lipid migrated into the material, an increasing carbonyl signal at 1730 cm^{-1} can be observed and was used to identify the migration of the components.

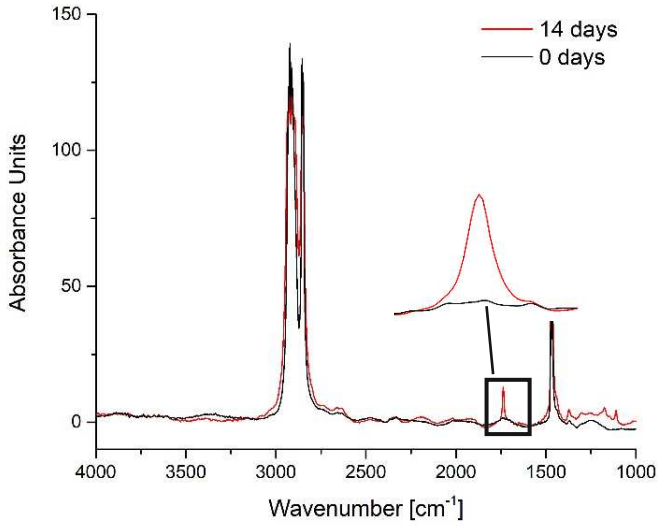

Figure 21 IR spectrum of vHDPE 1 (black) and vHDPE 1 incubated in isopropyl palmitate (red) after 14 days, at the wavenumber range of 1800-1700 cm^{-1}.

4.1.2 Migration measurement

In addition to identifying migration through IR spectroscopy, the diffusion process can be monitored and quantified for various components by measuring the change in weight of the polymer's specimens over time. Initially, the migration process was observed in virgin POs. All materials exhibited migration over time, characterized by an increase in weight change until saturation was achieved, as illustrated in Figure 22 a). Notably, certain materials, such as vLLDPE 1, reached maximum saturation (MS) significantly faster than others, such as vPP 1. The linearization of the data (according to Fick's second law, Equation 5) yielded various graphs with differing slopes, as shown in Figure 22 b). Consequently, vLLDPE 1 and vLDPE 1 exhibited the steepest slopes, indicating the highest D relative to vPP 1. A comparison of the weight change in the graphs presented in Figure 22 a) reveals that vPP 1 demonstrate the highest oil uptake, in contrast to the rapid oil migration observed in vLLDPE 1 and vLDPE 1.

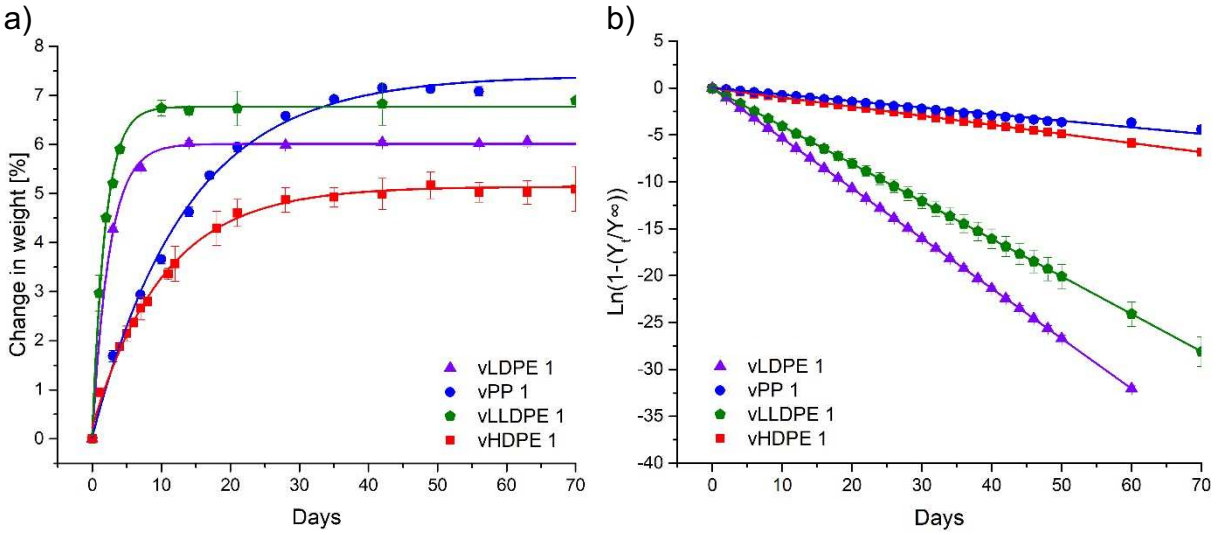

Figure 22 Migration of isopropyl palmitate at 40 °C into virgin POs, plotted as time against change in weight as a) asymptotic function and b) linearized function.

To gain a comprehensive understanding of the migration process and in order to differentiate among materials, it is essential to closely examine the migration conditions and polymer properties, as well as to expand the sample range to recycled materials. Recycled materials represent a sustainable option for future packaging and possess distinct properties compared to virgin materials, which can enhance our understanding of migration processes. Consequently, two recycled HDPE samples were analyzed and compared to two virgin samples, as illustrated in Figure 23. All samples exhibited

similar oil uptake and migration speeds for isopropyl palmitate. However, the variation in slope observed in Figure 23 b) indicates differing D among the samples, with rHDPE 1 and rHDPE 4 demonstrating substantially higher values than vHDPE 1 and vHDPE 2. This confirms that measuring the change in weight over time and determining the Ds of each sample will provide deeper insights into the migration processes of various POs, the migrating components, and the conditions involved, which will be further explored in the subsequent chapters.

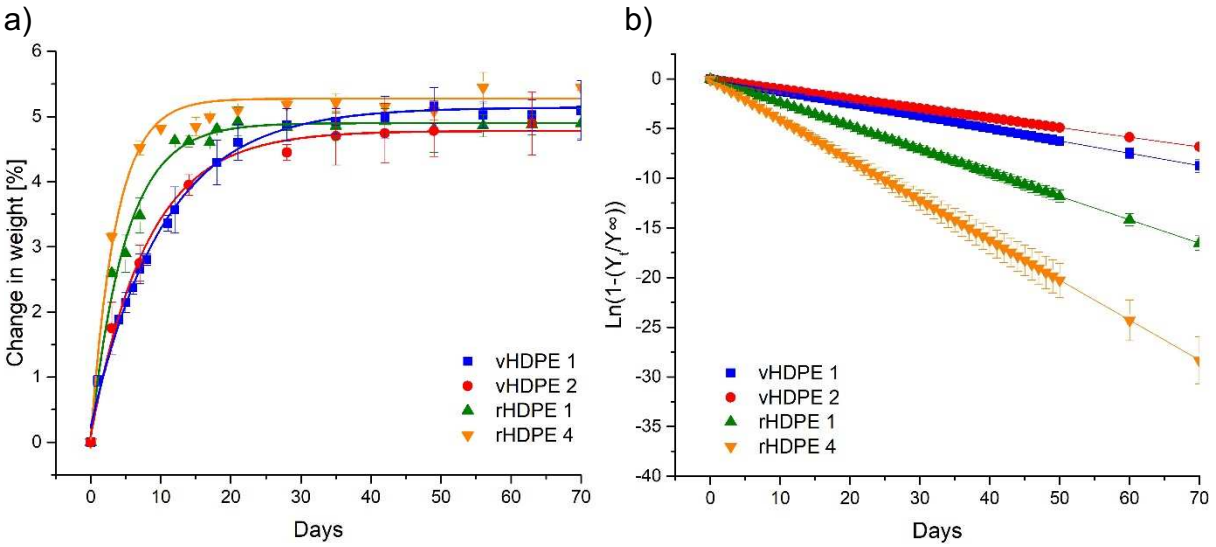

Figure 23 Migration of isopropyl palmitate at 40 °C into virgin and recycled HDPE plotted as time against the change in weight as a) an asymptotic function and b) a linearized function.

4.1.3 Influence of temperature on migration process

As seen in many cases before, diffusion is temperature-dependent, leading to the assumption that the migration of cosmetic components into polymers increases with higher temperatures [72]. For analysis of migration behavior at different temperatures, it must be considered that the properties of the lipid change with temperature (Table 7). As the temperature increased from 23 °C to 40 °C and subsequently to 66 °C, the viscosity decreased from 7 to 2 mPa*s. This reduction in viscosity, accompanied by decreased intermolecular interactions, enhances the flow of the component, resulting in accelerated migration. Additionally, higher temperatures provide more kinetic energy to the oil molecules, which promotes faster movement, leading to an increased diffusion within the plastic material. Further, a slight decrease in density and surface tension was observed. The density is correlating negatively with the temperature and decreases by 5 % from 25° to 55° [73, 74].

Table 7 Properties of isopropyl palmitate at 25 °C, 40 °C, and 66 °C.

T [°C]	η [mPa*s]	Density [g/cm^3]	Surface tension [mN/m]
25	7.0	0.853	28.90
40	4.5	0.838	27.53
66	2.5	0.819	25.59

The influence of temperature differences on polymeric materials is negligibly small within the specified range of measurement temperatures from 23 °C to 66 °C. These temperatures remain significantly below the melting temperature and well above the glass transition temperature of the polymers, as shown in Table 2. Considering the thermal expansion coefficient of HDPE, which ranges from 1.5 *10^{-4} to 2.3*10^{-4}/°C [75], an estimated volume increase of approximately 0.8% can be anticipated for vHDPE 1 when transitioning from 23 °C to 66 °C. This 0.8% increase in available space within the polymer chains would theoretically permit only an additional 0.04% of oil to migrate, if the maximum saturation of vHDPE 1 would have been 5 % before. PP with an even lower thermal expansion coefficient of 1.05 *10^{-4}/°C leads to even less oil that would migrate [76]. Consequently, it can be concluded that alterations in the molecular structure of the polymers will not significantly influence migration behavior within this temperature range.

The increase in oil movement with rising temperatures was also observed in the migration analysis for two HDPE and two PP materials at 23 °C, 40 °C, and 66 °C — temperatures commonly used in emulsion stability testing (Figure 24).

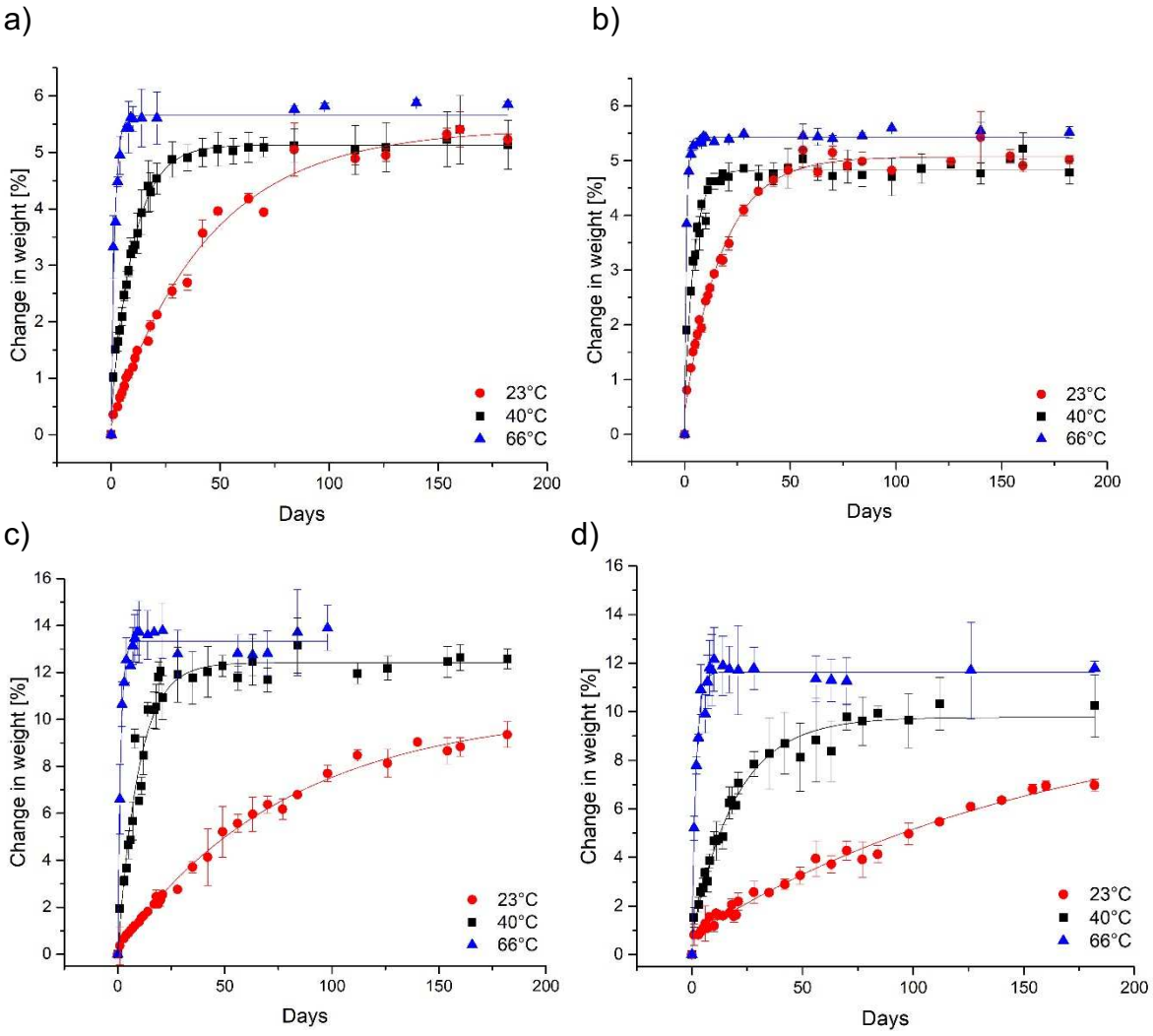

Figure 24 Change in weight over time after the migration of isopropyl palmitate at 23 °C, 40 °C and 66 °C into a) vHDPE 1, b) rHDPE 1, c) vPP 2, and d) rPP 2.

The four selected samples showed similar MS levels of isopropyl palmitate at different temperatures (Figure 24). For the HDPE materials, the MS is observed around 4.5-5.5% across all temperatures, while for PP, the MS reaches values up to 13%. Given the minimal changes in molecular structure across the three measured temperatures, it can be inferred that the MS would remain relatively constant within a single PO type. Notably, in Figure 24 d), rPP 2 demonstrates a higher MS for 66 °C, approaching 12% compared to almost 10% MS at 40 °C. While specific data on the thermal expansion coefficient for rPP 2 is not available, it can be reasonably assumed to be higher than that of the other polymer types, leading to an increased available

space within the polymer matrix. Additionally, the significant deviation observed at different time points indicates a notable degree of inhomogeneity within this PO material. This variability may further influence the migration behavior and overall performance of rPP 2 under varying thermal conditions. A deeper insight into the variations of the MS of different POs is given in chapter 4.2.1.

In contrast to the MS, significant variations of D can be observed at different temperatures within a sample. For all samples, D increases with rising temperature, as displayed in Table 8. Thereby supporting the hypothesis of enhanced molecular movement due to higher kinetic energy, less intermolecular interactions, and lower viscosity with increasing temperature. Within the PO materials, differences can be observed. In HDPE, the PCRs rHDPE 1 and rHDPE 3 exhibit higher D at all temperatures compared to vHDPE 1, with the greatest differences for rHDPE 3, ranging from 9 mm^2/day at 23 °C to 990 mm^2/day at 66 °C, while vHDPE 1 shows values of 2.97 mm^2/day at 23 °C to 64 mm^2/day at 66 °C. The PP materials, on the other hand, would also exhibit an increase in D with rising temperature but has higher D values for the virgin than the recycled materials. Comparing PP and HDPE materials, D at 23 °C and 40 °C of PP is similar to the virgin HDPE, while the 66 °C PP is higher than the vHDPE 1. Conversely, vLDPE 1 display much higher D at all temperatures than vHDPE 1, with an increase of D with temperature.

These findings indicate that each PO behaves differently, yet all exhibit an increase in D with higher temperatures. In the following experiments, all measurements were conducted at 40 °C to yield more precise values, as this temperature allows for a reasonable migration rate while still achieving maximum saturation within a manageable timeframe. The differences among the POs will be further analyzed in chapter 4.2.

Table 8 D in * 10^{-3} mm^2/day of isopropyl palmitate after migration into different virgin and recycled materials at 23 °C, 40 °C and 66 °C.

Pellet	23 °C	40 °C	66 °C
vHDPE 1	2.97 ± 0.63	10 ± 1	64 ± 9
rHDPE 1	4.8 ± 0.4	19 ± 2	89 ± 5
rHDPE 3	9 ± 1	40 ± 5	990 ± 150
vPP 2	1.43 ± 0.48	12 ± 3	100 ± 10
vPP 4	1.23 ± 0.08	9.97 ± 0.93	136 ± 1
rPP 1	0.46 ± 0.02	10.37 ± 0.86	77.20 ± 0.53
rPP 2	1.16 ± 0.59	6.21 ± 0.58	50 ± 10
vLDPE 1	9 ± 2	45 ± 3	110 ± 18

4.1.4 Comparison of different cosmetic components

Previous chapters analyzed the migration in POs and different temperatures for isopropyl palmitate. To thoroughly analyze migration behavior, it is essential to understand how the properties of the migrating substances influence the process. To this end, various mineral oil-based and natural oils, and as a fragrance compound, the monoterpene limonene, were evaluated for migration, as these substances are commonly found in different emulsions. It can be assumed that the structural characteristics and resulting properties, such as polarity, molecular size, and physical properties, impact the migration process. Figure 25 illustrates the migration of ten cosmetic components in one virgin and one recycled material. The influence of the chemical nature of the components is shown in Table 9, which summarizes the saturation values, D, and some physicochemical characteristics of the tested compounds.

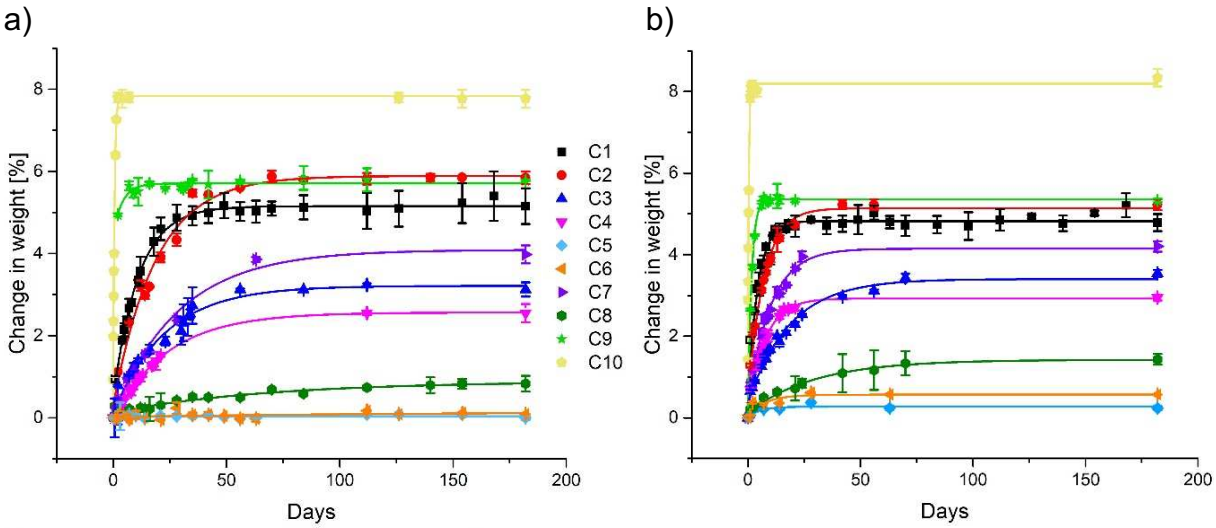

Figure 25 Migration of different components in a) vHDPE 1 and b) rHDPE 1, C1-C10 indicating the components listed in Table 5.

The migration of the ten cosmetic components has exhibited different behavior. While component C1 (limonene) demonstrates a high saturation level in both materials, C3 (butylene glycol dicaprylate/dicaprate) shows a relatively slow migration and lower saturation levels. Conversely, C5 (castor oil) does not migrate at all. A more detailed analysis of the migration behavior and the characteristics of the components is presented in Table 9 and discussed further.

Table 9 Properties of the migrating components into six different samples at 40 °C [77-80].

Name	Substance	η * at 20 °C [mPa*s]	MW* [g/mol]	Vm* [cm³/mol]	RI*	D * 10⁻³ [mm²/day]						MS [%]					
						vHDPE 1	rHDPE 1	rHDPE 3	vLDPE 1	vPP 2	rPP 5	vHDPE 1	rHDPE 1	rHDPE 3	vLDPE 1	vPP 2	rPP 5
C10	Limonene	1	136	162	1022	166.25 ± 0.75	211 ± 5	383 ± 3	424 ± 8	214 ± 2	220 ± 40	8.1 ± 0.2	8.3 ± 0.2	8.3 ± 0.2	16.1 ± 0.1	27.1 ± 0.6	20.0 ± 0.2
C9	Dicaprylyl ether	3	242	300	1657	22 ± 7	50 ± 1	39 ± 5	204 ± 7	30 ± 3	21.25 ± 0.59	5.7 ± 0.1	5.4 ± 0.1	7.3 ± 0.3	5.9 ± 0.9	16.3 ± 0.3	13.5 ± 0.1
C1	Isopropyl palmitate	7	300	352	1980	10 ± 1	19 ± 2	40 ± 5	45 ± 3	12 ± 3	8.91 ± 0.63	5.0 ± 0.2	4.8 ± 0.2	4.5 ± 0.1	5.6 ± 0.4	12.0 ± 0.1	11.3 ± 0.5
C2	C12-C15 alkyl benzoate	13	311	334	2168	5.8 ± 0.6	14 ± 1	27 ± 1	38 ± 1	5.45 ± 0.45	4.03 ± 0.06	5.4 ± 0.3	4.9 ± 0.1	4.6 ± 0.1	5.7 ± 0.1	7.5 ± 0.1	9.5 ± 0.1
C8	Caprylic/capric triglyceride	25	500	529	2958	1.19 ± 0.53	2.82 ± 0.87	2.07 ± 0.13	5.15 ± 0.09	3.06 ± 0.93	4.55 ± 0.79	1.3 ± 0.4	1.4 ± 0.6	2.0 ± 0.1	1.5 ± 0.1	2.5 ± 0.9	1.9 ± 0.8
C3	Butylene glycol dicaprylate/dicaprate	11	687	749	2484	2.81 ± 0.11	7 ± 2	12.43 ± 0.52	25 ± 1	2.06 ± 0.04	3.00 ± 0.07	2.7 ± 0.4	2.3 ± 0.4	2.8 ± 0.1	2.7 ± 0.2	7.8 ± 0.1	7.4 ± 0.1
C7	Paraffinum oil LV/669	27	382	449	-	2.63 ± 0.05	9 ± 2	7.97 ± 0.17	13.37 ± 0.08	2.06 ± 0.07	5 ± 2	4.2 ± 0.1	4.2 ± 0.1	4.7 ± 0.1	7.2 ± 0.1	12.2 ± 0.3	4.3 ± 0.9
C4	Paraffinum liquidum N 32	59	427	495	-	3.28 ± 0.54	11 ± 2	6.44 ± 0.31	30 ± 4	9.95 ± 0.36	19 ± 3	2.6 0.2	3.0 ± 0.1	4.3 ± 0.1	6.1 ± 0.4	3.5 ± 0.3	1.8 ± 0.1
C5	Castor oil	712	300	313	-	0	0	0	0	0	0	0	0	0	0	0	0

C6	Sunflower oil	55.0	-	-	-	0.05 ± 0.01	8 ± 2	3.7 ± 0.2	5 ± 1	2.38 ± 0.12	6.49 ± 0.77	0.39 ± 0.05	0.57 ± 0.01	0.87 ± 0.05	0.55 ± 0.04	0.25 ± 0.02	1.18 ± 0.09

*Symbols indicating viscosity (η), molecular weight (MW), molar volume (Vm), and retention index (RI) on a non-polar column.

Among the compounds tested, limonene (C10) exhibited the highest D and MS across all PO materials, followed by dicaprylyl ether (C9), then isopropyl palmitate (C1) and C12-C15 alkyl benzoate (C2), which exhibit similar MS values. The lowest D values were determined for the components caprylic/capric triglyceride (C8), butylene glycol dicaprylate/dicaprate (C3), paraffinum oil LV/669 (C7), and paraffinum liquidum N 32 (C4), while sunflower (C6) and castor oil (C5) exhibited minimal or no migration. When examining the oil uptake of the components in virgin and recycled polymers, the migration processes remain qualitatively consistent. For instance, isopropyl palmitate achieves approximately 5.0% oil uptake in each HDPE material. In LDPE, the oil uptake is slightly higher at 6.1%, while PP exhibits the highest oil uptake, reaching 12.0% and 9.0% in different samples. This trend is consistent across other components, which display similar oil uptake within the PO materials, with PP consistently showing higher oil uptake. Analyzing D values across different materials, it can be seen they are more inconsistent. HDPE materials, mainly virgin HDPE shows lower D values than PCR, but also, within the recycled HDPEs, there are great variations. For example, isopropyl palmitate shows D values of 10 mm^2/day in vHDPE 1, 19 mm^2/day in rHDPE 1, and 40 mm^2/day in rHDPE 3. In the virgin LDPE material, migration is the fastest for all components, for example isopropyl palmitate with 45 mm^2/day, compared to the other POs, while the oil uptake is similar to that of HDPE. The virgin and recycled PP materials have the highest oil uptake, while D is often the lowest. All those differences within the POs will be further discussed in section 4.2.1.

The differences among the components are based on their properties. Firstly, the molecular size displays a negative correlation with D and MS, which is defined by the MW and the Vm of the molecule. Limonene, with a MW of 136 g/mol and a Vm of 162 cm^3/mol, is very compact, facilitating almost unhindered migration into the polymer, with a D of $166.25*10^{-3}$ mm^2/day and a MS of 8,1% in vHDPE 1. In comparison, isopropyl palmitate has a lower MS (5%) and D ($10*10^{-3}$ mm^2/day), with a MW of 300 g/mol and a Vm of 352 cm^3/mol, while butylene glycol dicaprylate/dicaprate exhibits even lower values for D at $2.81*10^{-3}$ mm^2/day and MS at 2.7%, due to high values for MW at 687 g/mol and Vm at 749 cm^3/mol. This indicates that larger and bulky molecules, such as triglycerides, hinder smooth diffusion through the polymer chains, leading to reduced D and MS values.

Secondly, D is increasing with decreasing viscosity of the component. Limonene, with a viscosity of 1 mPa*s compared to castor oil with 712 mPa*s confirms the aspects described in the previous chapter regarding lower viscosity values due to reduced interactions, which offer less resistance and diffuse more quickly.

Thirdly, polarity of the components influences the strength of the interaction with the polymer. The polarity of components can be determined on the one hand using retention indices (RI) obtained during GC-MS measurements, which describe the interaction of an analyte with the non-polar column. Thus, high values indicate a strong interaction of a non-polar molecule with the non-polar column, while low values describe a weak interaction that is more typical of polar molecules [81]. POs are highly non-polar polymers, which primarily interact with non-polar components. Limonene possesses an RI of 1022, compared to isopropyl palmitate with an RI of 1980, followed by butylene glycol dicaprylate/dicaprate with an RI of 2484. In contrast, polar solvents such as water and ethanol exhibit minimal interaction with POs, with RIs of 317 and 459, respectively [1, 82, 83].
On the other hand, polarity can be visualized by the contact angle, which describes the wettability of the material, and the adhesive bonding of a component on the material's surface. Therefore, the contact angle of various components was measured on the surface of POs (Figure 26).

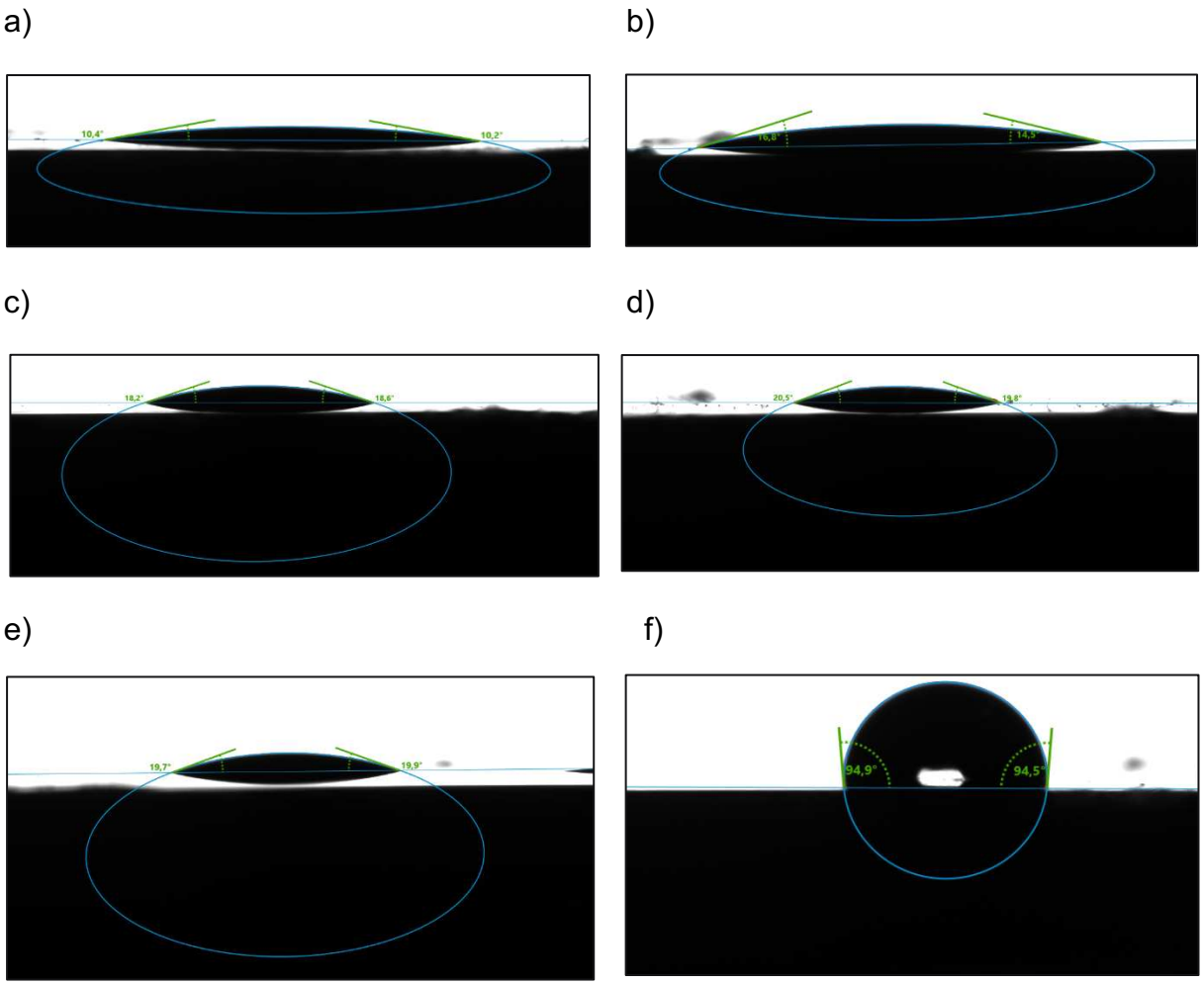

Figure 26 Contact angle of a) dicaprylyl ether, b) isopropyl palmitate, c) caprylic/capric triglycerid, d) paraffinum liquidum N 32, e) sunflower oil, and f) destilled water on top of vHDPE 1.

Comparing the images of the component droplets on vHDPE 1, it is evident that all oil droplets (Figure 26 a-e) exhibit the high affinity on the surface, while the water droplet in Figure 26 f retains a spherical shape The measured values are presented in Table 10.

Table 10 Contact angles of various components on different POs in ° ordered by increasing D of the components in vHDPE 1 (left to right) and isopropyl palmitate in different POs (top to bottom).

Pellet	Water	Sun-flower oil	Paraffinum liquidum N 32	Caprylic/ capric triglycerid	Isopropyl palmitate	Dicaprylyl ether
vPP1	92	33	22	25	29	10
rPP1	91	38	27	22	19	11
vHDPE 1	94	19	21	23	17	9
rHDPE 2	99	29	23	21	15	11
rHDPE 1	98	25	23	20	19	12
vLLDPE 1	91	27	24	20	15	11
vLDPE 1	99	32	17	18	14	9
rHDPE 3	90	28	20	18	14	12

Increase in D

Polar molecules, such as water, exhibit high contact angles (90° to 99°) on POs, indicating low surface affinity. In contrast, non-polar oils demonstrate low contact angles (<20°), signifying high affinity, wettability, sorption, and accelerated migration. However, PP exhibits higher contact angles for oil components compared to PE, resulting in weaker oil affinity and, consequently, slower D [84]. Figure 27 confirms that smaller contact angles result in higher D, with a negative Pearson correlation factor of -0.64.

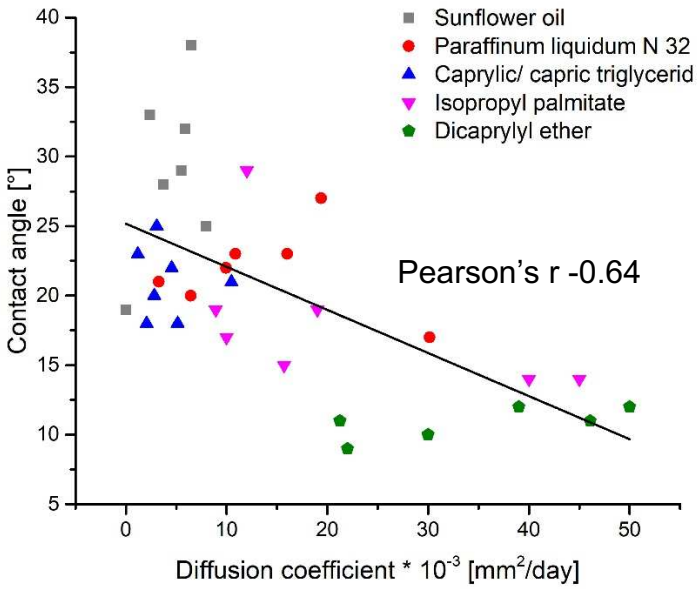

Figure 27 Correlation of contact angle and D.

Further properties of the components, such as density, spreadability, and surface tension, are given in the supporting material section in Table 34. The Pearson's r of all properties of the components, and D of vHDPE1 are shown below.

Table 11 Pearson's r of component properties correlation.

	D	η	MW	Vm	RI	ρ	Spreadability
Surface tension	-0.43	0.69	-0.08	-0.14	0.34	0.45	-0.80
Spreadability	0.36	-0.74	-0.16	-0.12	-0.68	-0.59	
ρ	-0.07	0.22	0.33	0.27	0.37		
RI	-0.81	0.92	0,82	0.80			
Vm	-0.59	0.99	-0,18				
MW	-0.59	-0.12					
η	-0.19						

*Pearson's r: +1: positive correlation; -1: negative correlation; 0: no correlation; diffusion coefficient (D) of vHDPE 1, viscosity at 25 °C (η), molecular weight (MW), maximum saturation (MS), molar volume (Vm), density at 25 °C (ρ), surface tension at 25 °C, and retention index (RI) on a non-polar column.

The heatmap presented in Table 11 illustrates a negative correlation of D with RI (-0.81), Vm (-0.59), and MW (-0.59). In contrast, the Pearson correlation coefficient for viscosity is notably lower at -0.19, indicating a lack of linear correlation with D; instead, viscosity exhibits an exponential relationship (Figure 28). Furthermore, the parameters analyzed show intercorrelations, as evidenced by the observation that spreadability increases with decreasing surface tension, lower viscosity, and enhanced non-polar characteristics.

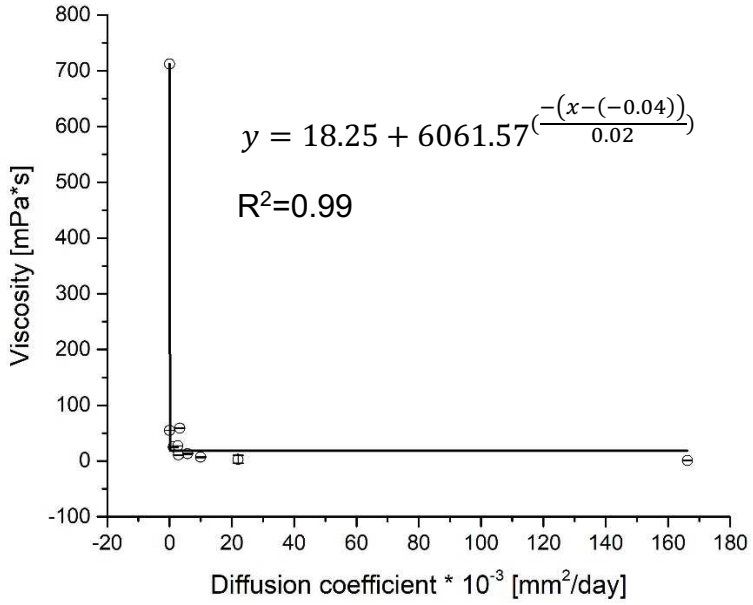

Figure 28 Correlation of viscosity at 25 °C and D of vHDPE 1.

4.1.5 Migration of component mixtures

Cosmetic emulsions usually comprise more than one emollient, making it essential to know how they mutually affect each other's migration. To this end, two mixtures of isopropyl palmitate plus C12-C15 alkyl benzoate (M1), and isopropyl palmitate plus butylene glycol dicaprylate/dicaprate (M2) were prepared. As expected, migration can be seen by the weight gain of the two HDPE samples, vHDPE 1 and rHDPE 1 (Figure 29).

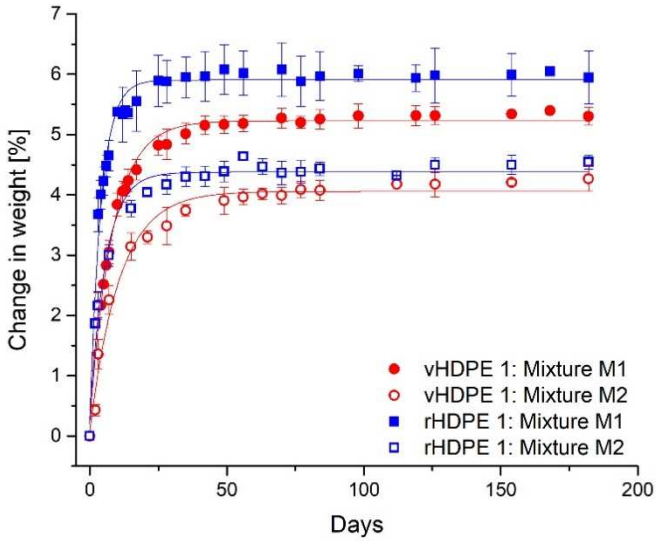

Figure 29 Change in weight over time after migration of Mixture M1 (isopropyl palmitate + C12-C15 alkyl benzoate) and M2 (isopropyl palmitate + butylene glycol dicaprylate/dicaprate) at 40 °C in vHDPE 1 and rHDPE 2.

However, it is impossible to distinguish between the different oils in the mixture and quantify the amount of the individual oils that migrated. Therefore, migration was followed by an IR microscope to distinguish between the two components (Figure 31). To obtain comparable results, the absorption was measured for both oils individually. In Figure 30, the IR spectrum of vHDPE 1 is shown after isopropyl palmitate and C12-C15 alkyl benzoate migrated for 28 days, at which point saturation was reached. The change in weight was measured at 5% for isopropyl palmitate and 5.4% for C12-C15 alkyl benzoate.

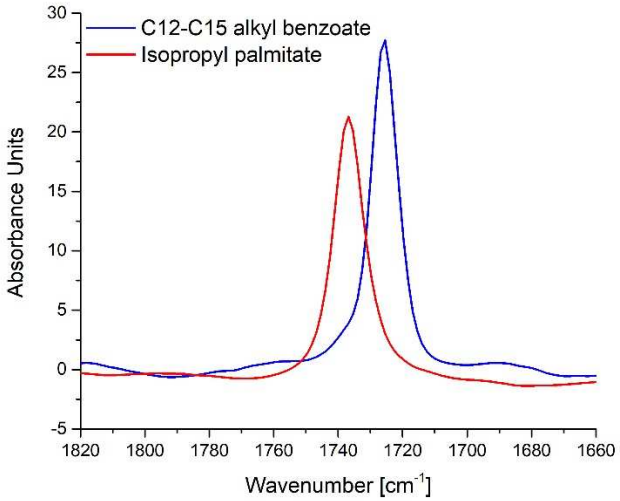

Figure 30 IR spectrum of vHDPE 1 incubated at 40°C in isopropyl palmitate (red) and C12-C15 alkyl benzoate (blue) after 28 days, at the wavenumber range of 1820-1660 cm^{-1}.

Both oils exhibit similar absorption characteristics, and the distinction between the two components can be made due to specific wavenumbers of their carbonyl absorption bands. Isopropyl palmitate displays a characteristic band ranging between 1725-1750 cm^{-1}, whereas C12-C15 alkyl benzoate absorbs between 1715-1732 cm^{-1}.

Using these results, the measurement of the oil mixture M1 was performed and analyzed with the IR microscope. Migration was stopped for some pellets after three, seven, 14 and 140 days and then cut into slices. Each pellet was analyzed using IR measurements to detect the carbonyl group signal, allowing for the qualification and quantification of the migrated oil and visualization of the migration process.

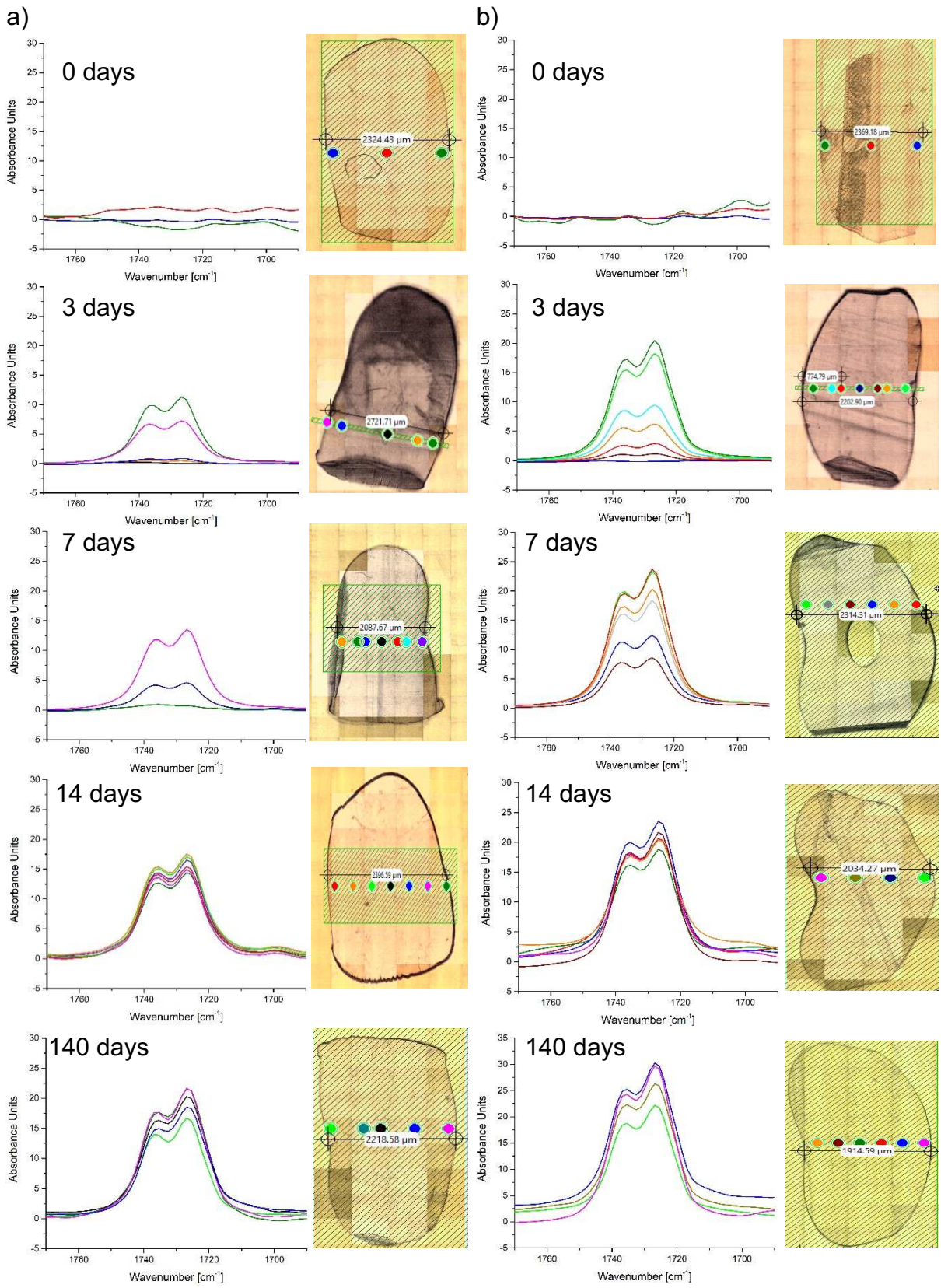

Figure 31 IR microscope images of 20 µm thick pellet slices of a) vHDPE 1 and b) rHDPE 1 at different time points of migration of isopropyl palmitate (carbonyl absorption band 1750-1725 cm^{-1}) and C12-C15 alkyl benzoate (carbonyl absorption band 1732-1715 cm^{-1}) at 40 °C into the pellet.

Notably after three days of migration, both absorption bands appear at approximately the same intensity, maintaining this same ratio even after 140 days. From this, it can be concluded that both oils migrate into the plastic pellets at the same speed and to the same extent. Further, both components migrate independently and do not displace each other. The maximum oil uptake of the pellets is approximately 5%, with equal quantities of both oils.

Color coding of the graphs and the images in Figure 31 illustrates the temporal progression of the migration process. After three days, the oils migrated 500 µm into vHDPE 1, extending to a depth of 700 µm by seven days. After 14 days, the pellet appears completely saturated with oils, and the achieved absorption intensity remains constant after 140 days.

In contrast, migration occurs much faster in rHDPE 1. After three days both oils migrated to a depth of 770 µm, reaching their saturation value by seven days with no further changes observed over 140 days. This behavior reflects that isopropyl palmitate and C12-C15 alkyl benzoate are oils demonstrating a similar D in the same material. (Table 12).

Moreover, it was of great interest to elucidate the behavior of a mixture M2, of a fast (isopropyl palmitate) and a very slow (butylene glycol dicaprylate/dicaprate) migrating oil. As indicated in Table 9, isopropyl palmitate migrates approximately three times faster than butylene glycol dicaprylate/dicaprate in the same material. Due to the overlapping wavenumbers of the carbonyl bands of both components, IR spectroscopy was not suitable for comparing the migration of this oil mixture Therefore, the pellets were extracted, and quantitative nuclear magnetic resonance (NMR) measurements were conducted on the extract (Figure 32).

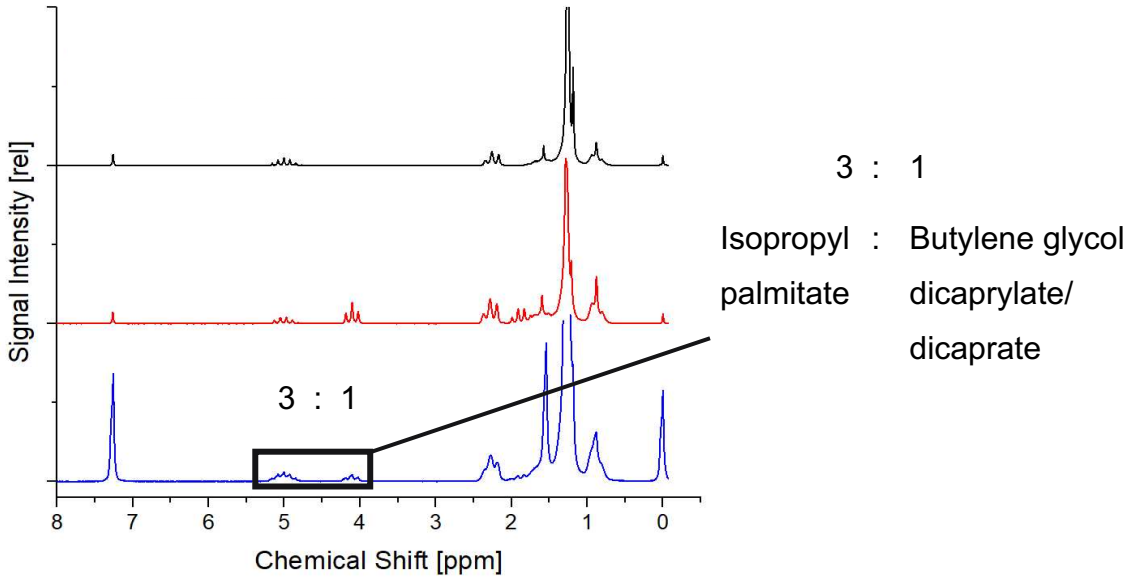

Figure 32 ^{1}H-NMR spectrum in $CDCl_3$ of isopropyl palmitate (black) and butylene glycol dicaprylate/dicaprate (red) and the mixture of both, Mixture M2 (blue) that migrated into the vHDPE 1 after 28 days.

Figure 32 demonstrates after integration of the signals that in line with D (Table 12), isopropyl palmitate was three times more abundant than butylene glycol dicaprylate/dicaprate. The D and MS have been determined for both mixtures and compared to the individual D and MS of the components in different materials.

Table 12 D and MS of plane lipids and lipid mixtures in vHDPE 1, rHDPE 1 and 3.

Migrating component	D * 10^{-3} [mm^2/day]			MS [%]		
	vHDPE 1	rHDPE 1	rHDPE 3	vHDPE 1	rHDPE 1	rHDPE 3
Lipid 1*	10 ± 1	19 ± 2	40 ± 5	5.0 ± 0.2	4.8 ± 0.2	4.5 ± 0.1
Lipid 2*	5.8 ± 0.6	14 ± 1	27 ± 1	5.8 ± 0.1	5.8 ± 0.1	6.7 ± 0.1
Lipid 3*	2.81 ± 0.11	7 ± 2	12.43 ± 0.52	3.1 ± 0.1	2.6 ± 0.1	2.0 ± 0.1
Mixture M1*	8.41 ± 0.78	18 ± 1	28 ± 5	5.1 ± 0.1	5.4 ± 0.5	6.1 ± 0.9
Mixture M2*	6.1 ± 0.7	12 ± 3	29 ± 3	4.1 ± 0.2	4.5 ± 0.2	4.9 ± 0.7

* Lipid 1: Isopropyl palmitate; Lipid 2: C12-C15 alkyl benzoate; Lipid 3: Butylene glycol dicaprylate/dicaprate; Mixture M1: 1+1 Isopropyl palmitate + C12-C15 alkyl benzoate; Mixture M2: 1+1 Isopropyl palmitate + Butylene glycol dicaprylate/dicaprate

Table 12 shows that D of the oil mixtures M1 and M2 are intermediate values to those of the individual oils. For instance, in vHDPE 1, the D of mixture M1 is $8.41*10^{-3}$ mm²/day, compared to that of pure isopropyl palmitate ($10*10^{-3}$ mm²/day) and C12-C15 alkyl benzoate ($5.8*10^{-3}$ mm²/day).

A similar pattern is observed for the MS. In vHDPE 1, the MS of the isopropyl palmitate and C12–C15 alkyl benzoate mixture (5.1%) is also an intermediate value between those of the individual oils. Since both oils have a similar molecular size, they exhibit comparable oil uptake. This implies that at 5.1% MS, the mixture in vHDPE 1 contains roughly equal amounts of both oils, as they migrate at similar speeds (Figure 31). Similar results are observed for the recycled materials as well.

When examining mixture M2, combining the very fast migrating oil isopropyl palmitate and the slow migrating oil butylene glycol dicaprylate/dicaprate, D and MS values are also intermediate between those of the individual oils in all materials. For example, in vHDPE 1, Mixture M2 reaches an MS of 4.1%, which exceeds that of pure butylene glycol dicaprylate/dicaprate (3.1%) but is lower than that of pure isopropyl palmitate (5.0%). NMR measurements (Figure 32) indicate that isopropyl palmitate migrates at approximately three times the rate of butylene glycol dicaprylate/dicaprate. Consequently, we can deduce that of the 4.1% MS in vHDPE 1, about 75% is isopropyl palmitate and 25% is butylene glycol dicaprylate/dicaprate.

The limited capacity of POs to accommodate oils means that the amount of oil that can migrate is contingent upon the size of the molecules. Specifically, larger oil molecules still migrate, but in lower quantities, because their diffusion is hindered compared to smaller molecules. In mixtures containing oils of different molecular sizes—such as isopropyl palmitate and butylene glycol dicaprylate/dicaprate—the smaller molecule (isopropyl palmitate) diffuses more rapidly and in greater quantity than the larger one (butylene glycol dicaprylate/dicaprate).

Although each oil diffuses independently, their combined migration behavior in the mixture results in an effective D that reflects an intermediate of the individual rates. This average D arises because both oils simultaneously interact with the polymer matrix, each contributing its own diffusion characteristics. The smaller and more mobile oil molecules tend to diffuse more rapidly, while the larger, more hindered molecules move more slowly. In a mixture, these differing behaviors effectively balance each other, producing a net diffusion rate.

4.1.6 Migration of oils as components of emulsions

Cosmetic final products consist of emulsifiers, stabilizers, salts, and emollients, besides water and oil phase. The interaction among all these constituents can mutually influence migration behavior. Therefore, different W/O and O/W emulsions were prepared, as shown in Table 6. The migration of plain isopropyl palmitate (black line) compared to the oil formulated in various O/W and W/O emulsions for one virgin and two recycled materials is presented in Figure 33.

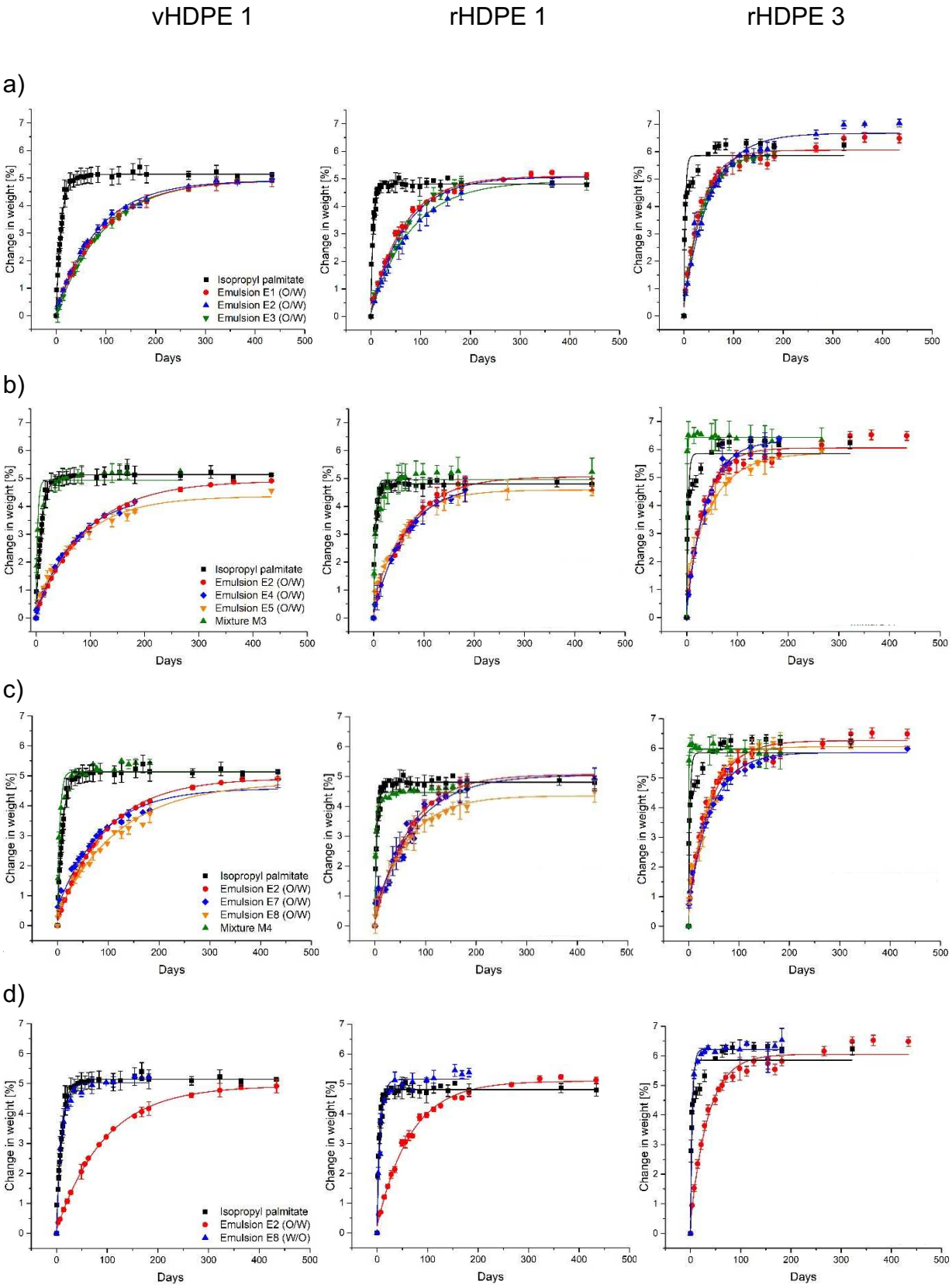

Figure 33 Migration of isopropyl palmitate into vHDPE 1, rHDPE 1 and rHDPE 3 compared to a) oil-in-water emulsions, b) and c) oil-in-water emulsions with thickening agents, and d) oil-in-water compared to water-in-oil emulsions.

Figure 33 a) illustrates the migration behavior of isopropyl palmitate from O/W emulsions (red, green, blue) compared to pure isopropyl palmitate (black). The O/W emulsions consistently show slower migration, requiring more time to reach equilibrium than the pure oil. Although these emulsions contain varying emulsifier concentrations (2% to 6%), their slopes remain similar, indicating that emulsifier concentration does not significantly influence D. Additionally, no major differences across the virgin and recycled materials can be observed. The reduced migration rate of the emulsions arises from the water phase surrounding the oil droplets, which slows the migration kinetics and delays the oil's access to the polymer surface, where it eventually spreads as a film and is absorbed [85].

Figure 33 b) and c) present O/W emulsions containing thickening agents (blue, yellow). For comparison, pure isopropyl palmitate (black), an O/W emulsion without thickener (E2, red), and an isopropyl palmitate mixture with 4% thickener (green) are shown. In row b) emulsions with different emulsifier levels (E4, blue, with 2% and E5, yellow, with 4%) and 2% cetyl alcohol show similar slopes, suggesting that the thickener does not affect the migration rate. Plain oil samples containing 4% cetyl alcohol (M3, green) also exhibit a migration pattern similar to pure oil, indicating that there is no influence of the thickener. Identical results were obtained for another thickener, tetradecyl tetradecanoate, as demonstrated in row c).

In Figure 33 d), the migration from the W/O emulsion E8 (blue) is compared to the previous pure oil (black) and O/W emulsion (E2, red). The W/O emulsion's migration curve closely matches that of pure oil, indicating significantly faster migration than that of the O/W emulsions. When further comparing virgin and recycled materials, major differences in D become apparent, with higher rates for the recycled material than the virgin. This increased migration rate is attributed to the outer oil phase in W/O emulsions, which allows direct oil contact with the packaging material and thus more rapid diffusion, unlike O/W emulsions, where the water phase impedes access to the polymer surface.

Table 13 summarizes the calculated D and MS values for all tested materials and emulsions. Across all HDPE materials, O/W emulsions yield much lower D values than pure oil or W/O emulsions. Additionally, pure oils mixed with a 4% thickener show high D values similar to W/O emulsions, highlighting the influence of the external phase in contact with the packaging wall on migration kinetics. Within a single HDPE material,

MS remains relatively consistent, showing similar values for vHDPE 1 and rHDPE 1, and a slightly higher MS for rHDPE 3.

For emulsions containing C12-C15 alkyl benzoate (E9-E16, M5-M6), a behavior similar to that observed for isopropyl palmitate is noted (Table 13), with slow migration from O/W emulsions and comparable migration rates from W/O emulsion and pure oil. When comparing the MS, high deviations can be observed, for example, the MS for vHDPE 1 ranges from 3.1% to 6.1%. The variations in MS values across the HDPE materials result from the slow migration of O/W emulsions, which do not reach saturation within the experimental timeframe. This incomplete saturation makes the asymptotic approximation of both MS and D less accurate.

Table 13 D*10^{-3} [mm^2/day] and MS of components, mixtures, and emulsions in HDPE.

Mixture/ Emulsion *	vHDPE 1		rHDPE 1		rHDPE 3	
	D	MS [%]	D	MS [%]	D	MS [%]
Isopropyl palmitate	10 ± 1	5.0 ± 0.2	19 ± 2	4.8 ± 0.2	40 ± 5	4.5 ± 0.1
E1	1.00 ± 0.03	5.0 ± 0.2	1.07 ± 0.09	4.9 ± 0.1	1.03 ± 0.03	6.0 ± 0.3
E2	1.12 ± 0.08	4.8 ± 0.2	1.25 ± 0.09	5.1 ± 0.1	1.19 ± 0.19	6.0 ± 0.1
E3	1.21 ± 0.06	4.7 ± 0.2	1.07 ± 0.07	5.3 ± 0.3	0.81 ± 0.01	6.5 ± 0.3
E4	1.21 ± 0.09	4.7 ± 0.9	1.83 ± 0.62	4.9 ± 0.1	1.20 ± 0.18	6.5 ± 0.2
E5	1.30 ± 0.13	4.0 ± 0.8	1.38 ± 0.02	4.3 ± 0.3	1.64 ± 0.71	5.7 ± 0.1
M3	10.0 ± 1.3	5.3 ± 0.5	20 ± 3	5.6 ± 0.6	33 ± 3	5.9 ± 0.5
E6	1.29 ± 0.15	4.4 ± 0.9	1.31 ± 0.42	4.8 ± 0.2	1.0 ± 0.1	6.4 ± 0.1
E7	1.06 ± 0.10	4.3 ± 0.8	1.36 ± 0.13	4.2 ± 0.2	0.98 ± 0.09	5.7 ± 0.1
M4	12.36 ± 0.99	5.2 ±0.5	21 ± 1	5.4 ± 0.1	37 ± 3	6.4 ± 0.4
E8	8.56 ± 0.75	5.1 ± 0.7	20 ± 1	5.1 ± 0.1	24 ± 3	6.3 ± 0.1
C12-C12 Alkyl Benzoate	5.8 ± 0.6	5.8 ± 0.1	14 ± 1	5.8 ± 0.1	27 ± 1	6.7 ± 0.1
E9	1.41 ± 0.07	3.8 ± 0.8	1.50 ± 0.77	4.6 ± 0.2	1.67 ± 0.84	5.8 ± 0.3
E10	1.47 ± 0.33	4.0 ± 0.4	1.34 ± 0.16	4.6 ± 0.7	1.0 ± 0.1	6.3 ± 0.3
E11	1.29 ± 0.45	4.1 ± 0.6	1.03 ± 0.40	4.7 ± 0.9	1.01 ± 0.12	5.9 ± 0.3
E12	1.18 ± 0.43	3.4 ± 0.1	1.56 ± 0.42	3.7 ± 0.1	1.52 ± 0.25	5.1 ± 0.1
E13	1.61 ± 0.22	3.5 ± 0.1	1.54 ± 0.25	3.9 ± 0.2	1.37 ± 0.37	5.6 ± 0.1
M5	6.10 ± 0.69	5.7 ± 0.2	13 ± 3	5.8 ± 0.5	22 ± 1	6.9 ± 0.4
E14	1.44 ± 0.17	4.5 ± 0.1	1.12 ± 0.02	4.7 ± 0.2	1.0 ± 0.4	7.1 ± 0.2
E15	1.39 ± 0.02	3.1 ± 0.1	1.41 ± 0.40	3.7 ± 0.2	0.70 ± 0.02	5.2 ± 0.2
M6	6.50 ± 0.65	5.2 ± 0.1	16 ± 1	6.0 ± 0.1	24 ± 2	5.9 ± 0.3
E16	5.78 ± 1.28	6.1 ± 0.6	16 ± 3	7.1 ± 0.2	27 ± 1	6.6 ± 0.1

* E1: O/W: Lipid 1 + 2% Emulsifier; E2: O/W: Lipid 1 + 4% Emulsifier; E3: O/W: Lipid 1 + 6% Emulsifier; E4: O/W: Lipid 1 + 2% Emulsifier + 2% Thickening Emollient e; E5: O/W: Lipid 1 + 4% Emulsifier + 2% Thickening Emollient e; M3: Lipid 1 + Thickening Emollient e; E6: O/W: Lipid 1 + 2% Emulsifier + 2% Thickening Emollient f; E7: O/W: Lipid 1 + 4% Emulsifier + 2% Thickening Emollient f; M4: Lipid 1 +Thickening Emollient f; E8: W/O: Lipid 1 + 2% Emulsifier + 2% Thickening Emollient g + Salt; E9: O/W: Lipid 2 + 2% Emulsifier; E10: O/W: Lipid 2 + 4% Emulsifier; E11: O/W: Lipid 2 + 6% Emulsifier; E12: O/W: Lipid 2 + 2% Emulsifier + 2% Thickening Emollient e; E13: O/W: Lipid 2 + 4% Emulsifier + 2% Thickening Emollient e; M5: Lipid 2 + Thickening Emollient e; E14: O/W: Lipid 2 + 2% Emulsifier + 2% Thickening Emollient f; E15: O/W: Lipid 2 + 4% Emulsifier + 2% Thickening Emollient f; M6: Lipid 2 +Thickening Emollient f; E16: W/O: Lipid 2 + 2% Emulsifier + 2% Thickening Emollient g + Salt

4.1.7 Migration of emulsions of different droplet sizes

In addition to the phase distribution of oil and water in an emulsion, this study aimed to investigate the impact of droplet size on the migration of isopropyl palmitate from O/W emulsions. To this end, an O/W emulsion containing isopropyl palmitate has been prepared by rotor-stator homogenization, yielding an average droplet size of 120 µm. A fraction of this emulsion was high-pressure homogenized, reaching an average droplet size of 0.35 µm. The migration of the emulsions and the plain oil are illustrated in Figure 34.

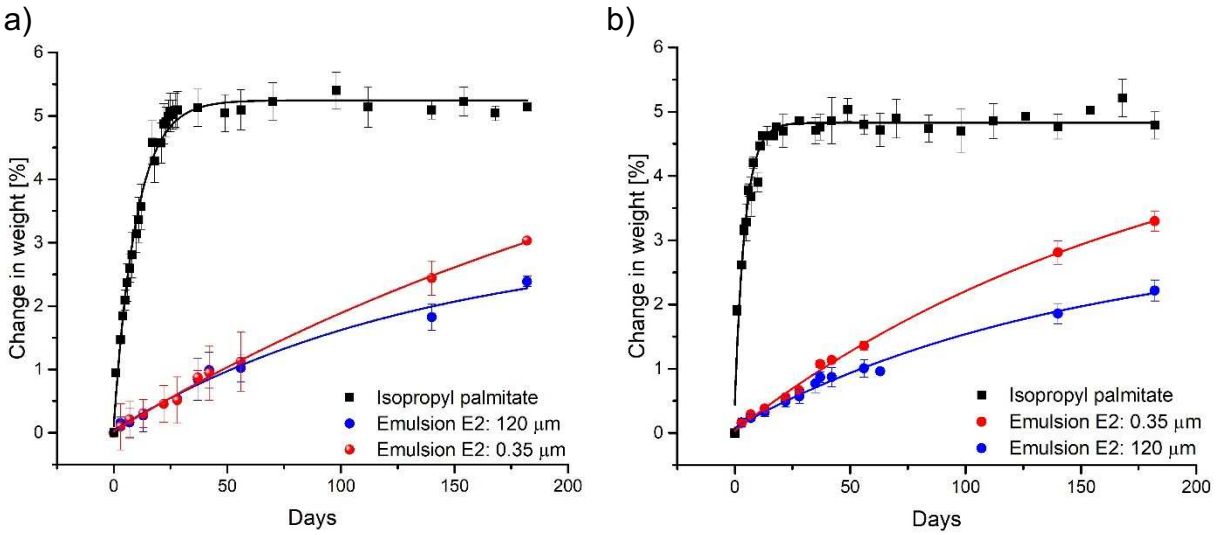

Figure 34 Change in weight over time after migration of isopropyl palmitate and emulsion E2 of different droplet sizes into a) vHDPE 1 and b) rHDPE 1.

Both emulsions are O/Ws and exhibit a slower migration speed than the plain oil, as already discussed in the previous chapter. But some clear differences between the emulsion types of different droplet sizes can be observed. The rate of migration was notably faster from the emulsion with smaller droplets (red) than with larger droplets (blue) in both virgin and recycled materials.

This can be attributed to several factors. Firstly, a larger surface area of smaller droplets in contact with the packaging wall leads to higher absorption of the oil and faster migration. Secondly, a greater surface area results in a thinner emulsifier layer surrounding the oil droplet, thereby reducing the effective shielding from the water phase. Thirdly, the droplets are separated by a thinner layer of the water phase, reducing the distance oil molecules travel through the aqueous phase by diffusion. Fourthly, Brownian motion describes the enhanced the movement of smaller droplets,

resulting higher energy and greater interaction with the packaging wall, promoting migration [86].

In summary, all these effects lead to a faster migration of isopropyl palmitate from a more finely dispersed O/W emulsion. D and MS for both emulsions and different materials can be seen in Table 14.

Table 14 D and MS of Emulsion E2 with different droplet size into different POs.

Name	120 µm Emulsion E2		0.35 µm Emulsion E2	
	D * 10^{-3} [mm^2/day]	MS [%]	D * 10^{-3} [mm^2/day]	MS [%]
vHDPE 1	1.00 ± 0.03	5.0 ± 0.2	1.68 ± 0.26	5.4 ± 0.1
vHDPE 3	1.07 ± 0.09	4.9 ± 0.1	1.56 ± 0.09	5.4 ± 0.3
vHDPE 5	1.03 ± 0.03	6.0 ± 0.3	1.42 ± 0.09	6.8 ± 0.5
rHDPE 1	1.07 ± 0.09	4.9 ± 0.1	3.30 ± 0.41	5.1 ± 0.3
rHDPE 3	1.03 ± 0.03	6.0 ± 0.3	2.31 ± 0.22	4.2 ± 0.1
rHDPE 11	1.00 ± 0.26	5.7 ± 0.9	2.68 ± 0.52	5.3 ± 0.1
rHDPE 12	0.82 ± 0.01	5.0 ± 0.2	2.37 ± 0.18	5.3 ± 0.2
vPP 5	0.12 ± 0.04	6.6 ± 0.3	0.36 ± 0.13	5.7 ± 0.1

The smaller droplet size is associated with a higher D in both virgin and recycled HDPE and PP materials. For the 120 µm droplet size, minimal differences in D were observed across the various HDPE materials. In contrast, for the 0.35 µm droplet size, the D increased in recycled materials compared to virgin materials. In the case of PP, both emulsions exhibited the lowest D, as also observed in plain oil migration. For the MS, similar values between the emulsions and among the different HDPE materials are expected. However, measurements have shown notable deviations. As previously discussed, the measurement timeframe may not have been sufficient to achieve complete saturation, resulting in the MS values being estimated and contributing to these deviations.

4.2 Migration influenced by polymers

4.2.1 Polyolefin types

In addition to product properties, such as emulsion composition and which conditions are chosen for the migration test, the influence of packaging material on oil migration is also considered. As shown in sections 4.1.2 and 4.1.3, where various PO materials were tested under varied conditions, this chapter aims to get a deeper insight into these differences between the various POs. Consequently, properties of POs — including contamination, molecular structure (such as crystallinity and branching), thermal processes, and processing conditions for the material into subsequent products — are examined and related to migration behavior. This analysis aims to understand the processes and variations observed across different materials. Multiple virgin and recycled POs are compared in terms of their migration of isopropyl palmitate. An incubation temperature of 40 °C was selected for the subsequent measurements, as it facilitates fast migration and reveals a distinct weight change. As an example of the migration process, Figure 35 illustrates the change in weight over time after the migration of isopropyl palmitate into one virgin and one recycled sample each of HDPE, LDPE, and PP.

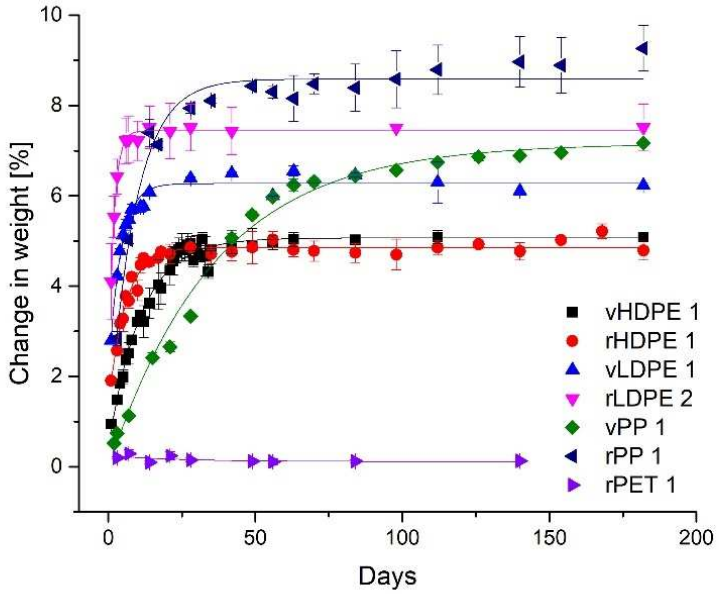

Figure 35 Migration of isopropyl palmitate into different POs at 40 °C.

The POs show a similar behavior characterized by a fast migration with high weight gain within the initial days until a MS is reached. While LDPE and PP demonstrate a higher saturation maximum than the HDPE samples, PP has a less steep slope and takes longer to reach its maximum. PET does not show any migration of isopropyl palmitate and serves as a negative reference and will be further discussed in chapter 4.2.2.

In Figure 36, all D and MS values for all tested materials are presented. It is evident that all HDPE materials reached nearly the same MS level, ranging from 4.5% to 5.5%. In contrast, LDPE shows a slightly higher MS, ranging from 6% to 7%, while LLDPE exhibits an MS between 6% and 11%. The highest saturation values and deviations were observed in PP materials, with values ranging from 7% to 65%. These results can be directly correlated with density and crystallinity of the POs. A summary of all measured materials is presented in Table 15, thereby density was given by the supplier and crystallinity measured via DSC. The parameters to calculate D for all polymers are provided in the appendix in Table 39.

a) b)

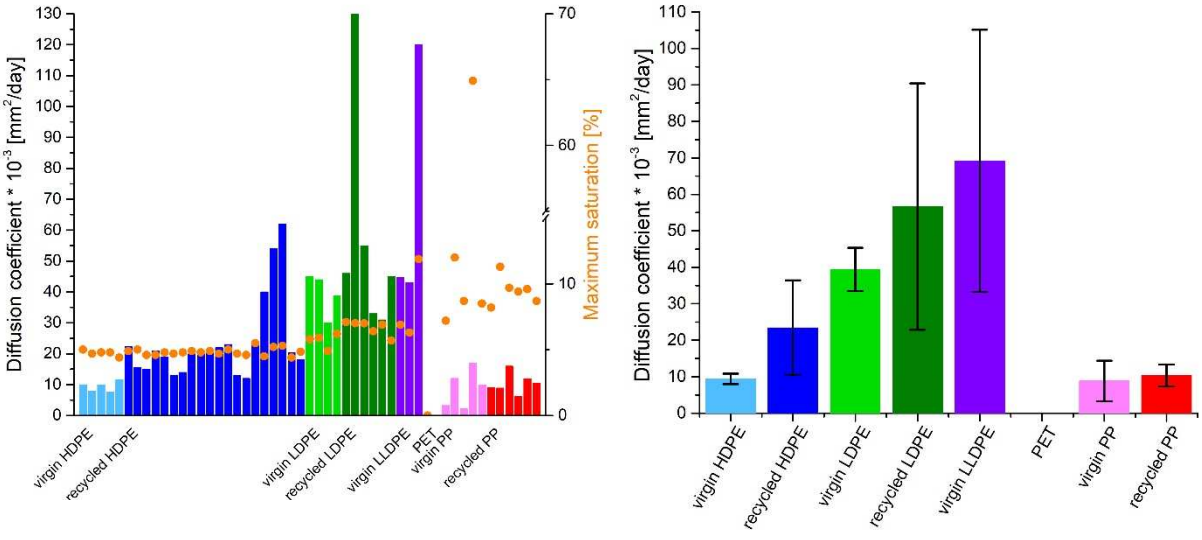

Figure 36 D and MS of isopropyl palmitate at 40 °C in a) various PO's and PET and b) the average of a polymer class.

Table 15 D, MS, crystallinity, and density of isopropyl palmitate into POs and PET.

Name	$D*10^{-3}$ [mm^2/day]	MS [%]	Crystallinity [%]	Density at 23 °C [g/cm^3]
vHDPE 1	10 ± 1	5.0 ± 0.2	69.2	0.958
vHDPE 2	7.66 ± 0.66	4.8 ± 0.1	64.5	0.950
vHDPE 3	10.12 ± 0.46	4.9 ± 0.2	67.7	0.958
vHDPE 4	8 ± 1	4.7 ± 0.3	63.5	0.955
vHDPE 5	11.53 ± 0.41	4.6 ± 0.1	57.5	0.945
rHDPE 1	19 ± 2	4.8 ± 0.2	66.7	0.944
rHDPE 2	15 ± 1	4.6 ± 0.1	65.9	0.960
rHDPE 3	40 ± 5	4.5 ± 0.1	62.1	0.955
rHDPE 4	54 ± 7	5.1 ± 0.2	60.3	-
rHDPE 5	62 ± 5	5.1 ± 0.2	56.4	0.956
rHDPE 6	24 ± 3	5.3 ± 0.2	65.2	0.950
rHDPE 7	12 ± 2	4.6 ± 0.2	63.0	0.955
rHDPE 8	22 ± 3	4.9 ± 0.4	59.4	0.956
rHDPE 9	15.64 ± 0.93	5.0 ± 0.1	66.1	0.950
rHDPE 10	21 ± 2	4.2 ± 0.2	63.6	0.965
rHDPE 11	13 ± 1	4.7 ± 0.1	59.4	0.960
rHDPE 12	14 ± 2	4.8 ± 0.1	69.4	-
rHDPE 13	20 ± 2	4.7 ± 0.3	63.1	-
rHDPE 14	20.79 ± 0.24	4.8 ± 0.1	69.8	0.955
rHDPE 15	20.13 ± 0.82	4.9 ± 0.1	62.1	0.970
rHDPE 16	22 ± 1	4.6 ± 0.1	61.5	0.950
rHDPE 17	13 ± 1	4.7 ± 0.1	65.0	0.960
rHDPE 18	23 ± 3	4.9 ± 0.2	65.7	0.955
rHDPE 19	20 ± 33	4.7 ± 0.1	62.8	0.960

rHDPE 20	18 ± 1	4.7 ± 0.2	66.7	0.950
rHDPE 21	59 ± 2	4.4 ± 0.1	61.4	0.960
vLDPE 1	45 ± 3	5.6 ± 0.4	39.8	0.924
vLDPE 2	44 ± 3	5.9 ± 0.1	41.4	0.919
vLDPE 3	30 ± 5	4.9 ± 0.1	46.0	0.927
vLDPE 4	38.68 ± 0.42	6.2 ± 0.1	43.1	0.922
rLDPE 1	46 ± 2	7.1 ± 0.5	32.4	0.920
rLDPE 2	100 ± 11	7.1 ± 0.1	31.7	0.920
rLDPE 3	55 ± 9	6.9 ± 0.5	31.9	-
rLDPE 4	33 ± 3	6.4 ± 0.2	35.4	-
rLDPE 5	31 ± 5	6.9 ± 0.1	28.1	-
rLDPE 6	45 ± 2	5.7 ± 0.1	22.7	-
vLLDPE 1	44.64 ± 0.54	6.9 ± 0.3	44.3	0.920
vLLDPE 2	43 ± 2	6.3 ± 0.1	43.1	0.918
vLLDPE 3	120 ± 10	11.9 ± 0.2	27.4	0.910
rPET 1	0	0	-	1.890
vPP1	3.27 ± 0.11	7.2 ± 0.1	51.6	0.905
vPP 2	12 ± 3	12.0 ± 0.2	45.5	0.905
vPP 3	17 ± 2	65 ± 3	17.8	-
vPP 4	9.97 ± 0.93	7.4 ± 0.1	13.6	-
vPP 5	2.11 ± 0.10	8.7 ± 0.3	47.8	-
rPP 1	10.37 ± 0.86	8.7 ± 0.2	38.4	0.900
rPP 2	6.21 ± 0.58	13.7 ± 0.8	44.6	-
rPP 3	11.89 ± 0.81	9.6 ± 0.3	41.2	0.910
rPP 4	9 ± 1	8.2 ± 0.2	38.1	-
rPP 5	8.91 ± 0.63	11.3 ± 0.5	35.1	-
rPP 6	16 ± 3	9.5 ± 0.4	40.2	-

PP has the lowest density with 0.89-0.92 g/cm^3, followed by LDPE and LLDPE, ranging from 0.91 to 0.93 g/cm^3 and HDPE with approximately 0.94-0.96 g/cm^3. Similar trends can be observed for the crystallinity of the polymers. HDPE materials possess a crystallinity within a range of 59% to 69%, while LDPE and LLDPE is between 27% and 46%, and PP ranges from 13% to 51%. Consequently, the amorphous phase of the POs is highest for PP, then LDPE and LLDPE, and lowest for HDPE. The ability of polymer chains to crystallize is based on the molecular structure. While virgin HDPE still has a high MW and only a few to no SCB, the crystalline phase is much larger than that of recycled HDPE and LDPE. LDPE, in particular, has a high amount of branching, increasing its amorphous phase, while recycled samples are exposed to thermal degradation and contamination with other POs that can lead to a decrease in MW and the formation of SCB. Since oils migrate within the amorphous phase, oil uptake is higher for PP, LLDPE and LDPE than for HDPE. A higher density and crystallinity of the polymer will prevent oil migration [1, 10, 23].

Furthermore, when evaluating D, it can be observed that the lowest values were found for all virgin HDPE materials, followed by the recycled HDPE materials, which exhibit a broad range from $12*10^{-3}$ to $62*10^{-3}$ mm^2/day, compared to the virgin ones. For LDPE, D is much higher than for HDPE, ranging from $30*10^{-3}$ to $100*10^{-3}$ mm^2/day with no observed substantial difference between the virgin and recycled materials. Three virgin samples of LLDPE were tested, revealing substantial variation in their D values and faster migration compared to LDPE. Conversely, PP exhibits slower migration than PE materials, with the average D for both virgin and recycled PP approximating that of virgin HDPE materials. As Figure 36 b) indicates that all D cover an area that also overlaps with the other PO materials, particularly for recycled materials.

Moreover, isopropyl palmitate migrates faster in recycled materials than in the virgin ones. This demonstrates substantial differences between the properties of different polymers and within one kind of PO that influence the ability of oils to migrate. The following chapters analyze the significant differences in D, especially for HDPE materials and in comparison, to other POs based on their properties.

4.2.2 Migration in PET

PET has not shown migration behavior of isopropyl palmitate in Figure 35 and is utilized as a negative reference. Due to its high density above 1 g/cm^3 (1.89 g/cm^3), and a high T_g of 72.4 °C, PET maintains a glass-like structure within the temperature range of the measurements (23-66 °C). This structure is characterized by densely packed and highly ordered polymer chains, which present a significant barrier for oils attempting to migrate. In contrast, PE and PP materials possess a T_g below 0 °C, resulting in a rubbery phase structure in the temperature range of the migration measurements, thereby facilitating migration processes.

In order to overcome the T_g of PET and transition into the rubbery state of the material, additional measurements at 105 °C for HDPE and PET were conducted. Figure 37 shows a high and fast migration of isopropyl palmitate into HDPE materials, while PET does not exhibit any migration. Although the T_g for PET is lower than 105 °C, allowing the material to transform from a glassy to a rubbery phase, the polymer structure and density continue to inhibit the migration process.

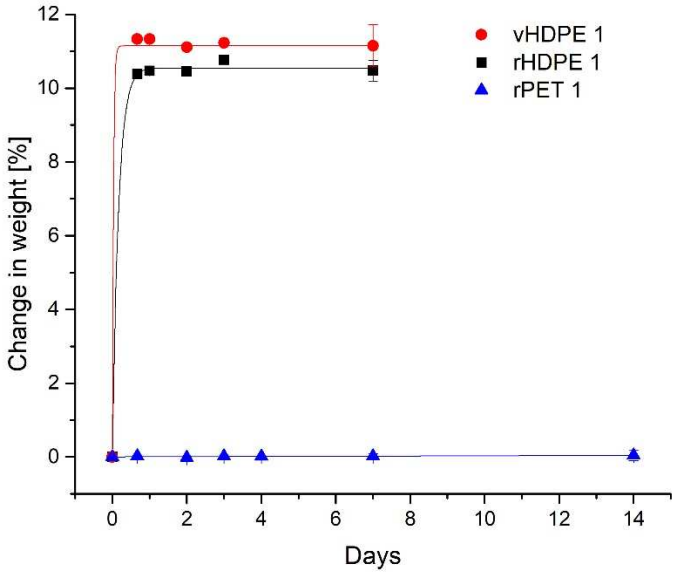

Figure 37 Change in weight after migration of isopropyl palmitate at 105 °C for vHDPE 1, rHDPE 1 and rPET 1.

4.2.3 Structural properties

The properties of a PO are mainly defined by the structure of the polymer, which influences the material's stiffness and rigidity, thereby determining the purpose of the material and the impact on the migration process. Therefore, it is essential to measure molecular properties like crystallinity, MW, MWD, SCB, as well as thermal characteristics like melting temperature in order to be able to identify possible correlations with the migration behavior.

4.2.3.1 Crystallinity

The results in Table 15 were used to analyze the relationship of crystallinity of the samples against the D. Figure 38 a) illustrates the influence of HDPE crystallinity on migration, while Figure 38 b) gives a broader overview by incorporating data from all PE materials.

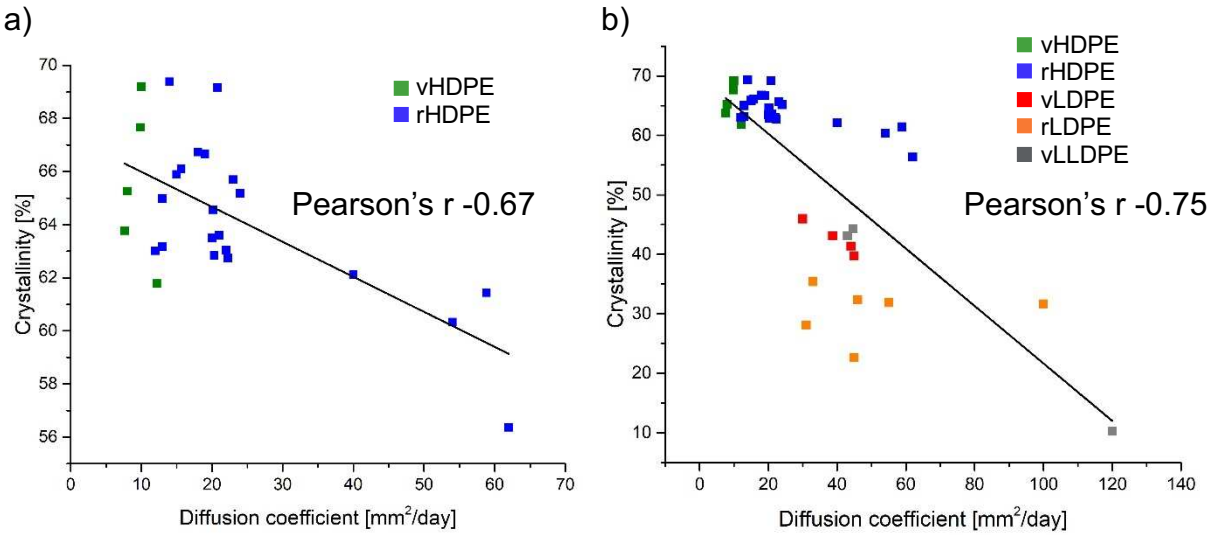

Figure 38 Correlation of crystallinity and D in a) only HDPE and b) all PEs.

A negative correlation is observed between D and the crystallinity. As crystallinity increases, polymer chains become more regularly aligned, resulting in closer packing. That leads to stronger intermolecular bonding and restricted chain mobility, thereby reducing the available space for migration and slows down the absorption of various compounds into the PE matrix [87]. For example, the virgin material vHDPE 1 has a D of $10*10^{-3}$ mm^2/day and a crystallinity of 73.6% whereas rHDPE 3, shows a D of $40*10^{-3}$ mm^2/day and a crystallinity of 62.1%.

When extending the analysis to include other PEs, such as LDPE and LLDPE, an even stronger negative correlation emerges. Figure 38 b) shows the relationship between crystallinity and D of all PE materials yielding a Pearson's r of -0.75. LDPE and LLDPE have different structural properties compared to HDPE, characterized by higher degree of branching, lower densities, and consequently, lower crystallinities [88-90]. Materials with a high degree of branches and crosslinks, exhibit restricted mobility within the chains, resulting in limited chain folding's during the crystallization process. This leads to imperfect crystallites and decreased crystallinity [91]. Thus, the polymer chain structure, as influence by crystallinity, plays a critical role with respect to D.

Crystallinity also has a substantial impact on the density of the material. HDPE, for instance, has a higher density and crystallinity compared to LDPE, suggesting a positive correlation between crystallinity and density in PEs. Figure 39 a) supports the assumption, with a positive correlation factor of 0.89 for all PE materials. However, when considering only the HDPE materials (Figure 39 b)), no clear correlation can be observed. This discrepancy may be attributed to the imprecision of the density values provided by the supplier, which often represent a range rather than an exact value. While a correlation might exist within HDPE materials, more precise density measurements would be necessary to confirm this relationship.

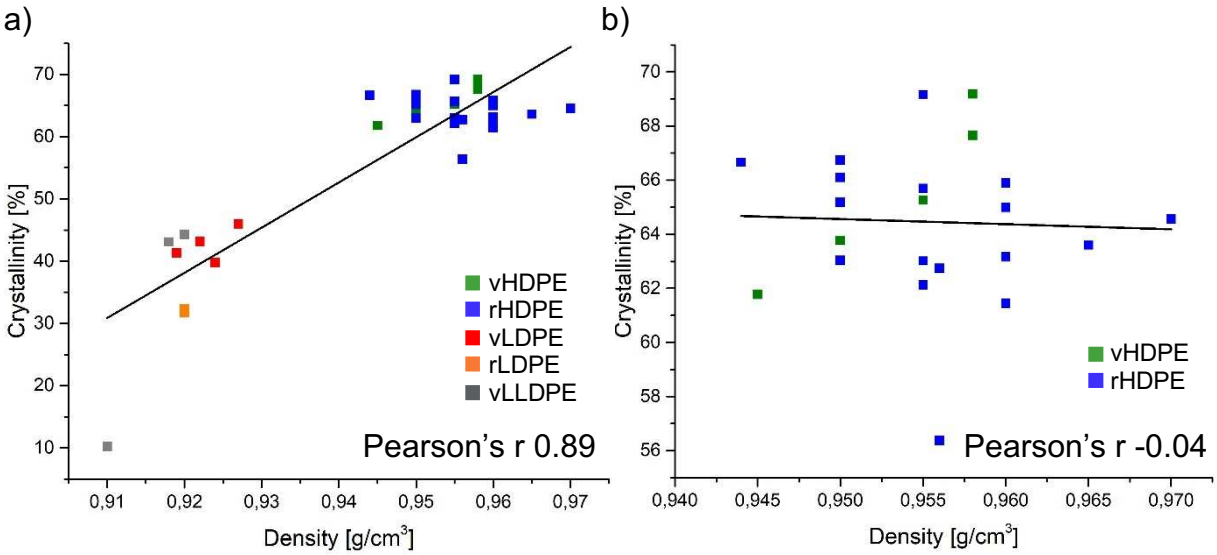

Figure 39 Correlation of crystallinity and density in a) all PEs, and b) only HDPE.

4.2.3.2 Short chain branching

SCB, arises primarily from intentional additives, degradation processes at high temperatures, and contamination of HDPE with other POs containing side chains such as PP, LDPE, and LLDPE. SCB is predominantly observed in PCR materials [68, 92]. The amount of SCB for a specific MW, as well as MW and MWD were measured at Fraunhofer Institute. The average SCB values, along with the MW and MWD of the materials, are summarized in Table 16 and plotted against D in Figure 40.

Table 16 Amount of SCB, MW and MWD of PEs.

Name	SCB	MW [g/mol]	MWD
vHDPE 1	1.4	431590	14.2
vHDPE 2	2.3	392260	12.5
vHDPE 3	0.7	554110	16.7
vHDPE 4	0.0	312390	6.6
vHDPE 5	6.6	326410	19.0
rHDPE 1	7.2	318350	7.2
rHDPE 2	10.9	322970	10.4
rHDPE 3	24.4	375230	14.9
rHDPE 4	17.9	404760	14.2
rHDPE 5	26.4	331560	11.4
rHDPE 6	4.8	338810	8.2
rHDPE 9	0.5	349950	10.2
rHDPE 10	4.3	293670	9.4
rHDPE 11	10.4	336750	11.8
rHDPE 12	5.7	266650	7.9
rHDPE 13	9.6	323840	10.3
rHDPE 14	-0.1	372200	9.9
rHDPE 15	7.5	351420	11.5

rHDPE 18_a	1.9	402000	11.7
vLDPE 1	19.9	230870	5.1
vLDPE 2	17.8	241850	7.5
rLDPE 5	15.2	190350	5.6
rLDPE 4	14.1	251940	6.9
rLDPE 6	45.4	245290	10.4
rLDPE 1	19.1	197020	5.5
rLDPE 2	15.2	203160	5.7
vLLDPE 1	7.5	217360	4.3
vLLDPE 3	26.7	172850	5.3

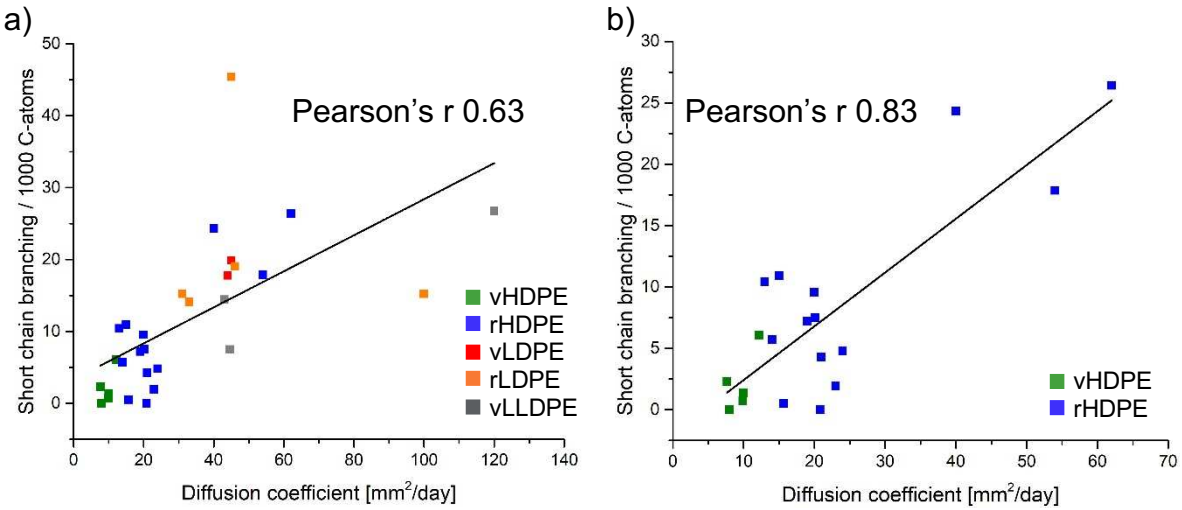

Figure 40 Correlation of SCB and D in a) PE materials and b) HDPE.

Figure 40 demonstrates a clear correlation between the SCB and D. In Figure 40 a) the data of HDPE material, alongside other PEs like LDPE and LLDPE are presented since they contain a high amount of long and short chain branches and a higher D compared to HDPE. A positive correlation between SCB and D with a Pearson's r of 0.63 is evident, indicating that a greater presence of SCB facilitates oil migration. Figure 40 b), focuses exclusively on HDPE, confirming the positive correlation between SCB and D. Most materials cluster between 0 and 15 SCB, with a few exceptions, while LDPE and LLDPE predominantly fall within the range of 13 to 30 SCB.

The presence of SCB alters the structural arrangement of the polymer chains, preventing them from aligning as they would have done before. This misalignment decreases chains local mobility, resulting in greater spacing between the chains, an increased amorphous phase, and decreased crystallinity, and consequently rises D [49]. Figure 41 represents the negative correlation of SCB and crystallinity.

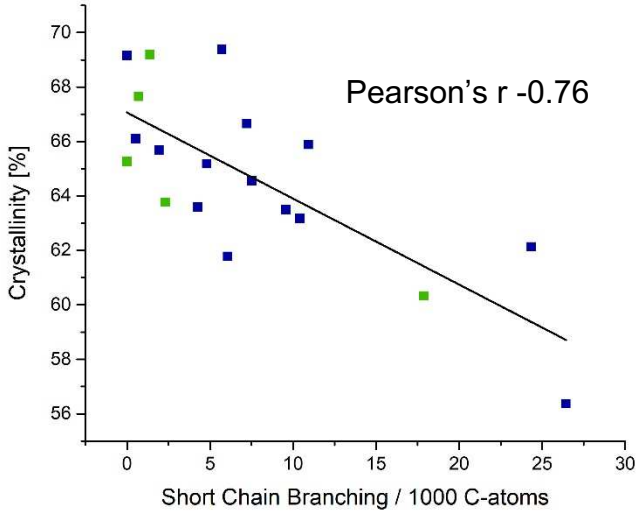

Figure 41 Correlation of SCB and Crystallinity in HDPE.

4.2.3.3 Molecular weight and molecular weight distribution

The measured MW and MWD values, are presented alongside the SCB data in Table 16 and further plotted against D in Figure 42. MW indicated the size of the polymer chain, while MWD characterizes the distribution of molecular weights within a polymer. Both are expected to decrease in recycled materials, due to degradation processes that break down longer polymer chains into shorter fragments, thereby narrowing the MWD [8]. The correlation between D and MW exhibits a negative trend, indicating that as MW increases, D decreases. Notably, the LDPE and LLDPE materials have lower MW and higher D compared to HDPE materials. However, the Pearson's r of only -0.56 suggest only a limited correlation. Similar results can be observed for the MWD in Figure 42 b) with a Pearson's r of -0.42, indicating a negative correlation trend.

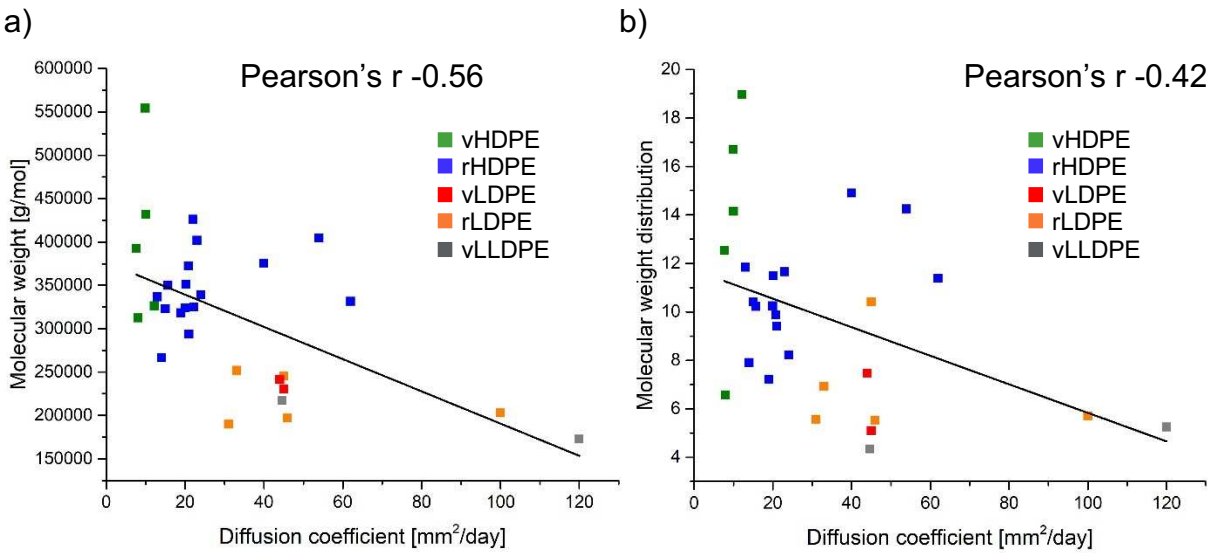

Figure 42 Correlation of a) MW and b) MWD with D for PEs.

However, when looking at HDPE alone, MW and D values scatter strongly and do not correlate (Figure 43). This means MW alone does not cause a difference in D, although it Figure 42 apparently suggest such a trend.

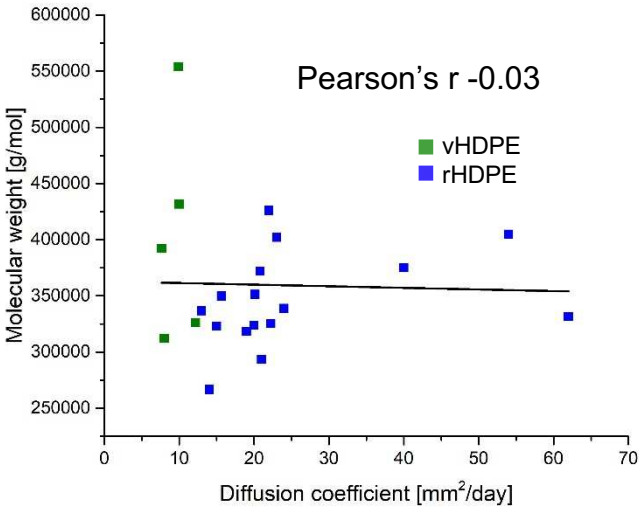

Figure 43 Correlation of MW and D in HDPE.

4.2.4 Thermal properties

Based on various molecular structures mentioned in chapter 4.2.3, thermal properties can change along and will further be analyzed. As mentioned in section 3.2, crystallinity and thermal properties can be determined by DSC measurements. Figure 44 shows the second heating (red) and the cooling curve (black) of vHDPE 1. The area under the melting peak in the heating curve is the enthalpy required for the phase transition from solid to liquid. This enthalpy was used in Equation 9 to calculate the degree of crystallinity, which was determined to be 73.6%. The melting point was identified as 132.7 °C, the temperature of crystallization was 117.8 °C, and no glass transition can be observed due to the material's high degree of crystallinity.

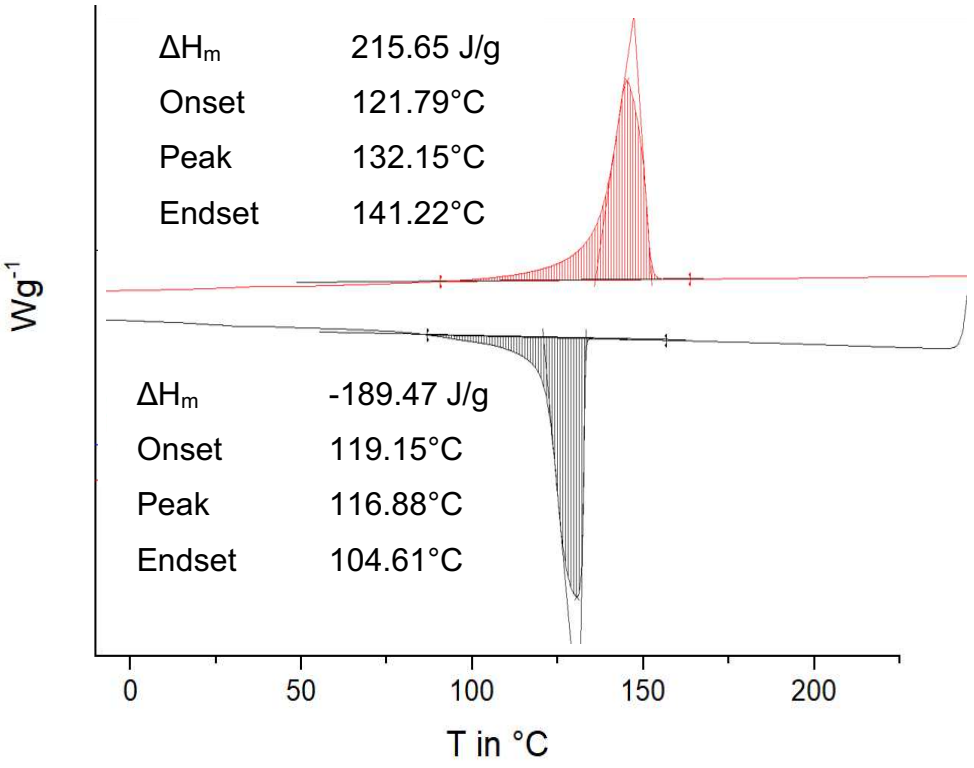

Figure 44 DSC second heating (red) and cooling (black) curve of vHDPE 1.

Thermal decomposition was further analyzed by TGA. From the heat flow curve, the onset and end temperature of the decomposition process, as well as the residual ash content, were determined. All data from thermal measurements of all materials are summarized in Table 17 and will be analyzed in the following chapter.

Table 17 Thermal properties of tested POs.

Name	T_m [°C]	T_c [°C]	Decomposition Onset T [°C]	Decomposition T range [°C]	Ash residue [%]
vHDPE 1	132.7	117.8	261.1	213.7	0.0
vHDPE 2	130.5	116.3	225.2	248.0	0.0
vHDPE 3	133.9	115.3	241.5	231.2	0.7
vHDPE 4	130.9	119.0	244.4	226.1	0.0
vHDPE 5	132.7	112.3	236.9	233.3	0.0
rHDPE 1	133.6	117.2	235.4	238.4	0.0
rHDPE 2	131.9	118.7	239.0	232.3	1.7
rHDPE 3	132.0	118.2	206.7	289.1	0.6
rHDPE 4	131.0	118.2	224.1	284.9	0.7
rHDPE 5	130.9	118.5	217.1	306.3	0.4
rHDPE 6	132.5	118.4	-	-	-
rHDPE 7	135.8	114.0	254.5	220.6	0.0
rHDPE 8	134.7	116.3	-	-	-
rHDPE 9	133.0	118.1	239.4	236.4	0.0
rHDPE 10	131.4	118.3	-	-	-
rHDPE 11	136.8	113.4	228.6	295.7	0.0
rHDPE 12	135.3	115.5	233.7	250.7	0.0
rHDPE 13	133.1	117.9	231.0	265.1	2.6
rHDPE 14	133.2	119.6	267.7	206.3	0.0
rHDPE 15	133.8	115.0	238.2	235.9	1.21
rHDPE 16	131.6	119.1	-	-	-
rHDPE 17	133.5	115.3	-	-	-
rHDPE 18_a	131.6	117.7	232.8	241.2	0.0
rHDPE 19	132.4	118.4	-	-	-
rHDPE 20_0h	132.6	118.7	-	-	-
rHDPE 21	132.0	118.2	-	-	-
vLDPE 1	114.0	100.6	215.0	246.2	0.0
vLDPE 2	110.5	94.8	-	-	-
vLDPE 3	114.5	100.1	-	-	-
vLDPE 4	111.0	95.0	-	-	-

rLDPE 1	109.2	96.8	225.0	252.75	0.1
rLDPE 2	108.8	96.9	-	-	-
rLDPE 3	109.9	99.8	-	-	-
rLDPE 4	109.2	97.8	-	-	-
rLDPE 5	110.1	98.9	-	-	-
rLDPE 6	114.5	100.1	-	-	-
vLLDPE 1	-	-	238.5	232.47	0.0
vLLDPE 2	123.5	107.9	-	-	-
vLLDPE 3	118.5	104.2	242.5	231.7	0.0
vPP1	163.6	124.2	-	-	-
vPP 2	161.5	128.4	-	-	-
vPP 3	167.2	112.0	-	-	-
vPP 4	150.8	118.5	-	-	-
vPP 5	165.5	115.7	-	-	-
rPP 1	161.8	123.9	-	-	-
rPP 2	164.3	116.0	-	-	-
rPP 3	163.2	124.8	-	-	-
rPP 4	163.2	122.8	-	-	-
rPP 5	161.5	124.2	-	-	-
rPP 6	164.2	124.2	-	-	-

4.2.4.1 Melting temperature

Figure 45 compares the melting temperatures of various POs, showing distinct values for each material: LDPE at 110 °C, LLDPE at 121 °C, HDPE at 126 °C, and PP at 166 °C. Further, the melting peak of the HDPE exhibits substantially higher intensity compared to the other POs, indicating that more energy is required to melt this material. This is attributed to its higher structural order and crystallinity.

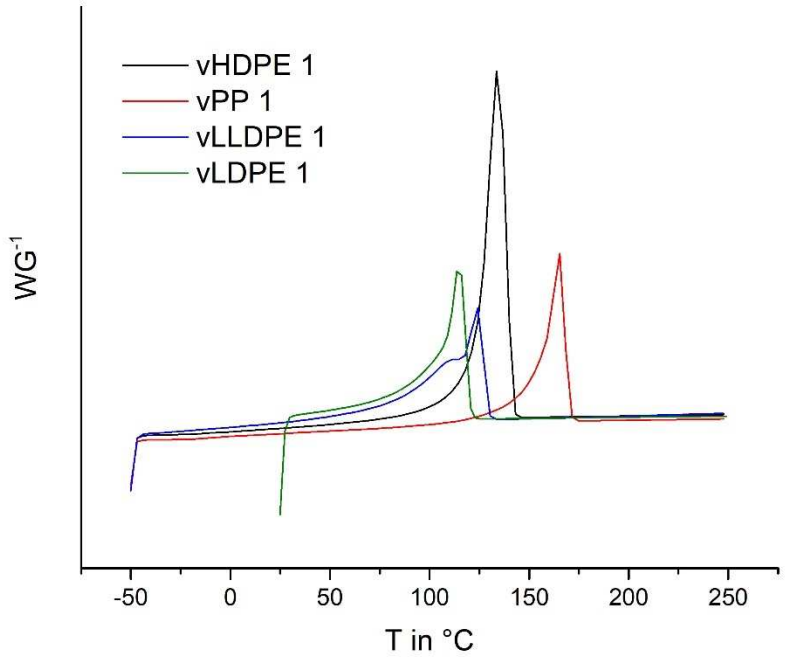

Figure 45 DSC second heating curve of different POs.

All measured T_m were analyzed and plotted against D, as shown in Figure 46 a). A negative correlation between T_m and D can be observed, which can be attributed to the polymer structure since T_m depends on the polymer chains arrangement.

Figure 46 b) demonstrates that T_m is positively correlated with crystallinity. This is because highly crystalline materials are characterized by thicker and more perfect crystallites, which require more energy to melt these highly structured polymer chains [91].

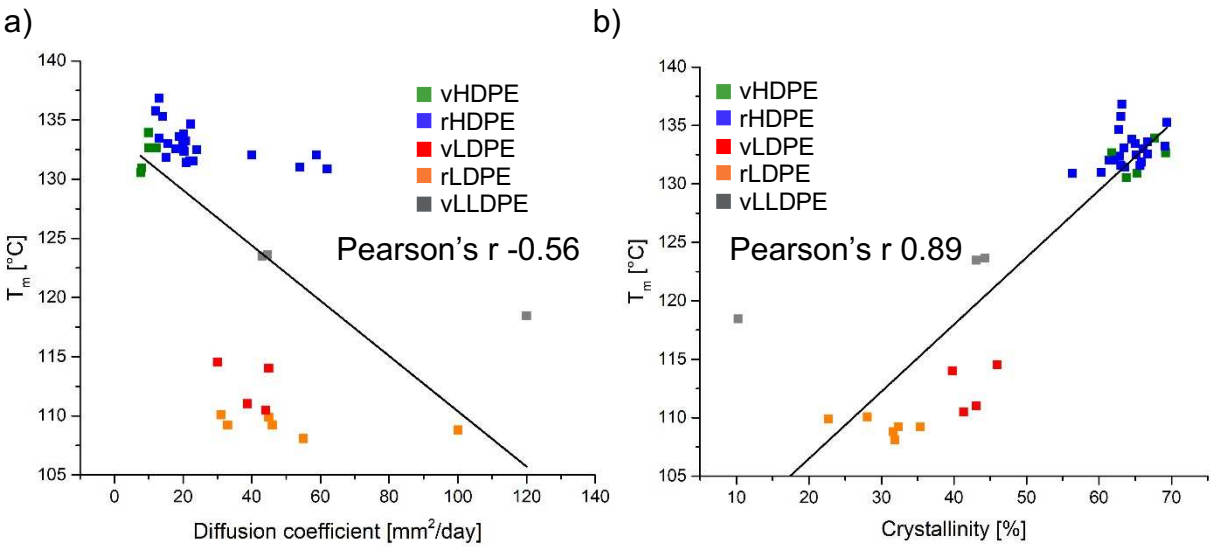

Figure 46 Correlation of T_m with a) D and b) crystallinity in PE.

These trends are observed across all PE materials. However, when only considering HDPE materials no clear correlation between T_m and D was found (Figure 47). The Pearson's r of -0.37 indicates the absence of a consistent positive or negative correlation. This means that both D and T_m are also influenced by properties beyond crystallinity, and additional factors must be considered to estimate the migration process more precisely.

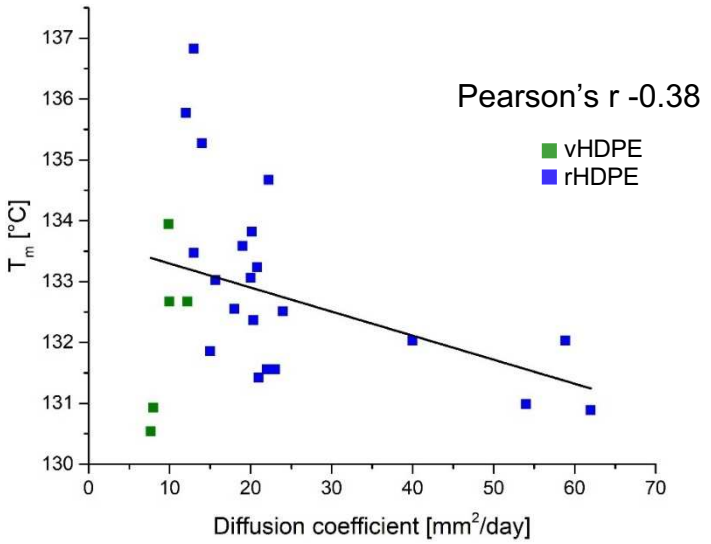

Figure 47 Correlation of T_m and D of isopropyl palmitate in HDPE.

4.2.4.2 Crystallizing temperature

The correlation of the materials' T_c is similar to the trends observed for T_m. Figure 48 a) demonstrates the negative trend correlation between D and T_c across all PE materials. Additionally, a positive correlation is observed between T_c and crystallinity, indicating that a higher crystallinity corresponds to higher T_c, and a lower D. These results further confirm previous observations that crystallinity strongly influences migration behavior.

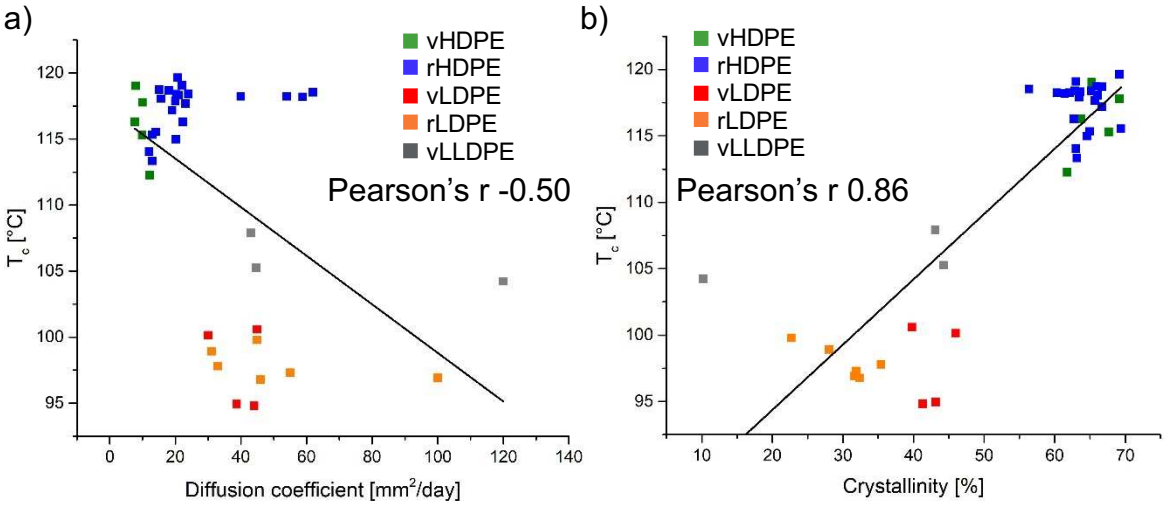

Figure 48 Correlation of T_c with a) D and b) crystallinity in PE.

In contrast, no correlation is visible within the HDPE materials (Figure 49). The Pearson's r of 0.37 is similar to the relationship with T_m and indicates no significant connection to D. Similar to T_m, T_c is influenced by the structure of the polymer chains. However, as previously mentioned, D is influenced by various factors beyond thermal behavior, necessitating a broader consideration of material properties.

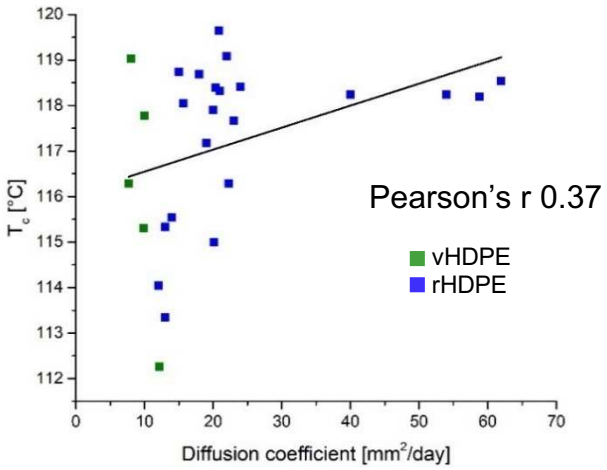

Figure 49 Correlation of T_c and D in HDPE.

4.2.4.3 Decomposition

Decomposition was analyzed using TGA, wherein the material was heated until the decomposition process was complete. During this process, changes in mass are measured, and the onset and offset temperature of decomposition were recorded, which give insights into structure and contamination of the samples. Additionally, the ash residue was weighed, as presented in chapter 4.2.2.1 Table 17. Figure 50 represents the weight loss during the decomposition.

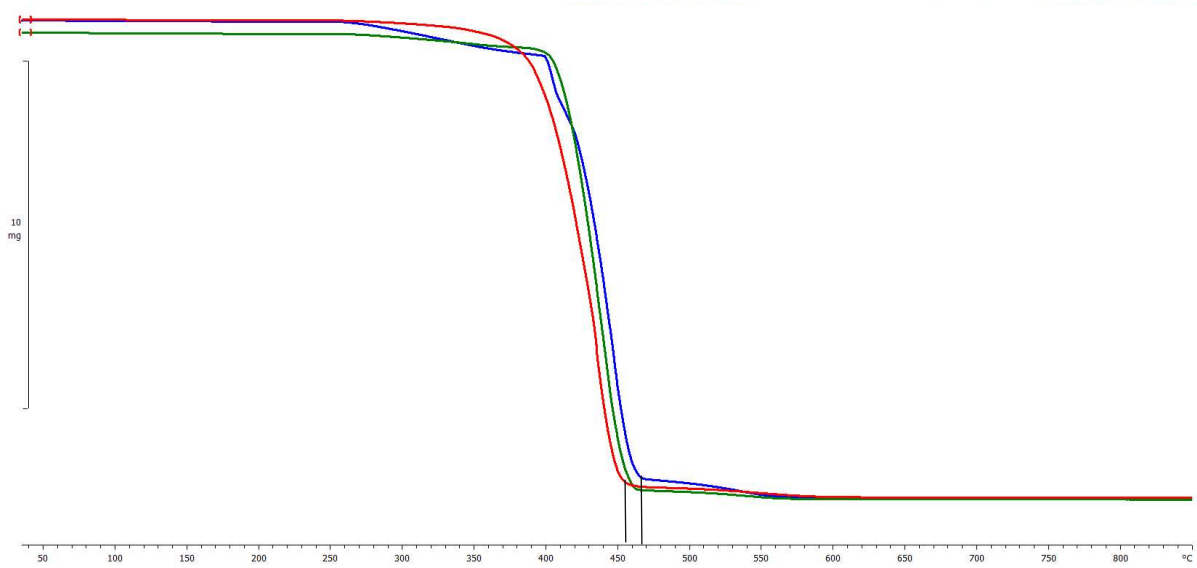

Figure 50 TGA curve of vHDPE 1 (green), rHDPE 1 (blue), and vLDPE 1 (red).

A comparison of the TGA curves for vHDPE 1, rHDPE 1, and vLDPE 1 (Figure 50) reveals that vLDPE 1 has the lowest onset temperature and starts the decomposition process before rHDPE 1 and then vHDPE 1. This leads to the conclusion that thermal stability of the polymer structure decreases in the following order: virgin HDPE, recycled HDPE, and LDPE.

Additionally, the presence of a DSC sensor during the measurement allows to record heat flow curves of the materials, as shown in Figure 51. Multiple peaks corresponding to melting, oxidation, and degradation processes were observed. Thereby the signals of rHDPE 1 were much stronger compared to those for vHDPE 1, indicating a higher presence of impurities or additives in rHDPE 1 that were oxidized and degraded [87, 93]. When comparing HDPE and LDPE, LDPE exhibited a lower onset temperature for degradation than HDPE, confirming the observations in Figure 50.

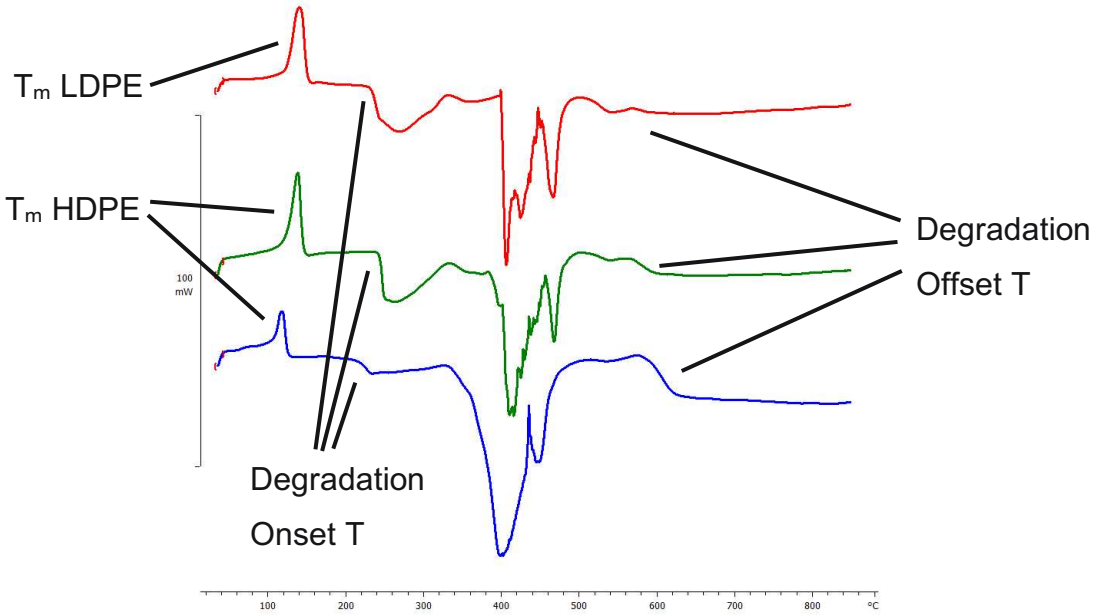

Figure 51 Heatflow curve of TGA measurement of rHDPE 1 (blue), vHDPE 1 (green), and vLDPE 1 (red).

The onset and offset temperatures for HDPE were analyzed and a correlation curve with D was plotted in Figure 52. In a), a negative correlation trend between D and the decomposition onset temperature is observed, whereas in b), the decomposition temperature range reveals a positive correlation with D.

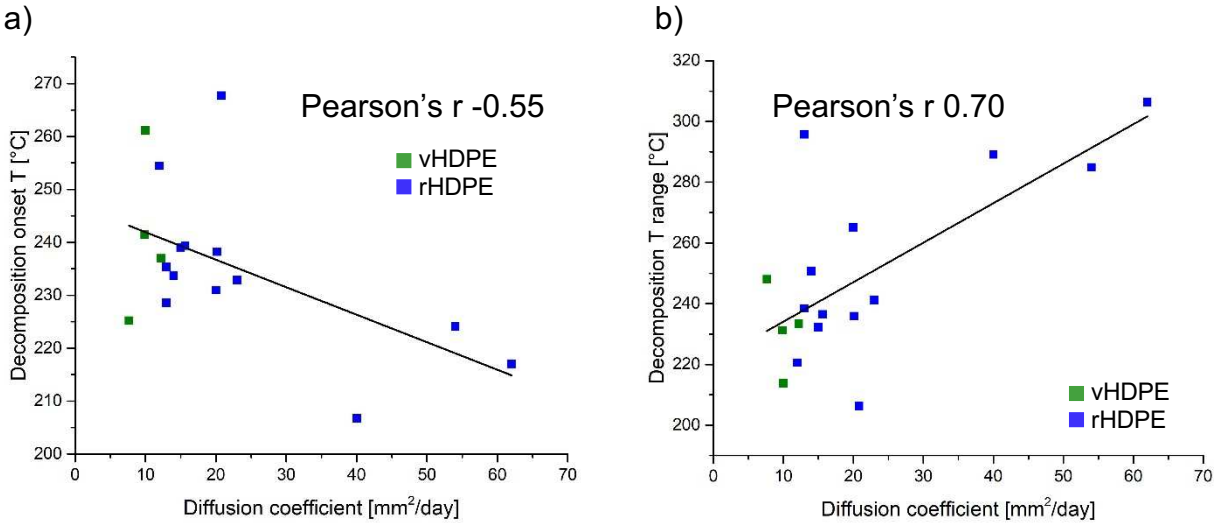

Figure 52 Correlation between D and a) the onset temperature and b) the temperature range of the decomposition process in HDPE.

The lower the onset temperature, the lower the material's thermal stability. This reduced stability is associated with factors such as lower MW, lower crystallinity, and higher branching, all of which reduce the energy required for decomposition of the PEs. Additionally, the onset temperature may indicate the presence of volatile components that evaporate, initiating the degradation process. A broader temperature range, on the other hand, suggests high reaction rates, indicating lower material stability and higher presence of impurities and additives. Furthermore, an oxygen atmosphere facilitates oxidative processes and thermal degradation, resulting in an increased number of observable signals during analysis [87].

When the onset temperature was related to D across different PE materials, the Pearson's r is only -0.25. Therefore, no positive or negative correlation with D can be observed. This indicates that thermal properties alone cannot explain the migration behavior (Figure 53).

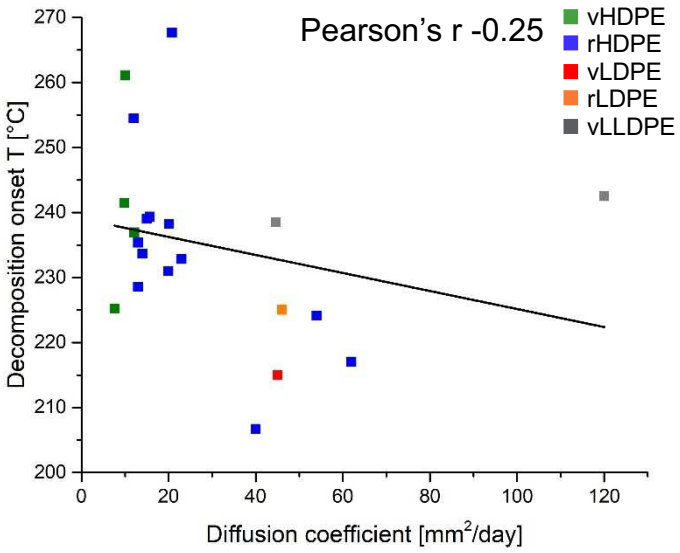

Figure 53 Correlation of decomposition Onset T and D in PEs.

After decomposition, some ash residues, possibly indicative for fillers and inorganic pigments, remain. The amount of ash residue was correlated to the D, as shown in Figure 54 [93]. Most materials, especially the virgin ones, showed negligible ash residues, as seen in Table 30, while some recycled materials have residues of 0.5-2.5%. However, no correlation to D was found, indicating that the ash residues do not significantly affect migration processes.

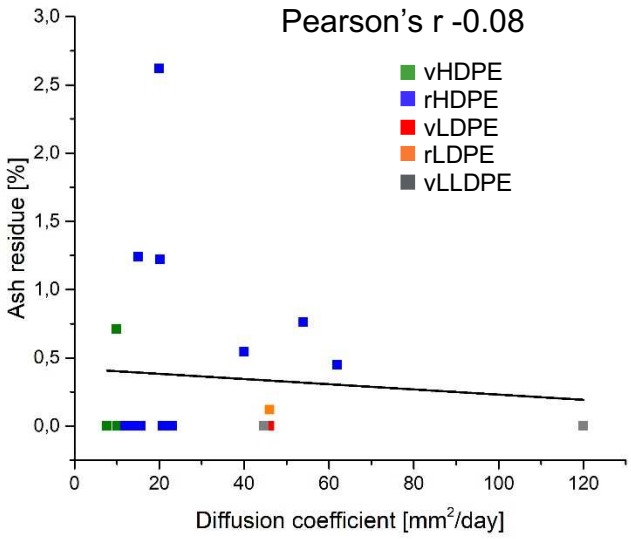

Figure 54 Correlation of ash residue and D in PEs.

4.2.4.4 Glass transition temperature

The final thermal property analyzed was T_g, which defines the temperature range in which a material transitions from a glass-like structure to a rubbery state. While the amorphous or rubbery state provides a much higher volume than the crystalline or glass state of a polymer, enhanced migration is observed in the amorphous phase during the rubbery phase [94]. In glassy state, the temperature is so low that the polymer chains are frozen due to low-energy molecular motion. Therefore, the change in volume within the polymer chains is shallow and would only increase above the T_g [16]. T_g is most prominent in amorphous structures like PET. Although semicrystalline POs like PP and PE also contain amorphous regions, their chain interactions are much weaker than those in PET. While PET contains ester groups that facilitates intermolecular forces like dipole-dipole interactions and hydrogen bonds, POs only exhibit weak Van der Waals interactions within the PO chains. The stronger the interaction within the polymer, the higher the change in specific heat capacity as the temperature increases, resulting in a more distinct glass transition area [16, 95]. Moreover, the melting and crystallizing processes might overlap with the amorphous phase's glass transition, making the T_g hard to detect.

Due to possible overlapping and weak interaction forces, it was not possible to determine the T_g of the POs, as shown in Figure 55. For PET, the T_g can be observed at 72,4 °C, marking the transition from a glass-like to a rubbery structure.

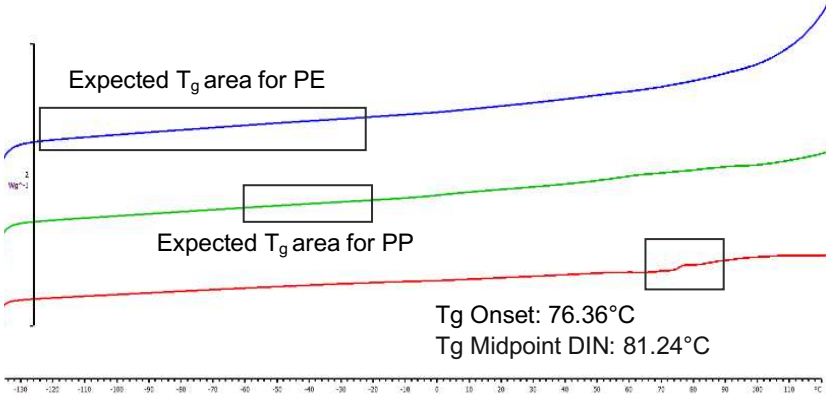

Figure 55 DSC curves of vHDPE 1 (blue), vPP 1 (green), rPET 1 (red) within the range of the T_g.

In the literature, T_g values for POs are known to be around -23 °C to -125 °C. The range is extensive due to difficult measurements, since PE is not commonly accessible in an utterly amorphous state and has a very high crystallization rate. Furthermore, the amount of branching varies within PEs, resulting in a wide range of different structured materials with different T_g's [95]. For PP, the T_g is around -40.15 °C [96]. All these T_g values are significantly below the temperature used for migration measurements, leaving the amorphous phase in a rubbery state with a higher free volume, that facilitates migration.

4.2.5 Mechanical properties

As discussed in previous chapters, various PE properties correlate with D. These properties also influence mechanical characteristics of the material and define, for example, tensile strength, elongation at break, and melt flow rate. The mechanical property data, provided by the supplier, and their correlation with D are summarized in Table 18. Data for the mechanical properties of all polymers are detailed in Table 35 in the appendix.

Table 18 Pearson's r of various mechanical properties and D of all PEs and only HDPE.

Pearson's r	D: HDPE, LDPE, LLDPE	D: HDPE
Density [g/cm^3]	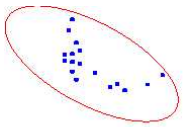	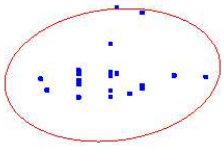
	-0.65	0.13
Charpy notched impact strength 23 °C [kJ/m^2]	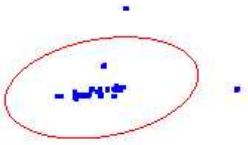	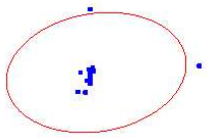
	0.14	0.14
Tensile modulus [MPa]	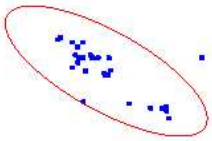	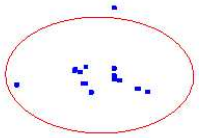
	-0.65	-0.02
Elongation at break [%]	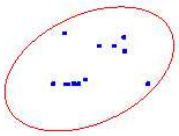	-
	0.38	-
Tensile strength [MPa]	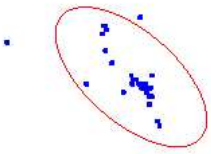	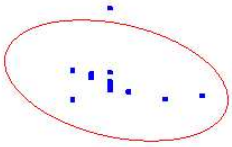
	-0.64	-0.32
MFR (5.00 kg) [g/10 min]	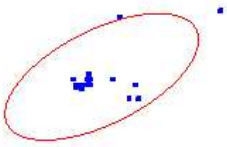	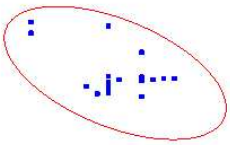
	0.52	-0.03

No relevant correlation was observed between mechanical properties and D for HDPE materials alone. For all PE materials, a negative trend can be observed for density, tensile strength, and tensile modulus. This trend suggests that HDPE, being a stiffer material compared to LDPE, exhibits slower migration rates. The stiffness of HDPE is attributed to its structural properties, such as higher crystallinity and less branching.

Thus, intercorrelations between mechanical properties and polymer characteristics are evident, both within HDPEs, as shown in Table 19, and across all PEs, as presented in Table 20.

Table 19 Pearson's r correlation of D, thermal, molecular and mechanical properties in HDPE.*

	MFR	TM	TS	CIS	χ	ρ	PP	SCB	T_m	MWD	MW
D	-0.52	-0.02	-0.32	0.14	-0.67	0.13	0.72	0.83	-0.38	0.10	-0.03
MW	-0.15	0.30	0.55	-0.06	0.15	0.01	-0.19	-0.16	-0.12	0.60	
MWD	-0.32	-0.43	0.39	-0.32	-0.27	-0.04	-0.08	0.20	-0.04		
T_m	0.26	-0.05	0.09	0.03	0.30	0.15	-0.07	-0.17			
SCB	-0.52	-0.42	-0.43	-0.03	-0.76	0.09	0.78				
PP	-0.65	-0.05	-0.48	0.35	-0.67	0.06					
ρ	-0.06	0.18	0.06	-0.26	-0.04						
χ	0.50	0.62	0.60	0.13							
CIS	-0.16	-0.70	-0.47								
TM	-0.48	0.51									
TS	-0.43										

* Pearson's r: +1: positive correlation; -1: negative correlation; 0: no correlation; Tensile strength (TS), Tensile modulus (TM), Charpy notched impact strength at 23 °C (CIS), density (ρ), crystallinity (χ), MWD, MW, MFR at 5.00 kg

In HDPE materials, crystallinity exhibits a positive correlation with tensile modulus (+0.62) and tensile strength (+0.60). Higher crystallinity enhances the material's resistance to stress [1]. Furthermore, MFR is influenced by PP contamination (-0.65), indicating an increased contamination reduces viscosity of the material.

Table 20 Pearson's r correlation of D, thermal, molecular and mechanical properties in PEs.*

	MFR	TM	TS	CIS	χ	ρ	PP	SCB	T_m	MWD	MW
D	0.52	-0.65	-0.64	0.14	-0.75	-0.65	0.42	0.63	-0.56	-0.42	-0.56
MW	-0.67	0.72	0.82	-0.06	0.77	0.75	0.05	-0.49	0.72	0.80	
MWD	-0.65	0.42	0.77	-0.32	0.56	0.64	0.11	-0.18	0.59		
T_m	-0.94	0.81	0.68	0.04	0.89	0.87	0.34	-0.59			
SCB	0.18	-0.80	-0.77	-0.03	-0.72	-0.53	0.57				
PP	-0.65	0.35	0.16	0.30	0.16	0.37					
ρ	-0.85	0.86	0.80	-0.27	0.89						
χ	-0.87	0.90	0.78	0.14							
CIS	-0.19	-0.67	-0.47								
TS	-0.88	0.78									
TM	-0.76										

* Pearson's r: +1: positive correlation; -1: negative correlation; 0: no correlation; Tensile strength (TS), Tensile modulus (TM), Charpy notched impact strength at 23 °C (CIS), density (ρ), crystallinity (χ), MWD, MW, MFR at 5.00 kg.

In PEs, all mechanical properties show a strong interrelation, highlighting significant structural differences. The observed properties are often influenced by multiple factors, leading to a complex network of different correlations within one specific polymer, which ultimately impact D.

For a detailed analysis of how and to what extent each property influences D, a multiple regression analysis was performed using the parameters from Table 19 and Table 20 for HDPE and all PE materials. Based on Equation 8, the coefficients and significant values ($p < 0.05$) were determined and are provided in the appendix (Table 37). For most samples, the dataset was incomplete due to missing information from suppliers regarding mechanical or molecular properties. This limitation resulted in a reduced number of samples relative to the number of parameters available for multiple regression analysis, causing issues with the reliability of the results. Specifically, the analysis suffered from overfitting, which led to misleadingly high R^2 values, unstable regression coefficients, and reduced statistical power [97, 98]. As a result, the dataset was considered unsuitable for making assumptions about the extent of the impact on D.

4.2.6 Contaminations

Various additives intended to maintain and enhance plastic properties, as well as unintentional contamination during consumption and the recycling process, can influence the migration of cosmetic components. Although the recycling process aims to eliminate these contaminants, the effectiveness of cleaning is often limited [99-102]. Using GC-MS, volatile and semi volatile components in the sample can be identified, while XRF is used to trace inorganic contaminants. Moreover, insufficient separation of polymer mixtures results in polymeric contamination, which can be identified by DSC. Table 21 summarizes the levels of organic volatile, semi volatile, inorganic contaminants, and residual PP. Complete inorganic contamination data are presented in the appendix (Table 36).

Table 21 Organic and inorganic contamination and properties of tested POs.

Name	Total elements [%]	Total semi volatiles [mg/kg]	Total volatiles [mg/kg]	PP content [%]
vHDPE 1	0.03	16.2	4.2	0.0
vHDPE 2	0.03	-	-	0.0
vHDPE 3	0.02	-	-	0.0
vHDPE 4	0.01	0.6	0.9	0.0
vHDPE 5	0.03	-	-	0.0
rHDPE 1	0.07	2.0	1.4	2.4
rHDPE 2	1.05	58.2	5.4	1.8
rHDPE 3	1.16	89.0	3.6	2.1
rHDPE 4	0.67	36.5	2.3	5.9
rHDPE 5	0.51	21.4	1.9	8.1
rHDPE 6	0.05	5.5	1.7	3.4
rHDPE 7	0.08	-	-	-
rHDPE 8	0.56	112.3	5.8	4.2
rHDPE 9	0.03	19.4	3.4	0.6
rHDPE 10	0.76	16.1	4.1	0.4
rHDPE 11	0.40	-	-	3.7
rHDPE 12	0.13	12.5	4.6	1.1
rHDPE 13	1.22	-	-	1.9
rHDPE 14	0.03	3.8	0.8	0.0

rHDPE 15	0.69	65.7	4.6	1.1
rHDPE 16	0.40	11.2	2.4	2.1
rHDPE 17	0.48	-	-	1.7
rHDPE 18_a	0.05	58.7	9.3	0.7
rHDPE 19	0.46	-	-	4.9
rHDPE 20_0h	0.04	-	8.8	0.5
rHDPE 21	1.37	22.8	7.2	3.9
vLDPE 1	0.01	-	-	0.0
vLDPE 2	0.02	-	-	0.0
vLDPE 3	0.01	-	-	0.0
vLDPE 4	0.02	-	-	0.0
rLDPE 1	0.15	5.8	3.4	0.0
rLDPE 2	0.13	23.1	9.5	0.0
rLDPE 3	0.18	69.4	-	0.0
rLDPE 4	0.31	38.8	-	0.0
rLDPE 5	0.23	61.9	-	0.0
rLDPE 6	1.02	356.6	-	0.0
vLLDPE 1	0.03	-	-	0.0
vLLDPE 2	0.03	-	-	0.0
vLLDPE 3	0.10	-	-	0.0
vPP1	0.08	54.4	7.7	100.0
vPP 2	0.15	51.7	9.3	100.0
vPP 3	-	-	-	59.2
vPP 4	0.02	64.9	6.5	45.3
vPP 5	-	-	-	-
rPP 1	0.31	-	-	-
rPP 2	0.22	29.0	4.5	-
rPP 3	0.68	-	-	-
rPP 4	-	43.4	9.8	-
rPP 5	0.85	87.5	4.4	-
rPP 6	0.72	89.5	12.6	-

4.2.6.1 Organic and inorganic contamination

To analyze the influence of contamination with inorganic material, total semi-volatiles, and total volatiles, the measured values (Table 21) were plotted against D, as illustrated in Table 22. Subsequently, the Pearson correlation factors in all POs and for HDPE were determined.

Table 22 Pearson's r of D and contamination levels in HDPE and all POs.

Pearson's r	Total elements	Total semi volatiles	Total volatiles
D: HDPE, LDPE, LLDPE, PP	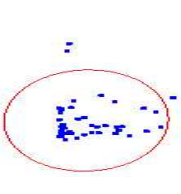	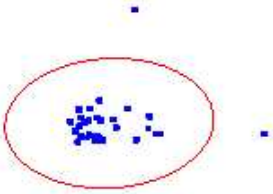	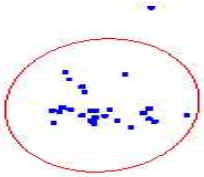
	0.05	0.09	0.01
D: HDPE	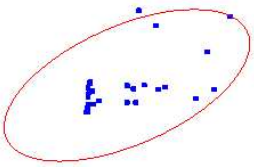	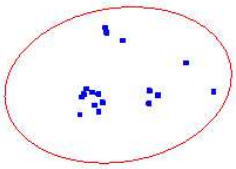	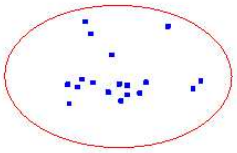
	0.55	0.13	-0.01

Pearson's r reveals no significant correlation between these parameters. Almost all values are close to zero, indicating that neither a positive nor a negative correlation can be observed between the contamination levels and D in the analyzed POs. The only exception is the correlation between HDPE and inorganic material, which showed a small positive trend with Pearson's r of 0.55. This is presumably due to the presence of calcium and titanium content in some recycled material, used as white pigments and fillers [103]. However, since this type of contamination applies only to white PCR samples, it can be disregarded as a parameter influencing the migration process.

Previous studies have demonstrated that the incorporation of antioxidants can improve melt behavior and decrease various degradation effects, resulting in improved mechanical properties for LDPE. However, for HDPE, no significant changes in mechanical properties or crystallinity were observed, leading to the conclusion that the migration process is also unaffected by the addition of antioxidants [104].

Degassing during recycling reduces volatile organic contaminants (VOCs). A study by Marcel Bruns at Beiersdorf AG found that extended degassing reduces volatile organic contamination, with longer degassing durations showing greater reductions (Figure 56) [100, 105].

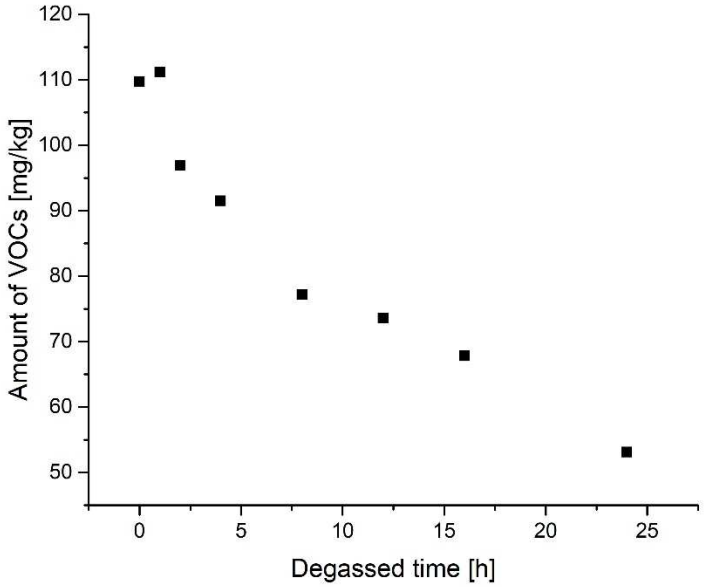

Figure 56 Amount of VOCs over degassed time.

To analyze the influence of the degassing process on migration behavior, samples that have been degassed for 0, 12, and 24 hours were taken for migration measurements. While the volatile contamination decreases with increasing degassing time, D and crystallinity remained the same (Table 23), confirming that VOC contamination does not influence migration behavior.

Table 23 D, VOC contamination and crystallinity in degassed samples.

Pellet Name	Degassing hours	D $*10^{-3}$ [mm^2/day]	VOC [mg/kg]	Crystallinity [%]
rHDPE 20_0h	0	18 ± 1	8.8	66.7
rHDPE 20_12h	12	17 ± 3	5.9	68.1
rHDPE 20_24h	24	22 ± 2	4.3	67.1

4.2.6.2 PP contamination in HDPE

Various analytical methods, including IR spectroscopy and DSC, can be applied to identify and quantify foreign polymeric contaminants in POs. Certain band signals in the IR spectrum apply for the various POs as shown in Table 24. For instance, PP exhibits signals at 2959, 2840, 2860, 2875, and 1377 cm^{-1}, which differentiate it from HDPE. However, the presence of overlapping signals from LDPE and LLDPE, making it challenging to distinguish and moreover quantify the amount of PP in the polymer (Figure 57).

Table 24 Peak intensities of the main absorptions of POs in the IR region [106].

Band [cm^{-1}]	HDPE	LDPE	LLDPE	PP	Assignment
2959	-	weak	weak	strong	CH_2 asymmetric stretching
2920	strong	strong	strong	strong	
2860, 2875	-	-	-	medium	
2850	strong	strong	strong	-	CH_2 symmetric stretching
2840	-	-	-	medium	
1473	strong	strong	strong	-	Bending deformation
1463	strong	strong	strong	strong	
1456	weak	weak	weak	medium	
1377	-	weak	weak	strong	CH_3 symmetric deformation
1366, 1351	medium	weaker than 1377	stronger than 1377	strong	Wagging deformation
1176	weak	weak	weak	medium	
731-720	medium	medium	medium	weak	Rocking deformation

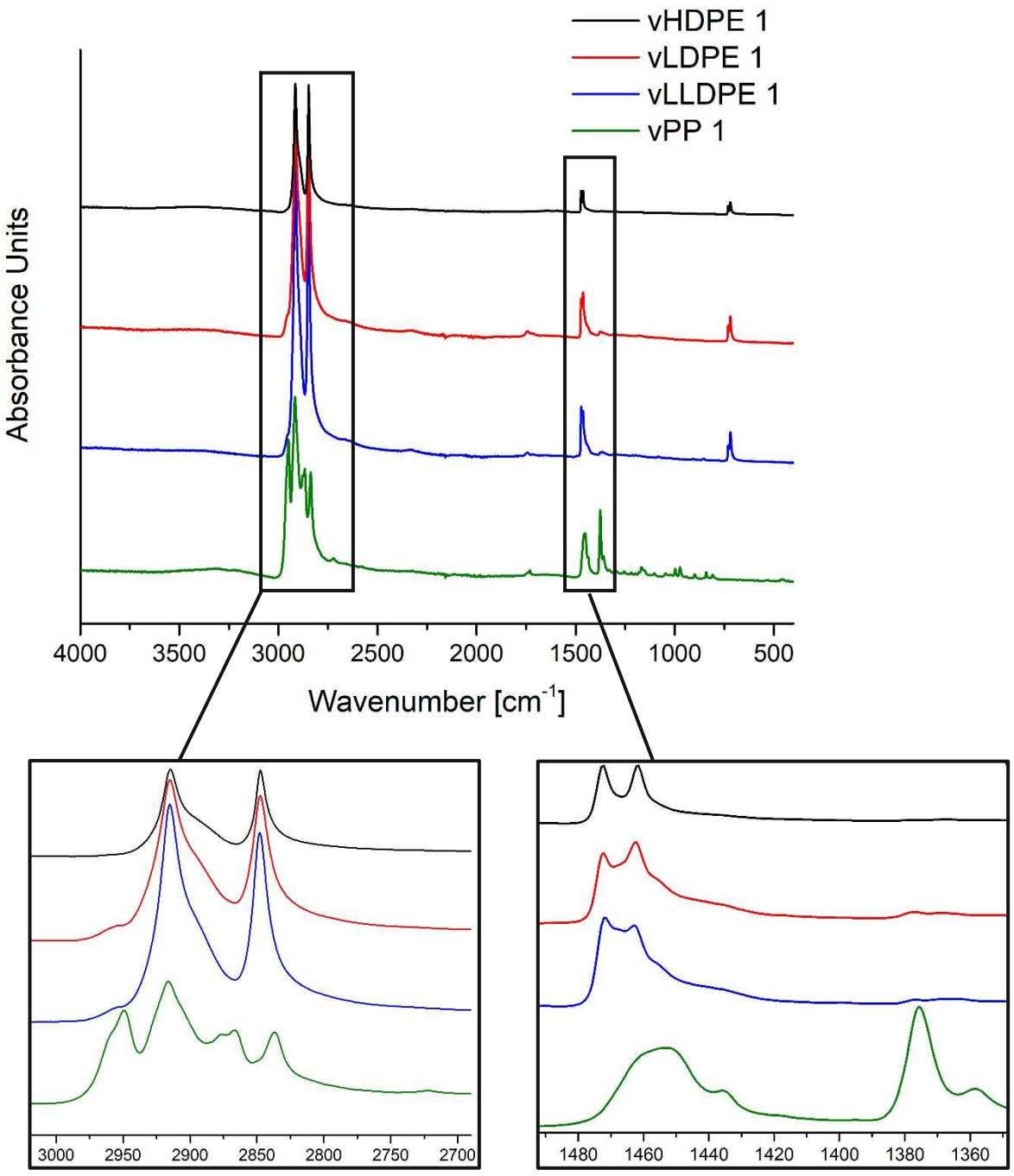

Figure 57 IR spectrum of the POs and their characteristic bands.

A comparison of vHDPE 2 and rHDPE 5 materials in Figure 58 reveals additional signals indicating the presence of PP in rHDPE 5. But due to overlapping absorption bands of LDPE and LLDPE to those of PP, FT-IR spectroscopy is not suitable for quantifying the contamination levels of other POs than PP.

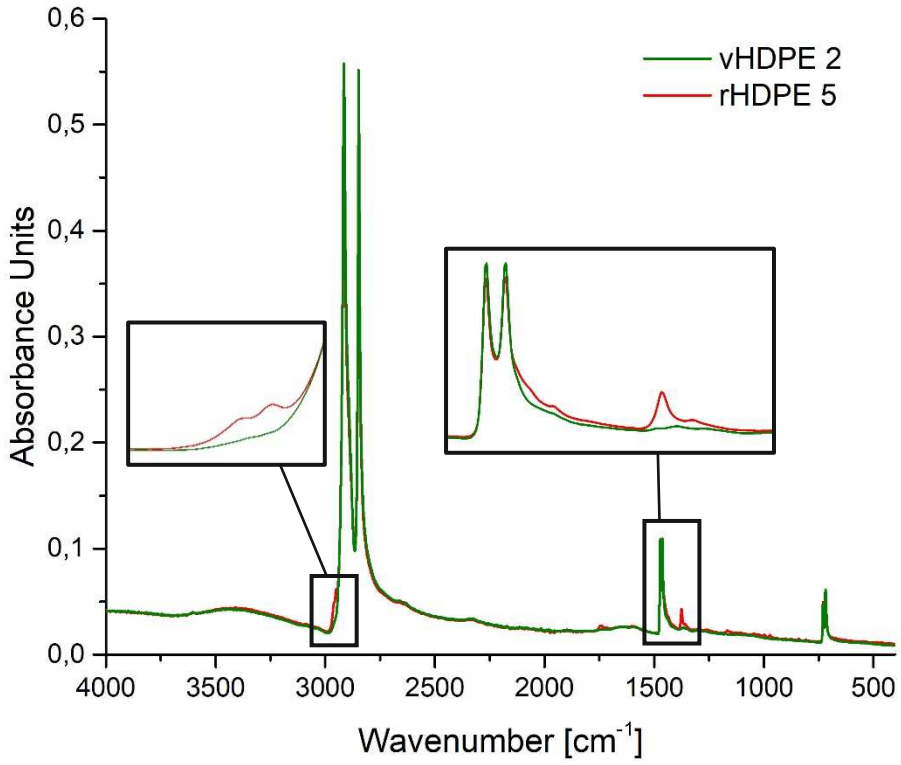

Figure 58 IR spectrum of vHDPE 2 in comparison to rHDPE 5.

In addition to FT-IR, DSC measurements were conducted. The resulting graph shows the heat flow within a PO over a specific temperature range. Aside from the determination of melting, crystallization, and glass transition temperature, DSC also allows to measure the melting enthalpy which can be used to calculate the degree of crystallinity and amount of contamination with other POs (Figure 59). After respective calibration, it is possible to assess the contamination levels of PP, LDPE, and LLDPE based on their distinct melting temperatures. Since PP and HDPE are immiscible in a molten state, two distinct peaks can be measured and quantified [107]. As shown in Figure 59 a), the heat flow curve of PP in red exhibits the melting peak at higher temperatures than the HDPE in blue. Analyzing PCR materials with unknown HDPE and PP content, as in Figure 59 b) and c), allows to quantify the amount and crystallinity of each PO by calculating the integral of both peaks.

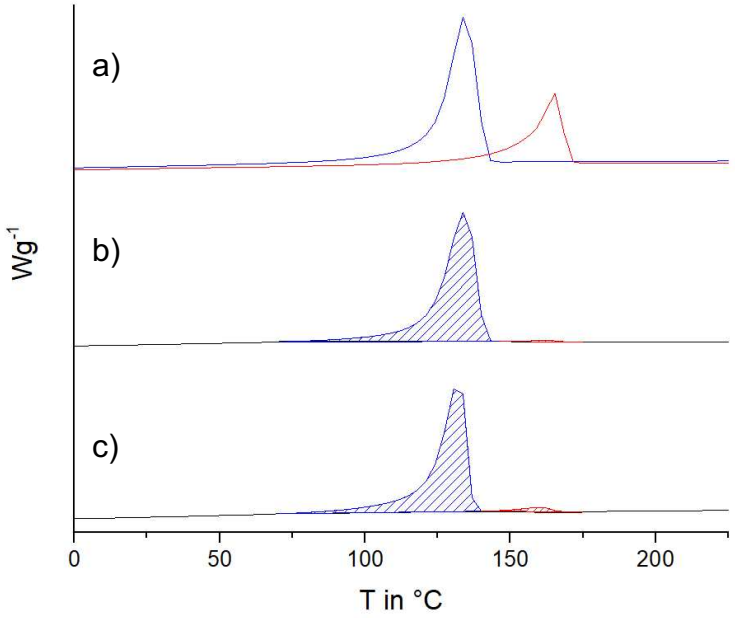

Figure 59 Second DSC heating curve of a) vHDPE 1 (blue) and vPP1 (red), b) rHDPE 2, and c) rHDPE 5.

To analyze the influence of PP contamination in HDPE, the contamination values were plotted against D. Figure 60 shows a positive correlation, with a Pearson's r of 0.72. This indicates that the higher PP content in the samples, the faster the migration, while the maximum oil uptake remains constant. Especially PCR materials contain up to 10% contaminants, as detailed in Table 21. Although IR measurements can effectively eliminate PP contamination at various stages of the recycling process, some residues persist, resulting in alterations to the structure and behavior of HDPE materials [108].

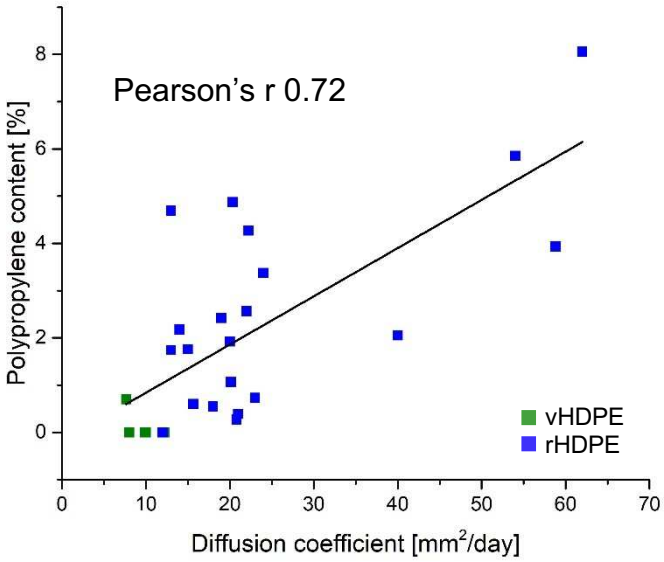

Figure 60 Correlation of PP contamination and D in HDPE.

To validate these findings, specimens with defined amounts of PP in vHDPE were prepared, and migration behavior and crystallinity was measured, as shown in Table 25.

Table 25 Migration results in HDPE+PP specimen.

Name	D $*10^{-3}$ [mm^2/day]	MS [%]	Crystallinity [%]
vHDPE + 1%PP	7.29 ± 0.34	4.9 ± 0.1	68.8
vHDPE + 3%PP	8.81 ± 0.44	5.4 ± 0.1	66.0
vHDPE + 5%PP	11 ± 1	4.9 ± 0.2	66.8

The data shown in Table 25 indicate an increase in D with rising amounts of PP in vHDPE. However, values for virgin material contaminated with 3% and 5% PP was significantly lower than for recycled material containing 5% PP. For instance, rHDPE 4 with 5.85% PP has a D of $54*10^{-3}$ mm²/day, compared to $11*10^{-3}$ mm²/day for virgin HDPE with 5% PP. This observation suggests that PP content alone cannot fully account for the different migration behavior of HDPE materials. MS on the other hand, yields similar values to those of other HDPE (Table 15). Crystallinity, on the other hand, decreases from 68.8% at 1% PP to 66% at 3% PP indicating a clear change in molecular structure, even though no further changes can be observed at 5% PP. Given that HDPE and PP are immiscible, the distribution of PP may not be homogeneous, potentially leading to inaccurate high values.

Furthermore, this raises the question of how other POs influence migration and whether LDPE and LLDPE contamination would yield similar results. Given their higher D compared to HDPE, as shown in Table 15, further studies will analyze how their contamination influences HDPE properties.

4.2.6.3 LDPE contamination

To analyze the influence of LDPE and LLDPE contamination, vHDPE samples with a defined amount of vLDPE, as well as vLPDE with a defined amount of vLLDPE were prepared, and migration measurements performed.

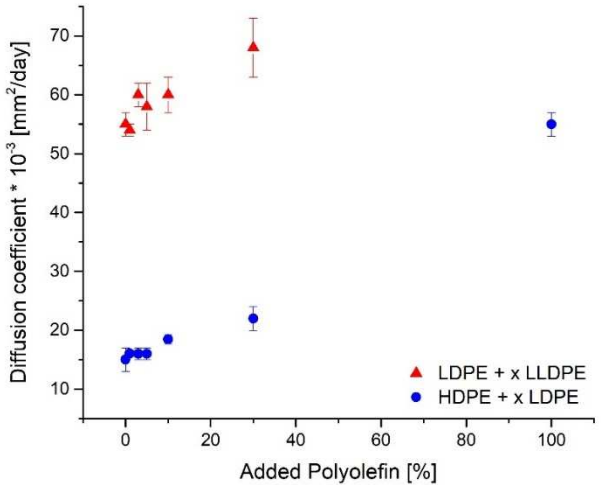

Figure 61 D in PE mixtures.

As shown in Figure 61, D increases with the amount of LDPE added to HDPE. However, between 0 and 10% LDPE in HDPE, only minimal differences in D were observed (Table 26). Since contamination levels in PCR materials are mainly below 10%, LDPE contamination is unlikely to significantly influence migration behavior. Similar results were obtained for LLDPE in LDPE samples.

Table 26 D and MS in PE mixtures.

Added PE (x) [%]	vHDPE + x vLDPE		vLDPE + x vLLDPE	
	$D * 10^{-3}$ [mm^2/day]	MS [%]	$D * 10^{-3}$ [mm^2/day]	MS [%]
0	16.55 ± 0.27	5.3 ± 0.4	55 ± 2	6.0 ± 0.1
1	16.03 ± 0.33	5.0 ± 0.1	54 ± 1	6.1 ± 0.1
3	16 ± 1	5.0 ± 0.1	60 ± 2	6.1 ± 0.1
5	16 ± 1	5.1 ± 0.1	58 ± 4	6.1 ± 0.1
10	18.47 ± 0.78	4.9 ± 0.1	60 ± 3	6.2 ± 0.1
30	22 ± 2	5.0 ± 0.1	68 ± 5	6.3 ± 0.2

While PP and HDPE are immiscible and exhibit distinct and separated peaks in DSC measurements, LDPE and HDPE possess a very similar structure, and are hard to distinguish. In DSC analyses, these two materials produce a single peak, indicative of a homogeneous mixture (Figure 62).

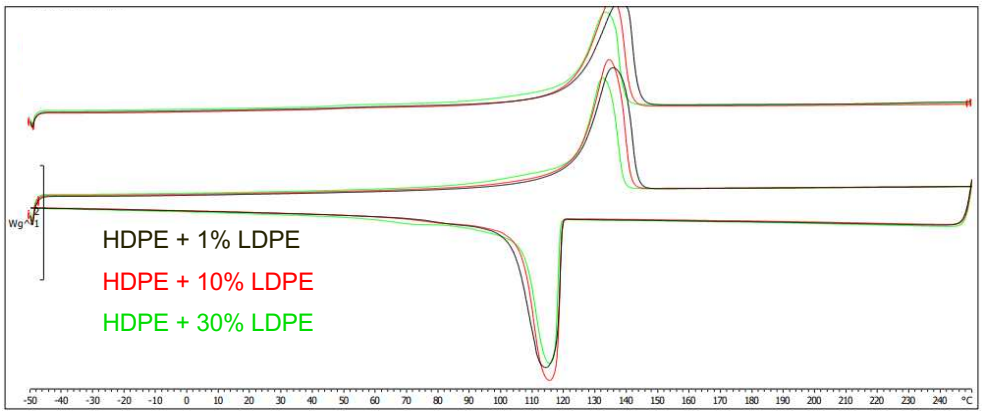

Figure 62 DSC curves of HDPE + LDPE mixtures.

In IR spectroscopy, the band at 2959 cm^{-1} is significant for LDPE but overlapped by PP signals in recycled material (Figure 57). Techniques such as ^{13}C-NMR can be employed for qualitative analysis, but they are not suitable for quantification, as the source of the side chain branches cannot be attributed to specific polymer chains. Similar challenges are faced with LLDPE when mixed with LDPE. Both materials are often blended to improve the processing properties. However, DSC and IR-spectroscopy cannot distinguish or quantify both materials, as they are highly miscible. The miscibility of HDPE, LDPE, and LLDPE is influenced by various factors, including branching content, MW, MWD, and composition distribution [88, 90]. The interaction among these properties and their influence on the miscibility are still unclear, but some assumptions have been made. LDPE, characterized by a somewhat chaotic structure resulting from free radical polymerization, exhibits favorable compatibility with the conformations of highly branched LLDPE. Specifically, LLDPE with a high branching content demonstrates greater miscibility with LDPE of comparable MW and MWD than LLDPE with lower branching content. Additionally, the compositional distribution plays a role in miscibility, for instance, Ziegler-Natta LLDPE is more miscible with LDPE than metallocene LLDPE at equivalent MW and branching content [89]. In terms of LDPE and HDPE miscibility, it has been observed that LDPE with a low branching content of 9 CH_3/1000C is highly miscible with HDPE of the same MW, while a higher branching content of 19 CH_3/1000C leads to changes in viscosity and elastic properties [88]. Overall, the analysis of PE mixtures containing LDPE and LLDPE presents significant challenges and is only accessible for determination of PP contamination. Despite these complexities, D remains constant below 10% contamination, suggesting that LDPE and LLDPE contamination has a negligible influence on the migration process.

4.2.7 Correlation of PE properties

In prior chapters, various thermal and molecular properties of the polymers influencing the migration process were defined. Their correlations are analyzed here using Pearson's r as shown in the heatmaps below (Table 27, Table 29).

Table 27 Pearson's r of properties in HDPE.*

	PP	T_c	T_m	χ	MFR	ρ	MWD	MW	SCB	D
D	0.72	0.37	-0.38	-0.67	0.13	-0.52	0.10	-0.03	0.83	1.00
SCB	0.78	0.09	-0.17	-0.76	0.09	-0.52	0.20	-0.16	1.00	
MW	-0.19	0.01	-0.12	0.15	0.01	-0.15	0.60	1.00		
MWD	-0.08	-0.50	-0.04	-0.27	-0.04	-0.32	1.00			
P	-0.65	0.06	0.26	0.50	-0.06	1.00				
MFR	0.06	-0.05	0.15	-0.04	1.00					
X	-0.67	0.05	0.30	1.00						
T_m	-0.07	-0.64	1.00							
T_c	0.16	1.00								
PP	1.00									

* Pearson's r: +1: positive correlation; -1: negative correlation; 0: no correlation; density (ρ), crystallinity (χ), MWD, MW, MFR at 5.00 kg.

D correlates with specific properties of HDPE materials, including:

- SCB: positive correlation (Pearson's r of 0.83, p-value $9.04*10^{-6}$)
- PP content: positive correlation (Pearson's r of 0.72, p-value $3.61*10^{-5}$)
- Crystallinity: negative correlation (Pearson's r of -0.67, p-value $1{,}76*10^{-4}$)

Increase in SCB and PP content are associated with higher D, while D decreases with increasing crystallinity. The presence of SCB and PP contributes to a less organized polymer structure, resulting in HDPE polymer chains being less capable of achieving an ordered arrangement. This structural disorder leads to a higher amorphous phase and a reduction in the crystalline phase, creating greater interstitial spaces between the polymer chains. Furthermore, SCB measurements allow for the detection and quantification of methyl and methylene groups. The side chains of HDPE, along with the multiple side chains present in LDPE, also account for the methyl groups in PP. Consequently, an increase in PP content correlates with an increase in the amount of SCB. Further, a multiple regression analysis was performed to determine to which extent the three parameters influence D in HDPE (Table 28).

Table 28 Coefficients of PP, SCB and crystallinity in a multiple regression analysis of D (R^2=0.75).

Parameter	Coefficient	Standard error	p-value
Intercept	48	62	0.455
SCB	0.91	0.45	0.064
PP content	2	1	0.130
Crystallinity	-0.58	0.93	0.544

The coefficients in Table 28 confirm the positive correlation of D with SCB and PP content, as well as the negative correlation with crystallinity. Among these, PP content exhibits the highest coefficient, indicating that an increase of one unit in PP content leads to an increase of 2 units in D, suggesting the strongest influence. However, the p-values indicate that no parameter is statistically significant ($p<0,05$). Additionally, the standard errors are notably large relative to the coefficients—particularly for crystallinity, where the standard error is approximately double the size of the coefficient. Such large errors suggest issues with the model and imprecise results, which may arise from several factors. First, multicollinearity could be present, meaning that independent variables are highly correlated. This destabilizes the estimated coefficients, making it difficult to distinguish the individual effects of each parameter and leading to large errors and reduced statistical significance. Second, interactions

between variables could alter the effect of individual parameters, further complicating the analysis. Third, extreme values or outliers might be distorting the coefficient estimates, reducing the precision of the results. Finally, overfitting may occur when the model includes too many parameters. In such cases, the model fits the sample data too closely, which compromises its ability to generalize to other datasets [97, 98]. Since there is a correlation between all three parameters, multicollinearity is present and would not allow the analysis of a multiple regression.

Further evaluation of Table 27 unexpectedly revealed no correlation of MW and MWD with any property of the HDPE materials. High MW would allow higher packing of the polymer chains resulting in higher density and crystallinity, which leads to a low D, but the values and effect of MW and MWD in HDPE must be negligible small. In addition to that, it is important to note that the data regarding density and MFR are sourced from recycling suppliers, which may be incomplete, outdated, or imprecise. Such limitations reduce their utility in correlation with other properties such as SCB, D, and PP content of HDPE. Nonetheless, an increase in SCB and PP content typically results in a less dense material. Last T_m and T_c have not demonstrated a correlation with any other property, as shown in chapter 4.2.4. Typically, an increase in crystallinity would be expected to correlate with an increase in T_m; however, the observed differences in T_m among the materials are too small to establish a significant correlation.

For the impact analysis of all parameters on D, a multiple regression was performed (Table 38). However, similar to the analysis in Table 37 the results are unreliable due to high standard errors and a lack of statistical significance. These issues arise from the limited number of samples relative to the number of parameters tested, as well as multicollinearity, overfitting, and the presence of extreme values. Consequently, this dataset was excluded from further analysis regarding the influence of various parameters on D.

In contrast, when examining the correlations among properties across all PE types, more correlations are observed, driven by structural differences among PE variants (Table 29). HDPE, characterized by minimal branching, allows polymer chains to organize closely, resulting in higher density and crystallinity. In contrast, LDPE and LLDPE possess numerous short and long chain branches, leading to greater spacing between polymer chains and lower density.

Table 29 Pearson's r of properties in PE materials. *

	T_c	T_m	χ	MFR	ρ	MWD	MW	SCB	D
D	-0.50	-0.56	-0.75	0.55	-0.65	-0.42	-0.56	0.63	1.00
SCB	-0.54	-0.59	-0.72	0.18	-0.53	-0.18	-0.49	1.00	
MW	0.74	0.72	0.77	-0.67	0.75	0.80	1.00		
MWD	0.55	0.59	0.56	-0.65	0.64	1.00			
P	0.87	0.87	0.89	-0.85	1.00				
MFR	-0.92	-0.94	-0.87	1.00					
X	0.87	0.89	1.00						
T_m	0.95	1.00							
T_c	1.00								

* Pearson's r: +1: positive correlation; -1: negative correlation; 0: no correlation; density (ρ), crystallinity (χ), MWD, MW, MFR at 5.00 kg.

Key correlations of D include:

- SCB and D: Positive correlation (r=0.63, p-value $2.18*10^{-4}$)
- Crystallinity and D: Negative correlation (r=−0.75, p-value $4.22*10^{-8}$)
- Density and D: Negative correlation (r=−0.65, p-value $6.43*10^{-5}$)

Furthermore, it is observed that higher crystallinity and density, resulting from increased SCB, lead to an increase in T_m and a decrease in MFR. Additionally, higher MW is associated with increases in density, crystallinity, and T_m, and T_c. Specifically, higher MW polymer chains are associated with increased density, as longer chains pack more closely together. This increase in density corresponds to a decrease in MFR, indicating a negative correlation. In conclusion, the properties of PEs are interconnected and collectively influence their behavior, including D. While variations in properties among HDPE samples are minimal, these differences become more pronounced when comparing different types of PEs.

4.3 Migration influenced by the processed PO

4.3.1 Extrusion influence

During the extrusion process, materials are heated to 240 °C for melting and homogenization. At these elevated temperatures, various processes such as chain scission, crosslinking, and branching can occur Table 30 presents data from the analysis of two HDPE materials, one virgin and one recycled, over multiple extrusion cycles, and corresponding migration measurements plotted in Figure 63.

Table 30 $D*10^{-3}$ [mm^2/day], MS [%], crystallinity [%], and T_m [°C] of HDPE materials after zero to eight extrusion cycles.

		0	1	2	3	4	5	6	7	8
vHDPE	D	16.55 ± 0.27	16 ± 1	16.07 ± 0.55	21 ± 3	20 ± 2	21.46 ± 0.50	22 ± 1	21 ± 3	23 ± 2
	MS	5.3 ± 0.4	5.1 ± 0.1	5.1 ± 0.1	5.0 ± 0.1	5.0 ± 0.1	5.1 ± 0.2	5.0 ± 0.1	5.0 ± 0.1	5.0 ± 0.2
	χ	69.5	69.2	68.8	68.9	68.9	69.2	68.7	68.6	68.1
	T_m	133.6	133.6	133.7	133.2	133.7	134.3	133.7	134.5	134.3
rHDPE	D	19 ± 2	18 ± 2	22 ± 2	25 ± 2	24 ± 1	26 ± 3	24 ± 2	25 ± 1	28 ± 4
	MS	4.9 ± 0.1	5.0 ± 0.1	5.0 ± 0.1	4.9 ± 0.1	4.9 ± 0.1	5.0 ± 0.1	5.0 ± 0.1	4.9 ± 0.1	4.9 ± 0.1
	χ	60.6	59.9	61.9	61.8	61.7	61.5	62.2	62.2	60.2
	T_m	132.4	131.9	131.7	131.6	131.7	131.6	131.7	131.6	131.7

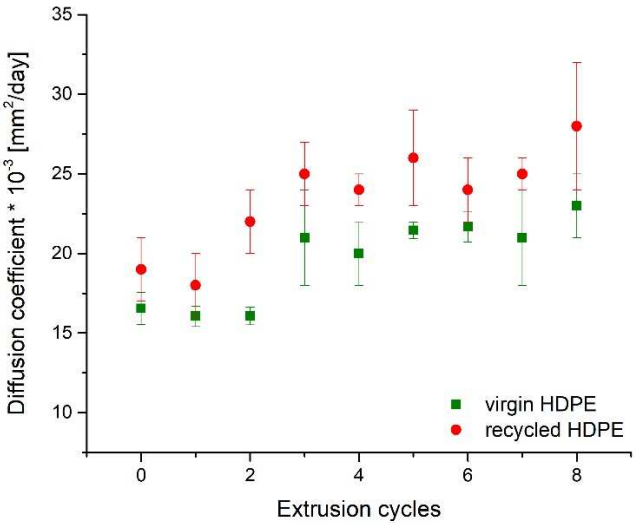

Figure 63 D of virgin and recycled HDPE of different extrusion cycles.

The analysis in Figure 63 indicates an increase in D for both virgin and recycled HDPE. Initially, after the first extrusion cycle, both materials exhibit comparable D values of approximately $17*10^{-3}$ mm²/day. However, over the course of eight extrusion cycles, the recycled HDPE has a higher increase in D, reaching $28*10^{-3}$ mm²/day, while the virgin HDPE reaches a D value of $23*10^{-3}$ mm²/day. Between cycles four to seven, no obvious change in D in either material was observed. Notably, D showed considerable deviations after the eighth cycle, especially for the recycled material, suggesting that degradation processes happened in varying intensities. During the first extrusion cycles, degradation processes such as SCB are likely to take place, contributing to the observed increase in D. Almost constant D values between the fourth and seventh cycle suggest that, although degradation processes may still be active, their influence on migration is negligible [99]. Previous studies have shown, that particularly during the first 30 cycles of extrusion, the material's flowability decreases, indicating that processes like crosslinking and branching are taking place. This results in a substantial change in mechanical properties, for example, MFR drops by 98.8%. After the 35th cycle, flowability increases, likely due to enhanced mobility of the molecules resulting from chain scission [109].

The materials were further analyzed for their T_m and crystallinity, revealing only small differences. While T_m slightly increased from 133.6 to 134.3 °C, the crystallinity slightly decreased from 69.2 to 68.1%. As illustrated in Figure 64, the melting peaks of the materials across different extrusion cycles remain largely unchanged in shape, indicating that no significant structural alterations attributable to chain scission are detectable via DSC.

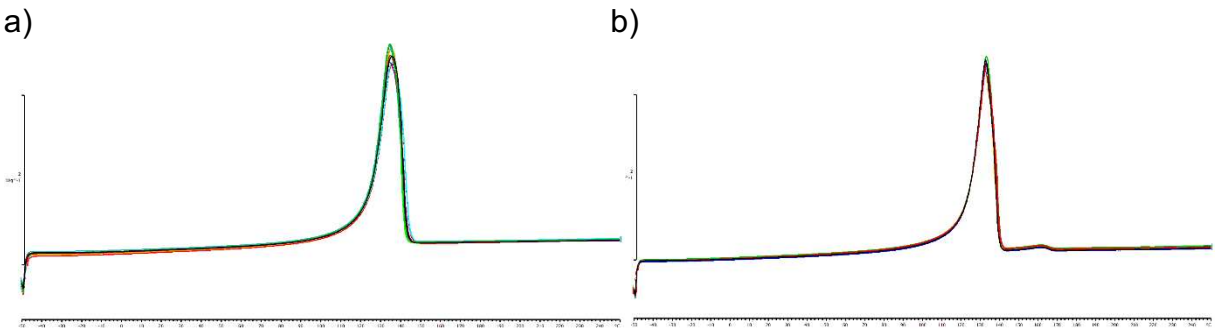

Figure 64 Second DSC heating curve of all extrusion cycles of a) vHDPE and b) rHDPE.

These results were consistent with previous studies, which reported no change in T_m within the first 30 extrusion cycles, with only slight decreases thereafter. Furthermore, crystallinity remains stable over 20 cycles of extrusion, followed by a reduction of approximately 10% and further by 18% after 70 extrusion cycles [99]. This suggests that the molecular ability to form crystalline regions is not reduced as a consequence of cross-linking and chain branching after a certain number of extrusion cycles. Another critical aspect of the analysis is MWD. With an increasing number of extrusion cycles, MWD broadens initially and subsequently decreases after 30 cycles. These changes result from degradation processes during extrusion. MW slowly decreases with the number of extrusion cycles, while MWD only shows minimal variation with repetitive extrusion cycles [100, 104, 107, 109, 110]. In previous studies, the degradation and the influence of extrusion were also analyzed for LLDPE. It was observed that with an increasing number of extrusion cycles, the viscosity increases due to the simultaneous formation of long chain branches and chain scission during degradation processes [92].

4.3.2 Migration in different batches of one material

In recent years, the recycling process has been optimized in terms of duration and temperature, particularly regarding the degassing phase. Additionally, the composition of collected feedstock has evolved over time, influenced by seasonal variations in waste and the introduction of new consumer products. To evaluate the consistency of recycled materials, eight distinct batches of the same recycled material have been analyzed, with results summarized in Table 31.

Table 31 Comparison of migration and polymer properties of different batches of rHDPE 18.

Name	D * 10^{-3} [mm^2/day]	MS [%]	Crystallinity [%]	PP content [%]
rHDPE 18_a	25 ± 2	4.9 ± 0.2	65.7	0.7
rHDPE 18_b	25 ± 3	4.5 ± 0.2	66.4	1.1
rHDPE 18_c	23 ± 1	5.1 ± 0.4	66.1	1.9
rHDPE 18_d	21.17 ± 0.33	4.7 ± 0.1	65.6	1.2
rHDPE 18_e	22.04 ± 0.70	4.6 ± 0.1	66.8	1.8
rHDPE 18_f	23 ± 4	4.8 ± 0.1	67.0	1.7
rHDPE 18_g	21 ± 2	4.5 ± 0.1	64.3	1.6
rHDPE 18_h	23 ± 2	4.5 ± 0.2	65.6	1.2

All batches demonstrate similar results across all measured properties. Notable small variations are observed, for instance in the PP content, which ranges from 0.7% to 1.9%. However, these discrepancies did not impact parameters such as D, MS, or crystallinity. This suggests that the observed differences result from inhomogeneities within the material and the heterogeneous sizes of the tested pellets, as the samples exhibit non-uniform shapes and dimensions. Given that a consistent mass of one gram of the sample is utilized for migration calculations, the variability in pellet sizes likely contributed to increased deviations in the results. Nonetheless, the overall migration behavior among different batches was consistent, as the structural morphology and contamination levels exhibited only minor differences, even when adjustments are made to the recycling process.

4.3.3 Processed shape and masterbatch effects

HDPE is extensively used in the cosmetic industry for packaging applications and can be processed using various manufacturing techniques, including pelletizing after extrusion, injection molding, and extrusion blow molding. Alterations in processing methods may impact migration behavior, making the investigation of these effects particularly relevant. The recycling company's supplier provides materials in the form of granules produced through pelletizing after extrusion. These granules can subsequently be processed into jars or plates via injection molding or bottles via extrusion blow molding (Figure 65).

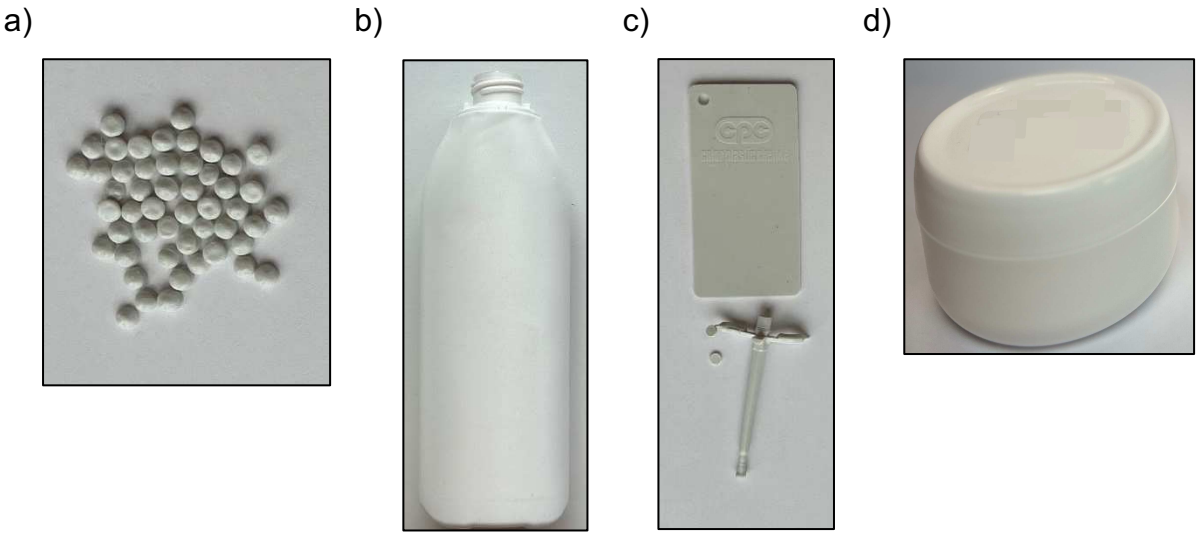

Figure 65 HDPE pellets (a) processed to bottles (b) or injection moldings (c+d).

To assess how different processing methods influence the material's structure and, consequently, the migration process, measurements were conducted, as summarized in Table 32. Samples of the same material were received as granules and further processed to create bottles through blow molding and plates through injection molding. Additionally, many materials are colored for their primary packaging purposes, utilizing various masterbatches (Figure 66). The following table compares different samples in various shapes, with or without masterbatches, concerning the migration of isopropyl palmitate.

Figure 66 vHDPE 3 bottles with no, white and blue MB.

Table 32 D and crystallinity in different HDPE shaped samples and MB.

Name	D * 10^{-3} [mm^2/day]			Crystallinity [%]		
	granules	bottles	IM	granules	bottles	IM
vHDPE 1	10.08 ± 0.98	-	9.24 ± 0.80	69.2	-	70.0
rHDPE 2	15.71 ± 0.21	-	14 ± 1	65.9	-	65.2
vHDPE 3 (natural)	10.12 ± 0.46	8.76 ± 0.65	9.08 ± 0.82	67.7	70.05	69.5
vHDPE 3_ bottle white	-	10.15 ± 0.90	-	-	67.7	-
vHDPE 3_ bottle blue	-	8.71 ± 0.20	-	-	69.6	-

No substantial difference in D were observed between the granules and the IM samples, indicating that processing these materials does not significantly alter the polymer structure for vHDPE 1 and rHDPE 2. In case of vHDPE 3, a slight decrease in D was noted when the material was processed into a bottle, accompanied by a small increase in crystallinity, which may account for the observed reduction in D. D and crystallinity of the IM samples (vHDPE 1, rHDPE 2) fall within the range of the values for granules and bottles. While minor deviations in D were observed, the differences among granules, bottles, and IM samples are still considered negligibly small. Furthermore, the incorporation of MB did not significantly impact the polymer structure between the blue and natural bottles; however, a minor increase in D for the white bottle was noted, attributed to a reduction in crystallinity. Again, these variations were minimal and did not significantly influence the migration of cosmetic components.

4.3.4 Mixtures of HDPE materials

The results so far indicate that virgin materials typically exhibit greater resistance to migration processes compared to recycled materials, which often demonstrate higher migration rates. To enhance the performance of recycled materials and address the issue of elevated D values, new materials were developed by blending virgin and recycled HDPE. Specifically, vHDPE 3 was combined with varying proportions of recycled materials, namely rHDPE 22 and rHDPE 23, at concentrations of 50% and 70% (Figure 67). The results of the migration measurements and crystallinity analyses are presented in Table 33.

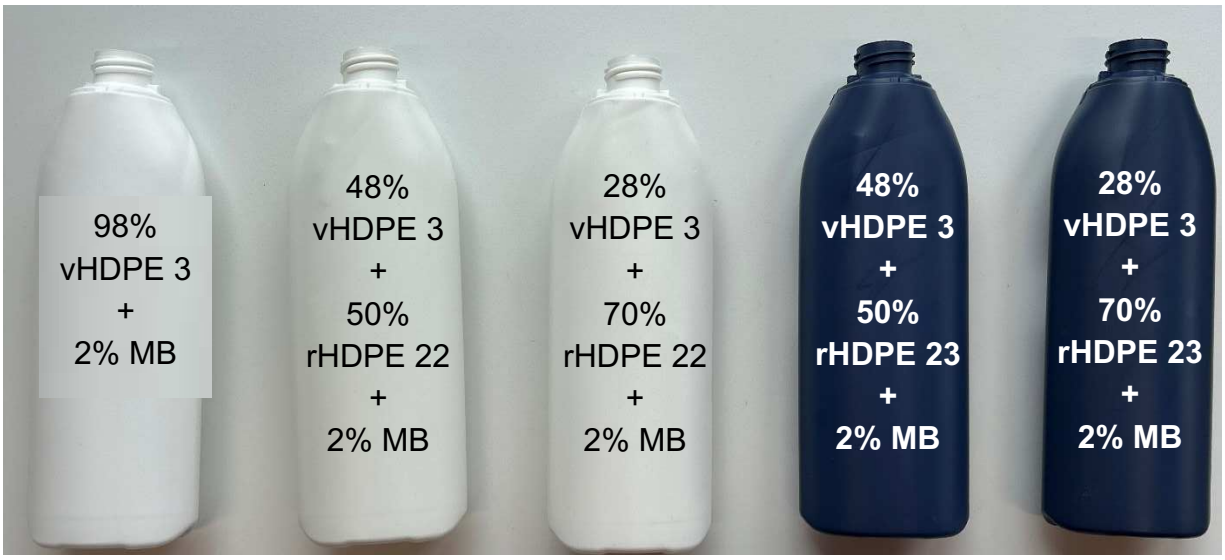

Figure 67 Bottles made of virgin and recycled HDPE.

Table 33 D and MS in mixtures of virgin and PCR material.

PCR [%]	D * 10^{-3} [mm^2/day]			Crystallinity [%]		
	vHDPE 3	rHDPE 22	rHDPE 23	vHDPE 3	rHDPE 22	rHDPE 23
0	10.15 ± 0.90	-	-	69.8	-	-
50	-	9.35 ± 0.92	10.27 ± 0.50	-	69.9	68.2
70	-	10 ± 1	11.91 ± 0.14	-	68.7	67.5

Migration measurements of the bottles from polymer blends indicate that D shows minimal variation with increased concentrations of PCR material. Neither of the PCR materials significantly influences migration behavior. Unlike findings in previous studies, which typically found that recycled materials exhibited higher D than virgin materials, the PCR materials analyzed in this study demonstrate a structure similar to virgin material. Consequently, their migration behavior was comparable to virgin materials, making them suitable substitutes for virgin HDPE in cosmetic packaging applications.

5 Summary

The interaction between cosmetic products and packaging materials is a critical issue in various industries, particularly in cosmetics. This study investigated key factors influencing the migration of product components into the packaging material to better understand the process.

The research focused on HDPE samples, as it is widely used to manufacture cosmetic bottles from both virgin and recycled sources. To assess migration variations across different HDPE samples, other POs were included for comparison. Migration measurements determined the diffusion coefficient as a comparative parameter for different polymer materials, various migration components, and their conditions.

Initially, product properties were analyzed for their migration behavior. Various components, primarily oils, displayed migration patterns influenced by polarity, molecular size, and viscosity. Smaller and more non-polar molecules demonstrated a faster migration. Further migration measurements under various environmental conditions, including those embedded in emulsions, revealed that higher temperatures and smaller emulsion droplet sizes facilitate faster oil migration. In emulsions, oil-based systems enabled faster migration compared to a water-based emulsions. The diffusion process of oils was facilitated when the oil formed the continuous phase in direct contact with the packaging wall. Other emulsion components, such as thickening emollients and emulsifiers, and their variations in the choice and concentration showed no impact on oil migration. These findings were consistent in all measured PO materials.

The study also observed differences in migration behavior across different PO samples. For comparative analysis, isopropyl palmitate at 40 °C was used as a model. The diffusion coefficient and oil uptake varied across POs. PP exhibited the highest oil uptake, followed by LDPE, LLDPE, and HDPE, correlating with material density. Lower-density materials, like PP, had greater inter-chain spacing, facilitating oil migration, while virgin and recycled HDPE showed migration but exhibited no differences in oil uptake. Conversely, migration speed, defined by the diffusion coefficient, did not correlate with oil uptake. Migration was fastest in LLDPE and LDPE, followed by HDPE, and slowest in PP. Thereby, recycled materials consistently

exhibited faster migration than virgin materials of the same type, showing a wide range of diffusion coefficients. Various properties were observed to understand the differences in migration behavior of HDPE. The key parameters influencing the migration included:

- Contamination with PP (0–10%),
- Molecular structure variations, such as the amount of short-chain branches, and
- Polymer crystallinity.

Lower crystallinity correlated with higher PP contamination or increased short-chain branching, both of which enhanced migration rates. These parameters are particularly significant in recycled materials due to inadequate separation processes of POs, other contaminants, and structural alterations during extrusion. Overall, recycled materials are inherently complex, with migration behavior driven by multiple factors, including feedstock, recycling methods, composition, and processing conditions, all of which influence the structure. Other properties, like molecular weight, molecular weight distribution, and contamination with other organic and inorganic substances, as well as mechanical properties, showed no correlation with the diffusion coefficient.

Finally, the effect of material processing on oil migration was evaluated. Pellet samples were compared with IM pellets and extrusion blow molded bottles. No differences were observed in oil uptake and diffusion coefficient. Furthermore, the addition of a masterbatch also did not exhibit a correlation with migration behavior and was considered negligible.

In conclusion, these results provide a comprehensive methodology for evaluating and monitoring the migration of cosmetic components into packaging materials. Differences within polymers, virgin and recycled materials, cosmetic components, and environmental conditions were analyzed. Specific parameters influencing the migration process were identified, offering potential strategies to minimize or prevent migration. However, polymers, particularly recycled ones, are complex systems with variable molecular structures and compositions that influence the migration behavior.

6 Zusammenfassung

Die Interaktion zwischen kosmetischen Produkten und Verpackungsmaterialien stellt ein zentrales Thema in verschiedenen Branchen dar, insbesondere in der Kosmetikindustrie. Diese Studie untersucht die wesentlichen Faktoren, die die Migration von Produktkomponenten in das Verpackungsmaterial beeinflussen, um den zugrunde liegenden Prozess besser zu verstehen.

Der Fokus der Forschung lag auf HDPE-Proben, da dieses Material häufig zur Herstellung von kosmetischen Flaschen aus sowohl virgin als auch recycelten Materialien verwendet wird. Um das Migrationsverhalten zwischen verschiedenen HDPE-Proben zu bewerten, wurden auch andere Polyolefine zum Vergleich herangezogen. Die Migrationsmessungen ermöglichten die Bestimmung des Diffusionskoeffizienten als vergleichbaren Parameter für unterschiedliche Polymermaterialien, verschiedene Migrationskomponenten sowie deren Bedingungen und Zusammensetzungen.

Zunächst wurden die Produkteigenschaften hinsichtlich ihres Migrationsverhaltens analysiert. Verschiedene Komponenten, insbesondere Öle, zeigten, dass die Migration von Polarität, Molekülgröße und Viskosität beeinflusst wurde. Kleinere und weniger polare Moleküle wiesen eine schnellere Migration auf. Weitere Messungen unter verschiedenen Umweltbedingungen, einschließlich solcher in Emulsionen, zeigten, dass höhere Temperaturen und kleinere Emulsionströpfchen die Ölmigration beschleunigen. In Emulsionen ermöglichten ölbasierten Systeme eine schnellere Migration im Vergleich zu wasserbasierten Emulsionen, da das Öl als kontinuierliche Phase in direktem Kontakt mit der Verpackungswand steht. Andere Emulsionskomponenten, wie unterschiedliche Verdicker und Emulgatoren in verschiedenen Konzentrationen, hatten keinen Einfluss auf die Ölmigration. Diese Ergebnisse waren in allen gemessenen Polyolefinen konsistent.

Die Studie beobachtete zudem Unterschiede im Migrationsverhalten zwischen verschiedenen Polyolefinen. Für die vergleichende Analyse wurde Isopropyl Palmitat bei 40 °C als Modell verwendet. Der Diffusionskoeffizient und die Ölaufnahme variierten zwischen den Polyolefinen. PP wies die höchste Ölaufnahme auf, gefolgt von LDPE, LLDPE und HDPE, was negativ mit der Materialdichte korrelierte. Materialien mit niedrigerer Dichte, wie PP, hatten einen größeren Abstand der

Polymerketten, was die Ölmigration erleichterte. Zwischen virgin und recyceltes HDPE gab es jedoch keine Unterschiede in der Menge des aufgenommenen Öls. Im Gegensatz dazu konnte keine Korrelation der Diffusionsgeschwindigkeit und der aufgenommenen Menge Öl beobachtet werden. Die Migration war in LLDPE und LDPE am schnellsten, gefolgt von HDPE und am langsamsten in PP. Recycelte Materialien wiesen dabei konsistent eine schnellere Migration auf als virgin Materialien desselben Polyolefins und zeigten deutlich größere Unterschiede im Diffusionskoeffizienten. Um die Unterschiede im Migrationsverhalten von HDPE zu verstehen, wurden verschiedene Eigenschaften untersucht. Die Schlüsselfaktoren, die die Migration beeinflussen, umfassen:

- Kontamination mit PP (0–10%),
- Variationen in der molekularen Struktur, wie die Menge an kurzkettigen Verzweigungen, und
- Polymerkristallinität.

Eine niedrigere Kristallinität korrelierte mit einer höheren PP-Kontamination oder einer größeren Anzahl an kurzkettigen Verzweigungen, die beide die Migrationsraten erhöhten. Diese Parameter sind besonders signifikant in recycelten Materialien aufgrund unzureichender Trennprozesse von POs, anderer Kontaminanten und struktureller Veränderungen während der Extrusion. Insgesamt sind recycelte Materialien von Natur aus komplexer, wobei das Migrationsverhalten von mehreren Faktoren beeinflusst wird, einschließlich Rohstoffen, Recyclingmethoden, Zusammensetzung und Verarbeitungsbedingungen, die die Struktur beeinflussen. Andere Eigenschaften, wie Molekulargewicht, Molekulargewichtsverteilung und Kontamination mit anderen organischen und anorganischen Substanzen sowie mechanische Eigenschaften, zeigten keine Korrelation mit dem Diffusionskoeffizienten.

Abschließend wurde der Einfluss der Materialverarbeitung auf die Ölmigration bewertet. Pellets wurden mit Spritzguss-Pellets (IM) und extrusionsgeblasenen Flaschen verglichen. Es wurden keine Unterschiede in der Ölaufnahme und dem Diffusionskoeffizienten beobachtet. Darüber hinaus zeigte die Zugabe eines Masterbatches ebenfalls keine Korrelation mit dem Migrationsverhalten und wurde als vernachlässigbar angesehen.

Die vorliegende Arbeit bietet eine umfassende Methodik zur Analyse der Migration von kosmetischen Komponenten in Verpackungsmaterialien. Es wurden Unterschiede zwischen verschiedenen Polymeren, einschließlich virgin und recycelten Materialien, kosmetischen Komponenten und Umweltbedingungen analysiert. Dabei konnten spezifische Parameter identifiziert werden, die den Migrationsprozess beeinflussen, was potenzielle Strategien zur Minimierung oder Vermeidung von Migration ermöglicht. Es ist jedoch zu beachten, dass Polymere, insbesondere recycelte, komplexe Systeme mit variablen molekularen Strukturen und Zusammensetzungen sind, die das Migrationsverhalten maßgeblich beeinflussen.

7 Indices

7.1 List of tables

7.2 List of figures

7.3 List of equations

References

1. Seymour, R.B. and C.E. Carraher, *Properties of Polyolefins*, in *Structure—Property Relationships in Polymers*, R.B. Seymour and C.E. Carraher, Editors. 1984, Springer US: Boston, MA. p. 133-145.
2. Eriksen, M.K. and T.F. Astrup, *Characterisation of source-separated, rigid plastic waste and evaluation of recycling initiatives: Effects of product design and source-separation system.* Waste Manag, 2019. **87**: p. 161-172.
3. Eriksen, M.K., J.D. Christiansen, A.E. Daugaard, and T.F. Astrup, *Closing the loop for PET, PE and PP waste from households: Influence of material properties and product design for plastic recycling.* Waste Manag, 2019. **96**: p. 75-85.
4. Abbas-Abadi, M.S., M.N. Haghighi, and H. Yeganeh, *Effect of the melt flow index and melt flow rate on the thermal degradation kinetics of commercial polyolefins.* Journal of Applied Polymer Science, 2012. **126**(5): p. 1739-1745.
5. Zahedi, M., M. Ahmadi, and M. Nekoomanesh, *Influence of molecular weight distribution on flow properties of commercial polyolefins.* Journal of Applied Polymer Science, 2008. **108**(6): p. 3565-3571.
6. Elgharbawy, A.S. and R.M. Ali, *A comprehensive review of the polyolefin composites and their properties.* Heliyon, 2022. **8**(7): p. e09932.
7. Tumu, K., K. Vorst, and G. Curtzwiler, *Understanding intentionally and non-intentionally added substances and associated threshold of toxicological concern in post-consumer polyolefin for use as food packaging materials.* Heliyon, 2024. **10**(1): p. e23620.
8. Schyns, Z.O.G. and M.P. Shaver, *Mechanical Recycling of Packaging Plastics: A Review.* Macromol Rapid Commun, 2021. **42**(3): p. e2000415.
9. Kenneth S. Whiteley, T.G.H., Hartmut Koch, Ralph L. Mawer, Wolfgang Immel, *Polyolefins*. 2000: Ullmann's Encyclopedia of Industrial Chemistry. p. A21_487.
10. Kotek, R., M. Afshari, H. Avci, and M. Najafi, *7 - Production of polyolefins*, in *Polyolefin Fibres (Second Edition)*, S.C.O. Ugbolue, Editor. 2017, Woodhead Publishing. p. 189-264.
11. Gugumus, F., *Physico-chemical aspects of polyethylene processing in an open mixer.* Polymer Degradation and Stability, 2005. **87**: p. 449-463.
12. Laria, J.G., R. Gaggino, J. Kreiker, L.E. Peisino, M. Positieri, and A. Cappelletti, *Mechanical and processing properties of recycled PET and LDPE-HDPE composite materials for building components.* Journal of Thermoplastic Composite Materials, 2020. **36**(1): p. 418-431.
13. Jose, S., A.S. Aprem, B. Francis, M.C. Chandy, P. Werner, V. Alstaedt, and S. Thomas, *Phase morphology, crystallisation behaviour and mechanical properties of isotactic polypropylene/high density polyethylene blends.* European Polymer Journal, 2004. **40**(9): p. 2105-2115.
14. Cho, K., B.H. Lee, K.-M. Hwang, H. Lee, and S. Choe, *Rheological and mechanical properties in polyethylene blends.* Polymer Engineering & Science, 1998. **38**(12): p. 1969-1975.
15. Huang, D.E., A.P. Kotula, C.R. Snyder, and K.B. Migler, *Crystallization Kinetics in an Immiscible Polyolefin Blend.* Macromolecules, 2022. **55**(24).
16. Wang, Y.-h., W.-h. Wang, Z. Zhang, L. Xu, and P. Li, *Study of the glass transition temperature and the mechanical properties of PET/modified silica nanocomposite by molecular dynamics simulation.* European Polymer Journal, 2016. **75**: p. 36-45.

17. Thomsen, T.B., C.J. Hunt, and A.S. Meyer, *Standardized method for controlled modification of poly (ethylene terephthalate) (PET) crystallinity for assaying PET degrading enzymes.* MethodsX, 2022. **9**: p. 101815.
18. Furukawa, T., H. Sato, Y. Kita, K. Matsukawa, H. Yamaguchi, S. Ochiai, H. Siesler, and Y. Ozaki, *Molecular Structure, Crystallinity and Morphology of Polyethylene/Polypropylene Blends Studied by Raman Mapping, Scanning Electron Microscopy, Wide Angle X-Ray Diffraction, and Differential Scanning Calorimetry.* Polymer Journal, 2006. **38**: p. 1127-1136.
19. Rojas, G., E.B. Berda, and K.B. Wagener, *Precision polyolefin structure: Modeling polyethylene containing alkyl branches.* Polymer, 2008. **49**(13-14): p. 2985-2995.
20. Vassallo, N. and P. Refalo, *Reducing the Environmental Impacts of Plastic Cosmetic Packaging: A Multi-Attribute Life Cycle Assessment.* Cosmetics, 2024. **11**(2).
21. Gatt, I.J. and P. Refalo, *Reusability and recyclability of plastic cosmetic packaging: A life cycle assessment.* Resources, Conservation & Recycling Advances, 2022. **15**: p. 200098.
22. Santos, A.S.F., J.A.M. Agnelli, D.W. Trevisan, and S. Manrich, *Degradation and stabilization of polyolefins from municipal plastic waste during multiple extrusions under different reprocessing conditions.* Polymer Degradation and Stability, 2002. **77**(3): p. 441-447.
23. Fazylzyanova, G.R., E.S. Okhotnikova, Y.M. Ganeeva, T.N. Yusupova, I.N. Frolov, and Y.L. Karabut, *Sorption Properties of Recycled Polyethylenes and Their Thermal Behavior in the Mixture with Oil.* Polymer Science, Series A, 2022. **64**(6): p. 633-640.
24. Zengeya, P., K. Mao, and V. Goodship, *The effects of cooling rate (mould temperature) on HDPE gears produced through injection moulding.* Wear, 2023. **530-531**: p. 205000.
25. Lin, S.-K., *Handbook of Polymers. By George Wypych*. Polymers. Vol. 5. 2012: ChemTec Publishing.
26. Shenoy, A.V. and D.R. Saini, *Melt flow index: More than just a quality control rheological parameter. Part I.* Advances in Polymer Technology, 1986. **6**(1): p. 1-58.
27. Bradley, E.C., L., *An Investigation into the Reaction and Breakdown Products from Starting Substances used to Produce Food Contact Plastics*, in *Central Science Laboratory SAC Commercial Ltd*. 2007: Food Standards Agency: London, UK.
28. Wong, O.-W.L.S.-K., *Contamination in food from packaging material.* Journal of Chromatography A, 2000. **882**: p. 255-270.
29. Murat, P., S. Harohalli Puttaswamy, P.J. Ferret, S. Cosledan, and V. Simon, *Identification of Potential Extractablesand Leachables in Cosmetic Plastic Packagingby Microchambers-Thermal Extraction and Pyrolysis-Gas Chromatography-Mass Spectrometry.* Molecules, 2020. **25**(9).
30. Achilias, D., E.V. Antonakou, C. Roupakias, P. Megalokonomos, and A. Lappas, *Recycling techniques of polyolefins from plastic wastes.* Global Nest Journal, 2008. **10**: p. 114-122.
31. Baird, D.G. and D.I. Collias, *Polymer Processing: Principles and Design*. 2014: Wiley.
32. Bharath Kumar, B.R., M. Doddamani, S.E. Zeltmann, N. Gupta, M.R. Ramesh, and S. Ramakrishna, *Processing of cenosphere/HDPE syntactic foams using an industrial scale polymer injection molding machine.* Materials & Design, 2016. **92**: p. 414-423.

33. Usman, M. and A.S. Siddiqui, *Blow Molding of Polyethylene*, in *Handbook of Industrial Polyethylene and Technology*. 2017. p. 475-534.
34. Service, E.P.R. *Revision of the Packaging and Packaging Waste Directive*. 2023 30.11.2023]; Available from: https://www.europarl.europa.eu/RegData/etudes/BRIE/2023/745707/EPRS_BRI(2023)745707_EN.pdf.
35. Manufacturers, P.E.-A.o.P. *Plastics – the Facts 2021*. 2021 30.11.2023]; Available from: https://plasticseurope.org/knowledge-hub/plastics-the-facts-2021/.
36. Manufacturers, P.E.-A.o.P. *The Circular Economy for Plastics – A European Overview 2022*. 2022 30.11.2023]; Available from: https://plasticseurope.org/knowledge-hub/the-circular-economy-for-plastics-a-european-overview-2/.
37. OECD, *Global Plastics Outlook*. 2022.
38. Thomas Hundertmark, M.M., Chris McNally, Theo Jan Simons, Christof Witte. *How plastics waste recycling could transform the chemical industry*. 2018 06.03.2024]; Available from: https://www.mckinsey.com/industries/chemicals/our-insights/how-plastics-waste-recycling-could-transform-the-chemical-industry#/.
39. Reports, M.I.I. *Analyse der Marktgröße und des Anteils von Kosmetikverpackungen - Wachstumstrends und Prognosen (2023 - 2028)*. 2023 30.11.2023]; Available from: https://www.mordorintelligence.com/de/industry-reports/global-cosmetic-packaging-market-industry.
40. Research, Z.M. *Global Cosmetic Products Market Will Reach USD 863 Billion by 2024: Zion Market Research*. 2018 30.11.2023]; Available from: https://www.globenewswire.com/news-release/2018/06/22/1528369/0/en/Global-Cosmetic-Products-Market-Will-Reach-USD-863-Billion-by-2024-Zion-Market-Research.html.
41. comission, E. *Packaging Waste*. 2022 [cited 2024 07.08.2024]; Available from: https://environment.ec.europa.eu/topics/waste-and-recycling/packaging-waste_en#objectives.
42. Manufacturers, P.E.-A.o.P. *Plastics – the Facts 2022*. 2022 07.03.2024]; Available from: https://plasticseurope.org/knowledge-hub/plastics-the-facts-2022/.
43. Thompson, R.C., C.J. Moore, F.S. vom Saal, and S.H. Swan, *Plastics, the environment and human health: current consensus and future trends.* Philos Trans R Soc Lond B Biol Sci, 2009. **364**(1526): p. 2153-66.
44. Craft, C., *Next generation of sustainable packaging for Danish skincare scale-up*. 2022, LUND UNIVERSITY; Packaging Logistics.
45. Vrabič-Brodnjak, U. and I. Jestratijević, *The future of baby cosmetics packaging and sustainable development: A look at sustainable materials and packaging innovations – A systematic review.* Sustainable Development, 2023. **32**(3): p. 2208-2222.
46. Feil, A. and T. Pretz, *Mechanical recycling of packaging waste*, in *Plastic Waste and Recycling: Environmental Impact, Societal Issues, Prevention, and Solutions*. 2020. p. 283-319.
47. Alavi, S.A.R., M.T. Angaji, and Z. Gholami, *Twin-Screw Extruder and Effective Parameters on the HDPE Extrusion Process.* World Academy of Science, Engineering and Technology, International Journal of Chemical, Molecular, Nuclear, Materials and Metallurgical Engineering, 2009. **3**: p. 60-63.

48. Gryn'ova, G., J.L. Hodgson, and M.L. Coote, *Revising the mechanism of polymer autooxidation.* Org Biomol Chem, 2011. **9**(2): p. 480-90.
49. Alzerreca, M., M. Paris, O. Boyron, D. Orditz, G. Louarn, and O. Correc, *Mechanical properties and molecular structures of virgin and recycled HDPE polymers used in gravity sewer systems.* Polymer Testing, 2015. **46**: p. 1-8.
50. Venkataramani, D., A. Tsulaia, and S. Amin, *Fundamentals and applications of particle stabilized emulsions in cosmetic formulations.* Adv Colloid Interface Sci, 2020. **283**: p. 102234.
51. Goodarzi, F. and S. Zendehboudi, *A Comprehensive Review on Emulsions and Emulsion Stability in Chemical and Energy Industries.* The Canadian Journal of Chemical Engineering, 2018. **97**(1): p. 281-309.
52. Tadros, T.F., *Emulsion Formation and Stability*. 2013: Wiley.
53. Hayase, M., *Chapter 10 - Introduction to Cosmetic Materials*, in *Cosmetic Science and Technology*, K. Sakamoto, et al., Editors. 2017, Elsevier: Amsterdam. p. 149-154.
54. Vold, R.D. and R.C. Groot, *Parameter of Emulsions Satbility.* Journal of Cosmetic Science, 1962. **14**(5): p. 233-244.
55. Terescenco, D., G. Savary, C. Picard, F. Clemenceau, E. Merat, and M. Grisel, *Influence of the emollient on emulsions containing lamellar liquid crystals: from molecular organization towards applicative properties.* International Journal of Cosmetic Science, 2018. **40**(6): p. 565-574.
56. Li, Y., Z. Zhou, X. Zhao, H. Zhao, and X. Qu, *The rheological and skin sensory properties of cosmetic emulsions: Influence of thickening agents.* Journal of Cosmetic Science, 2018. **69**(1): p. 67-75.
57. Isaac, V.L.B., L.C. Cefali, B.G. Chiari, M.G.J. Almeida, H.M. Ribeiro, and M.A. Corrêa, *Effect of Various Thickening Agents on the Rheological Properties of Oil-in-Water Emulsions Containing Nonionic Emulsifier.* Journal of Dispersion Science and Technology, 2013. **34**(6): p. 880-885.
58. Groh, K.J., T. Backhaus, B. Carney-Almroth, B. Geueke, P.A. Inostroza, A. Lennquist, H.A. Leslie, M. Maffini, D. Slunge, L. Trasande, A.M. Warhurst, and J. Muncke, *Overview of known plastic packaging-associated chemicals and their hazards.* Sci Total Environ, 2019. **651**(Pt 2): p. 3253-3268.
59. Geueke, B., K. Groh, and J. Muncke, *Food packaging in the circular economy: Overview of chemical safety aspects for commonly used materials.* Journal of Cleaner Production, 2018. **193**: p. 491-505.
60. Bereketoglu, C. and A. Pradhan, *Plasticizers: negative impacts on the thyroid hormone system.* Environ Sci Pollut Res Int, 2022. **29**(26): p. 38912-38927.
61. Ercan, O. and G. Tarcin, *Overview on Endocrine disruptors in food and their effects on infant's health.* Global Pediatrics, 2022. **2**: p. 100019.
62. Hahladakis, J.N., E. Iacovidou, and S. Gerassimidou, *An overview of the occurrence, fate, and human risks of the bisphenol-A present in plastic materials, components, and products.* Integrated Environmental Assessment and Management, 2023. **19**(1): p. 45-62.
63. Fasano, E., F. Bono-Blay, T. Cirillo, P. Montuori, and S. Lacorte, *Migration of phthalates, alkylphenols, bisphenol A and di(2-ethylhexyl)adipate from food packaging.* Food Control, 2012. **27**(1): p. 132-138.
64. Gimeno, P., A.F. Maggio, C. Bousquet, A. Quoirez, C. Civade, and P.A. Bonnet, *Analytical method for the identification and assay of 12 phthalates in cosmetic products: application of the ISO 12787 international standard "Cosmetics-Analytical methods-Validation criteria for analytical results using chromatographic techniques".* J Chromatogr A, 2012. **1253**: p. 144-53.

65. Rochman, C.M., E. Hoh, B.T. Hentschel, and S. Kaye, *Long-term field measurement of sorption of organic contaminants to five types of plastic pellets: implications for plastic marine debris.* Environ Sci Technol, 2013. **47**(3): p. 1646-54.
66. Fahr, A., *Voigt Pharmazeutische Technologie*. 2015, Deutscher Apotheker Verlag: Stuttgart.
67. Gupta, R.K., S. Pipliya, S. Karunanithi, G.M. Eswaran U, S. Kumar, S. Mandliya, P.P. Srivastav, T. Suthar, A.M. Shaikh, E. Harsányi, and B. Kovács, *Migration of Chemical Compounds from Packaging Materials into Packaged Foods: Interaction, Mechanism, Assessment, and Regulations.* Foods, 2024. **13**(19): p. 3125.
68. Felgel-Farnholz, A., A. Schweighuber, C.W. Klampfl, and J. Fischer, *Comparative study on the degradation of HDPE, LLDPE and LDPE during multiple extrusions.* Polymer Degradation and Stability, 2023. **216**: p. 110486.
69. Sinha, V., M.R. Patel, and J.V. Patel, *Pet Waste Management by Chemical Recycling: A Review.* Journal of Polymers and the Environment, 2010. **18**(1): p. 8-25.
70. Ferreira, A.M., I. Sucena, V. Otero, E.M. Angelin, M.J. Melo, and J.A.P. Coutinho, *Pretreatment of Plastic Waste: Removal of Colorants from HDPE Using Biosolvents.* Molecules, 2021. **27**(1): p. 1-18.
71. Rodgers, J.L. and W.A. Nicewander, *Thirteen Ways to Look at the Correlation Coefficient.* The American Statistician, 1988. **42**(1): p. 59-66.
72. Brandsch, R., M. Pemberton, D. Schuster, and F. Welle, *Impact of partitioning in short-term food contact applications focused on polymers in support of migration modelling and exposure risk assessment.* Molecules, 2022. **27**(1).
73. Wang, C., S. Liu, J. Wu, and Z. Li, *Effects of temperature-dependent viscosity on fluid flow and heat transfer in a helical rectangular duct with a finite pitch.* Brazilian Journal of Chemical Engineering, 2014. **31**(3): p. 787-797.
74. Iwahashi, M. and Y. Kasahara, *Dynamic molecular movements and aggregation structures of lipids in a liquid state.* Current Opinion in Colloid & Interface Science, 2011. **16**(5): p. 359-366.
75. Kunststoffedirekt, *Technisches Datenblatt-Polyethylen PE-HD* 2017: Essen.
76. Wypych, G., *PP polypropylene*, in *Handbook of Polymers*, G. Wypych, Editor. 2012, Elsevier: Oxford. p. 479-486.
77. Araújo, E.C.C., E.R. Silveira, M.A.S. Lima, M.A. Neto, I.L. de Andrade, M.A.A. Lima, G.M.P. Santiago, and A.L.M. Mesquita, *Insecticidal Activity and Chemical Composition of Volatile Oils from Hyptis martiusii Benth.* Journal of Agricultural and Food Chemistry, 2003. **51**(13): p. 3760-3762.
78. Peng, C.T., *Prediction of retention indices: V. Influence of electronic effects and column polarity on retention index.* Journal of Chromatography A, 2000. **903**(1): p. 117-143.
79. Andriamaharavo, N.R. *Retention Data. NIST Mass Spectrometry Data Center*. 2014 [cited 30.11.2023; Available from: https://webbook.nist.gov/cgi/cbook.cgi?Source=2014AND%2319410M&Mask=2792.
80. Korhonen, I.O.O., *Gas-liquid chromatographic analyses. XLV. Retention behaviour of C1-C12 n-alkyl esters of benzoic, 4-nitrobenzoic and 3,5-dinitrobenzoic acids on SE-30 and OV-351 capillary columns.* Journal of Chromatography A, 1986. **356**(C): p. 285-299.
81. Bizzo, H.R., N.S. Brilhante, Y. Nolvachai, and P.J. Marriott, *Use and abuse of retention indices in gas chromatography.* Journal of Chromatography A, 2023. **1708**: p. 464376.

82. Landault, C. and G. Guiochon, *Séparation des amines par chromatographie gaz—liquide en utilisant le teflon comme support.* Journal of Chromatography A, 1964. **13**: p. 327-336.
83. Golovnya, R.V., T.E. Kuz'menko, and A.L. Samusenko, *Gas-chromatographic method of evaluation ofn-alkanol ability for self-association in pure liquid.* Russian Chemical Bulletin, 2000. **49**(2): p. 317-320.
84. Cakir, M.F., *An inexpensive contact angle measurement system.* Revista Mexicana de Física, 2022. **68**(2 Mar-Apr).
85. Arzhakova, O.V., A.Y. Kopnov, A.I. Nazarov, A.A. Dolgova, and A.L. Volynskii, *"Green" environmental crazing of polymers in oil-in-water emulsions with high water content.* Polymer, 2020. **186**: p. 122020.
86. Mörters, P. and Y. Peres, *Brownian Motion*. 2010: Cambridge University Press.
87. Zhang, J., V. Hirschberg, and D. Rodrigue, *Blending Recycled High-Density Polyethylene HDPE (rHDPE) with Virgin (vHDPE) as an Effective Approach to Improve the Mechanical Properties.* Recycling, 2023. **8**(1).
88. Hameed, T. and I.A. Hussein, *Effect of Short Chain Branching of LDPE on its Miscibility with Linear HDPE.* Macromolecular Materials and Engineering, 2004. **289**(2): p. 198-203.
89. Elhrari, W., *The Influence of LDPE Content on the Mechanical Properties of HDPE/LDPE Blends.* Research & Development in Material Science, 2018. **7**(5).
90. Hussein, I.A., T. Hameed, B.F.A. Sharkh, and K. Mezghani, *Miscibility of hexene-LLDPE and LDPE blends: influence of branch content and composition distribution.* Polymer, 2003. **44**(16): p. 4665-4672.
91. Gu, J., H. Xu, and C. Wu, *Thermal and Crystallization Properties of HDPE and HDPE/PP Blends Modified with DCP.* Advances in Polymer Technology, 2013. **33**(1).
92. Dordinejad, A.K., F. Sharif, M. Ebrahimi, and R. Rashedi, *Rheological and thermorheological assessment of polyethylene in multiple extrusion process.* Thermochimica Acta, 2018. **668**: p. 19-27.
93. Jesus, T.W.S.d., D. Pasquini, and T. Benvenuti, *Characterization of PS/PP/HDPE/LDPE Polymer Blend Obtained from PlasticWaste Collected on Beaches in Ilhéus-Bahia, Brazil.* Polymers, 2023. **15**(4155).
94. White, R.P. and J.E.G. Lipson, *Polymer Free Volume and Its Connection to the Glass Transition.* Macromolecules, 2016. **49**(11): p. 3987-4007.
95. Fakirov, S. and B. Krasteva, *On the Glass Transition Temperature of Polyethylene as Revealed by Microhardness Measurements.* Journal of Macromolecular Science, Part B, 2007. **39**(2): p. 297-301.
96. Sun, H., Y. Tang, G. Wu, and F. Zhang, *Investigation of the relationship of the glass-transition temperature and the polymer structure by fuzzy set theory.* Journal of Polymer Science Part B: Polymer Physics, 2002. **40**(5): p. 454-459.
97. Chan, J., S. Leow, K. Bea, W.K. Cheng, S.W. Phoong, Z.-W. Hong, and Y.-L. Chen, *Mitigating the Multicollinearity Problem and Its Machine Learning Approach: A Review.* Mathematics, 2022. **10**: p. 1283.
98. Kirtland, K.M. *Outlier detection and multicollinearity in sequential variable selection: A least angle regression-based approach*. 2017.
99. Ortiz, I.Z.A., *Quality changes of virgin and post-consumer recycled polypropylene exposed to simulated mechanical recycling cycles*, in *Hamburg University of Technology Institute of Environmental Technology and Energy Economics*. 2022, Hamburg University of Technology. p. 90.
100. Mylläri, V., S. Hartikainen, V. Poliakova, R. Anderson, I. Jönkkäri, P. Pasanen, M. Andersson, and J. Vuorinen, *Detergent impurity effect on recycled HDPE:*

Properties after repetitive processing. Journal of Applied Polymer Science, 2016. **133**(31).
101. Hans Zweifel, R.-D.M., Michael Schiller, *Plastic Additives Handbook*. 6th ed. 2009, Munich: Carl Hanser Verlag.
102. Sarjas, A., B. Pongrac, and D. Gleich, *Automated Inorganic Pigment Classification in Plastic Material Using Terahertz Spectroscopy.* Sensors (Basel), 2021. **21**(14).
103. Ghosh, A., *Enhancing the thermoplastic behavior and mechanical performance of recycled HDPE/CaCO composites using oxidized polyethylene.* Journal of Applied Polymer Science, 2023. **140**(23): p. e53923.
104. Abad, M.J., A. Ares, L. Barral, J. Cano, F.J. Díez, S. García-Garabal, J. López, and C. Ramírez, *Effects of a mixture of stabilizers on the structure and mechanical properties of polyethylene during reprocessing.* Journal of Applied Polymer Science, 2004. **92**(6): p. 3910-3916.
105. Bruns, M., *Untersuchung von Strategien zur Minimierung der NIAS in recycelten Polyolefinen mittels GC-MS Analysen*. 2023, Technische Hochschule Ostwertfalen-Lippe. p. 38.
106. Gulmine, J.V., P.R. Janissek, H.M. Heise, and L. Akcelrud, *Polyethylene characterization by FTIR.* Polymer Testing, 2002. **21**(5): p. 557-563.
107. Camacho, W. and S. Karlsson, *Assessment of thermal and thermo-oxidative stability of multiextruded recycled PP, HDPE and a blend thereof.* Polymer Degradation and Stability, 2002. **78**(2): p. 385-391.
108. Karaagac, E., T. Koch, and V.M. Archodoulaki, *The effect of PP contamination in recycled high-density polyethylene (rPE-HD) from post-consumer bottle waste and their compatibilization with olefin block copolymer (OBC).* Waste Manag, 2021. **119**: p. 285-294.
109. Oblak, P., J. Gonzalez-Gutierrez, B. Zupančič, A. Aulova, and I. Emri, *Processability and mechanical properties of extensively recycled high density polyethylene.* Polymer Degradation and Stability, 2015. **114**: p. 133-145.
110. Zhang, J., V. Hirschberg, A. Goecke, M. Wilhelm, W. Yu, M. Orfgen, and D. Rodrigue, *Effect of mechanical recycling on molecular structure and rheological properties of high-density polyethylene (HDPE).* Polymer, 2024. **297**: p. 126866.

8 Appendix

Table 34 Physical properties of cosmetic components, with viscosity (η), molecular weight (MW), molar volume (Vm), retention index (I) on non-polar column.

Name	Substance	η at 25 °C [mPa*s]	MW [g/mol]	Vm [cm^3/mol]	RI	Density at 25 °C [g/cm^3]	Spreadability [mm^2/10min]	Surface tension at 25 °C [mN/m]
C10	Limonene	0.9	136	162	1022	0.848	835	27.6
C9	Dicaprylyl ether	3.0	242	300	1657	0.801	1030	27.5
C1	Isopropyl palmitate	7.0	300	352	1980	0.853	810	28.9
C2	C12-C15 alkyl benzoate	13.0	311	334	2168	0.929	770	32.6
C8	Caprylic/capric triglyceride	25.0	500	529	2958	0.946	620	29.2
C3	Butylene glycol dicaprylate/dicaprate	11.0	687	749	2484	0.917	780	27.9
C7	Paraffinum oil LV/669	27.0	382	449	-	0.851	600	29.8
C4	Paraffinum liquidum N 32	59.0	427	495	-	0.863	440	30.8
C5	Castor oil	712.0	300	313	-	0.959	180	34.8
C6	Sunflower oil	55.0	-	-	-	0.919	480	32.9

Table 35 Physical and mechanical properties of POs and PET, with Melt Flow Rate (MFR) at 190 °C for PE and 230 °C for PP materials.

Name	Density [g/cm^3]	Crystallinity [%]	Charpy notched impact strength 23 °C [kJ/m^2]	Tensile modulus [MPa]	Flexural modulus [MPa]	Elongation at break [%]	Tensile strain at yield [%]	Tensile strength [MPa]	Shore Hardness (Shore D)	MFR (2.16 kg) [g/10 min]	MFR (5.0 kg) [g/10 min]
vHDPE 1	0.958	73.6	-	1420	-	-	7	30	64	0.35	1.2
vHDPE 2	0.950	64.5	12	1000	-	-	10	23	60	0.4	1.5
vHDPE 3	0.958	67.7	-	1400	-	800	-	30	66	0.25	1.1
vHDPE 4	0.955	63.5	0.19	1497	1241	>700	-	28	65	0.35	-
vHDPE 5	0.945	57.5	-	340	-	-	390	26	-	0.3	1.2
rHDPE 1	0.944	66.7	-	-	850	-	-	-	-	-	1.0-2.0
rHDPE 2	0.960	65.9	15	1250	-	10	-	25	-	0.2	1
rHDPE 3	-	62.1	-	-	850	-	-	-	-	-	1.0-2.0
rHDPE 4	-	60.3	-	-	700-1200	-	-	19-26	-	-	0.3-0.7
rHDPE 5	-	56.4	-	-	700-1200	-	-	21-26	-	-	0.3-0.7
rHDPE 6	0.950	65.2	195	-	740	-	-	23	-	0.3	-
rHDPE 7	0.955	63.0	-	-	-	-	-	-	-	0.3	-
rHDPE 8	0.956	59.4	-	1200	9	-	-	24	-	0.3	1.2
rHDPE 9	0.950	66.1	20	1200	-	9	-	25	-	0.3	1.2
rHDPE 10	-	63.6	25	852	-	-	49	24	-	-	1.7
rHDPE 11	0.960	59.4	20	930	-	-	10	25	-	0.3	-
rHDPE 12	-	69.4	-	-	-	-	-	-	-	0.5-0.7	-
rHDPE 13	-	63.1	4-5	900-1500	-	-	-	-	-	-	1.1-2.0
rHDPE 14	0.955	69.8	-	-	-	-	-	-	-	0.4	1.8
rHDPE 15	0.970	62.1	20	900	-	-	-	24	-	-	1.3
rHDPE 16	0.950	61.5	18	860	-	80	12	24	61	-	1.5
rHDPE 17	0.960	65.0	20	950	-	-	10	25	-	0.2	-
rHDPE 18_a	0.955	65.7	24	950	-	-	10	25	-	0.2	-
rHDPE 19	0.960	60.6	20	1200	-	9	-	25	-	0.3	1.2

rHDPE 20_0h	0.950	66.7	20	1200	-	9	-	25	-	0.3	1.2
rHDPE 21	0.960	61.4	20	1200	-	9	-	25	-	0.3	1.2
vLDPE 1	0.924	39.8	-	159	-	520	-	11	-	0.8	-
vLDPE 2	0.919	41.4	-	200	-	-	15	17	45	1.5	-
vLDPE 3	0.927	46.0	-	300	-	600	-	27	-	0.3	-
vLDPE 4	0.922	43.1	-	210	-	600	-	20	-	2.1	-
rLDPE 1	0.920	32.4	-	13	-	-	180	13	-	0.9-1.6	3.6-5.8
rLDPE 2	0.920	31.7	>10	>180	-	>200	-	>14	-	0.7-1.0	4.5-5.5
rLDPE 3	-	31.9	-	-	-	-	-	-	-	-	-
rLDPE 4	-	35.4	-	-	-	-	-	-	-	-	-
rLDPE 5	-	28.1	-	-	-	-	-	-	-	-	-
rLDPE 6	-	22.7	-	-	-	-	-	-	-	-	-
vLLDPE 1	0.920	44.3	-	237	-	740	-	11	-	1.0	-
vLLDPE 2	0.918	43.1	-	210	-	-	850	12	-	1.0	-
vLLDPE 3	0.910	27.4	-	-	-	>500	-	15	45	2.6.0	-
rPET 1	-	-	-	-	-	-	-	-	-	-	-
vPP1	0.905	51.6	4	1600	1500	9	-	34	-	42.0	-
vPP 2	0.905	45.5	8	1500	1450	-	5	27	-	20.0	-
vPP 3	-	17.8	70	-	330	-	35	9	36	0.8	-
vPP 4	-	13.6	6	1100	-	-	12	28	-	13.0	-
vPP 5	-	47.8	4	1550	1550	-	9	35	-	12.0	-
rPP 1	0.900	38.4	6	1200	-	6	-	26	-	20.0	-
rPP 2	-	44.6	-	-	-	-	-	-	-	38.0-42.0	-
rPP 3	0.910	41.2	6	1200	-	6	-	26	-	20.0	-
rPP 4	-	38.1	7	1250	1150	-	30	26	-	-	-
rPP 5	-	35.1	-	-	-	-	-	-	-	20.0-25.0	-
rPP 6	0.930	40.2	6	1200	-	6	-	26	-	45.0	-

Table 36 Inorganic contamination of all polymers in %.

Name	Al	Si	P	S	Cl	K	Ca	Ti	V	Fe	Ni	Cu	Zn
vHDPE 1	0.008	<0.001	0.006	0.000	0.002	<0.001	0.007	0.000	0.000	0.001	0.001	0.000	<0.001
vHDPE 4	0.004	<0.001	0.002	0.000	0.000	0.000	0.002	<0.001	0.000	0.000	0.001	0.000	0.001
vHDPE 3	0.006	<0.001	0.002	0.000	0.002	0.000	0.006	0.000	0.000	<0.001	0.000	0.000	0.001
vHDPE 2	0.007	0.000	0.000	0.001	0.002	0.000	0.012	0.003	0.000	0.000	0.001	0.000	0.000
vHDPE 5	0.012	<0.001	0.003	0.003	0.002	0.001	0.003	0.000	0.000	0.000	0.001	0.000	<0.001
rHDPE 8	0.014	0.002	0.012	0.004	0.002	0.000	0.192	0.320	0.002	<0.001	0.002	0.000	0.001
rHDPE 9	0.007	<0.001	0.002	0.001	0.004	0.000	0.007	0.010	0.000	0.000	0.001	0.000	0.001
rHDPE 2	0.025	0.008	0.003	0.010	0.005	0.001	0.051	0.888	0.007	0.001	0.001	0.001	0.039
rHDPE 10	0.016	0.002	0.003	0.006	0.016	0.001	0.469	0.235	0.001	0.003	0.001	0.000	0.005
rHDPE 1	0.026	<0.001	0.005	0.003	0.004	0.000	0.018	0.008	0.001	0.002	0.002	0.001	0.003
rHDPE 11	0.024	0.014	0.002	0.008	0.004	0.003	0.142	0.157	0.001	0.002	0.001	0.015	0.008
rHDPE 12	0.013	0.011	0.002	0.002	0.003	0.002	0.017	0.073	0.001	0.003	0.001	0.001	0.002
rHDPE 13	0.022	0.009	0.002	0.002	0.003	0.001	0.485	0.686	0.004	<0.001	0.003	<0.001	0.001
rHDPE 14	0.005	0.003	0.006	0.001	0.002	0.000	0.010	0.004	0.000	0.000	0.001	0.000	0.001
rHDPE 15	0.019	0.005	0.002	0.005	0.003	0.001	0.035	0.582	0.006	0.002	0.001	0.000	0.023
rHDPE 16	0.026	0.004	0.002	0.003	0.003	0.001	0.036	0.313	0.004	<0.001	0.002	0.000	0.001
rHDPE 18_e	0.006	<0.001	0.001	0.001	0.002	0.000	0.019	0.014	0.000	0.000	0.001	<0.001	0.001
rHDPE 17	0.019	0.004	0.002	0.005	0.004	0.001	0.030	0.385	0.003	0.001	0.001	0.001	0.017
rHDPE 7	0.011	0.002	0.005	0.002	0.002	0.001	0.014	0.039	0.001	0.001	0.001	0.000	0.001
rHDPE 6	0.006	<0.001	0.008	0.003	0.002	0.000	0.022	0.003	0.000	0.000	0.001	0.000	0.001
rHDPE 18_f	0.007	<0.001	0.002	0.001	0.002	0.000	0.045	0.025	0.000	0.000	0.002	0.000	0.001
rHDPE 3	0.163	0.225	0.007	0.037	0.063	0.031	0.338	0.228	0.001	0.018	0.002	0.025	0.019
rHDPE 4	0.020	0.003	0.002	0.002	0.006	0.001	0.230	0.395	0.003	<0.001	0.002	0.000	0.001
rHDPE 5	0.035	0.032	0.002	0.005	0.013	0.009	0.170	0.206	0.001	0.006	0.001	0.014	0.017
rHDPE 18_g	0.007	<0.001	0.002	0.001	0.003	0.000	0.038	0.025	0.000	0.002	0.001	0.000	0.004
rHDPE 18_h	0.006	<0.001	0.001	0.001	0.002	0.000	0.030	0.024	0.000	0.002	0.001	0.000	0.003
rHDPE 18_d	0.007	<0.001	0.002	0.001	0.003	0.000	0.050	0.029	0.000	0.002	0.001	0.000	0.004
rHDPE 18_a	0.007	<0.001	0.002	0.001	0.002	0.000	0.051	0.022	0.000	0.002	0.001	0.000	0.004
rHDPE 20_12h	0.007	0.001	0.003	0.001	0.005	0.001	0.010	0.009	0.000	0.001	0.001	0.000	0.002

rHDPE 20_24h	0.016	0.007	0.002	0.001	0.004	0.001	0.010	0.010	0.000	0.001	0.001	0.000	0.002
rHDPE 18_b	0.006	<0.001	0.001	0.001	0.002	0.000	0.033	0.023	0.000	0.001	0.001	0.000	0.003
rHDPE 18_c	0.008	<0.001	0.002	0.002	0.004	0.001	0.036	0.035	0.000	0.002	0.001	0.000	0.004
rHDPE 19	0.025	0.016	0.002	0.007	0.007	0.005	0.221	0.135	0.001	0.004	0.001	0.017	0.007
rHDPE 20_0h	0.007	<0.001	0.002	0.001	0.004	0.001	0.009	0.010	0.000	0.001	0.001	0.000	0.002
rHDPE 21	0.025	0.016	0.002	0.007	0.007	0.005	0.221	0.135	0.001	0.004	0.001	0.017	0.007
VLDPE 1	0.006	<0.001	<0.001	0.000	0.000	0.000	0.000	<0.001	0.000	0.000	0.001	0.000	<0.001
vLDPE 2	0.008	<0.001	<0.001	0.001	0.002	0.001	0.000	0.000	0.000	0.000	0.001	0.000	<0.001
vLDPE 3	0.006	<0.001	<0.001	0.001	0.002	0.001	0.000	<0.001	0.000	0.000	0.001	0.000	<0.001
vLDPE 4	0.009	0.005	<0.001	0.001	0.001	0.000	0.001	0.000	0.000	0.001	0.001	0.000	<0.001
rLDPE 1	0.017	0.039	0.002	0.003	0.003	0.002	0.039	0.030	0.000	0.004	0.001	0.001	0.009
rLDPE 2	0.006	0.004	0.001	0.000	0.000	0.000	0.001	0.000	0.000	0.001	0.001	0.000	0.118
rLDPE 3	0.019	0.057	0.003	0.004	0.003	0.002	0.042	0.032	0.000	0.005	0.001	0.001	0.009
rLDPE 4	0.014	0.009	0.001	0.002	0.007	0.001	0.261	0.001	0.000	0.002	0.001	0.000	0.011
rLDPE 5	0.017	0.027	0.003	0.003	0.016	0.002	0.108	0.014	0.000	0.004	0.001	0.001	0.036
rLDPE 6	0.033	0.055	0.004	0.025	0.081	0.004	0.431	0.245	0.001	0.024	0.001	0.005	0.024
vLLDPE 1	0.008	<0.001	0.008	0.000	0.004	<0.001	0.009	0.000	0.000	0.000	0.001	0.000	<0.001
vLLDPE 2	0.010	<0.001	0.002	0.001	0.004	0.001	0.000	0.000	0.000	0.000	0.001	0.000	0.013
vLLDPE 3	0.022	<0.001	0.069	0.000	0.005	0.000	0.000	0.001	0.001	0.000	0.001	0.000	0.001
vPP1	0.017	0.052	0.001	0.000	0.001	0.000	0.005	0.000	0.000	0.002	0.001	0.000	<0.001
vPP 2	0.010	0.125	0.002	0.000	0.001	0.000	0.005	0.000	0.000	0.003	0.001	0.000	<0.001
vPP 4	0.011	<0.001	<0.001	<0.001	<0.001	<0.001	0.007	<0.001	<0.001	<0.001	<0.001	<0.001	<0.001
rPP 2	0.017	0.047	0.003	0.001	0.003	0.001	0.138	0.003	0.000	0.003	0.001	0.000	0.001
rPP 3	0.034	0.045	0.003	0.002	0.007	0.001	0.157	0.407	0.003	0.004	0.001	0.001	0.009
rPP 1	0.022	0.025	0.003	0.003	0.014	0.001	0.097	0.124	0.001	0.011	0.001	0.005	0.005
rPP 5	0.035	0.026	0.003	0.004	0.158	0.003	0.319	0.258	0.001	0.014	0.001	0.004	0.017
rPP 6	0.023	0.053	0.003	0.002	0.004	0.001	0.165	0.454	0.003	0.003	0.001	0.000	0.008

Table 37 Coefficient values from multiple regression analysis of molecular and mechanical properties in HDPE and PP, R^2=0.99 (PE), R^2=0.99 (HDPE).

	HDPE			PE		
Parameter*	Coefficient	Standard error	p-value	Coefficient	Standard error	p-value
Intercept	3298	156	0.054	911.40	0.57	1169.012
MFR	-26	76	0.734	15.42	0.60	21.268
MW	0.0482	4.91e−05	0.342	0.01	0.18	0.00007
MWD	-1	12	0.521	-7.98	0.18	2.415
T_m	-18	13	0.198	2	1	1.270
SCB	16.32	0.42	0.002	3.89	0.21	1.375
PP	1	16	0.684	-6.38	0.36	4.092
Density at 25 °C	-1011	121	0.418	-1550.61	0.44	1304.721
Crystallinity	0.31	12	0.812	3.70	0.26	1.650
CIS	0.02	0.05	0.692	-	-	-
Tension strength	-0.25	15	0.877	2.07	0.38	0.385
Tension modulus	-0.01	0.01	0.813	-0.06	0.20	0.209

* SCB: number of short chain branching per 1000 C-atoms, MW: molecular weight, MWD: molecular weight distribution, T_m: melting temperature, PP: polypropylene content, MFR (melt flow rate) at 5.00 kg and 190 °C (HDPE) and 230°C (PP), CIS: charpy notched impact strength.

Table 38 Coefficient values from multiple regression analysis of molecular and mechanical properties in HDPE and PP, with R^2=0.99 (PE) and R^2=0.99 (HDPE).

	HDPE	PE

Parameter	Coefficient	Standard error	p-value	Coefficient	Standard error	p-value
Intercept	-1340	172	0,016	-708	828	0,432
SCB	-0,16	0,18	0,458	0,04	0,16	0,972
MW	$-1,82 * 10^{-5}$	$1,67* 10^{-5}$	0,390	$8,54 * 10^{-4}$	$1,06 * 10^{-4}$	0,458
MWD	2,15	0,53	0,055	-1	2	0,831
T_m	5,83	0,94	0,025	5	5	0,416
T_c	4,45	0,66	0,021	4	3	0,279
PP	5	1	0,044	-	-	-
Density at 25 °C	205	94	0,162	-37	702	0,960
Crystallinity	-2,68	0,63	0,052	-6	4	0,176
MFR	14	3	0,053	15	17	0,411

* SCB: short chain branching at 1000 C-atoms, MW: molecular weight, MWD: molecular weight distribution, T_m: melting temperature, T_c: crystalizing temperature, PP: polypropylene content, MFR (melt flow rate) at 5.00 kg and 190 °C.

Table 39 Parameter values of the asymptotic function $y=a-b*c^x$ and the slope k, for the linearized function to calculate D in each polymer.

Cosmetic component	T [°C]	Material name	a	b	c	k	D [mm^2/day]
Isopropyl palmitate	40	vHDPE 1	5.09325	5.10215	0.90043	-0.10488	10.3052876
Isopropyl palmitate	40	vHDPE 1	4.96111	4.90988	0.89532	-0.11057	10.864375
Isopropyl palmitate	40	vHDPE 1	4.60161	4.41306	0.9197	-0.08373	8.22713324
Isopropyl palmitate	40	vHDPE 1	5.14001	4.90964	0.90755	-0.09701	9.53199804
Isopropyl palmitate	40	vHDPE 1	5.09336	5.09292	0.90012	-0.10523	10.3396779
Isopropyl palmitate	40	vHDPE 1	4.87033	4.50007	0.89194	-0.1144	11.2407028
Isopropyl palmitate	40	vHDPE 1_IM	4.93873	4.93394	0.56767	-0.56622	10.6077279
Isopropyl palmitate	40	vHDPE 1_IM	4.9243	4.91552	0.63884	-0.4481	8.78983153
Isopropyl palmitate	40	vHDPE 1_IM	4.67918	4.66991	0.65759	-0.41917	8.69616185
Isopropyl palmitate	40	vHDPE 1_IM	4.67184	4.65211	0.62986	-0.46226	8.8626803
Isopropyl palmitate	40	vHDPE 2	4.78006	4.68341	0.88298	-0.12445	8.67205894
Isopropyl palmitate	40	vHDPE 2	4.87026	4.64872	0.90657	-0.09809	6.83521303
Isopropyl palmitate	40	vHDPE 2	4.77227	4.39554	0.89558	-0.11033	7.68813389
Isopropyl palmitate	40	vHDPE 2	4.76022	4.52121	0.89855	-0.10697	7.45399875
Isopropyl palmitate	40	vHDPE 3	4.87145	4.77423	0.93555	-0.06662	9.917
Isopropyl palmitate	40	vHDPE 3	4.88721	4.73296	0.93363	-0.06868	10.2236
Isopropyl palmitate	40	vHDPE 3	4.66329	4.5734	0.92938	-0.07324	10.9024
Isopropyl palmitate	40	vHDPE 3	4.70319	4.60318	0.92863	-0.07405	11.023
Isopropyl palmitate	40	vHDPE 3_IM	4.821	4.81622	0.74205	-0.49834	10.0464
Isopropyl palmitate	40	vHDPE 3_IM	4.95595	4.91772	0.67681	-0.39036	8.0376
Isopropyl palmitate	40	vHDPE 3_IM	4.80795	4.86288	0.64476	-0.43887	9.1632
Isopropyl palmitate	40	vHDPE 3_ natural bottle	4.71	4.63	0.71	-0.34523	7.8843
Isopropyl palmitate	40	vHDPE 3_ natural bottle	4.56	4.51	0.66	-0.42022	9.4146
Isopropyl palmitate	40	vHDPE 3_ natural bottle	4.61	4.57	0.67	-0.3987	8.99
Isopropyl palmitate	40	vHDPE 3_ white bottle	4.57	4.58	0.59	-0.52484	9.212
Isopropyl palmitate	40	vHDPE 3_ white bottle	4.46	4.43	0.61	-0.48794	10.4431
Isopropyl palmitate	40	vHDPE 3_ white bottle	4.47	4.5	0.48	-0.73827	11.0403
Isopropyl palmitate	40	vHDPE 3_ blue bottle	4.63	4.68	0.51	-0.67997	8.8175
Isopropyl palmitate	40	vHDPE 3_ blue bottle	4.69	4.6	0.73	-0.31752	8.4351
Isopropyl palmitate	40	vHDPE 3_ blue bottle	4.56	4.49	0.71	-0.3464	8.8861
Isopropyl palmitate	40	vHDPE 3 + 50% rHDPE 22	4.84924	4.88422	0.52167	-0.65072	8.3592
Isopropyl palmitate	40	vHDPE 3 + 50% rHDPE 22	4.83889	4.86056	0.51577	-0.66207	8.5854
Isopropyl palmitate	40	vHDPE 3 + 50% rHDPE 22	4.9287	4.97517	0.44765	-0.80303	9.8318
Isopropyl palmitate	40	vHDPE 3 + 50% rHDPE 22	4.63165	4.64805	0.47974	-0.73388	10.6045
Isopropyl palmitate	40	vHDPE 3 + 70% rHDPE 22	4.83959	4.86188	0.50629	-0.68065	8.8263
Isopropyl palmitate	40	vHDPE 3 + 70% rHDPE 22	4.87775	4.91417	0.52271	-0.64872	8.7295
Isopropyl palmitate	40	vHDPE 3 + 70% rHDPE 22	4.86644	4.91452	0.46149	-0.77183	10.4812
Isopropyl palmitate	40	vHDPE 3 + 70% rHDPE 22	4.65471	4.66117	0.35338	-1.03951	12.109
Isopropyl palmitate	40	vHDPE 3 + 50% rHDPE 23	4.92281	4.91737	0.68268	-0.38173	10.0242
Isopropyl palmitate	40	vHDPE 3 + 50% rHDPE 23	5.00359	4.95951	0.68588	-0.37705	10.365
Isopropyl palmitate	40	vHDPE 3 + 50% rHDPE 23	4.82979	4.75054	0.66518	-0.4077	9.6684
Isopropyl palmitate	40	vHDPE 3 + 50% rHDPE 23	4.59092	4.57329	0.55836	-0.58275	11.0132

Isopropyl palmitate	40	vHDPE 3 + 50% rHDPE 23	5.10788	5.10193	0.61356	-0.48848	11.8726
Isopropyl palmitate	40	vHDPE 3 + 50% rHDPE 23	4.90158	4.8427	0.6221	-0.47465	12.1044
Isopropyl palmitate	40	vHDPE 3 + 50% rHDPE 23	4.8691	4.76695	0.63398	-0.45574	11.76
Isopropyl palmitate	40	rHDPE 2	4.58073	4.43154	0.79959	-0.22366	15.5536
Isopropyl palmitate	40	rHDPE 2	4.53374	4.394	0.79435	-0.23024	16.0112
Isopropyl palmitate	40	rHDPE 2	4.64256	4.37719	0.7995	-0.22377	15.5612
Isopropyl palmitate	40	rHDPE 2_IM	4.50826	4.50685	0.481	-0.73123	13.5046
Isopropyl palmitate	40	rHDPE 2_IM	4.51963	4.51647	0.52813	-0.63841	13.0532
Isopropyl palmitate	40	rHDPE 2_IM	4.52288	4.52281	0.48326	-0.72689	14.8623
Isopropyl palmitate	40	rHDPE 2_IM	4.46895	4.4621	0.51848	-0.65687	13.7148
Isopropyl palmitate	40	rHDPE 2_IM	4.51991	4.55566	0.52101	-0.65198	13.8019
Isopropyl palmitate	40	rHDPE 18_d	4.78868	4.70185	0.65772	-0.41898	21.2737
Isopropyl palmitate	40	rHDPE 18_d	4.74117	4.65974	0.66508	-0.40786	20.7091
Isopropyl palmitate	40	rHDPE 18_d	4.60975	4.49522	0.66052	-0.41473	21.0579
Isopropyl palmitate	40	rHDPE 18_d	4.72266	4.6261	0.65316	-0.42593	21.6266
Isopropyl palmitate	40	rHDPE 18_h	4.6254	4.40957	0.77366	-0.25665	20.8022
Isopropyl palmitate	40	rHDPE 18_h	4.59767	4.37461	0.75303	-0.28365	22.9907
Isopropyl palmitate	40	rHDPE 18_h	4.20732	4.10348	0.72305	-0.32428	26.2838
Isopropyl palmitate	40	rHDPE 18_g	4.66576	4.52059	0.71373	-0.33726	19.2083
Isopropyl palmitate	40	rHDPE 18_g	4.65793	4.503	0.72677	-0.41915	23.8722
Isopropyl palmitate	40	rHDPE 18_g	4.45414	4.33112	0.70114	-0.35505	20.2215
Isopropyl palmitate	40	rHDPE 18_g	4.41812	4.29495	0.70443	-0.35038	19.9555
Isopropyl palmitate	40	rHDPE 18_ e	4.63606	4.54276	0.67947	-0.38644	21.8823
Isopropyl palmitate	40	rHDPE 18_ e	4.70595	4.59168	0.66357	-0.41012	23.2232
Isopropyl palmitate	40	rHDPE 18_ e	4.50749	4.39251	0.68396	-0.37987	21.5103
Isopropyl palmitate	40	rHDPE 18_ e	4.35912	4.2602	0.68347	-0.38057	21.5499
Isopropyl palmitate	40	rHDPE 18_b	4.61237	4.26387	0.75474	-0.28143	29.0403
Isopropyl palmitate	40	rHDPE 18_b	4.71016	4.45621	0.80491	-0.21702	22.3939
Isopropyl palmitate	40	rHDPE 18_b	4.33945	3.96142	0.79061	-0.23495	24.2441
Isopropyl palmitate	40	rHDPE 18_c	5.68541	5.4918	0.73514	-0.30771	21.0008
Isopropyl palmitate	40	rHDPE 18_c	4.83789	4.61675	0.69726	-0.3606	24.6105
Isopropyl palmitate	40	rHDPE 18_c	4.83079	4.61284	0.70187	-0.35401	24.1608
Isopropyl palmitate	40	rHDPE 18_c	4.93207	4.69285	0.71006	-0.34243	23.3704
Isopropyl palmitate	40	rHDPE 18_a	5.10877	4.96875	0.79281	-0.23217	23.162
Isopropyl palmitate	40	rHDPE 18_a	4.87454	4.86391	0.75509	-0.28092	28.0255
Isopropyl palmitate	40	rHDPE 18_a	4.66654	4.22954	0.77493	-0.25498	25.4376
Isopropyl palmitate	40	rHDPE 18_f	4.77625	4.75525	0.76534	-0.26744	20.4607
Isopropyl palmitate	40	rHDPE 18_f	4.92134	4.93289	6.81E-01	-0.38473	29.4341
Isopropyl palmitate	40	rHDPE 18_f	4.82261	4.6925	0.75252	-0.28434	21.7537
Isopropyl palmitate	40	vHDPE_1x E	5.19513	4.87861	0.71436	-0.33637	2.947845805
Isopropyl palmitate	40	vHDPE_1x E	5.13605	5.05481	0.61738	-0.48227	3.253968254
Isopropyl palmitate	40	vHDPE_1x E	5.04202	4.82936	0.75089	-0.2865	2.877624168
Isopropyl palmitate	40	vHDPE_1x E	4.90321	4.78027	0.7182	-0.33101	2.73015873
Isopropyl palmitate	40	vHDPE_1x E	5.1464	5.04535	0.71503	-0.33543	3.063316347
Isopropyl palmitate	40	vHDPE_1x E	4.94964	4.81917	0.77506	-0.25481	2.746721877
Isopropyl palmitate	40	vHDPE_2x E	5.16101	5.04665	0.72465	-0.32207	2.943233791
Isopropyl palmitate	40	vHDPE_2x E	5.11922	4.89685	0.70836	-0.3448	3.03657695
Isopropyl palmitate	40	vHDPE_2x E	5.08094	4.87035	0.73543	-0.3073	2.976190476
Isopropyl palmitate	40	vHDPE_2x E	4.92635	4.80627	0.72633	-0.31975	2.645502646
Isopropyl palmitate	40	vHDPE_2x E	4.96188	4.78485	0.74481	-0.29463	2.623571017
Isopropyl palmitate	40	vHDPE_3x E	5.05078	4.95479	0.68512	-0.37816	2.886002886
Isopropyl palmitate	40	vHDPE_3x E	5.16565	4.90847	0.73491	-0.30801	2.873475221
Isopropyl palmitate	40	vHDPE_3x E	4.87672	4.7158	0.74228	-0.29803	2.607709751
Isopropyl palmitate	40	vHDPE_3x E	4.92575	4.80707	0.72928	-0.3157	2.623571017
Isopropyl palmitate	40	vHDPE_4x E	5.09343	4.97057	0.69693	-0.36107	2.837301587
Isopropyl palmitate	40	vHDPE_4x E	5.01873	4.87457	0.72504	-0.32153	2.877624168
Isopropyl palmitate	40	vHDPE_4x E	5.03109	4.81596	0.73624	-0.3062	2.841220083
Isopropyl palmitate	40	vHDPE_4x E	4.89028	4.75744	0.76781	-0.26421	2.546534201
Isopropyl palmitate	40	vHDPE_4x E	4.95336	4.7789	0.76761	-0.26447	2.720446063
Isopropyl palmitate	40	vHDPE_5x E	5.36685	5.25595	0.75359	-0.28291	2.947845805
Isopropyl palmitate	40	vHDPE_5x E	5.11193	4.87771	0.75897	-0.27579	2.920634921
Isopropyl palmitate	40	vHDPE_5x E	5.00015	5.00015	0.69277	-0.36706	2.861186938
Isopropyl palmitate	40	vHDPE_5x E	4.91758	4.74942	0.76703	-0.26523	2.594858262
Isopropyl palmitate	40	vHDPE_6x E	5.10577	4.99683	0.68881	-0.37279	2.853124372
Isopropyl palmitate	40	vHDPE_6x E	4.98	4.82529	0.70059	-0.35583	2.84913124
Isopropyl palmitate	40	vHDPE_6x E	4.99773	4.84512	0.7157	-0.33449	2.829537612
Isopropyl palmitate	40	vHDPE_6x E	4.89782	4.75803	0.72887	-0.31626	2.577400597
Isopropyl palmitate	40	vHDPE_6x E	4.93277	4.7578	0.75366	-0.28281	2.607709751

Isopropyl palmitate	40	vHDPE_7x E	5.11975	4.98426	0.74013	-0.30093	2.886002886
Isopropyl palmitate	40	vHDPE_7x E	5.02754	4.85136	0.73384	-0.30946	2.877624168
Isopropyl palmitate	40	vHDPE_7x E	5.08663	4.88305	0.73108	-0.31323	2.903091061
Isopropyl palmitate	40	vHDPE_7x E	4.89324	4.7722	0.72332	-0.3239	2.664887794
Isopropyl palmitate	40	vHDPE_7x E	4.97429	4.80609	0.75087	-0.28652	2.612942613
Isopropyl palmitate	40	vHDPE_8x E	5.31969	5.30794	0.7134	-0.47031	2.795760802
Isopropyl palmitate	40	vHDPE_8x E	4.92727	4.39601	0.70469	-0.35	2.877624168
Isopropyl palmitate	40	vHDPE_8x E	4.91916	4.41193	0.71174	-0.34004	2.837301587
Isopropyl palmitate	40	vHDPE_8x E	4.94305	4.7476	0.7381	-0.30368	2.565296697
Isopropyl palmitate	40	vHDPE_8x E	4.87562	4.65536	0.75135	-0.28588	2.584807822
Isopropyl palmitate	40	vHDPE_8x E	5.05924	4.82505	0.75322	-0.2834	2.612942613
Isopropyl palmitate	40	vHDPE + 1%PP	4.9318	4.93	0.80934	-0.21154	7.6835
Isopropyl palmitate	40	vHDPE + 1%PP	4.84277	4.84	0.82557	-0.19168	6.8634
Isopropyl palmitate	40	vHDPE + 1%PP	5.02666	5.0002	0.81686	-0.20229	7.3127
Isopropyl palmitate	40	vHDPE + 3%PP	5.47237	5.47	0.78907	-0.2369	8.6454
Isopropyl palmitate	40	vHDPE + 3%PP	5.37729	5.37	0.77251	-0.25811	9.4195
Isopropyl palmitate	40	vHDPE + 3%PP	5.21073	5.21	0.79146	-0.23388	8.3745
Isopropyl palmitate	40	vHDPE + 5%PP	4.58263	4.56827	0.71108	-0.34097	12.0925
Isopropyl palmitate	40	vHDPE + 5%PP	5.20501	5.2	0.76137	-0.27264	9.8091
Isopropyl palmitate	40	vHDPE + 5%PP	5.06863	4.8954	0.76887	-0.26283	9.8652
Isopropyl palmitate	40	vHDPE + 5%PP	4.91028	4.71032	0.69791	-0.35967	13.6256
Isopropyl palmitate	40	rHDPE 19	4.95483	4.24484	0.78471	-0.24244	17.0905
Isopropyl palmitate	40	rHDPE 19	4.84153	4.60324	0.74899	-0.28903	20.3748
Isopropyl palmitate	40	rHDPE 19	4.86252	4.66863	0.75	-0.25431	17.8921
Isopropyl palmitate	40	rHDPE 19_1x E	5.22653	5.10676	0.71845	-0.33066	16.0886
Isopropyl palmitate	40	rHDPE 19_1x E	5.10877	5.02205	0.61906	-0.47955	15.5786
Isopropyl palmitate	40	rHDPE 19_1x E	5.02058	4.91678	0.69792	-0.35965	18.9432
Isopropyl palmitate	40	rHDPE 19_1x E	4.90585	4.84155	0.61791	-0.48141	20.0013
Isopropyl palmitate	40	rHDPE 19_1x E	4.90425	4.81252	0.71565	-0.33456	19.2027
Isopropyl palmitate	40	rHDPE 19_2x E	5.10283	5.07912	0.72471	-0.32198	17.8469
Isopropyl palmitate	40	rHDPE 19_2x E	5.02136	5.06274	0.7177	-0.3317	22.2572
Isopropyl palmitate	40	rHDPE 19_2x E	4.88287	4.78061	0.67915	-0.38691	23.9939
Isopropyl palmitate	40	rHDPE 19_2x E	4.90363	4.71377	0.6837	-0.38024	23.4687
Isopropyl palmitate	40	rHDPE 19_3x E	4.98209	4.95811	0.66873	-0.40237	23.0948
Isopropyl palmitate	40	rHDPE 19_3x E	4.84883	4.74237	0.69543	-0.36322	24.2617
Isopropyl palmitate	40	rHDPE 19_3x E	4.72644	4.59809	0.67344	-0.39536	26.7703
Isopropyl palmitate	40	rHDPE 19_4x E	5.01847	4.88558	0.70836	-0.3448	21.8917
Isopropyl palmitate	40	rHDPE 19_4x E	4.82101	4.69573	0.64852	-0.43306	24.9792
Isopropyl palmitate	40	rHDPE 19_4x E	4.91186	4.82314	0.63339	-0.45667	23.8051
Isopropyl palmitate	40	rHDPE 19_5x E	4.87156	4.67328	0.68815	-0.37375	20.5084
Isopropyl palmitate	40	rHDPE 19_5x E	5.01584	4.91976	0.68903	-0.37247	27.0742
Isopropyl palmitate	40	rHDPE 19_5x E	5.16983	4.9183	0.62516	-0.46975	27.0955
Isopropyl palmitate	40	rHDPE 19_5x E	4.86734	4.71399	0.66497	-0.40801	27.7518
Isopropyl palmitate	40	rHDPE 19_5x E	4.84725	4.76614	0.62476	-0.47039	27.6694
Isopropyl palmitate	40	rHDPE 19_6x E	5.05972	5.00044	0.68337	-0.38072	22.6135
Isopropyl palmitate	40	rHDPE 19_6x E	5.01101	4.95094	0.67275	-0.39638	22.8635
Isopropyl palmitate	40	rHDPE 19_6x E	4.88836	4.76193	0.69287	-0.36691	23.5138
Isopropyl palmitate	40	rHDPE 19_6x E	5.01352	4.90534	0.60999	-0.49431	28.3719
Isopropyl palmitate	40	rHDPE 19_7x E	5.0284	4.96465	0.6716	-0.39809	23.4165
Isopropyl palmitate	40	rHDPE 19_7x E	4.94315	4.8838	0.68849	-0.37325	23.9201
Isopropyl palmitate	40	rHDPE 19_7x E	4.75016	4.70966	0.64165	-0.44371	25.8462
Isopropyl palmitate	40	rHDPE 19_7x E	4.86281	4.76456	0.65365	-0.42518	25.3769
Isopropyl palmitate	40	rHDPE 19_8x E	4.99526	4.94154	0.67213	-0.3973	22.6913
Isopropyl palmitate	40	rHDPE 19_8x E	4.99516	4.98427	0.66077	-0.41435	25.3317
Isopropyl palmitate	40	rHDPE 19_8x E	4.83922	4.52634	0.62336	-0.47263	30.8552
Isopropyl palmitate	40	rHDPE 19_8x E	4.80962	4.75487	0.58225	-0.54086	32.9084
Isopropyl palmitate	40	vHDPE + 0% vLDPE	5.15901	5.12882	0.71017	-0.34225	16.8329
Isopropyl palmitate	40	vHDPE + 0% vLDPE	5.15578	5.08895	0.71961	-0.32905	16.1836
Isopropyl palmitate	40	vHDPE + 0% vLDPE	5.0724	5.01017	0.71325	-0.33792	16.6199
Isopropyl palmitate	40	vHDPE + 1% vLDPE	5.01041	4.8713	0.73801	-0.3038	16.5018
Isopropyl palmitate	40	vHDPE + 1% vLDPE	5.05302	4.99935	0.70621	-0.34784	15.578
Isopropyl palmitate	40	vHDPE + 1% vLDPE	5.06211	4.89543	0.74591	-0.29315	16.0044
Isopropyl palmitate	40	vHDPE + 1% vLDPE	5.03854	4.59189	0.71234	-0.3392	16.061

Isopropyl palmitate	40	vHDPE + 3% vLDPE	5.00654	5.04236	0.66939	-0.40139	15.8025
Isopropyl palmitate	40	vHDPE + 3% vLDPE	4.9616	4.93065	0.69003	-0.37102	17.7608
Isopropyl palmitate	40	vHDPE + 3% vLDPE	4.95512	4.96136	0.63619	-0.45226	14.4938
Isopropyl palmitate	40	vHDPE + 3% vLDPE	4.99806	4.95923	0.70131	-0.35481	17.2636
Isopropyl palmitate	40	vHDPE + 5% vLDPE	5.12612	5.11364	0.62286	-0.47343	17.965
Isopropyl palmitate	40	vHDPE + 5% vLDPE	5.23968	5.18849	0.67921	-0.38682	16.7405
Isopropyl palmitate	40	vHDPE + 5% vLDPE	5.09638	4.96943	0.72256	-0.32495	14.5529
Isopropyl palmitate	40	vHDPE + 5% vLDPE	5.05173	5.01804	0.61441	-0.48709	15.1868
Isopropyl palmitate	40	vHDPE + 10% vLDPE	5.07624	5.03199	0.6239	-0.47177	19.2556
Isopropyl palmitate	40	vHDPE + 10% vLDPE	5.05372	5.07873	0.52423	-0.64582	19.1696
Isopropyl palmitate	40	vHDPE + 10% vLDPE	4.78887	4.7913	0.60013	-0.51061	17.3813
Isopropyl palmitate	40	vHDPE + 10% vLDPE	4.80754	4.47494	0.65393	-0.42475	18.0655
Isopropyl palmitate	40	vHDPE + 30% vLDPE	5.1828	5.2371	0.48102	-0.73103	22.4777
Isopropyl palmitate	40	vHDPE + 30% vLDPE	5.08949	5.07299	0.60255	-0.50658	21.1713
Isopropyl palmitate	40	vHDPE + 30% vLDPE	4.86344	4.78035	0.57929	-0.54595	24.7276
Isopropyl palmitate	40	vHDPE + 30% vLDPE	5.05888	4.98089	0.53598	-0.62366	19.9868
Isopropyl palmitate	40	vLDPE + 0% vLLDPE	6.03874	6.02646	0.29375	-1.22525	53.0254
Isopropyl palmitate	40	vLDPE + 0% vLLDPE	5.92628	5.9119	0.20995	-1.5604	54.8791
Isopropyl palmitate	40	vLDPE + 0% vLLDPE	5.98775	5.98116	0.27647	-1.2854	57.8927
Isopropyl palmitate	40	vLDPE + 1% vLLDPE	6.21199	6.2041	0.28564	-1.25254	52.3468
Isopropyl palmitate	40	vLDPE + 1% vLLDPE	6.12802	6.11463	0.30643	-1.18318	55.4101
Isopropyl palmitate	40	vLDPE + 1% vLLDPE	6.00751	6.00837	0.25619	-1.36241	54.2906
Isopropyl palmitate	40	vLDPE + 3% vLLDPE	6.09026	6.09053	0.30143	-1.19951	58.0483
Isopropyl palmitate	40	vLDPE + 3% vLLDPE	6.01421	6.0157	0.2279	-1.47885	61.8049
Isopropyl palmitate	40	vLDPE + 5% vLLDPE	6.20943	6.21318	0.24163	-1.4208	52.5848
Isopropyl palmitate	40	vLDPE + 5% vLLDPE	6.04954	6.0423	0.23109	-1.46441	59.0611
Isopropyl palmitate	40	vLDPE + 5% vLLDPE	6.02486	6.02124	0.26954	-1.3118	63.4824
Isopropyl palmitate	40	vLDPE + 10% vLLDPE	6.3012	6.29926	0.23861	-1.43351	58.5096
Isopropyl palmitate	40	vLDPE + 10% vLLDPE	6.37399	6.36591	0.28805	-1.24365	57.601
Isopropyl palmitate	40	vLDPE + 10% vLLDPE	6.07968	6.07846	0.21922	-1.51709	64.5249
Isopropyl palmitate	40	vLDPE + 10% vLLDPE	6.12419	6.11986	0.21715	-1.52662	60.4677
Isopropyl palmitate	40	vLDPE + 30% vLLDPE	6.50538	6.50659	0.21649	-1.52963	64.6802
Isopropyl palmitate	40	vLDPE + 30% vLLDPE	6.39396	6.39623	0.17073	-1.76767	61.3667
Isopropyl palmitate	40	vLDPE + 30% vLLDPE	6.17063	6.1709	0.20787	-1.57216	70.0117
Isopropyl palmitate	40	vLDPE + 30% vLLDPE	6.16129	6.16036	0.18352	-1.69421	75.3613
Isopropyl palmitate	40	rHDPE 20_0h	4.74788	4.3655	0.86291	-0.14744	16.4533
Isopropyl palmitate	40	rHDPE 20_0h	4.95282	4.64743	0.8356	-0.17961	20.0432

Isopropyl palmitate	40	rHDPE 20_0h	4.38634	4.02783	0.85279	-0.15924	17.7701
Isopropyl palmitate	40	rHDPE 20_12h	3.11413	2.90084	0.72898	-0.31611	21.1099
Isopropyl palmitate	40	rHDPE 20_12h	4.66369	4.24848	0.79622	-0.22788	15.2178
Isopropyl palmitate	40	rHDPE 20_12h	4.72859	4.34305	0.80314	-0.21923	14.6402
Emulsion L	40	vHDPE 1	5.02932	4.90594	0.90958	-0.09477	9.3119
Emulsion L	40	vHDPE 1	5.22112	4.81235	0.923569	-0.07951	7.8125
Emulsion L	40	rHDPE 1	5.15047	4.87384	0.76412	-0.26903	21.6073
Emulsion L	40	rHDPE 1	5.001235	4.98665	0.712356	-0.23918	19.2099
Emulsion L	40	rHDPE 3	6.21492	6.20792	0.5022	-0.68878	27.3073
Emulsion L	40	rHDPE 3	6.43256	6.012356	0.596352	-0.51692	20.4938
Emulsion L	40	rHDPE 3	6.32349	6.1636	0.55236	-0.5458	25.5002
Emulsion V	40	vHDPE 1	6.14949	5.88432	0.93072	-0.0718	7.0549
Emulsion V	40	vHDPE 1	6.02365	5.9636	0.955236	-0.0458	4.5002
Emulsion V	40	vHDPE 1	6.90745	6.75306	0.78418	-0.24312	19.5263
Emulsion V	40	vHDPE 1	7.2365	7.1235	0.76589	-0.16672	13.3902
Emulsion V	40	vHDPE 1	6.69983	6.66473	0.49718	-0.69888	27.7077
Emulsion V	40	vHDPE 1	6.51235	6.2365	0.51235	-0.66873	26.5124
Emulsion C	40	vHDPE 1	4.94717	4.90117	0.98972	-0.01033	1.015
Emulsion C	40	vHDPE 1	5.11068	4.63088	0.99018	-0.00987	0.9698
Emulsion C	40	vHDPE 1	4.84196	4.71831	0.98954	-0.01052	1.0337
Emulsion D	40	vHDPE 1	4.6112	4.46843	0.98784	-0.01223	1.2017
Emulsion D	40	vHDPE 1	4.92639	4.80049	0.98952	-0.01054	1.0356
Emulsion D	40	vHDPE 1	4.71322	4.6345	0.99001	-0.01321	1.1654
Emulsion E	40	vHDPE 1	4.4708	4.3091	0.98722	-0.01286	1.2636
Emulsion E	40	vHDPE 1	4.90657	4.72511	0.98838	-0.01169	1.1486
Emulsion E	40	vHDPE 1	4.77556	4.52671	0.98788	-0.01199	1.25432
Emulsion C	40	rHDPE 1	4.76024	4.75137	0.9869	-0.01319	1.0594
Emulsion C	40	rHDPE 1	4.89644	4.71214	0.98804	-0.01203	0.9662
Emulsion C	40	rHDPE 1	5.06506	4.93331	0.9855	-0.01461	1.1734
Emulsion D	40	rHDPE 1	5.09583	4.9579	0.98561	-0.01449	1.1638
Emulsion D	40	rHDPE 1	5.03133	4.80212	0.98342	-0.01672	1.3429
Emulsion D	40	rHDPE 1	5.07983	4.88852	0.98902	-0.01289	1.3989
Emulsion E	40	rHDPE 1	4.91398	4.80512	0.98764	-0.01244	0.9991
Emulsion E	40	rHDPE 1	5.59752	5.46259	0.98583	-0.01427	1.1461
Emulsion E	40	rHDPE 1	5.2733	5.02288	0.97713	-0.01199	1.1061
Emulsion C	40	rHDPE 3	5.97312	5.73457	0.97331	-0.02705	1.0724
Emulsion C	40	rHDPE 3	5.97877	4.85805	0.97516	-0.02515	0.9971
Emulsion C	40	rHDPE 3	5.89791	5.65914	0.97485	-0.02547	1.0098
Emulsion D	40	rHDPE 3	5.89687	5.70421	0.96561	-0.035	1.3876
Emulsion D	40	rHDPE 3	6.0358	5.61879	0.97512	-0.02519	0.9987
Emulsion D	40	rHDPE 3	5.9338	5.68889	0.97002	-0.028	1.0067
Emulsion E	40	rHDPE 3	6.50189	6.30843	0.97981	-0.0204	0.8088
Emulsion E	40	rHDPE 3	6.55006	6.04505	0.97914	-0.02108	0.8357
Emulsion E	40	rHDPE 3	6.54356	6.2133	0.97712	-0.02099	0.8201
120 µm Emulsion C	40	vHDPE 1	5.25326	5.2225	0.98837	-0.0117	0.7712
120 µm Emulsion C	40	vHDPE 1	5.64639	5.58813	0.992992	-0.01703	1.1225
120 µm Emulsion C	40	rHDPE 1	4.84452	4.01	0.98505	-0.01506	1.2096
120 µm Emulsion C	40	rHDPE 1	5.44065	5.47217	0.9847	-0.01542	1.2385
120 µm Emulsion C	40	rHDPE 3	4.0382	4.107	0.97677	-0.0235	0.9317
120 µm Emulsion C	40	rHDPE 3	4.26863	4.23384	0.96161	-0.03915	1.5521
120 µm Emulsion C	40	rHDPE 3	4.28763	4.20064	0.96981	-0.03078	1.3411
120 µm Emulsion C	40	vHDPE 5	7.0814	7.01958	0.97553	-0.02477	0.4498
120 µm Emulsion C	40	vHDPE 5	6.2284	6.05704	0.97381	-0.02654	0.482
120 µm Emulsion C	40	vHDPE 5	6.54582	6.05868	0.9735	-0.02686	0.4999
120 µm Emulsion C	40	vPP 5	5.55931	5.52508	0.99272	-0.00731	0.1246
120 µm Emulsion C	40	vPP 5	4.97267	4.57888	0.99067	-0.00937	0.1649
120 µm Emulsion C	40	vPP 5	9.20825	8.85924	0.99651	-0.0035	0.0612
120 µm Emulsion C	40	vHDPE 3	4.59285	4.54194	0.96955	-0.03092	0.6322
120 µm Emulsion C	40	vHDPE 3	4.86895	4.9634	0.96061	-0.04019	0.8333
120 µm Emulsion C	40	vHDPE 3	4.6987	4.71021	0.967812	-0.03891	0.7189
120 µm Emulsion C	40	rHDPE 12	4.82209	4.70181	0.96068	-0.04011	0.8259
120 µm Emulsion C	40	rHDPE 12	5.26098	5.15222	0.96183	-0.03892	0.8126
120 µm Emulsion C	40	rHDPE 12	5.17654	5.01128	0.96117	-0.03917	0.8199
120 µm Emulsion C	40	rHDPE 11	4.69293	4.66655	0.94199	-0.05976	1.2651
120 µm Emulsion C	40	rHDPE 11	6.66289	6.33902	0.96526	-0.03536	0.7383
120 µm Emulsion C	40	rHDPE 12	5.26098	5.15222	0.96183	-0.03892	0.8126
0,35 µm Emulsion C	40	vHDPE 1	5.2653	5.11206	0.97793	-0.02232	1.4712
0.35 µm Emulsion C	40	vHDPE 1	5.49459	5.47154	0.971759	-0.02865	1.8885
0.35 µm Emulsion C	40	rHDPE 1	4.7914	4.75005	0.9548	-0.04625	3.7146
0.35 µm Emulsion C	40	rHDPE 1	5.29917	5.26336	0.96469	-0.03595	2.8873

0.35 µm Emulsion C	40	rHDPE 3	4.21128	4.1825	0.94857	-0.0528	2.0933
0.35 µm Emulsion C	40	rHDPE 3	4.17926	4.16441	0.93811	-0.06389	2.533
0.35 µm Emulsion C	40	rHDPE 3	4.39926	4.1712	0.94098	-0.06088	2.5743
0.35 µm Emulsion C	40	vHDPE 5	6.20348	6.40299	0.94321	-0.05847	1.075
0.35 µm Emulsion C	40	vHDPE 5	7.32345	7.12872	0.95295	-0.04819	0.8969
0.35 µm Emulsion C	40	vHDPE 5	6.731	6.94914	0.94209	-0.05965	1.0967
0.35 µm Emulsion C	40	vPP 5	4.89142	5.09124	0.98094	-0.01924	0.3387
0.35 µm Emulsion C	40	vPP 5	4.97593	4.93953	0.97023	-0.03022	0.5286
0.35 µm Emulsion C	40	vPP 5	7.14332	7.06836	0.98766	-0.01242	0.2172
0.35 µm Emulsion C	40	vHDPE 3	5.67035	6.11458	0.9262	-0.07667	1.4803
0.35 µm Emulsion C	40	vHDPE 3	5.05255	5.56869	0.92224	-0.08095	1.6435
0.35 µm Emulsion C	40	vHDPE 3	5.50255	5.96700	0.92398	-0.079143	1.5996
0.35 µm Emulsion C	40	rHDPE 12	5.50025	6.06112	0.88535	-0.12177	2.5424
0.35 µm Emulsion C	40	rHDPE 12	5.06849	5.58784	0.89784	-0.10776	2.1878
0.35 µm Emulsion C	40	rHDPE 12	5.35649	5.91284	0.89001	-0.11890	2.4762
0.35 µm Emulsion C	40	rHDPE 11	5.37405	5.79476	0.90074	-0.10454	2.1676
0.35 µm Emulsion C	40	rHDPE 11	5.1016	5.62933	0.85707	-0.15424	3.1981
0.35 µm Emulsion C	40	rHDPE 11	5.2076	5.5987	0.8923	-0.14976	3.0165
Emulsion H	40	vHDPE 1	5.53817	5.4222	0.89131	-0.11506	11.3056
Emulsion H	40	vHDPE 1	5.01421	4.83457	0.91458	-0.08929	8.7734
Emulsion H	40	rHDPE 1	4.95277	4.75743	0.75455	-0.28163	22.6193
Emulsion H	40	rHDPE 1	6.17488	6.56883	0.73278	-0.21091	16.9393
Emulsion H	40	rHDPE 3	6.43532	6.43539	0.4668	-0.76257	30.2328
Emulsion H	40	rHDPE 3	5.48578	5.48578	0.4059	-0.90266	35.7868
Emulsion H	40	rHDPE 3	6.17488	6.56883	0.73278	-0.21091	33.9393
Emulsion K	40	vHDPE 1	5.14847	5.13705	0.89075	-0.11569	11.3675
Emulsion K	40	vHDPE 1	5.33262	5.09679	0.8729	-0.13593	13.3562
Emulsion K	40	rHDPE 1	5.41453	5.27651	0.76151	-0.27245	21.882
Emulsion K	40	rHDPE 1	5.47298	5.24241	0.73823	-0.25035	20.107
Emulsion K	40	rHDPE 3	5.97409	5.97416	0.36315	-1.01345	40.1792
Emulsion K	40	rHDPE 3	6.72831	6.72783	0.42196	-0.86306	34.2168
Emulsion K	40	rHDPE 3	6.19434	6.27556	0.40013	-0.89959	37.8974
Emulsion G	40	vHDPE 1	4.36269	3.94433	0.98811	-0.01196	1.1752
Emulsion G	40	vHDPE 1	3.53013	3.2872	0.9856	-0.0145	1.4247
Emulsion G	40	rHDPE 1	4.58838	4.06635	0.98328	-0.01686	1.3541
Emulsion G	40	rHDPE 1	3.90913	3.55106	0.98276	-0.01739	1.3967
Emulsion G	40	rHDPE 3	5.60382	4.89715	0.94241	-0.05931	2.3514
Emulsion G	40	rHDPE 3	5.72548	5.06638	0.97691	-0.02336	0.9261
Emulsion G	40	rHDPE 3	5.701765	5.00003	0.96113	-0.03786	1.6787
Emulsion F	40	vHDPE 1	4.43965	4.23105	0.98694	-0.01315	1.2921
Emulsion F	40	vHDPE 1	4.89635	4.023568	0.988653	-0.01141	1.1211
Emulsion F	40	rHDPE 1	4.7986	4.59755	0.98504	-0.01507	1.2104
Emulsion F	40	rHDPE 1	4.96532	4.56352	0.96998	-0.03048	2.448
Emulsion F	40	rHDPE 3	6.315	6.02889	0.97456	-0.02577	1.0217
Emulsion I	40	rHDPE 3	6.75632	6.53265	0.965685	-0.03492	1.3844
Emulsion I	40	rHDPE 3	6. 5678	6.32444	0.96997	-0.03043	1.1876
Emulsion I	40	vHDPE 1	4.76288	4.18309	0.98848	-0.01159	1.1388
Emulsion I	40	vHDPE 1	4.03128	3.54834	0.98536	-0.01475	1.4493
Emulsion I	40	rHDPE 1	4.54344	4.02177	0.97869	-0.02154	1.73
Emulsion I	40	rHDPE 1	4.98197	4.80616	0.98902	-0.01104	0.8867
Emulsion I	40	rHDPE 3	6.27814	5.16472	0.97435	-0.02598	1.03
Emulsion I	40	rHDPE 3	6.44131	5.95571	0.98082	-0.01937	0.7679
Emulsion I	40	rHDPE 3	6.33131	5.53571	0.97991	-0.02875	0.8823
Emulsion J	40	vHDPE 1	4.73984	4.34177	0.99024	-0.00981	0.9639
Emulsion J	40	vHDPE 1	3.8226	3.64798	0.98822	-0.01185	1.1644
Emulsion J	40	rHDPE 1	4.04245	3.78489	0.98164	-0.01853	1.4882
Emulsion J	40	rHDPE 1	4.3692	4.07592	0.98482	-0.0153	1.2288
Emulsion J	40	rHDPE 3	5.69858	5.13785	0.97351	-0.02685	1.0645
Emulsion J	40	rHDPE 3	5.7195	5.17599	0.97776	-0.02249	0.8916
Emulsion J	40	rHDPE 3	5.7087	5.15982	0.97477	-0.02601	0.9576
Emulsion M	40	vHDPE 1	4.08941	3.95585	0.98505	-0.01506	1.4798
Emulsion M	40	vHDPE 1	3.66329	3.521	0.98636	-0.01373	1.3491
Emulsion M	40	rHDPE 1	4.26371	4.07051	0.96838	-0.03213	2.5805
Emulsion M	40	rHDPE 1	4.74791	4.45569	0.98644	-0.01365	1.0963
Emulsion M	40	rHDPE 1	4.74886	4.43666	0.98972	-0.01033	0.8297
Emulsion M	40	rHDPE 3	6.10973	5.70404	0.93047	-0.07207	2.8573
Emulsion M	40	rHDPE 3	5.77522	5.39306	0.97341	-0.02695	1.0685
Emulsion M	40	rHDPE 3	5.46187	5.04651	0.97307	-0.0273	1.0823
Emulsion N	40	vHDPE 1	3.64306	3.42088	0.98186	-0.01831	1.7991
Emulsion N	40	vHDPE 1	4.42711	4.00163	0.98846	-0.01161	1.1408

Emulsion N	40	rHDPE 1	3.89452	3.69219	0.9813	-0.01888	1.5164
Emulsion N	40	rHDPE 1	5.27412	4.59498	0.98512	-0.01499	1.2039
Emulsion N	40	rHDPE 3	5.86327	5.42861	0.97324	-0.02712	1.0752
Emulsion N	40	rHDPE 3	6.65565	5.7301	0.97946	-0.02075	0.8227
Emulsion N	40	rHDPE 3	6.04575	5.59678	0.978632	-0.024786	0.9556
Emulsion O	40	vHDPE 1	3.48008	3.24149	0.98249	-0.01767	1.7362
Emulsion O	40	vHDPE 1	4.62086	4.23689	0.99154	-0.0085	0.8352
Emulsion O	40	rHDPE 1	3.78293	3.53577	0.98236	-0.0178	1.4296
Emulsion O	40	rHDPE 1	5.67673	5.19491	0.99223	-0.0078	0.6265
Emulsion O	40	rHDPE 3	5.64398	5.36777	0.97195	-0.02845	1.1279
Emulsion O	40	rHDPE 3	6.16043	5.31692	0.97801	-0.02224	0.8817
Emulsion O	40	rHDPE 3	5.93047	5.35876	0.97734	-0.024878	0.9256
Emulsion R	40	vHDPE 1	5.90525	5.71094	0.94641	-0.05508	5.412
Emulsion R	40	vHDPE 1	5.52727	5.32561	0.93324	-0.06909	6.7886
Emulsion R	40	rHDPE 1	5.3177	5.14032	0.81418	-0.20557	16.5105
Emulsion R	40	rHDPE 1	6.32084	6.11223	0.72803	-0.11741	9.4298
Emulsion R	40	rHDPE 3	6.47847	6.47279	0.56242	-0.57551	22.8166
Emulsion R	40	rHDPE 3	7.31069	7.30205	0.59562	-0.51815	20.5425
Emulsion R	40	rHDPE 3	7.01556	6.93456	0.5578	-0.54876	21.765
Emulsion P	40	vHDPE 1	3.28274	3.06914	0.98382	-0.01631	1.6026
Emulsion P	40	vHDPE 1	3.56385	3.02365	0.99236	-0.00767	0.7536
Emulsion P	40	rHDPE 1	3.77208	3.53205	0.98584	-0.01426	1.1453
Emulsion P	40	rHDPE 1	3.68956	3.60235	0.97568	-0.02462	1.9774
Emulsion P	40	rHDPE 3	5.23603	4.69286	0.96849	-0.03202	1.2695
Emulsion P	40	rHDPE 3	5.02365	4.98568	0.95638	-0.0446	1.7682
Emulsion P	40	rHDPE 3	5.17546	4.88963	0.96875	-0.04047	1.5356
Emulsion Q	40	vHDPE 1	3.57755	3.30678	0.98155	-0.01862	1.8296
Emulsion Q	40	vHDPE 1	3.50527	3.33463	0.98602	-0.01408	1.3835
Emulsion Q	40	rHDPE 1	4.03095	3.66024	0.97793	-0.02232	1.7926
Emulsion Q	40	rHDPE 1	3.71424	3.50924	0.98407	-0.01606	1.2899
Emulsion Q	40	rHDPE 3	5.46412	5.00378	0.95711	-0.04384	1.7381
Emulsion Q	40	rHDPE 3	5.69739	5.20688	0.9751	-0.02522	0.9999
Emulsion Q	40	rHDPE 3	5.54756	5.13463	0.96257	-0.0374	1.5634
Emulsion U	40	vHDPE 1	5.15074	4.89844	0.92981	-0.07278	7.1512
Emulsion U	40	vHDPE 1	5.22454	5.08716	0.94223	-0.05951	5.8473
Emulsion U	40	rHDPE 1	6.00204	5.89964	0.75607	-0.19962	16.0326
Emulsion U	40	rHDPE 1	5.99702	5.82214	0.81465	-0.205	16.4647
Emulsion U	40	rHDPE 3	5.66414	5.66417	0.51718	-0.65935	26.1405
Emulsion U	40	rHDPE 3	6.26532	6.26042	0.5838	-0.5382	21.3374
Emulsion U	40	rHDPE 3	601456	6.03567	0.56898	-0.58996	22.6546
Emulsion S	40	vHDPE 1	4.51144	4.05898	0.98716	-0.01292	1.2695
Emulsion S	40	vHDPE 1	4.48857	4.10185	0.98367	-0.01646	1.6173
Emulsion S	40	rHDPE 1	4.91604	4.58001	0.9862	-0.0139	1.1164
Emulsion S	40	rHDPE 1	4.50768	4.44073	0.98613	-0.01397	1.122
Emulsion S	40	rHDPE 3	6.92957	6.21851	0.96626	-0.03432	1.3606
Emulsion S	40	rHDPE 3	7.27719	6.91278	0.9858	-0.0143	0.5669
Emulsion S	40	rHDPE 3	7.03567	6.8474	0.97346	-0.02276	1.0765
Emulsion T	40	vHDPE 1	3.0547	2.91584	0.98577	-0.01433	1.408
Emulsion T	40	vHDPE 1	3.17097	3.02426	0.98614	-0.01396	1.3717
Emulsion T	40	rHDPE 1	3.47548	3.32449	0.98754	-0.01254	1.0072
Emulsion T	40	rHDPE 1	3.86395	3.80368	0.97764	-0.02261	1.8159
Emulsion T	40	rHDPE 3	4.95873	4.55154	0.98193	-0.01824	0.7231
Emulsion T	40	rHDPE 3	5.38116	4.92211	0.98286	-0.01729	0.6855
Emulsion T	40	rHDPE 3	5.03453	4.73463	0.982145	-0.017987	0.69945
Sunflower oil	40	vPP 2	0.22977	0.23342	0.28841	-0.022429	2.4985
Sunflower oil	40	vPP 2	0.26508	0.27503	0.44742	-0.020298	2.2611
Sunflower oil	40	vPP 2	0.233456	0.246547	0.3768	-0.021134	2.37645
Paraffinum oil LV/669	40	vPP 2	11.90879	11.46696	0.98108	-0.0191	2.1276
Paraffinum oil LV/669	40	vPP 2	12.4325	11.96304	0.98224	-0.01792	1.9962
Paraffinum oil LV/669	40	vPP 2	12.0356	11.675	0.98156	-0.018567	1.9999
C12-C15 alkyl benzoate	40	vPP 2	7.62236	7.48901	0.94842	-0.05296	5.8995
C12-C15 alkyl benzoate	40	vPP 2	7.43102	6.90675	0.95616	-0.04483	4.9938
C12-C15 alkyl benzoate	40	vPP 2	7.5789	7.2452	0.95156	-0.04996	5.2456
Caprylic/Capric triglyceride	40	vPP 2	3.75094	3.48451	0.9687	-0.0318	3.5423

Caprylic/capric triglyceride	40	vPP 2	1.3874	1.22996	0.9843	-0.01582	1.7623
Caprylic/capric triglyceride	40	vPP 2	2.37858	2.23906	0.96583	-0.03477	3.8732
Dicaprylyl ether	40	vPP 2	15.94315	15.9752	0.74595	-0.2931	32.6497
Dicaprylyl ether	40	vPP 2	16.5949	16.30769	0.7837	-0.24373	27.1502
Dicaprylyl ether	40	vPP 2	15.7949	15.5657	0.7665	-0.2675	29.645
Butylene glycol dicaprylate/dicaprate	40	vPP 2	7.82715	7.79227	0.98203	-0.01813	2.0196
Butylene glycol dicaprylate/dicaprate	40	vPP 2	7.7756	7.51469	0.98141	-0.01876	2.0898
Butylene glycol dicaprylate/dicaprate	40	vPP 2	7.8356	7.6768	0.98199	-0.01822	2.0345
C12-C15 alkyl benzoate	40	vPP 1	7.0447	6.89915	0.99094	-0.0091	1.0363
C12-C15 alkyl benzoate	40	vPP 1	7.35348	7.13736	0.99242	-0.00761	0.8667
C12-C15 alkyl benzoate	40	vPP 1	7.0245	7.0024	0.99356	-0.00824	0.9356
Caprylic/capric triglyceride	40	vPP 1	2.30495	2.55924	0.82667	-0.19035	21.6778
Caprylic/capric triglyceride	40	vPP 1	0.40928	0.35848	0.95801	-0.0429	4.8856
Caprylic/capric triglyceride	40	vPP 1	0.53528	0.42534	0.98742	-0.01266	1.4418
Dicaprylyl ether	40	vPP 1	8.37208	7.4335	0.91327	-0.09072	10.3316
Dicaprylyl ether	40	vPP 1	8.88242	8.83712	0.9237	-0.07937	9.039
Dicaprylyl ether	40	vPP 1	8.5765	8.0076	0.91776	-0.0865	9.1345
Butylene glycol dicaprylate/dicaprate	40	vPP 1	1.68848	1.62852	0.96528	-0.03534	4.0247
Butylene glycol dicaprylate/dicaprate	40	vPP 1	1.7147	1.57654	0.97323	-0.02713	3.0897
Butylene glycol dicaprylate/dicaprate	40	vPP 1	1.7003	1.60057	0.96987	-0.0476	3.6795
C12-C15 alkyl benzoate	40	rPP 5	9.49371	9.14614	0.97696	-0.02331	3.9717
C12-C15 alkyl benzoate	40	rPP 5	9.44389	9.05558	0.97624	-0.02405	4.0978
C12-C15 alkyl benzoate	40	rPP 5	9.45787	9.0786	0.97656	-0.02397	4.0215
Caprylic/capric triglyceride	40	rPP 5	2.96125	3.23649	0.92869	-0.07398	12.6051
Caprylic/capric triglyceride	40	rPP 5	1.66396	1.55248	0.99101	-0.00903	1.5386
Caprylic/capric triglyceride	40	rPP 5	1.0946	0.99874	0.98317	-0.01697	2.8914
Dicaprylyl ether	40	rPP 5	13.3715	13.00541	0.87968	-0.1282	21.8433
Dicaprylyl ether	40	rPP 5	13.57217	12.98585	0.8858	-0.12126	20.6609
Dicaprylyl ether	40	rPP 5	13.4256	12.99936	0.8814	-0.12546	20.996
Butylene glycol dicaprylate/dicaprate	40	rPP 5	7.40069	7.30428	0.98219	-0.01797	3.0618
Butylene glycol dicaprylate/dicaprate	40	rPP 5	7.44235	7.15998	0.98296	-0.01719	2.9289
Butylene glycol dicaprylate/dicaprate	40	rPP 5	7.42654	7.27658	0.982865	-0.01785	3.0223
Sunflower oil	40	rPP 2	1.0894	1.14048	0.57011	-0.056193	5.7206
Sunflower oil	40	rPP 2	1.27312	1.33063	0.49012	-0.071312	7.2598
Sunflower oil	40	rPP 2	1.16546	1.2765	0.5876	-0.06976	6.8768
Paraffinum oil LV/669	40	rPP 2	3.30998	2.9348	0.94158	-0.0602	6.1286
Paraffinum oil LV/669	40	rPP 2	5.33271	4.89176	0.97268	-0.0277	2.82
Paraffinum oil LV/669	40	rPP 2	4.5772	3.99768	0.95875	-0.0543	5.245
C12-C15 alkyl benzoate	40	rPP 2	8.63441	8.13495	0.97564	-0.02466	2.5105
C12-C15 alkyl benzoate	40	rPP 2	8.34167	7.80299	0.96978	-0.03069	3.1243
C12-C15 alkyl benzoate	40	rPP 2	8.54563	7.99755	0.97003	-0.02764	2.8546
Caprylic/capric triglyceride	40	rPP 2	4.38314	4.25971	0.94988	-0.05142	5.2347

Caprylic/capric triglyceride	40	rPP 2	2.23497	2.05378	0.9667	-0.03387	3.4481
Caprylic/capric triglyceride	40	rPP 2	2.64547	2.46213	0.95247	-0.0487	4.9578
Dicaprylyl ether	40	rPP 2	9.83944	9.90746	0.76018	-0.2742	27.9145
Dicaprylyl ether	40	rPP 2	12.22167	11.83952	0.84951	-0.1631	16.6041
Dicaprylyl ether	40	rPP 2	10.2356	10.6546	0.80067	-0.185	20.7545
Butylene glycol dicaprylate/dicaprate	40	rPP 2	9.18996	9.12552	0.97664	-0.02364	2.4066
Butylene glycol dicaprylate/dicaprate	40	rPP 2	6.6545	5.97313	0.98069	-0.0195	1.9852
Butylene glycol dicaprylate/dicaprate	40	vLDPE 1	2.8375	2.61377	0.78493	-0.24216	24.7799
Butylene glycol dicaprylate/dicaprate	40	vLDPE 1	2.42381	2.29796	0.76795	-0.26403	27.0179
Butylene glycol dicaprylate/dicaprate	40	vLDPE 1	2.88228	2.63424	0.79596	-0.22821	23.3524
Butylene glycol dicaprylate/dicaprate	40	vLDPE 1	2.47869	2.32775	0.78365	-0.24379	24.9467
C12-C15 alkyl benzoate	40	vLDPE 1	5.75028	5.5211	0.694	-0.36574	37.4257
C12-C15 alkyl benzoate	40	vLDPE 1	5.655	5.465	0.676	-0.39165	40.0771
C12-C15 alkyl benzoate	40	vLDPE 1	5.79246	5.54246	0.70032	-0.35622	36.4516
C12-C15 alkyl benzoate	40	vLDPE 1	5.70737	5.49044	0.68523	-0.378	38.6803
Dicaprylyl ether	40	vLDPE 1	4.95312	4.95563	0.12673	-2.06252	211.0551
Dicaprylyl ether	40	vLDPE 1	5.00099	5.00591	0.14499	-1.927	197.1875
Dicaprylyl ether	40	vLDPE 1	4.99099	4.9976	0.1339	-1.997	205.0456
Caprylic/capric triglyceride	40	vLDPE 1	1.5388	1.4253	0.95005	-0.05124	5.2433
Caprylic/capric triglyceride	40	vLDPE 1	1.52808	1.43726	0.95172	-0.04948	5.0632
Caprylic/capric triglyceride	40	vLDPE 1	1.53657	1.43634	0.9507	-0.050014	5.2654
Paraffinum oil LV/669	40	vLDPE 1	7.14628	6.71546	0.87681	-0.13146	13.4521
Paraffinum oil LV/669	40	vLDPE 1	7.2326	6.81882	0.87825	-0.12982	13.2843
Paraffinum oil LV/669	40	vLDPE 1	7.19657	6.7976	0.87764	-0.130156	13.3765
Castor oil	40	vLDPE 1	0.12456	0.12456	0.15921	-1.83583	187.8582
Castor oil	40	vLDPE 1	0.1318	0.07006	0.90727	-0.09732	9.9586
Castor oil	40	vLDPE 1	0.12855	0.1076	0.70134	-0.78755	4.7654
Sunflower oil	40	vLDPE 1	0.58178	0.47432	0.93475	-0.06748	6.9051
Sunflower oil	40	vLDPE 1	0.51158	0.4695	0.95402	-0.04707	4.8166
Sunflower oil	40	vLDPE 1	0.55764	0.47065	0.94765	-0.0514	5.4654
C12-C15 alkyl benzoate	40	vHDPE 1	5.68752	5.50581	0.93662	-0.06548	6.4339
C12-C15 alkyl benzoate	40	vHDPE 1	5.89067	5.5988	0.94805	-0.05335	5.2421
C12-C15 alkyl benzoate	40	vHDPE 1	5.75546	5.57545	0.93997	-0.06024	6.2865
Caprylic/capric triglyceride	40	vHDPE 1	0.85607	0.77573	0.98261	-0.01754	1.7234
Caprylic/capric triglyceride	40	vHDPE 1	1.65306	1.51323	0.99326	-0.00676	0.6642
Caprylic/capric triglyceride	40	vHDPE 1	1.0356	1.0245	0.990013	-0.00897	1.45356
Dicaprylyl ether	40	vHDPE 1	5.77027	5.37038	0.85415	-0.15765	15.4904
Dicaprylyl ether	40	vHDPE 1	5.68036	5.669	0.74207	-0.29831	29.3113
Dicaprylyl ether	40	vHDPE 1	5.69036	5.565	0.80656	-0.20024	20.0356
Butylene glycol dicaprylate/dicaprate	40	vHDPE 1	3.09908	2.93062	0.97295	-0.02742	2.6942
Butylene glycol dicaprylate/dicaprate	40	vHDPE 1	3.15579	2.9812	0.97074	-0.0297	2.9183
Butylene glycol dicaprylate/dicaprate	40	vHDPE 1	3.05789	2.93567	0.9717	-0.0289	2.8456
Paraffinum oil LV/669	40	vHDPE 1	4.7836	4.62746	0.97315	-0.02722	2.6746

Paraffinum oil LV/669	40	vHDPE 1	4.69571	4.54657	0.97408	-0.02626	2.5803
Paraffinum oil LV/669	40	vHDPE 1	4.72351	4.59976	0.973154	-0.026998	2.61345
C12-C15 alkyl benzoate	40	rHDPE 1	4.831	4.477	0.834	-0.18128	14.5596
C12-C15 alkyl benzoate	40	rHDPE 1	4.699	4.352	0.833	-0.18294	14.6929
C12-C15 alkyl benzoate	40	rHDPE 1	4.92721	4.53922	0.84305	-0.17073	13.7123
C12-C15 alkyl benzoate	40	rHDPE 1	5.1011	4.63409	0.86542	-0.14454	11.6088
Butylene glycol dicaprylate/dicaprate	40	rHDPE 1	2.521	2.32	0.89	-0.11652	9.3584
Butylene glycol dicaprylate/dicaprate	40	rHDPE 1	2.38593	2.17966	0.88744	-0.11941	9.5905
Butylene glycol dicaprylate/dicaprate	40	rHDPE 1	3.2672	2.92981	0.93798	-0.06403	5.1426
Butylene glycol dicaprylate/dicaprate	40	rHDPE 1	3.40229	3.02095	0.94798	-0.05342	4.2905
Caprylic/capric triglyceride	40	rHDPE 1	0.90458	0.84952	0.89748	-0.10816	8.6869
Caprylic/capric triglyceride	40	rHDPE 1	0.70098	0.63439	0.88899	-0.11767	9.4507
Caprylic/capric triglyceride	40	rHDPE 1	2.21876	2.23027	0.95502	-0.04602	3.6961
Caprylic/capric triglyceride	40	rHDPE 1	1.63625	1.49196	0.976	-0.02429	1.9509
Dicaprylyl ether	40	rHDPE 1	5.39271	5.34013	0.53358	-0.62814	50.4494
Dicaprylyl ether	40	rHDPE 1	5.3646	5.32047	0.54025	-0.61573	49.4527
Dicaprylyl ether	40	rHDPE 1	5.40171	5.34704	0.53524	-0.62504	50.2004
Dicaprylyl ether	40	rHDPE 1	5.36644	5.3219	0.54058	-0.61511	49.4029
Paraffinum oil LV/669	40	rHDPE 1	3.96701	3.73161	0.8941	-0.11194	8.9905
Paraffinum oil LV/669	40	rHDPE 1	3.71742	3.47878	0.88008	-0.12774	10.2595
Paraffinum oil LV/669	40	rHDPE 1	5.23507	4.78023	0.94113	-0.06067	4.8727
Paraffinum oil LV/669	40	rHDPE 1	3.71742	3.47878	0.88008	-0.12774	10.2595
Castor oil	40	rHDPE 1	0.38074	0.34038	0.87775	-0.13039	10.4723
Castor oil	40	rHDPE 1	0.2913	0.28313	0.85947	-0.15144	12.163
Castor oil	40	rHDPE 1	0.33654	0.32342	0.86754	-0.14753	11.5435
Sunflower oil	40	rHDPE 1	0.58178	0.47432	0.93475	-0.06748	5.4197
Sunflower oil	40	rHDPE 1	0.56762	0.49723	0.88479	-0.1224	9.8306
Sunflower oil	40	rHDPE 1	0.57762	0.48234	0.99367	-0.0876	8.4678
C12-C15 alkyl benzoate	40	rHDPE 3	4.598	4.521	0.529	-0.63713	25.2596
C12-C15 alkyl benzoate	40	rHDPE 3	4.581	4.509	0.497	-0.69847	27.6915
C12-C15 alkyl benzoate	40	rHDPE 3	4.58354	4.51011	0.52553	-0.64334	25.5058
C12-C15 alkyl benzoate	40	rHDPE 3	4.55922	4.49198	0.49256	-0.7081	28.0733
Butylene glycol dicaprylate/dicaprate	40	rHDPE 3	2.70978	2.52642	0.74208	-0.2983	11.8264
Butylene glycol dicaprylate/dicaprate	40	rHDPE 3	2.91192	2.78786	0.7219	-0.32587	12.9194
Butylene glycol dicaprylate/dicaprate	40	rHDPE 3	2.69898	2.52145	0.7387	-0.30286	12.0072
Butylene glycol dicaprylate/dicaprate	40	rHDPE 3	2.90973	2.78678	0.72123	-0.3268	12.9563
Caprylic/capric triglyceride	40	rHDPE 3	2.08533	1.7914	0.94607	-0.05544	2.198
Caprylic/capric triglyceride	40	rHDPE 3	1.92433	1.7095	0.95227	-0.04891	1.9391
Caprylic/capric triglyceride	40	rHDPE 3	1.9994	1.7764	0.9487766	-0.055876	2.657
Castor oil	40	rHDPE 3	-1280.5086	-1280.6022	1	0	0
Castor oil	40	rHDPE 3	-769.70837	-769.75116	0.99999	-1.00E-05	0.0004
Castor oil	40	rHDPE 3	-945.7835	-986.71134	0.99999	-1.00E-05	0.0004

Paraffinum oil LV/669	40	rHDPE 3	4.72415	4.40929	0.82135	-0.19681	7.8027
Paraffinum oil LV/669	40	rHDPE 3	4.72896	4.42273	0.81456	-0.20511	8.1318
Paraffinum oil LV/669	40	rHDPE 3	4.72112	4.416543	0.822754	-0.2000134	8.12854
Dicaprylyl ether	40	rHDPE 3	7.66816	7.65826	0.4189	-0.87032	34.5046
Dicaprylyl ether	40	rHDPE 3	6.97078	6.97266	0.33177	-1.10285	43.7235
Dicaprylyl ether	40	rHDPE 3	7.02578	7.27580	0.39356	-1.0134	40.6235
Sunflower oil	40	rHDPE 3	0.8166	0.71668	0.92088	-0.08243	3.268
Sunflower oil	40	rHDPE 3	0.92357	0.78594	0.93025	-0.0723	2.8664
Sunflower oil	40	rHDPE 3	0.95857	0.76245	0.92995	-0.08895	2.80245
Limonene	40	vHDPE 1	8.24514	7.68481	0.22269	-1.50152	165.5045
Limonene	40	vHDPE 1	7.90873	7.48048	0.18455	-1.69E+00	166.993
Limonene	40	vHDPE 1	8.10873	7.55048	0.20415	-1.60E+00	165.990
Limonene	40	vPP 2	27.64747	26.81964	0.15109	-1.89E+00	211.9216
Limonene	40	vPP 2	26.55612	25.87721	0.14332	-1.94E+00	216.355
Limonene	40	vPP 2	26.77612	25.9121	0.15532	-1.92E+00	214.344
Limonene	40	rPP 5	20.13526	19.57834	0.25292	-1.37E+00	176.1292
Limonene	40	rPP 5	19.78281	19.39669	0.27947	-1.27E+00	266.4727
Limonene	40	rPP 5	19.9935	19.49766	0.26145	-1.31E+00	186.5527
Limonene	40	rHDPE 1	8.49616	7.88222	0.0725	-2.62E+00	206.4321
Limonene	40	rHDPE 1	8.14714	7.62654	0.05989	-2.81E+00	216.337
Limonene	40	rHDPE 1	8.37723	7.71343	0.063453	-2.71E+00	211.342
Limonene	40	rHDPE 3	8.49138	8.40749	1.76E-05	-1.09E+01	386.5939
Limonene	40	rHDPE 3	8.16544	7.97822	9.96E-05	-9.22E+00	379.6441
Limonene	40	rHDPE 3	8.3134	8.24134	4.46E-05	-5.67E+00	381.6166
Limonene	40	vLDPE 1	16.04894	14.9115	0.0305	-3.48E+00	432.5109
Limonene	40	vLDPE 1	16.08334	15.08661	0.02813	-3.57E+00	415.7169
Limonene	40	vLDPE 1	16.08334	15.08661	0.02813	-3.57E+00	415.7169
Mixture A	40	vHDPE 1	5.23195	5.0967	0.91643	-0.08727	8.575
Mixture A	40	vHDPE 1	5.22723	4.96009	0.90722	-0.09737	9.5674
Mixture A	40	vHDPE 1	5.14558	4.95419	0.926941	-0.07587	7.4548
Mixture A	40	rHDPE 1	5.01314	4.95765	0.80305	-0.21934	17.6164
Mixture A	40	rHDPE 3	4.52123	4.52096	0.47099	-0.75464	31.8666
Mixture A	40	rHDPE 3	4.84564	4.54564	0.4435	-0.75197	29.8126
Mixture A	40	rHDPE 3	4.37654	4.302546	0.4986	-0.73456	28.11343
Mixture B	40	vHDPE 1	4.39046	4.35227	0.92724	-0.07554	7.4224
Mixture B	40	vHDPE 1	4.17305	3.72805	0.94323	-0.05845	5.7432
Mixture B	40	rHDPE 1	4.30555	4.09288	0.90639	-0.09829	7.8942
Mixture B	40	rHDPE 3	3.75872	3.75977	0.53269	-0.62982	24.9698
Mixture B	40	rHDPE 3	3.85456	3.1346	0.50767	-0.67876	25.9865
Mixture B	40	rHDPE 3	3.59879	3.2342	0.55876	-0.602456	24.01345
Isopropyl palmitate	23	vHDPE 1	5.43952	5.22305	0.9784	-0.036694	3.6055
Isopropyl palmitate	23	vHDPE 1	5.66109	5.65562	0.97646	-0.02382	2.3405
Isopropyl palmitate	23	vHDPE 1	5.67345	5.4234	0.97774	-0.03246	2.94564
Isopropyl palmitate	66	vHDPE 1	5.71069	5.64805	0.52381	-0.64663	63.5365
Isopropyl palmitate	66	vHDPE 1	5.6796	5.55217	0.581	-0.543	53.354
Isopropyl palmitate	66	vHDPE 1	5.55099	5.49143	0.46298	-0.77069	75.7264
Isopropyl palmitate	23	rHDPE 1	5.05139	4.81609	0.9447	-0.05689	4.5692
Isopropyl palmitate	23	rHDPE 1	5.16974	4.78243	0.94669	-0.05478	4.3997
Isopropyl palmitate	23	rHDPE 1	4.89133	4.66291	0.93602	-0.06612	5.3105
Isopropyl palmitate	66	rHDPE 1	5.40685	5.40475	0.35375	-1.03982	83.5137
Isopropyl palmitate	66	rHDPE 1	5.43379	5.41456	0.31139	-1.16775	93.7885
Isopropyl palmitate	66	rHDPE 1	5.42719	5.40236	0.34432	-1.09834	88.25898
Isopropyl palmitate	23	rHDPE 3	4.42355	4.38178	0.78301	-0.24461	9.6978
Isopropyl palmitate	23	rHDPE 3	4.38775	4.12108	0.76188	-0.27197	10.7825
Isopropyl palmitate	23	rHDPE 3	4.81284	4.70793	0.83122	-0.18486	7.3289
Isopropyl palmitate	66	rHDPE 3	4.88633	4.88531	3.08E-13	-28.82739	1142.8887
Isopropyl palmitate	66	rHDPE 3	4.86593	4.15279	7.44E-10	-21.01882	833.3107
Isopropyl palmitate	66	rHDPE 3	4.87793	4.65675	5.54E-10	-25.02282	989.3887
Isopropyl palmitate	23	vPP 2	11.53475	11.30014	0.9899	-0.01015	1.1307
Isopropyl palmitate	23	vPP 2	8.79686	8.79018	0.98128	-0.0189	2.1054
Isopropyl palmitate	23	vPP 2	22.1567	22.68365	0.99059	-0.00945	1.0527
Isopropyl palmitate	66	vPP 2	12.4714	12.42857	0.37671	-0.97659	108.7868
Isopropyl palmitate	66	vPP 2	15.48613	15.09027	0.45801	-0.78057	86.9513
Isopropyl palmitate	66	vPP 2	14.49476	14.23195	0.44858	-0.80137	89.2683
Isopropyl palmitate	23	rPP 2	11.43068	10.74266	0.995	-0.00501	0.51
Isopropyl palmitate	23	rPP 2	8.44221	7.70328	0.98995	-0.0101	1.0282
Isopropyl palmitate	23	rPP 2	4.94056	4.53124	0.98123	-0.01895	1.9292
Isopropyl palmitate	66	rPP 2	11.16661	11.09429	0.55213	-0.59397	60.4681

Isopropyl palmitate	66	rPP 2	14.30953	13.71362	0.69889	-0.35826	36.4721
Isopropyl palmitate	66	rPP 2	11.77749	11.41936	0.65114	-0.42903	43.6767
Isopropyl palmitate	23	vPP 4	9.45315	9.2973	0.99094	-0.0091	1.241
Isopropyl palmitate	23	vPP 4	8.80952	8.63376	0.98992	-0.01013	1.3814
Isopropyl palmitate	23	vPP 4	8.89546	8.9857	0.99022	-0.01001	1.37866
Isopropyl palmitate	66	vPP 4	9.40488	8.68688	0.36955	-0.99417	135.574
Isopropyl palmitate	66	vPP 4	8.70136	8.01508	0.24377	-1.00978	137.7027
Isopropyl palmitate	66	vPP 4	8.99012	8.4522	0.29234	-1.00011	137.0023
Isopropyl palmitate	23	rPP 1	9.33542	9.25699	0.99389	-0.00613	0.5244
Isopropyl palmitate	23	rPP 1	9.69318	9.61458	0.9946	-0.00541	0.4628
Isopropyl palmitate	23	rPP 1	9.72178	9.40781	0.9940	-0.00600	0.49345
Isopropyl palmitate	66	rPP 1	9.15467	8.55983	0.40271	-0.90875	77.7384
Isopropyl palmitate	66	rPP 1	9.36324	8.79175	0.4075	-0.89628	76.6717
Isopropyl palmitate	66	rPP 1	9.25631	8.65143	0.4033	-0.89991	76.9324
Isopropyl palmitate	23	vLDPE 1	3.24561	2.99	0.89942	-0.10601	10.8479
Isopropyl palmitate	23	vLDPE 1	4.29868	3.6578	0.91933	-0.08801	8.9377
Isopropyl palmitate	23	vLDPE 1	5.11237	4.79097	0.92851	-0.07417	7.5897
Isopropyl palmitate	66	vLDPE 1	5.05721	4.92178	0.41261	-0.88402	90.4607
Isopropyl palmitate	66	vLDPE 1	5.05523	4.98279	0.31233	-0.98992	100.5505
Isopropyl palmitate	66	vLDPE 1	5.05155	5.00697	0.2929	-1.2252	125.3732
Isopropyl palmitate	40	rHDPE 5	5.1977	5.17588	0.69285	-0.36694	60.9411
Isopropyl palmitate	40	rHDPE 5	5.42881	5.39302	0.71939	-0.32936	54.6999
Isopropyl palmitate	40	rHDPE 5	5.29616	5.25328	0.71213	-0.33949	56.3822
Isopropyl palmitate	40	rHDPE 5	5.03883	4.73629	0.66886	-0.40218	66.7938
Isopropyl palmitate	40	rHDPE 5	4.72248	4.28697	0.68628	-0.37647	62.5239
Isopropyl palmitate	40	rHDPE 5	4.91641	4.58427	0.66227	-0.41208	68.4379
Isopropyl palmitate	40	rHDPE 3	4.42243	4.43459	0.44436	-0.80996	32.1116
Isopropyl palmitate	40	rHDPE 3	4.29067	4.29073	0.30984	-1.17056	46.4079
Isopropyl palmitate	40	rHDPE 3	4.38459	4.38528	0.40502	-0.9027	35.7884
Isopropyl palmitate	40	rHDPE 3	4.30588	4.25594	0.36264	-1.14069	45.2237
Isopropyl palmitate	40	rHDPE 3	4.32739	4.2776	0.3727	-1.01376	40.1915
Isopropyl palmitate	40	rHDPE 3	4.32169	4.26901	0.36603	-1.01311	40.1657
Isopropyl palmitate	40	rHDPE 3	4.35675	4.302	0.37884	-0.98549	39.0707
Isopropyl palmitate	40	rHDPE 1	4.67946	4.64791	0.78972	-0.23608	18.9524
Isopropyl palmitate	40	rHDPE 1	4.89969	4.82107	0.81997	-0.19849	15.9347
Isopropyl palmitate	40	rHDPE 1	4.96837	4.57761	0.78785	-0.23845	19.1427
Isopropyl palmitate	40	rHDPE 1	4.46567	4.39249	0.76829	-0.2636	21.1617
Isopropyl palmitate	40	rHDPE 4	5.27414	5.22038	0.75858	-0.27631	43.5373
Isopropyl palmitate	40	rHDPE 4	5.35332	5.27841	0.69863	-0.35863	56.5082
Isopropyl palmitate	40	rHDPE 4	5.19067	4.95096	0.72518	-0.32134	50.6325
Isopropyl palmitate	40	rHDPE 4	4.74938	4.48735	0.66743	-0.40432	63.7074
Isopropyl palmitate	40	rHDPE 21	4.25575	4.12886	0.65386	-0.42488	62.6966
Isopropyl palmitate	40	rHDPE 21	4.4295	4.23808	0.67733	-0.3896	57.4906
Isopropyl palmitate	40	rHDPE 21	4.3963	4.21741	0.67637	-0.39102	57.7001
Isopropyl palmitate	40	rHDPE 21	4.30618	4.11604	0.67785	-0.38885	57.3799
Isopropyl palmitate	40	rHDPE 8	4.2597	4.20111	0.77717	-0.2521	28.1282
Isopropyl palmitate	40	rHDPE 8	5.2587	5.07302	0.84043	-0.24384	27.2065
Isopropyl palmitate	40	rHDPE 8	5.12229	4.93383	0.84109	-0.17306	19.3092
Isopropyl palmitate	40	rHDPE 8	4.80238	4.59868	0.81971	-0.19883	22.1845
Isopropyl palmitate	40	vHDPE 5	3.68898	3.68317	0.57899	-0.54647	11.0167
Isopropyl palmitate	40	vHDPE 5	4.64569	4.64544	0.40966	-0.89109	17.3307
Isopropyl palmitate	40	vHDPE 5	4.68709	4.73511	0.65083	-0.42951	8.9678
Isopropyl palmitate	40	vHDPE 5	4.63101	4.67462	0.58383	-0.53815	11.5491
Isopropyl palmitate	40	vHDPE 5	4.5895	4.60033	0.56424	-0.57228	12.0316
Isopropyl palmitate	40	rHDPE 14	4.79166	4.74959	0.78199	-0.24591	20.8876
Isopropyl palmitate	40	rHDPE 14	4.84062	4.73722	0.78605	-0.24073	20.4476
Isopropyl palmitate	40	rHDPE 14	4.83493	4.48335	0.78079	-0.24745	21.0184
Isopropyl palmitate	40	rHDPE 9	4.95675	4.82151	0.84654	-0.16661	14.9663
Isopropyl palmitate	40	rHDPE 9	4.98779	4.83593	0.83301	-0.18271	16.4126
Isopropyl palmitate	40	rHDPE 9	5.23279	5.23279	0.85107	-0.16126	14.4858
Isopropyl palmitate	40	rHDPE 9	4.95508	4.62944	0.8305	-0.18576	16.6866
Isopropyl palmitate	40	rHDPE 10	4.67503	4.47865	0.89648	-0.10928	21.0297
Isopropyl palmitate	40	rHDPE 10	4.45979	4.20938	0.8857	-0.12138	23.3582
Isopropyl palmitate	40	rHDPE 10	3.9746	3.97488	0.90877	-0.09566	18.4087
Isopropyl palmitate	40	rHDPE 15	4.89185	4.89894	0.65292	-0.42629	21.1794
Isopropyl palmitate	40	rHDPE 15	4.83849	4.82991	0.67969	-0.38612	19.1836
Isopropyl palmitate	40	rHDPE 15	4.86685	4.86572	0.66814	-0.40326	20.0352
Isopropyl palmitate	40	rHDPE 12	4.78581	4.78371	0.52414	-0.646	12.8388
Isopropyl palmitate	40	rHDPE 12	4.7969	4.79662	0.42278	-0.85954	16.5958
Isopropyl palmitate	40	rHDPE 12	4.87391	4.89026	0.55282	-0.59272	12.2898

Isopropyl palmitate	40	vHDPE 4	4.73634	4.64232	0.92222	-0.08097	6.5364
Isopropyl palmitate	40	vHDPE 4	4.69062	4.59028	0.91114	-0.09306	7.5124
Isopropyl palmitate	40	vHDPE 4	4.13379	3.9864	0.88697	-0.11994	9.6823
Isopropyl palmitate	40	rHDPE 16	4.68202	4.64325	0.7734	-0.25696	20.5835
Isopropyl palmitate	40	rHDPE 16	4.63804	4.41541	0.75021	-0.2874	23.0219
Isopropyl palmitate	40	rHDPE 16	4.66959	4.6043	0.74437	-0.29522	23.6483
Isopropyl palmitate	40	rHDPE 16	4.58764	4.25204	0.75358	-0.28292	22.663
Isopropyl palmitate	40	rHDPE 6	5.50356	5.44729	0.77628	-0.25324	22.4727
Isopropyl palmitate	40	rHDPE 6	5.45072	5.32701	0.77802	-0.251	22.2739
Isopropyl palmitate	40	rHDPE 6	5.01546	4.58827	0.72569	-0.32063	28.4529
Isopropyl palmitate	40	rHDPE 11	4.66293	4.65928	0.53143	-0.63219	13.1081
Isopropyl palmitate	40	rHDPE 11	4.83617	4.83526	0.47876	-0.73559	14.9346
Isopropyl palmitate	40	rHDPE 11	4.73153	4.71417	0.54552	-0.60601	12.7407
Isopropyl palmitate	40	rHDPE 11	4.71308	4.75617	0.56892	-0.56402	11.6947
Isopropyl palmitate	40	rHDPE 7	4.71706	4.71518	0.59347	-0.52177	10.6683
Isopropyl palmitate	40	rHDPE 7	4.73953	4.73876	0.48877	-0.71586	14.4315
Isopropyl palmitate	40	rHDPE 7	4.40726	4.42706	0.6106	-0.49331	9.945
Isopropyl palmitate	40	rHDPE 17	4.64583	4.64439	0.57316	-0.55659	11.3004
Isopropyl palmitate	40	rHDPE 17	4.64712	4.64681	0.49641	-0.7003	14.1178
Isopropyl palmitate	40	rHDPE 13	4.72441	4.68569	0.69576	-0.36275	21.8
Isopropyl palmitate	40	rHDPE 13	4.85806	4.83381	0.70563	-0.34867	20.9538
Isopropyl palmitate	40	rHDPE 13	5.01597	4.89943	0.75792	-0.27718	16.6575
Isopropyl palmitate	40	rHDPE 13	4.35206	3.92387	0.69871	-0.35852	21.5458
Isopropyl palmitate	40	vLDPE 1	5.89161	5.79478	0.63336	-0.45672	46.7356
Isopropyl palmitate	40	vLDPE 1	5.82678	5.76327	0.63321	-0.45695	46.7591
Isopropyl palmitate	40	vLDPE 1	5.0747	4.84493	0.6698	-0.40078	41.0113
Isopropyl palmitate	40	LDPE 2	6.96715	6.88576	0.53534	-0.62485	26.3892
Isopropyl palmitate	40	LDPE 2	6.97008	6.91812	0.50121	-0.69072	29.1711
Isopropyl palmitate	40	LDPE 2	6.87839	6.78569	0.40658	-0.90076	38.0417
Isopropyl palmitate	40	LDPE3	6.1416	6.13812	0.45904	-0.77882	32.579
Isopropyl palmitate	40	LDPE3	6.56763	6.52139	0.48533	-0.72332	30.2574
Isopropyl palmitate	40	LDPE3	6.44081	6.37439	0.40873	-0.89504	37.4407
Isopropyl palmitate	40	LDPE3	6.43015	6.39704	0.4464	-0.80705	33.7599
Isopropyl palmitate	40	LDPE4	5.66881	5.64525	0.4741	-0.74716	42.483
Isopropyl palmitate	40	LDPE4	5.65242	5.64086	0.44633	-0.80746	45.9116
Isopropyl palmitate	40	LDPE4	5.8613	5.80387	0.4334	-0.83622	47.5469
Isopropyl palmitate	40	LDPE5	7.19701	7.18561	0.39183	-0.937	51.3679
Isopropyl palmitate	40	LDPE5	6.19017	6.22365	0.44001	-0.8212	45.0196
Isopropyl palmitate	40	LDPE5	7.22203	7.20054	0.29034	-1.23669	67.7974
Isopropyl palmitate	40	rLDPE 2	7.20487	7.18772	0.34189	-1.07261	172.3427
Isopropyl palmitate	40	rLDPE 2	7.10495	7.10218	0.50563	-0.68194	109.5714
Isopropyl palmitate	40	rLDPE 2	6.94913	6.99483	0.50902	-0.67525	108.4965
Isopropyl palmitate	40	rLDPE 2	4.43337	4.54009	0.58715	-0.53247	85.5551
Isopropyl palmitate	40	rLDPE 2	6.9653	6.93403	0.42609	-0.85351	137.1386
Isopropyl palmitate	40	rLDPE 2	7.90732	7.81265	0.37303	-0.98542	158.3333
Isopropyl palmitate	40	vLLDPE 3	11.90352	11.95254	0.32736	-1.11599	122.3574
Isopropyl palmitate	40	vLLDPE 3	11.82846	11.7879	0.38186	-0.96315	105.6
Isopropyl palmitate	40	vLLDPE 3	12.22465	12.18576	0.30863	-1.17655	128.9972
Isopropyl palmitate	40	rLDPE 1	11.8229	11.81123	0.26351	-0.833336	49.2338
Isopropyl palmitate	40	rLDPE 1	7.60407	7.56063	0.47515	-0.74403	43.9576
Isopropyl palmitate	40	rLDPE 1	6.61928	6.56146	0.4614	-0.7737	45.7105
Isopropyl palmitate	40	vLDPE 3	4.92301	4.85041	0.15795	-1.84169	35.0411
Isopropyl palmitate	40	vLDPE 3	4.90197	4.83769	0.22788	-1.47799	29.3741
Isopropyl palmitate	40	vLDPE 3	4.86659	4.8544	0.30362	-1.19052	22.6516
Isopropyl palmitate	40	vLDPE 3	4.90299	4.90251	0.19316	-1.64215	32.6367
Isopropyl palmitate	40	vLDPE 4	6.24865	6.17306	0.11754	-2.14101	39.2439
Isopropyl palmitate	40	vLDPE 4	6.20313	6.1137	0.11981	-2.12335	38.9202
Isopropyl palmitate	40	vLDPE 4	6.25844	6.24439	0.12358	-2.08781	38.2688
Isopropyl palmitate	40	vLDPE 4	6.25195	6.25197	0.12358	-2.08791	38.2706
Isopropyl palmitate	40	vLDPE 2	5.91	5.83282	0.10539	-2.24821	41.5207
Isopropyl palmitate	40	vLDPE 2	5.8501	5.77844	0.10834	-2.22677	40.8159
Isopropyl palmitate	40	vLDPE 2	5.92724	5.92251	0.07961	-2.53498	46.8169
Isopropyl palmitate	40	vLDPE 2	5.92802	5.92803	0.07952	-2.53555	46.4757
Isopropyl palmitate	40	vLLDPE 1	6.75354	6.92873	0.59545	-0.51844	43.9249
Isopropyl palmitate	40	vLLDPE 1	6.73499	6.66943	0.58631	-0.53391	45.2356
Isopropyl palmitate	40	vLLDPE 1	6.70621	6.66384	0.58967	-0.52819	44.751
Isopropyl palmitate	40	vLLDPE 2	6.19891	6.03399	0.09679	-2.33855	44.8231
Isopropyl palmitate	40	vLLDPE 2	6.27317	6.11047	0.08601	-2.45642	45.7076
Isopropyl palmitate	40	vLLDPE 2	6.3588	6.34705	0.11194	-2.19222	42.0184
Isopropyl palmitate	40	vLLDPE 2	6.30708	6.3071	0.11194	-2.19414	40.8272

Isopropyl palmitate	40	vPP 2	12.28749	12.84763	0.87231	-0.13661	15.2176
Isopropyl palmitate	40	vPP 2	11.98096	11.48558	0.91452	-0.08936	9.9542
Isopropyl palmitate	40	vPP 2	11.77363	11.79703	0.91553	-0.08825	9.8306
Isopropyl palmitate	40	rPP 2	8.53302	8.69009	0.93544	-0.06674	6.7944
Isopropyl palmitate	40	rPP 2	10.18127	9.6935	0.94618	-0.05532	5.6318
Isopropyl palmitate	40	rPP 3	9.17208	9.12835	0.89822	-0.10734	12.1535
Isopropyl palmitate	40	rPP 3	9.56957	9.42288	0.91037	-0.0939	10.6318
Isopropyl palmitate	40	rPP 3	10.02072	10.02261	0.89249	-0.11374	12.8782
Isopropyl palmitate	40	rPP 3	9.73599	9.74913	0.90013	-0.10522	11.9135
Isopropyl palmitate	40	rPP 1	8.54481	8.39208	0.88953	-0.11706	10.0138
Isopropyl palmitate	40	rPP 1	8.68581	8.53613	0.89544	-0.11044	9.4475
Isopropyl palmitate	40	rPP 1	8.96965	8.81119	0.88681	-0.12012	10.2756
Isopropyl palmitate	40	rPP 1	8.41751	8.45213	0.87152	-0.13752	11.7641
Isopropyl palmitate	40	vPP 3	60.35483	60.34583	0.3872	-0.94896	19.8134
Isopropyl palmitate	40	vPP 3	65.33185	65.32767	0.40029	-0.9148	14.6591
Isopropyl palmitate	40	vPP 3	65.57846	65.512	0.38641	-0.94973	16.6247
Isopropyl palmitate	40	vPP 3	68.18267	67.93812	0.36577	-1.00488	18.8383
Isopropyl palmitate	40	rPP 4	8.4152	8.50358	0.7072	-0.34644	7.3843
Isopropyl palmitate	40	rPP 4	7.93703	7.96909	0.60876	-0.49633	10.3629
Isopropyl palmitate	40	vPP 5	8.73418	8.78713	0.90283	-0.10222	2.2387
Isopropyl palmitate	40	vPP 5	8.37762	8.37704	0.9067	-0.09794	1.9885
Isopropyl palmitate	40	vPP 5	9.02202	8.92237	0.90711	-0.09749	2.1065
Isopropyl palmitate	40	rPP 5	11.784	11.082	0.954	-0.04714	8.0319
Isopropyl palmitate	40	rPP 5	11.502	10.943	0.946	-0.05566	9.4836
Isopropyl palmitate	40	rPP 5	10.554	10.339	0.947	-0.05412	9.2212
Isopropyl palmitate	40	rPP 6	9.99734	9.62163	0.89154	-0.1148	15.6076
Isopropyl palmitate	40	rPP 6	9.37521	8.68784	0.9165	-0.08719	11.8539
Isopropyl palmitate	40	rPP 6	9.01108	8.49542	0.86848	-0.14101	19.171
Isopropyl palmitate	40	vPP 4	7.3085	7.3238	0.92191	-0.08131	11.0882
Isopropyl palmitate	40	vPP 4	7.40176	7.36299	0.9292	-0.07343	10.0136
Isopropyl palmitate	40	vPP 4	7.54391	7.38939	0.93747	-0.06457	8.8053
Isopropyl palmitate	40	vPP 1	7.28467	7.32275	0.97275	-0.02763	3.1542
Isopropyl palmitate	40	vPP 1	7.07174	7.06352	0.97209	-0.02831	3.2319
Isopropyl palmitate	40	vPP 1	7.10692	7.08924	0.97047	-0.02997	3.4214